

THE UNIVERSITY OF HULL

MOLECULAR LEVEL EFFECTS OF LOW SEAWATER PH ON THE
MARINE POLYCHAETE PLATYNEREIS DUMERILII

being a Thesis submitted for the Degree of

DOCTOR OF PHILOSOPHY

in the University of Hull

by

JANINE WÄGE, B.Sc. University of Göttingen

August, 2015

This copy of the thesis has been supplied on condition that anyone who consults it is understood to recognise that its copyright rests with its author and that no quotation from the thesis and no information derived from it may be published without the author's prior consent.

ABSTRACT

Global changes lead to a measurable reduction of ocean pH. These rapid water chemistry changes are expected to have negative effects on ecosystems and keystone sensitive species. It is predicted that many different physiological processes will be altered under low pH conditions. To date, most studies focus on calcifying organisms however there is a need for further investigations into the precise molecular level changes that occur in other marine organisms.

This work investigates the molecular level changes taking place in a non-calcifying, polychaete species *P. dumerilii* after exposure to acidified seawater, induced by HCl and CO₂. Using laboratory-cultured worms, a targeted approach was employed to examine key genes involved in acid-base regulation and metabolism, as well as a global approach to find other potential mechanisms involved in low pH response. Genes involved in general metabolism and defence processes were down-regulated after exposure with HCl, indicating impacts following exposure. However, the up-regulation of the acid-base transporter *NHE* and an additional expression of *NHE* in the anus area of *P. dumerilii* larvae, may suggest possible compensation mechanisms.

Gene expression profiles were also obtained from *P. dumerilii*, collected from inside and outside natural CO₂ vents (Ischia, Italy), as well as following a pH translocation experiment. Expression analysis of *target* genes showed significant differences between the worms from vent sites in comparison to non-vent sites, suggesting that worms in the natural low pH areas are adapted to the different seawater conditions. Collectively this work shows that low seawater pH, induced by both HCl and CO₂, alters the gene expression in *P. dumerilii*. This provides new knowledge regarding the acid-base regulation mechanisms in a marine polychaete and will help to predict how *P. dumerilii* may respond to ocean acidification.

ACKNOWLEDGEMENTS

I would like to thank my supervisors Dr Jörg D. Hardege and Prof Jeanette M. Rotchell for their guidance throughout the PhD and suggestions for this thesis, as well as assistance in preparing manuscripts. In addition, I would especially like to thank Emma C. Chapman and Dr Adelaide Lerebours for all the technical support during the laboratory work.

I would also like to express my gratitude to Prof Detlev Arendt and the Arendt lab (EMBL Heidelberg), especially, Dr Oleg Simakov, Dr Tomas Larsson and Dr Silvia Rohr for teaching me new methods, providing worm samples and answering my several questions.

A special thanks to Dr Anja Schulze (Marine Biology Department, Texas A&M University) for preparing the sequence alignments and phylogenetic tree and to Dr Maria Cristina Gambi (Stazione Zoologica Anton Dohrn - Napoli) for help with animal collections.

Finally, I would like to thank Dr Helga Bartels-Hardege and Alessandro Recchioni for help with proofreading this dissertation and my family and close friends for their constant support throughout my studies.

PUBLICATIONS

Some chapters of this PhD work have been published:

Wäge, J., Hardege, J.D., Larsson, T.A., Simakov, O., Chapman, E.C., Arendt, D. and Rotchell, J.M. (2015) Effects of low seawater pH on the marine polychaete *Platynereis dumerilii*. *Mar Pollut Bull* 95, 166-172.

Wäge, J., Lerebours, A., Hardege, J.D. and Rotchell, J.M. (2016) Exposure to low pH induces molecular level changes in the marine worm, *Platynereis dumerilii*. *Ecotox Environ Safe* 124, 105-110.

CONTENTS

1. Introduction	20
1.1 Aquatic systems and changes	20
1.2 Regulatory mechanisms	21
1.2.1 Homeostasis	21
1.2.2 Acid-Base balance	22
1.3 Pollutants	24
1.4 Ocean acidification	27
1.4.1 High CO ₂ concentration in atmosphere	27
1.4.2 Effects on ocean chemistry	28
1.4.3 OA models	30
1.4.4 Impacts of lower pH on marine organisms	32
1.4.5 Ability for genetic adaptation to OA	38
1.5 Naturally venting sites as models	40
1.6 A model organism	42
1.6.1 Polychaeta	43
1.6.2 <i>Platynereis dumerilii</i> (Audouin & Milne-Edwards, 1933)	43
1.7 Objectives of this thesis	48
2. Isolation and characterisation of target genes involved in acid-base regulation, ion transport and metabolism	51
2.1 Introduction	51
2.2 Material and Methods	58
2.2.1 Animals	58
2.2.2 Total RNA isolation and purification from worm tissue	59
2.2.3 Synthesis of cDNA	61
2.2.4 Oligonucleotide primer design	61
2.2.5 Amplification of DNA by the Polymerase Chain Reaction (PCR)	62
2.2.6 Agarose gel electrophoresis of DNA	63
2.2.7 Quantification of DNA	64
2.2.8 Sequencing the potential gene	64
2.2.9 Phylogenetic analysis	65
2.2.9.1 <i>NHE</i>	65

2.2.9.2	<i>CA</i>	66
2.2.9.3	<i>CaM</i>	67
2.2.10	Determination of gene expression levels	67
2.2.10.1	Primer optimization and assay performance	67
2.2.10.2	Amplification using qPCR	68
2.2.10.3	Analysis of qPCR products	69
2.2.10.4	Quantification of <i>target</i> gene expression	70
2.3	Results	71
2.3.1	<i>Target</i> gene isolation and characterisation	71
2.3.1.1	Isolation of a partial <i>NHE-like</i> cDNA sequence from <i>P. dumerilii</i>	71
2.3.1.2	Isolation of a partial <i>CA</i> cDNA sequence from <i>P. dumerilii</i>	73
2.3.1.3	Isolation of a partial <i>CaM</i> cDNA sequence from <i>P. dumerilii</i>	75
2.3.2	Quantification qPCR analysis of <i>NHE</i> , <i>CA</i> and <i>CaM</i> mRNA expression	77
2.3.2.1	Real-time amplification	77
2.3.2.2	Assay performance	80
2.4	Discussion	82
3.	Effects of short term low pH on acid-base regulation	87
3.1	Introduction	87
3.2	Material and Methods	89
3.2.1	Animals and experimental exposure	89
3.2.2	Total RNA isolation and purification from worm tissue	91
3.2.3	Synthesis of cDNA	91
3.2.4	<i>Target</i> gene isolation and characterisation	91
3.2.5	Amplification using qPCR	92
3.2.6	Statistical analyses	92
3.2.7	<i>In situ</i> hybridisation of <i>NHE</i>	93
3.2.7.1	Experimental animals	93
3.2.7.2	Probe synthesis	93
3.2.7.2.1	Oligonucleotide primer design	93
3.2.7.2.2	Amplification of DNA by PCR	93
3.2.7.2.3	Agarose gel electrophoresis of DNA	94

3.2.7.2.4	Purification of PCR product	94
3.2.7.2.5	TOPO [®] Cloning reaction-Ligation and Transformation	95
3.2.7.2.6	Overnight culture	95
3.2.7.2.7	Plasmid DNA isolation	95
3.2.7.2.8	Quantification of DNA	96
3.2.7.2.9	Sequencing	96
3.2.7.2.10	Vector opening and clean up from enzymatic reaction	96
3.2.7.2.11	RNA-probe preparation	97
3.2.7.3	Preparation of larvae and fixation	98
3.2.7.4	Rehydration and ProtK digestion	98
3.2.7.5	Hybridisation	99
3.2.7.6	Primary staining	99
3.2.7.7	Analysis of staining	100
3.3	Results	100
3.3.1	qPCR analysis of <i>NHE</i> , <i>CA</i> and <i>CaM</i> mRNA expression	100
3.3.2	<i>In situ</i> hybridisation of <i>NHE</i>	102
3.4	Discussion	103
3.5	Conclusions	107
4.	Molecular level responses in <i>P. dumerilii</i> after exposure to acidified seawater	109
4.1	Introduction	109
4.2	Material and Methods	112
4.2.1	Animals and experimental exposure	112
4.2.2	Total RNA isolation and purification from worm tissue	113
4.2.3	RNA Integrity	113
4.2.4	RNA Precipitation	113
4.2.5	cDNA synthesis and Amplification by LD PCR	113
4.2.6	Rsa I Digestion	115
4.2.7	Adapter Ligation	115
4.2.8	Suppression subtractive hybridisation	118
4.2.8.1	First hybridisation	118
4.2.8.2	Second hybridisation	118

4.2.9	PCR amplification	118
4.2.10	Cloning of PCR generated fragments	119
4.2.11	Bioinformatics	122
4.2.12	qPCR validation	122
4.2.13	Statistical analyses	124
4.3	Results	124
4.3.1	SSH analysis	124
4.3.2	Validation of differential mRNA transcriptions	125
4.4	Discussion	130
4.5	Conclusion	134
5.	Short term effects of CO₂ induced low pH exposure on specific gene expressions	135
5.1	Introduction	135
5.2	Material and Methods	138
5.2.1	Animals and experimental exposure	138
5.2.2	Total RNA isolation and purification from worm tissue	139
5.2.3	Synthesis of cDNA	139
5.2.4	<i>Target</i> gene isolation and characterisation	140
5.2.5	Amplification using qPCR	140
5.2.6	Statistical analyses	141
5.3	Results	142
5.3.1	qPCR analysis of <i>NHE</i> , <i>CA</i> and <i>CaM</i> mRNA expression	142
5.3.2	Analysis of weight differences	142
5.4	Discussion	144
5.5	Conclusions	148
6.	Phylogenetic and gene expression profiles of worms at CO₂ vents	149
6.1	Introduction	149
6.2	Material and Methods	152
6.2.1	Study area	152
6.2.2	Animal collection	153
6.2.3	Laboratory exposure experiments	155
6.2.3.1	S. Anna – reference site worms	155
6.2.3.2	Castello S3 – vent worms	156

6.2.4	Total RNA isolation and cDNA synthesis	156
6.2.5	<i>Target</i> gene isolation and characterisation	156
6.2.6	Amplification using qPCR	157
6.2.7	Restriction enzyme analysis to determine species	158
6.2.7.1	Generation of COI PCR product	158
6.2.7.2	BstZ17I restriction digest	159
6.2.8	Phylogenetic analyses	159
6.3	Statistical analyses	161
6.4	Results	162
6.4.1	Experimental parameters	162
6.4.1.1	Seawater pH during exposure experiment	162
6.4.1.2	Punctual value records of sample collection sides	162
6.4.1.3	Body mass differences from the three sampling sites	163
6.4.2	qPCR analysis of <i>target</i> gene mRNA expression	164
6.4.3	Restriction enzyme analysis of Castello S3 and N3	168
6.4.4	Re-analysis of qPCR data (taking restriction enzyme analysis into account)	170
6.4.5	Phylogenetic analyses of different populations and heteronereids	170
6.5	Discussion	172
6.6	Conclusion	178
7.	General discussion	179
	Appendices	205
	References	207

LIST OF FIGURES

1. Introduction

- Figure 1.1 Relationship of cells, body systems, and homeostasis. Adapted from Sherwood et al., 2005. 22
- Figure 1.2 Schematic illustration of the carbonate system in the ocean. CO₂ from the atmosphere dissolves in the seawater forming carbonic acid (H₂CO₃). This acid releases H⁺ and HCO₃⁻, which can then release H⁺ again and form CO₃²⁻. 28
- Figure 1.3 Partial pressure of dissolved CO₂ at the ocean surface (blue curves) and in situ pH (green curves) measured at two stations in the Atlantic Ocean (dark blue/dark green and blue/green) as well as at a station in the Pacific Ocean (light blue/light green) (IPCC, 2013). 30
- Figure 1.4 Model mean time series of global surface pH change based on the scenarios RCP2.6, RCP4.5, RCP6.0 and RCP8.5 in 1850-2100. Adapted from IPCC (2013). 31
- Figure 1.5 Maps of multi-model surface pH for the scenarios RCP2.6, RCP4.5, RCP6.0 and RCP8.5 in 2081-2100 relative to 1986-2005. Adapted from IPCC (2013). 31
- Figure 1.6 Diverse ocean life near the island of Ischia in Italy (left picture). The CO₂ vent, which is only a few hundreds of meters away shows a decreased diversity of species (right picture). Image credit: David Liittschwager, National Geographic. 41
- Figure 1.7 Close-up picture of *P. dumerilii* head (source: <http://bit.ly/1ahJJsl>; accessed on 17.07.2015). 44
- Figure 1.8 Life cycle of *P. dumerilii* (Hagger et al., 2002) 45
- Figure 1.9 Prostomium and peristomium of small atokous *P. dumerilii*. Adapted from Fischer et al. (2010). 47
- Figure 1.10 Trunk of small atokous *P. dumerilii*. Further segments are budding off from the posterior growth zone. The worm increases in diameter. The size of the anterior segments is still growing in size. Adapted from Fischer et al. (2010). 47

2. Isolation and characterisation of target genes involved in acid-base regulation, ion transport and metabolism

- Figure 2.1 Schematic overview of effects of low pH on animal's body. Ocean *p*CO₂ is increasing (dark green) and decreases water pH (red). CO₂ distributes by diffusion (black arrows), causing pH disturbance in extra and intracellular compartments and influences directly or indirectly (red broken arrows) tissues, cells and their inherent processes and functions (blue) (Wittmann and Pörtner, 2013). 51

Figure 2.2	Examples for the three-dimensional protein structures of the selected <i>target</i> genes NHE, CA and CaM. A (a) Ribbon structure presentation of the crystal structure of NhaA of <i>E. coli</i> . Presented is a view parallel to the membrane. The 12 transmembrane segments are numbered with roman numerals. The letters C and N describe the N- and C-termini. The black lines present the cytoplasmic and periplasmic funnels. (b) Cross-section of the antiporter, without front part. The cytoplasmic and periplasmic funnels are marked in white. Hydrated cations can potentially access the cytoplasmic funnel down to the white arrow, whereas below the red arrow only non-hydrated Na ⁺ and Li ⁺ can enter. The green star indicated the ion-binding site (Padan, 2009). B Structure of human CA II at 2.0Å resolution. The zinc ion is presented in the active site. From PDB 1CA2. C Structure of CaM during Ca ²⁺ -regulated conformational change. (a) Ca ²⁺ -free and (b) as Ca ²⁺ ₄ -CaM. Presented are the methionine side chains in purple to represent the location of potential hydrophobic pockets in both domains. Through the binding of Ca ²⁺ , large changes in the helices in both domains are triggered and result in an exposure of several hydrophobic residues (Chin and Means, 2000).	56
Figure 2.3	Overview of methodical approach for gene isolation.	59
Figure 2.4	Alignment of partial <i>P. dumerilii</i> NHE (FARO denovo 101100021518), <i>A. aegypti</i> NHE (AAF80554.1) and <i>D. melanogaster</i> NHE2 (NP_001137847.1) amino acid sequences. Dashes represent alignment gaps and asterisks represent homology. Colons represent sites with conserved amino acid substitutions and dots represent semi-conserved amino acid substitutions (similar shape). Light grey shaded regions represent functional protein domains.	72
Figure 2.5	Phylogeny of predicted partial amino acid sequences for NHE, using an amino acid sequence with gaps. Sequences were aligned and edited in Jalview 2.8.0b1 and for the Maximum likelihood analysis Mega6 was used. The Jones-Taylor-Thornton (JTT) model was applied and for the heuristic search the Nearest Neighbour Interchange (NNI) method was performed. The numbers in the nodes represent bootstrap probabilities with 1000 replicates.	73
Figure 2.6	Alignment of partial <i>P. dumerilii</i> CA (TUEB denovo 100100001529), <i>P. vulgata</i> CA (CCJ09594.1) and <i>N. vectensis</i> CA1 (DAA06053.1) predicted amino acid sequences. Dashes represent alignment gaps and asterisks represent homology. Colons represent sites with conserved amino acid substitutions and dots represent semi-conserved amino acid substitutions (similar shape). Light grey shaded regions represent functional protein domains. Dark grey shaded regions represent active sites on the conserved domain and the hash sign the zinc binding sites.	74

- Figure 2.7 Phylogeny of partial amino acid sequences for *CA*, using an amino acid sequence with gaps. Sequences were aligned and edited in Jalview and for the Maximum likelihood analysis Mega6 was used. The Jones-Taylor-Thornton (JTT) model was applied and for the heuristic search the Nearest Neighbour Interchange (NNI) method was performed. The numbers in the nodes represent bootstrap probabilities with 1000 replicates. 75
- Figure 2.8 Alignment of partial *P. dumerilii CaM* (HEIDELBERG denovo 100500002325), *L. vannamei CaM A* (AEK21539.1) and *B. taurus CaM* (NP_001159980.1) predicted amino acid sequences. Dashes represent alignment gaps and asterisks represent homology. Colons represent sites with conserved amino acid substitutions and dots represent semi-conserved amino acid substitutions (similar shape). Light grey shaded regions represent functional protein domains. Dark grey shaded regions represent Ca²⁺ binding site on a conserved domain. The EF hand is a calcium-binding motif, which is the most common calcium-binding motif found in proteins. It usually has a helix-loop-helix motif (Lewit-Bentley and Réty, 2000). 76
- Figure 2.9 Phylogeny of partial amino acid sequences for *CaM*, using an amino acid sequence with gaps. Sequences were aligned and edited in Jalview 2.8.0b1 and for the Maximum likelihood analysis Mega6 was used. The Jones-Taylor-Thornton (JTT) model was applied and for the heuristic search the Nearest Neighbour Interchange (NNI) method was performed. The numbers in the nodes represent bootstrap probabilities with 1000 replicates. 77
- Figure 2.10 qPCR products derived from *18S*, *α-Tub*, *NHE*, *CA* and *CaM* primers sets were separated using 1% agarose gel in TBE buffer. A 100 bp DNA Ladder was loaded to the right of the samples 78
- Figure 2.11 Melt curve and melt peak of the real-time amplification of *P. dumerilii 18S* (A1, A2), *α-TUB* (B1, B2), *NHE* (C1, C2), *CA* (D1, D2) and *CaM* (E1, E2). 79
- Figure 2.12 qPCR standard curves generated from *18S rRNA*, *α-TUB*, *NHE*, *CA* and *CaM* amplification data. The slope, y-intercept and correlation coefficient (R²) of the calibration curve are presented. This is the minimum information needed for real-time PCR experiment publications stated by Bustin et al. (2009). Graphs were designed with XACT 8.03 (SciLab, Germany). 78 81

3. Effects of short term low pH on acid-base regulation

- Figure 3.1 Normalised average relative mRNA transcription \pm standard error of the mean in *P. dumerilii* for (a) *NHE* (b) *CA* and (c) *CaM* after 1 h and after 7 d in seawater with pH 8.2 and pH 7.8. Analysis was performed by unpaired *t*-test.* indicates significant differences ($p < 0.05$) of mRNA transcription between pH 8.2 and pH 7.8. 101
- Figure 3.2 Localized *NHE* expression in 7 dpf larvae maintained at pH 8.2 (a and b) and 7.8 (c and d). Bright-field images were taken using a Zeiss Axiophot microscope with a 200 \times magnification (Carl Zeiss, Jena, Germany). 102

4. Molecular level responses in *P. dumerilii* after exposure to acidified sea water

- Figure 4.1 Scheme of the preparation of adaptor-ligated tester cDNAs for hybridisation and PCR. Each tester cDNA is ligated to the appropriate adaptor. A The forward subtraction represents the intended experiment. B The reverse subtraction is required for differential screening of the subtracted cDNA library. C A control subtraction is performed with skeletal cDNA (Scheme taken from the SelectTM cDNA Subtraction Kit User Manual, Clontech). 117
- Figure 4.2 Overview of the main steps employed for the subcloning procedure. 120
- Figure 4.3 Pie chart presenting the three different groups identified as up-regulated mRNA transcripts in *P. dumerilii* kept at low pH seawater conditions relative to normal pH conditions. 124
- Figure 4.4 Pie chart presenting the different groups identified as down-regulated mRNA transcripts in *P. dumerilii* kept at low pH seawater conditions relative to normal pH conditions. 125
- Figure 4.5 qPCR analysis of selected transcripts (a) *paramyosin* (b) *calponin* (c) *cytochrome c oxidase* (d) *NADH dehydrogenase* identified by SSH as differentially expressed in worms maintained at low pH seawater conditions relative to normal pH conditions. All treatments present n=8 samples, only *paramyosin* has n=7 for pH 8.2, * $p < 0.05$. 126

5. Short term effects of CO₂ induced low pH on specific gene expressions

- Figure 5.1 Normalised average relative mRNA transcription \pm standard error of the mean in *P. dumerilii* for (a) *NHE* (b) *CA* and (c) *CaM* after 1 h and after 7 d in seawater with pH 8.2 and pH 7.8. Analysis was performed by two-way ANOVA. *NHE* showed a clear trend ($p=0.069$) for the effect of pH and *CA* a significant effect ($p=0.005$). Both did not show a significant effect of time ($p=0.128$; $p=1.000$). *CaM* did not show a significant for pH ($p=0.806$) or time ($p=0.374$). Graphs were designed with XACT 8.03 (SciLab, Germany). 143

6. Phylogenetic and gene expression profiles of worms at CO₂ vents

- Figure 6.1 CO₂ vent around the island of Ischia (Italy). The picture was provided by Jason Hall-Spencer (Plymouth University). Image credit: David Liittschwager, National Geographic (2010). 154
- Figure 6.2 Map of the sampling site in Italy on the island Ischia around Castello Aragonese and the S. Anna islets, highlighted with red rectangles. 155
- Figure 6.3 Map of the sampling site for the phylogenetic analysis around the Mediterranean Sea, Atlantic Ocean and Bristol Channel. Approximate sampling locations are highlighted with pins (blue-Bristol, red-Arcachon, yellow-Blanes, light green-Stareso, light blue-Ischia, pink-Nisida, dark green-Palinuro, orange-Ustica, purple-Vulcano, brown-S. Catarina). 161
- Figure 6.4 Body mass of all *P. dumerilii* collected from S. Anna in low $p\text{CO}_2$ environment and within the two CO₂ vents (Castello S3 and N3) with elevated $p\text{CO}_2$ conditions. 163
- Figure 6.5 Normalised average relative mRNA transcription \pm SEM in *P. dumerilii* for *NADH dehydrogenase* (a), *NHE* (b), *CA* (c) and *paramyosin* (d) in field samples (S. Anna, Castello S3, Castello N3) and after 7 d in sea water with pH 8.0 (C-C, control and A-C, treatment) and pH 7.7 (C-A, treatment and A-A, control). Analysis was performed by nonparametric Kruskal-Wallis test ($p < 0.05$). In case of significance a Mann-Whitney U test was used to evaluate significance. For all analyses, statistical significance was accepted at $p < 0.05$. Significant effects are labelled with asterisks (* $p < 0.05$; ** $p < 0.01$; *** $p < 0.001$). Non-significant results are labelled with ns. 167

- Figure 6.6 Alignment of selected *S. Anna* and Castello S3 COI sequences from GenBank. Regions showing homology are indicated by an asterisk. Grey shaded region shows restriction site for BstZ17I in Castello S3. Red arrow indicates cutting position. GenBank accession numbers for sequences are: S3_10 (KC591836.1), S3_8 (KC591834.1), S3_12 (KC591838.1), *S. Anna*_29 (KC591867.1), *S. Anna*_26 (KC591865.1) and *S. Anna*_22 (KC591864.1). 169
- Figure 6.7 Image of a 1% GelRed-stained (Biotium, Cambridge Bioscience, Cambridge, UK) agarose-gel of BstZ17I digested COI PCR products from Castello S3 and N3 worms used in qPCR analysis. A 100 bp ladder (L) (New England BioLabs, Hitchin, UK) was run to the right of the sample wells. 169
- Figure 6.8 50% majority rules consensus tree resulting from Bayesian Inference analysis of 139 sequences of *Platynereis* spp. (including pelagic heteronereis) from CO₂ vents in Ischia and Vulcano and from 12 control locations. Double asterisks (**) at nodes indicate branch support of 100% posterior probability; single asterisks indicate branch support of $\geq 95\%$ posterior probability. The figure was produced by Dr Anja Schulze (Texas A&M University). 171

7. General discussion

- Figure 7.1 OA has direct and indirect effects on many physiological processes which, in turn, can have consequences on the fitness of an organism (adapted from Dupont and Thorndyke (2009)). 182

LIST OF TABLES

1. Introduction

Table 1.1	Summary of the available literature published on gene expression responses of marine fauna in response to low pH conditions induced by CO ₂ . The table shows different species ordered in their phyla, the CO ₂ system parameters used in the experiment as well as a short description of the main gene expression differences and the corresponding reference.	36
-----------	---	----

2. Isolation and characterisation of target genes involved in acid-base regulation, ion transport and metabolism

Table 2.1	Oligonucleotide primer sequences for the two <i>reference</i> (<i>18S</i> and <i>α-TUB</i>), and the three <i>target</i> genes (<i>NHE</i> , <i>CA</i> and <i>CaM</i>) and their amplicon size in bp.	62
Table 2.2	Amino acid sequences for <i>NHE</i> obtained from NCBI used for the alignment and following phylogenetic analyses. The sequence for the outgroup is marked with an asterisk (*).	65
Table 2.3	Amino acid sequences for <i>CA</i> obtained from NCBI used for the alignment and following phylogenetic analyses. The sequence for the outgroup is marked with an asterisk (*).	66
Table 2.4	Amino acid sequences for <i>CaM</i> obtained from NCBI used for the alignment and following phylogenetic analyses. The sequence for the outgroup is marked with an asterisk (*).	67
Table 2.5	Primer concentrations for qPCR in nM, melting temperature in °C, efficiency of amplification in % and amplification of the oligonucleotide primers for <i>18S</i> , <i>α-TUB</i> , <i>NHE</i> , <i>CA</i> and <i>CaM</i> .	78

3. Effects of short term low pH on acid-base regulation

Table 3.1	Oligonucleotide primer of <i>NHE_{Probe}</i> for <i>in situ</i> hybridisation with sequence and amplicon size in bp.	93
-----------	--	----

4. Molecular level responses in *P. dumerilii* after exposure to acidified sea water

Table 4.1	<i>Target</i> and <i>reference</i> gene primer sequences, amplicon sizes and primer concentrations used for qPCR.	123
Table 4.2	Differentially expressed (subtracted) mRNAs identified in <i>P. dumerilii</i> maintained at low pH conditions. For each identified gene the corresponding accession number and nucleotide base pair length of the transcript is presented, as well as the homologues species match including E-value and GenBank accession number. Furthermore the functional category with small explanation and reference is presented. * indicates hits with PLATYpopsys database only and corresponding E-value represents the re-blast result of the matched sequence.	127

5. Short term effects of CO₂ induced low pH on specific gene expressions

Table 5.1	Oligonucleotide primer sequences for the <i>18S</i> , <i>NHE</i> , <i>CA</i> and <i>CaM</i> , as well as the new primer pair for the second <i>reference</i> gene <i>α-TUB₂</i> . For all <i>target</i> and <i>reference</i> genes the amplicon size in base pairs (bp) are presented.	141
-----------	---	-----

6. Phylogenetic and gene expression profiles of worms at CO₂ vents

Table 6.1	Oligonucleotide primers for the four <i>target</i> genes and the two <i>reference</i> genes with forward and reverse sequence, amplicon size in bp and primer concentration used in nM.	157
Table 6.2	Melting temperature (°C) and efficiency of amplification (%) of the oligonucleotide primers for <i>18S rRNA</i> , <i>α-TUB₂</i> , <i>NHE</i> , <i>CA</i> , <i>NADH dehydrogenase</i> and <i>paramyosin</i> .	158
Table 6.3	Seawater pH (mean ± SEM) in <i>P. dumerilii</i> holding glass bowls during 7 d exposure experiment.	162
Table 6.4	Average punctual value records (n=13) and SEM of salinity, temperature and pH at the three sampling station Sant' Anna, Castello S3 and Castello N3 in June 2014.	162
Table 6.5	Body mass (mean ± SEM) in mg of <i>P. dumerilii</i> direct field samples from the three sampling station S. Anna, Castello S3 and Castello N3 as well as for the individuals used in the transplant experiment (C-C, C-A and A-A, A-C).	163

7. General discussion

Table 7.1	Summary of the responses of <i>P. dumerilii</i> to low pH induced by HCl and CO ₂ of long term laboratory cultured worms labelled with * and field populations called non-vent, vent S3 and vent N3. All expressions are relative to normal pH conditions (~pH 8.2/ 8.0). Only, the relative expression of Vent S3 is relative to low pH (~pH 7.7). The second part of the table is a comparison of the relative expression of the non-vent population to the vent S3 and N3 population. ↑ indicates an up-regulation, ↓ indicates a down-regulation, ↔ indicates no significant change, F indicates a failed amplification, - stands for not investigated. All * next to the arrows present significant results.	187
Table 7.2	Comparison of five main approaches used to investigate the effects of OA. Five stages were used for the ranking: very high, high, medium, low and very low (Gattuso et al., 2014).	192

ABBREVIATIONS

ANOVA	analysis of variance
bp	base pair
CA	carbonic anhydrase
Calpo	calponin
CaM	calmodulin
cDNA	complementary deoxyribonucleic acid
COI	cytochrome <i>c</i> oxidase I
$C_q = C_T$	threshold cycle
Cyto	cytochrome <i>c</i> oxidase
DIC	dissolved inorganic carbons
DMSO	dimethyl sulfoxide
DNA	deoxyribonucleic acid
dNTPs	deoxynucleoside triphosphate
dsDNA	double-Stranded DNA
EMBL	European Molecular Biology Laboratory
EST	expressed sequence tag
FOCE	Free Ocean CO ₂ Enrichment
gDNA	genomic DNA
Kb	kilo base
LD PCR	Long-Distance Polymerase Chain Reaction
mRNA	messenger RNA
NADH	NADH dehydrogenase
NHE	sodium hydrogen antiporter
OA	ocean acidification
Para	paramyosin
PCBs	polychlorinated biphenyls
pCO_2	partial pressure of CO ₂
PCR	polymerase chain reaction
qPCR	quantitative real-time PCR
RCPs	Representative Concentration Pathways
RNA	ribonucleic acid
SEM	standard error of the mean
18S	18S ribosomal RNA
SSH	suppression subtractive hybridization
α -Tub	alpha-tubulin

1.1 Aquatic Systems and changes

Oceans cover approximately 70.8 % of the earth's surface, which is equivalent to 361.1 million km². At first glance the marine habitat appears monotone due to the aqueous environment. However, the marine biotope is very diverse and comprised of many different ecosystems. Generally the marine biotope can be subdivided into pelagic, meaning to be in the water or surrounded by water, and benthic, meaning to be on the bottom or on a solid surface, zone (Tardent, 2005). The seawater is comprised of a diverse number of organic and inorganic components. The latter, are dominated by salts such as chloride (Cl⁻), sodium (Na⁺), magnesium (Mg²⁺), sulphate (SO₄²⁻), calcium (Ca²⁺), potassium (K⁺), bicarbonate (HCO₃⁻), bromide (Br⁻), boric acid (B(OH)₃), strontium (Sr²⁺) and fluorine (F⁻) (Millero et al., 2008). The amount of dissolved gases, primarily from the atmosphere, depend on the physical parameters (temperature, salinity and hydrodynamic) as well as biological processes (assimilation and respiration). The two life's essential gases are oxygen (O₂) and carbon dioxide (CO₂) (Tardent, 2005). During the course of the earth's history the concentration of O₂ increased slowly to its current levels (Berkner and Marshall, 1965), whereas the CO₂ concentration is increasing rapidly since the Industrial Revolution due to the combustion of fossil fuels (IPCC, 2014). At the same time wood clearing eliminates CO₂-consumers, which are besides marine phytoplankton important to stabilise the CO₂-cycle. The subsequent increasing levels of CO₂ in the seawater lower the surface ocean pH (IPCC, 2014). Impacts of environmental alterations may vary across functional groups and trophic levels. It can alter food-web-structures and potentially lead to ecosystem-level changes (Edwards and Richardson, 2004).

1.2 Regulatory mechanisms

1.2.1 Homeostasis

Claude Bernard (1878) was the first who stated that life is sustained through the constancy of the fluid matrix or ‘milieu intérieur’. Half a century later, Cannon characterised the term homeostasis (*homoios* meaning like + *stasis* meaning fixity), describing the maintenance of an internal stability under interrupted normal condition (Cannon, 1929). In order to be able to function properly homeostasis is essential for all cells (Recordati and Bellini, 2004) (Fig. 1.1). A key part for homeostasis is the extracellular fluid, which is in contact with all cells and helps to make exchanges between the external and internal environment (Bernard, 1878). Several different factors of the internal environment are often homeostatically regulated: concentration of energy-rich molecules (e.g. ATP and NADH); concentration of CO₂ and O₂; concentration of waste products; pH and concentration of salt (e.g. Na⁺ and Cl⁻), water and electrolytes. Some animals additionally regulate the volume and pressure of the cell as well as the temperature (Sherwood et al., 2005).

Looking more closely at pH and the concentration of CO₂, both will play a major role in the present dissertation. The removal of CO₂ is very important to prevent the increase of acidity (hydrogen ions (H⁺) concentration) in the internal environment. Changes in pH (acidity) can have negative effects on electrical signalling mechanisms of nerve cells and the enzyme activity of cells (Sherwood et al., 2005). However, homeostasis does not mean that the internal environment is completely unchanged. Homeostasis is a dynamic condition with changes being reduced through physiological reactions (Selye, 1975). All organisms have to allocate resources between different life functions. This is known as “The Principle of Allocation” (Hillis et al., 2012). The highest priority is usually the maintenance of homeostasis. Under stressful physical conditions the investment in

homeostasis is very high and little energy is available for foraging, growth, defence and reproduction (Hillis et al., 2012). The most important feature of living organisms is reproduction, whereby resources i.e. energy need to be allocated between the interlinked processes of somatic and reproductive events (Jha, 2008). Both processes require to be maintained in a balance as the maturation of somatic compartments determines the reproductive success (Jha, 2008).

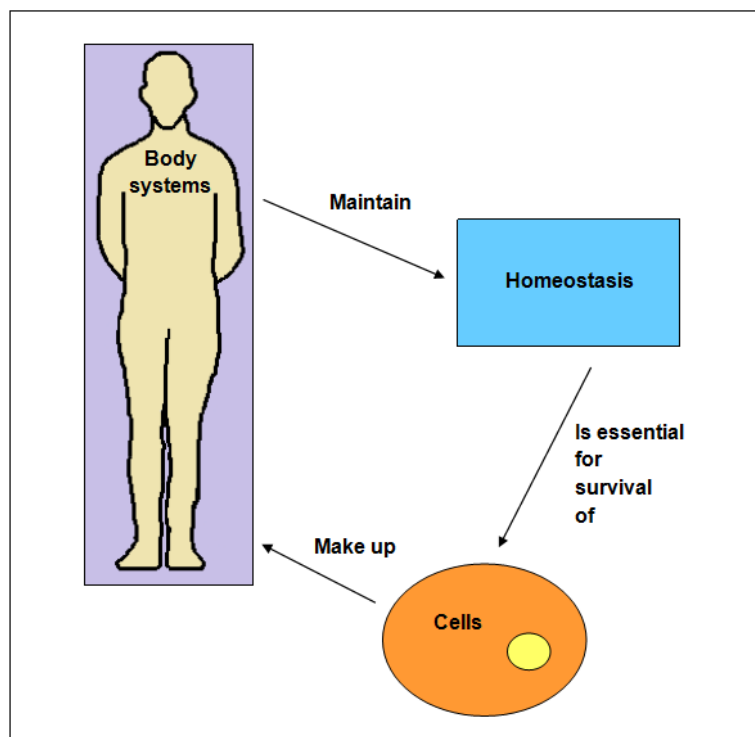


Figure 1.1 Relationship of cells, body systems, and homeostasis

Adapted from Sherwood et al., 2005.

1.2.2 Acid-Base balance

As mentioned in section 1.2.1 acidity is homeostatically regulated. This is known as acid-base balance, which is the regulation of H^+ in the body fluids (Siggaard-Andersen, 2005). Most life functions have a small pH range within they are functioning correctly. For instance, protein conformations are altered by H^+ which may also therefore affect their biochemical activity (Petsko and Ringe, 2004). The activity of an enzyme decreases

outside the optimum pH range and greater changes can lead to denaturation (Ochei and Kolhatkar, 2000). If an organism is not able to compensate an acid-base imbalance, it can suffer from metabolic suppression (Guppy and Withers, 1999) and / or the oxygen transport in the blood will be negatively affected due to reduced oxygen binding (Jensen, 2004). To illustrate, such effects have been observed in the jumbo squid, *Dosidicus gigas* (Rosa and Seibel, 2008). Malfunctions could also be detected in muscle cells (Orchard and Kentish, 1990). Further effects of acid-base changes were found in the synaptic transmission, neurotransmitter function and receptors of organisms (Ahn and Klinman, 1983; Ryu et al., 2003; Sinning and Hübner, 2013). The regulation of acid and bases requires energy-consuming ion pumps and can therefore cause changes in the energy budget depending on the function of the tissue (Pörtner et al., 2000). This could affect reproduction, growth, defence and thus the overall fitness of an organism (Hillis et al., 2012). Only once the maintenance of the integrity of the body is ensured, resources can be invested in other processes (Hillis et al., 2012).

Changes in the acid-base balance can be caused by either internal or external alterations. The increasing levels of atmospheric CO₂ through enhanced burning of fossil fuels by humans, is an example for external disturbance (Sherwood et al., 2005). Acidification of bodily fluids (hypercapnia) in marine animals through elevated external CO₂ can take place in a few hours (Royal Society, 2005). Also, increasing CO₂ concentrations can lead to changes in HCO₃⁻ and other ionic levels. Only small changes can be buffered within cells, large concentration variations require the employment of specialised active secretion systems, to carry the excess ions out of the body (Royal Society, 2005). A study on clownfish (*Amphiprion percula*) showed that high CO₂ levels affect neurotransmitter function by changing the direction of the ion current at a GABA-gated ion channel (Nilsson et al., 2012). This affects the olfactory-mediated behaviour

such as loss of avoidance of predator smell (Nilsson et al., 2012; Leduc et al., 2013). Pörtner et al. (2004) highlighted that high levels of CO₂ can have several effects including metabolic changes in animals. A previous study (Pörtner et al., 2000) showed that acid-base regulation is significantly costly. Adjustments of the cellular acid base regulation can be seen as an approach to save energy under metabolic depression caused through environmental stress.

1.3 Pollutants

A variety of different chemicals are considered as pollutants. Pollutants comprise simple inorganic ions as well as complex organic molecules (Walker et al., 2012). The two groups of inorganic ions are metals and anions. Metals are natural substances and their levels determine toxicity (Walker et al., 2012). Many essential processes such as growth and reproduction can be negatively affected by metals (Biesinger and Christensen, 1972; Florea and Büsselberg, 2006). Anions such as nitrates and phosphates are not directly toxic but the excessive use in agriculture as fertilizers can for example lead to an enhanced growths of algae (Nosengo, 2003). Organic pollutants contain carbon and their molecular structure (size, shape and functional groups) is crucial for the toxicity. Examples of organic pollutants are hydrocarbons, polychlorinated biphenyls (PCBs), organochlorine insecticides, phenoxy herbicides, detergents and pharmaceuticals. Furthermore, organometallic compounds, radioactive isotopes, nanoparticles and gases are classified as pollutants (Walker et al., 2012). Focusing on gaseous pollutants the main important and studied are ozone and oxides of carbon, nitrogen and sulphur (Cooley and Manning, 1987; Dockery and Pope, 1994; Wang et al., 2001). CO₂ levels hardly ever reach toxic concentrations. However, the continuously increasing levels of CO₂ in the atmosphere due to combustion of fossil fuels and deforestation and their potential subsequent

environmental effects increasingly raise the interest of scientists (Gattuso and Hansson, 2011; Bopp et al., 2013; IPCC, 2014). Not only in the atmosphere and terrestrial systems CO₂ has an impact, but also it leads to the acidification of world's oceans (IPCC, 2014).

In addition to acidification through CO₂, acid rain and industrial point sources can also lower the pH of seawater. Many coastal waters have naturally low pH, which is enhanced by acid rain and nutrient eutrophication (Doney et al., 2007; Cai et al., 2011). In the New York Bight for example, it is established that chemical waste including sulfuric acid have been discarded into the water since 1948 (Redfield and Walford, 1951).

Acidification events occur not only in marine habitats, but also in lakes and rivers. Since the 1960s air pollution resulted in acid deposition in many lakes in Canada and northern Europe (Day, 2006). Burning fossil fuels leads to so called acid rain which has been an internationally recognized problem for many years (Likens et al., 1979). In the atmosphere sulfur and nitrogen oxides react with water, ozone and other chemicals and form acids. These partials then fall from the clouds as acid rain, which has a pH of about 5, in contrast to normal rain with a pH of approximately 5.5 (Day, 2006). pH is an important factor for the aquatic species composition and pH levels below 6 are potentially harmful (Walker et al., 2012). Loss of planktonic diatoms is a first sign of acidification and pH levels below 5.5 cause a decline in species that occur in circumneutral water (Battarbee et al., 1984). At the same time, low pH levels lead to an increase in acidophilous taxa (Battarbee et al., 1984). A study on lakes in Ontario (Canada) showed that acidification leads to an extinction of fish species (Beamish, 1976). In these acidified lakes fish showed a reduction in growth and females lost their ability to spawn successfully (Beamish, 1976). Also lakes studied in the Czech Republic showed acidification events (Fott et al., 1994). In 1936, the surface pH of the lake Čertovo was 5.7-6.9 and for Černé 6.9-7.0, yet in the 1990s the pH values were only 4.3-4.8 in both

lakes (Fott et al., 1994). The Kyrömjoki River estuary in the Baltic Sea circumvent acidification due to drainage from acidic soil (Urho et al., 1990). This has led to an unsuitable environment in some parts of the estuary for the reproduction of fish (Urho et al., 1990). Periodical input of acidic river waters can also have negative effects on the water chemistry of coastal ecosystems (Salisbury et al., 2008). This may especially impact on shelled pteropods, which are an important food source for commercially important fish, as a result of the acidic river discharges (Salisbury et al., 2008).

The contamination of the marine environment has increased in recent years (Moore, 2008; IPCC, 2014). This is caused by anthropogenic activities and has negative effects on water and sediment quality (Chapman, 1996; Vitousek et al., 1997). Growing concern about water quality has led to the development of methods to identify, estimate, assess and manage such risks (Cajaraville et al., 2000). One of the objectives of environmental monitoring is to measure environmental pollution levels to avoid negative effects on the environment. Furthermore, possible ecosystem changes can be predicted (Mangun and Henning, 1999).

As a sensitive “early warning” tool for biological effect measurement biological markers or ‘biomarkers’ have been suggested (Cajaraville et al., 2000; Van der Oost, 2003). They could be used to assess the environmental quality (Cajaraville et al., 2000). A biomarker describes a biological or cellular alteration that can be measured and is an indicator that an organism has been exposed to a stressor from chemical or anthropogenic origin (Shugart et al., 1992). Biomarkers show changes in a biological response, including molecular, cellular, physiological and behavioural events, which can be caused through exposure to environmental chemicals or their toxic effects (Peakall, 1994). They can be highly specific and or nonspecific. Highly specific biomarkers perceive specific pollutants and their possible effects, whereas nonspecific biomarkers detect general

exposure to a pollutant without identifying it (Walker et al., 2012). Biomarkers can be divided into three different groups: biomarkers of exposure, effect and susceptibility. By a biomarker of exposure a detection of either an exogenous substance, its metabolite or a product of a following interaction is defined. Biomarkers of effect are measurable alterations of biochemical, physiological conditions as well as other changes within the system that have negative effects on the health or can be recognised as a disease. A biomarker of susceptibility is a marker that indicates that the health of a system is particularly responsive to an endogenous component (NRC, 1987).

Due to the similarity of biochemical and cellular structures and function within most organisms biomarkers can be potentially used on a variety of species and different ecosystem types (Shugart et al., 1992). Therefore, biomarkers can be a powerful and informative tool to monitor exposure and effects of environmental contamination (Shugart et al., 1992).

1.4 Ocean acidification

1.4.1 High CO₂ concentration in atmosphere

The reduction of the ocean's pH, mainly by the uptake of CO₂ from the atmosphere over a period of time, is known as ocean acidification (OA) (Gattuso and Hansson, 2011). Because of increasing anthropogenic CO₂ emissions, the absorption of CO₂ by the oceans has dramatically increased the average acidity from pre-industrial levels (IPCC, 2014). Atmospheric CO₂ is a chemically inert gas, but when dissolved in seawater it becomes reactive and takes part in several chemical, physical, biological and geological reactions (Royal Society, 2005) (Fig. 1.2).

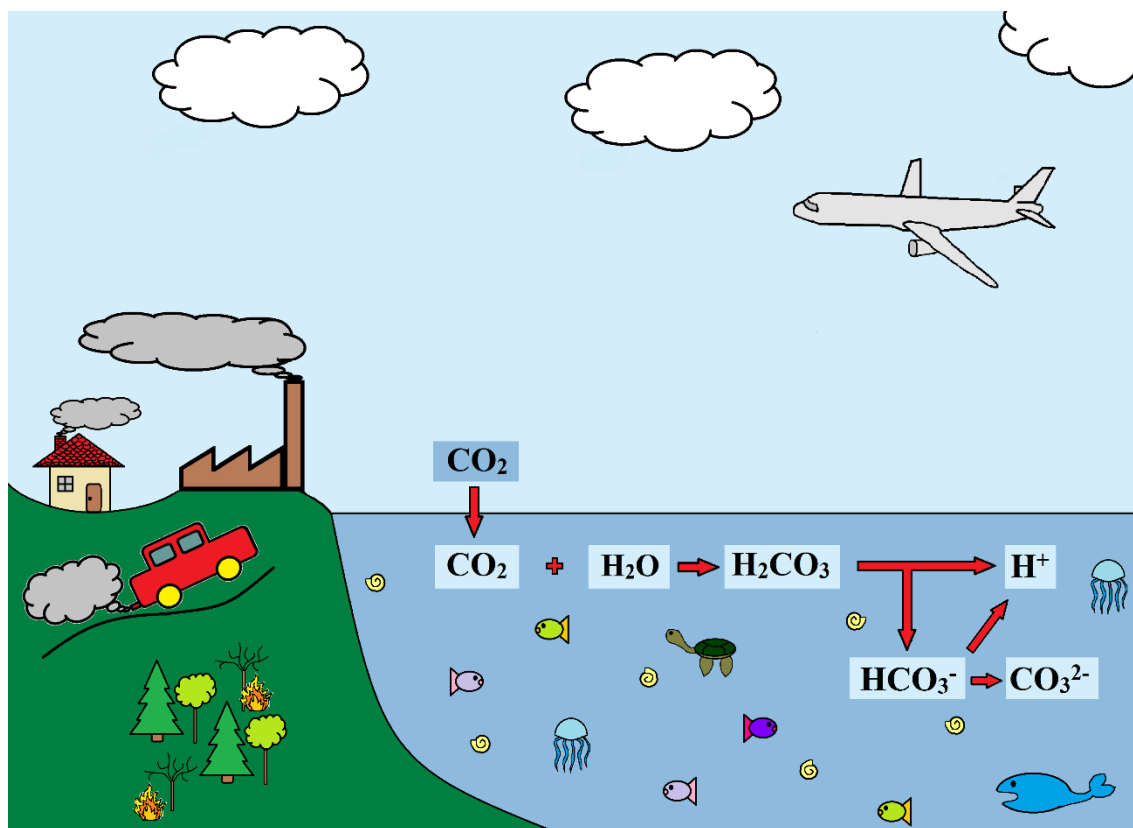


Figure 1.2 Schematic illustration of the carbonate system in the ocean. CO_2 from the atmosphere dissolves in the seawater forming carbonic acid (H_2CO_3). This acid releases H^+ and HCO_3^- , which can then release H^+ again and form CO_3^{2-} .

CO_2 is the fourth most common gas in the earth's atmosphere, after nitrogen, oxygen and argon. Additionally, it has a greenhouse effect comparable to that of water vapour. In comparison to nitrogen and oxygen most CO_2 in the atmosphere - ocean system is dissolved in water (98%). Unlike other gases, CO_2 reacts with seawater to form HCO_3^- and carbonate ions (CO_3^{2-}) (Fig. 1.2). Therefore, CO_2 exists in three different inorganic forms in the ocean: free CO_2 , $\text{CO}_2(\text{aq})$ = aqueous carbon dioxide, HCO_3^- and as CO_3^{2-} (Zeebe and Wolf-Gladrow, 2001).

1.4.2 Effects on ocean chemistry

One important effect of dissolved CO_2 in seawater is the increase of H^+ . This is the outcome of a reaction between water (H_2O) and CO_2 to form carbonic acid (H_2CO_3).

Because H_2CO_3 is a weak acid, it releases H^+ to form the other types of dissolved inorganic carbon.



The acidity of an ocean depends on the concentration of H^+ . Therefore, the more acidic a solution, the more H^+ are present and the lower the pH (Royal Society, 2005). The acidity is expressed in a logarithmic scale of 1 to 14:

$$\text{pH} = -\log_{10} [\text{H}^+] \quad (2)$$

A pH value of 7 is defined as neutral, a value below 7 as acidic and a value above 7 as alkaline (Mortimer and Müller, 2014). The pH of the oceans' surface has decreased by 0.1 pH-units since preindustrial time, which lead to a pH of about 8.1. This is an increase of 26% in acidity (IPCC, 2014). Therefore, the expression "OA" is focusing on the reduction in pH but does not mean that the pH of surface ocean waters will become acidic (below 7.0) in the near future (Gattuso and Lavigne, 2009). An increase in the partial pressure of dissolved CO_2 and a decrease in the oceans pH was observed in different parts of the world's ocean surfaces (Fig. 1.3). The amount of CO_2 dissolved in the seawater is proportional to the CO_2 in the atmosphere, however not the dissolved inorganic carbon (C_T) (Zeebe and Wolf-Gladrow, 2001). The change in C_T (CO_2 , HCO_3^- and CO_3^{2-}) is not proportional due to the buffer capacity of seawater. This is described by the Revelle factor or buffer factor. A doubling of the CO_2 concentration in the atmosphere only leads to an increase in C_T of about 10 % (Zeebe and Wolf-Gladrow, 2001). In seawater, three biogenic carbonate (CaCO_3) minerals are present: aragonite, calcite and magnesian calcite, whereby aragonite is more soluble than calcite. Both the carbonate ions and the CaCO_3 saturation stated are decreasing with increasing OA, which leads to a reduction in calcification rate (Gattuso and Hansson, 2011).

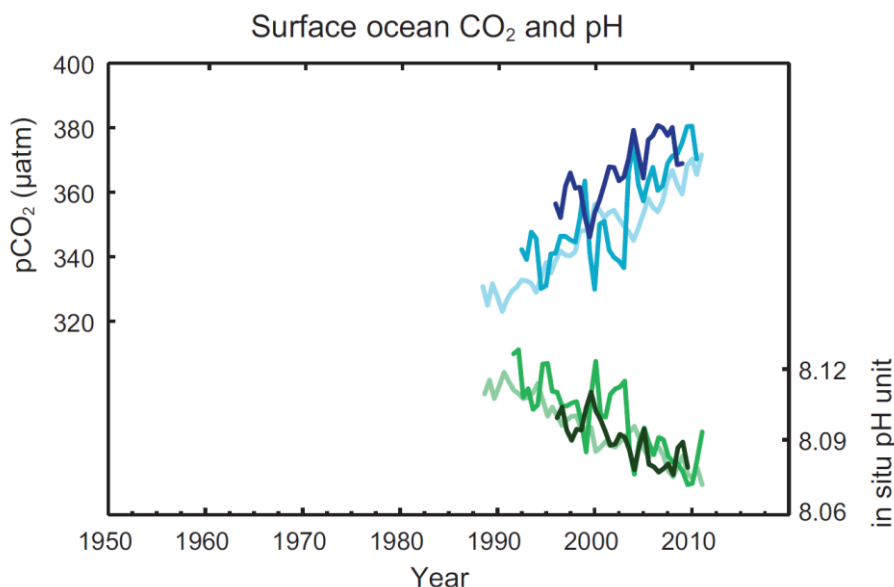


Figure 1.3 Partial pressure of dissolved CO₂ at the ocean surface (blue curves) and in situ pH (green curves) measured at two stations in the Atlantic Ocean (dark blue/dark green and blue/green) as well as at a station in the Pacific Ocean (light blue/light green) (IPCC, 2013).

1.4.3 OA models

It is clear that continuous emissions of greenhouse gases will cause further changes in all components of the climate system. Nevertheless, there are still various opinions to what extent OA will continue (IPCC, 2014). With the use of hierarchy climate models changes are simulated based on a set of scenarios of anthropogenic forcing. The Representative Concentration Pathways (RCPs) are a new set of scenarios used for climate model simulations. Four scenarios were presented including one mitigation scenario (RCP2.6) leading to a CO₂ concentration of 421 ppm, two stabilising scenarios (RCP4.5 and RCP6.0; 538 ppm and 670 ppm) and one scenario with very high greenhouse gas emissions (RCP8.5) reaching a CO₂ concentration of 936 ppm by the year 2100 (IPCC, 2013). Under all RCPs a worldwide increase of OA is predicted (Fig. 1.4). Expected decreases of the global-mean surface pH are 0.06-0.07 (15 to 17 % increase in acidity) for RCP2.6, 0.14-0.15 (38-41 %) for RCP4.5, 0.20-0.21 (58-62 %) for RCP6.0 and 0.30-0.32 (100-109 %) for RCP8.5 (Fig. 1.4, Fig. 1.5) (IPCC, 2014).

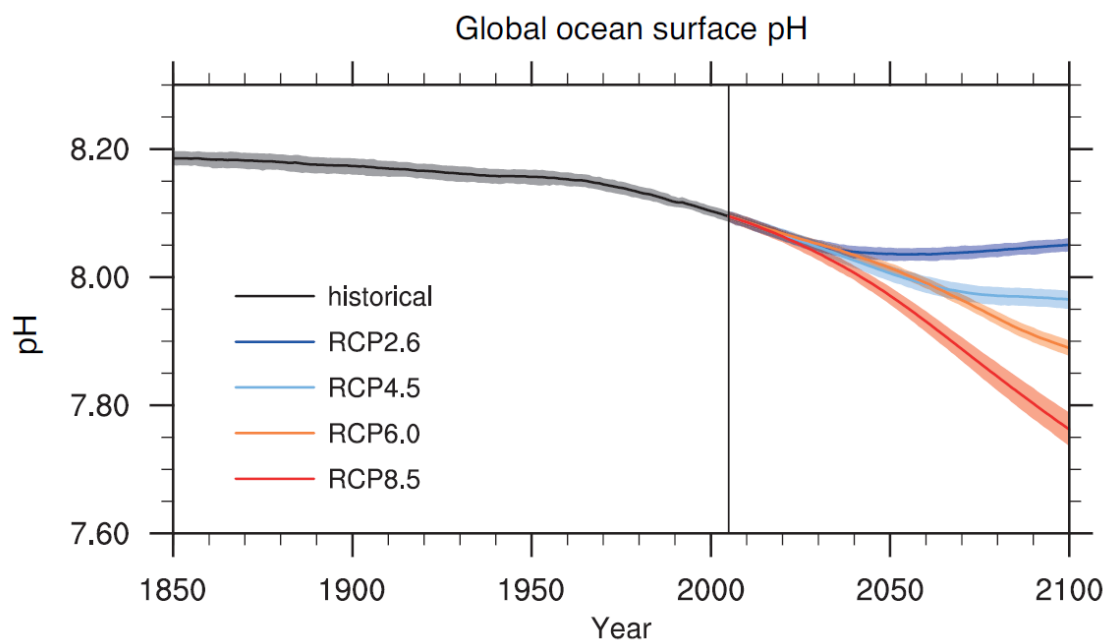


Figure 1.4 Model mean time series of global surface pH change based on the scenarios RCP2.6, RCP4.5, RCP6.0 and RCP8.5 in 1850-2100. Adapted from IPCC (2013).

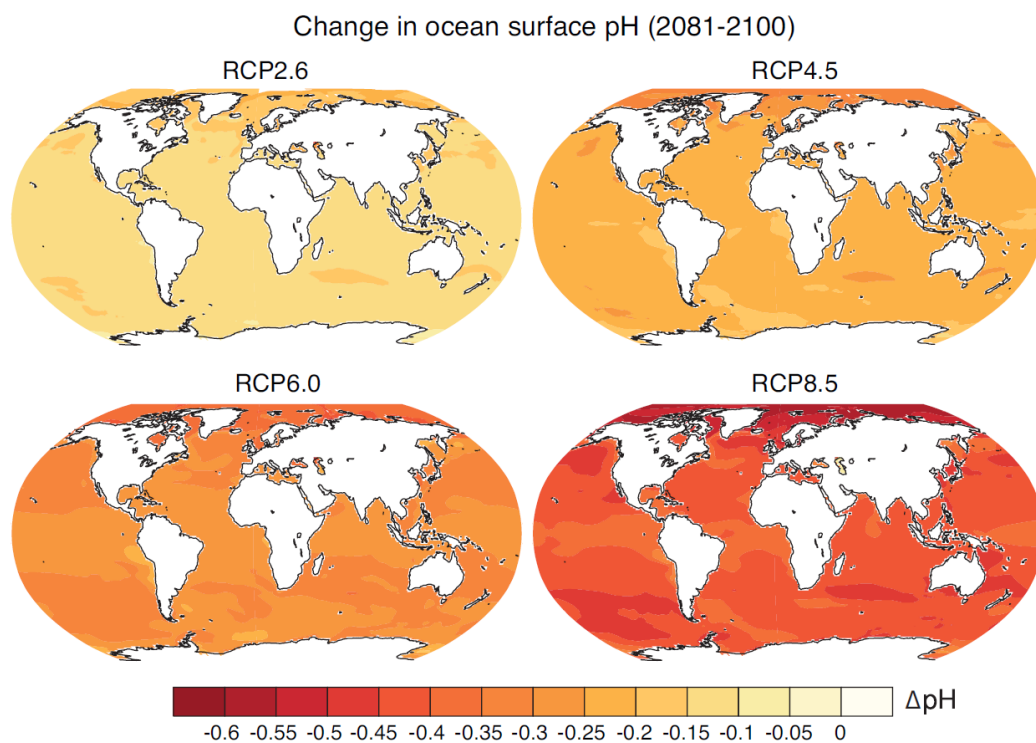


Figure 1.5 Maps of multi-model surface pH for the scenarios RCP2.6, RCP4.5, RCP6.0 and RCP8.5 in 2081-2100 relative to 1986-2005. Adapted from IPCC (2013).

1.4.4 Impact of lower pH on marine organisms

In the past 200 years, the observed increase of CO₂ in the surface water has caused a decrease of water pH by approximately 0.1 pH units (IPCC, 2014). The responses of marine fauna to those changes are expected to be diverse, especially the impacts on marine organisms through elevated partial pressure of CO₂ (*p*CO₂). Effects are expected to be caused by a decrease in CaCO₃ saturation of the seawater, which therefore can affect calcification rates (Gattuso et al., 1998). Furthermore, a disturbance in acid-base (metabolic) physiology can take place (Fabry et al., 2008).

The use of CaCO₃ skeletal structure is common across different animal groups and is forming a protective layer against predators (Knoll, 2003). The calcification rate of corals is suggested to be reduced due to the decrease in CaCO₃ saturation levels caused by increasing CO₂ concentrations in the atmosphere (Gattuso et al., 1998). Not only corals are expected to be affected by the expected seawater changes, planktonic Foraminifera and Mollusca also have shown negative effects on shell mass and calcification rates as well as shell dissolution (De Moel et al., 2009; Comeau et al., 2009; Moy et al., 2009; Gazeau et al., 2010). The shells of planktonic foraminifer *Globigerinoides ruber* in the Arabian Sea showed significantly lighter shells in the upper sediment layer than shells in a lower layer (De Moel et al., 2009). In the Southern Ocean a foraminifer species (*Globigerina bulloides*) showed that today's shells appear lighter in shell weights (30-35 %) in comparison to shells from the Holocene-aged sediments (Moy et al., 2009). Similarly to the Foraminifera, the blue mussel *Mytilus edulis* responded with a reduction in shell size and thickness under decreasing pH conditions (Gazeau et al., 2010). The two phytoplankton species *Emiliana huxleyi* and *Gephyrocapsa oceanica* showed a reduced calcite production under elevated CO₂ levels (Riebesell et al., 2000). Also for the arctic

pelagic mollusc *Limacina helicina* a reduction of 28 % on calcification under high $p\text{CO}_2$ levels was reported (Comeau et al., 2009).

Besides impact on calcification processes a lot of other effects of high $p\text{CO}_2$ are observed in the field or during laboratory studies (Kurihara et al., 2004; Kurihara and Shirayama, 2004; Michaelidis et al., 2005; Shirayama and Thornton, 2005; Watanabe et al., 2006; Attrill et al., 2007; Widdicombe and Needham, 2007; Bibby et al., 2008; Gazeau et al., 2010; Schalkhausser et al., 2013). Data on jellyfish abundance in the North Sea reveal an increase in frequency with decreasing pH (Attrill et al., 2007). This could have negative impacts for the pelagic ecosystem as jellyfish are key predators and are considered themselves as a “trophic dead-end”, because of their low nutritional value (Arai, 2005). The king scallop, *Pecten maximus*, showed a reduced exercise performance with a reduction in clapping force, which could make *P. maximus* more vulnerable for predation (Schalkhausser et al., 2013). Experimental data revealed a decrease of *M. edulis* hatching rates (Gazeau et al., 2010) as well as a decrease in phagocytosis proposing a change in immune response (Bibby et al., 2008). A 6 months experiment using a gastropod (*Strombus luhuanus*) and two sea urchin species (*Hemicentrotus pulcherrimus* and *Echinometra mathaei*), showed an effect on the growth of both groups (Shirayama and Thornton, 2005). Also, the Mediterranean bivalve, *M. galloprovincialis*, was shown to be affected by elevated CO_2 levels in its growth (Michaelidis et al., 2005). Michaelidis et al. (2005) propose that the slowing growth rate is correlated with the reduction in metabolic rate. A study on two planktonic copepods, *Acartia steueri* and *A. erythraea*, demonstrated decreasing egg hatching success as well as an increase in nauplius embryo mortality rate (Kurihara et al., 2004). This agrees with a study on several copepods from the western North Pacific of Watanabe et al. (2006) which found an increasing mortality with increasing CO_2 levels and increasing exposure time. Also, the sea urchins

H. pulcherrimus and *E. mathaei* were negatively impacted in terms of fertilization rate, cleavage rate developmental speed and the size of pluteus larval (Kurihara and Shirayama, 2004). The “bioturbator” polychaete *Nereis virens* also showed high tolerance towards changing seawater pH, however more studies are needed, as other ecosystem engineers could be negatively impacted and therefore affecting the nutrient cycle (Widdicombe and Needham, 2007).

Not only invertebrates are affected by high CO₂ exposure, vertebrates can also be affected. Several studies on fish such as: the starspotted dogfish *Mustelus manazo* (Hayashi et al., 2004), Japanese whiting *Sillago japonica* (Kikkawa et al., 2006), Japanese flounder *Paralichthys olivaceus* (Hayashi et al., 2004), Eastern little tuna *Euthynnus affinis* (Kikkawa et al., 2003) and red sea bream *Pagrus major* (Kikkawa et al., 2004) showed mortality after exposure to elevated CO₂ levels.

Recently there are more studies focusing on OA combined with other stressors such environmental pollutants. The study of Lewis et al. (2013) on the polychaete *Pomatoceros lamarckii* examined the combined effect of OA and copper. The survival of larvae was found to be sensitive to high CO₂ and a significant link to copper was reported. Another study on *Arenicola marina* discovered an increase of copper toxicity on sperm DNA damage and larval survival together with OA conditions (Campbell et al., 2014). Also responses of OA with elevated temperatures were conducted. The net calcification of the crustose coralline alga *Lithophyllum cabiochae* was negatively impacted by high pCO₂ and temperature, but not changed by higher temperature or higher pCO₂ alone (Martin and Gattuso, 2009). Also a study on the Sydney rock oyster, *Saccostrea glomerata* showed that temperature and high pCO₂ together effect fertilization and development differently (Parker et al., 2009). In the previous years, experimental studies also focused on gene and protein expression changes. Experiments investigated

mainly calcifying species such as barnacles, corals, sea urchins and oysters. The Table 1.1 presents a summary of the current literature published for gene expression studies on marine fauna under OA conditions.

Table 1.1 Summary of the available literature published on gene expression responses of marine fauna in response to low pH conditions induced by CO₂. The table shows different species ordered in their phyla, the CO₂ system parameters used in the experiment as well as a short description of the main gene expression differences and the corresponding reference.

Species	Common name	CO ₂ system parameters	Expression change summary	Reference
Arthropoda				
<i>Balanus amphitrite</i>	Barnacle	<u>Control:</u> pH 8.1 <u>Treatment:</u> pH 7.6 <u>Exposure:</u> 4 d	•Up- and down-regulation of proteins involve in energy-metabolism, respiration and molecular chaperons	Wong et al., 2011
Cnidaria				
<i>Pocillopora damicornis</i>	Coral	<u>Control:</u> pH 8.1 <u>Treatment:</u> pH 7.8 pH 7.4 pH 7.2 <u>Exposure:</u> 3 w	•Up-regulation in genes coding for calcium and carbonate transport, conversion of CO ₂ into HCO ₃ ⁻ and organic matrix •Down-regulation of genes involved in signal transduction	Vidal-Dupiol et al., 2013
<i>Acropora millepora</i>	Coral	<u>Control:</u> CO ₂ 380 ppm <u>Treatment:</u> CO ₂ 750 ppm CO ₂ 1000 ppm <u>Exposure:</u> 3 d	•Down-regulation of 37 metabolic genes (most of them only at high pCO ₂) •Down-regulation of membrane-associated or secreted carbonic anhydrases	Moya et al., 2012
<i>A. millepora</i>	Coral	<u>Control:</u> pH 8.0-8.2 <u>Treatment:</u> pH 7.8-7.9 pH 7.6-7.7 <u>Exposure:</u> 1 d, 28 d	•Metabolic suppression •Increase in oxidative stress, apoptosis and symbiont loss	Kaniewska et al., 2012
Echinodermata				
<i>Lytechinus pictus</i>	Sea urchin	<u>Control:</u> CO ₂ ~380 ppm <u>Treatment:</u> CO ₂ ~970 ppm <u>Exposure:</u> 48 hpf	•Genes central to energy metabolism and biomineralisation down regulated •Genes involved in ion regulation and acid-base balance up-regulated	O'Donnell et al., 2010
<i>Strongylocentrotus purpuratus</i>	Sea urchin	<u>Control:</u> CO ₂ ~400 µatm <u>Treatment:</u> CO ₂ ~900 µatm <u>Exposure:</u> 50 d, sampled every other day	•Allelic changes in 40 functional classes of proteins including genes for biomineralisation, lipid metabolism and ion homeostasis	Pespeni et al., 2013
		<u>Control:</u> pH 8.1 <u>Treatment:</u> pH 7.7 <u>Exposure:</u> 2, 4, 7 dpf	•Down regulation calcification related genes •Up regulation of metabolic genes	Stumpp et al., 2011

		<u>Control:</u> ~pH 8.01 <u>Treatment:</u> ~pH 7.96 ~pH 7.88 <u>Exposure:</u> ~29, ~40, ~70 hpf	<ul style="list-style-type: none"> •Decrease in gene expression in biomineralisation, cellular stress response, metabolism and apoptosis 	Todgham and Hofmann, 2009
<i>Paracentrotus lividus</i>	Sea urchin	<u>Control:</u> pH 8.1 <u>Treatment:</u> pH 7.9, 7.7, 7.5, 7.25, 7.0 <u>Exposure:</u> 22, 46, 52, 69 h post fertilization	<ul style="list-style-type: none"> •Up regulation of candidate genes involved in development and biomineralisation 	Martin et al., 2011
Mollusca				
<i>Crassostrea hongkongensis</i>	Oyster	<u>Control:</u> pH 8.2 <u>Treatment:</u> pH 7.9 pH 7.6 <u>Exposure:</u> 29 d post fertilization	<ul style="list-style-type: none"> •Number of expressed proteins and their phosphorylation level decreased •Down-regulation in larval energy metabolism and calcification •Up-regulation in cell motility and production of cytoskeletal proteins 	Dineshram et al., 2013
<i>C. gigas</i>	Oyster	<u>Control:</u> ~pH 8.0 <u>Treatment:</u> ~pH 7.5 <u>Exposure:</u> 6 d	<ul style="list-style-type: none"> •Reduction of global protein expression with decrease or loss of 71 proteins (depression of metabolic gene expression) •Calcium metabolism genes and cytoskeleton down-regulated •Energy related proteins down-regulated •Cellular proton transportation up-regulated 	Dineshram et al., 2012
<i>S. glomerata</i>	Oyster	<u>Control:</u> CO ₂ 375 ppm <u>Treatment:</u> CO ₂ 1000 ppm <u>Exposure:</u> 4 d	<ul style="list-style-type: none"> •No significant difference of larval proteins between elevated and ambient pCO₂, but between oyster lines (wild line, 6th generation selectively bred) 	Parker et al., 2011
<i>C. virginica</i>	Oyster	<u>Control:</u> ~39 Pa P _{CO2} <u>Treatment:</u> ~357 Pa P _{CO2} <u>Exposure:</u> 2 w	<ul style="list-style-type: none"> •Up-regulation of proteins involved in cytoskeleton and oxidative stress •Collagen expression decreased (cytoskeleton-related protein) •Down-regulation of Rap 1b (signalling protein) 	Tomanek et al., 2011
Chordata				
<i>Oryzias latipes</i>	Japanese rice fish	<u>Control:</u> 0.04 kPa P _{CO2} <u>Treatment:</u> 0.12 kPa P _{CO2} 0.42 kPa P _{CO2} 0.7 kPa P _{CO2} <u>Exposure:</u> 48 h (adult fish) Stage 32-33 (dev. fish)	<ul style="list-style-type: none"> •Down-regulation of genes involved in metabolism pathways in developing fish •Up-regulation of acid-base relevant genes and amino acid metabolism in developing fish •Up-regulation of acid-base relevant genes in adult fish 	Tseng et al., 2013

1.4.5 Ability for genetic adaptation to OA

Over the future centuries, the absorption of anthropogenic CO₂ from fossil fuels by oceans will possibly result in larger pH changes than those recorded from geological samples from the past 300 million years (Caldeira and Wickett, 2003). Therefore, organisms will be exposed to faster changes than they have ever experienced before. Environmental changes induce selection pressure on traits that are important for fitness. According to Gienapp et al. (2008), populations have three possible ways of responding to these changes: 1) Populations can move to a different habitat with better conditions. 2) Populations can stay in their original habitat and adjust to the changes by phenotypic plasticity. 3) Populations can adapt to the changes at the genetic level through evolution. Barry et al. (2011) additionally describe the event of extinction. As OA is a global change, and different habitats have other environmental conditions, the option of moving to a different territory seems limited for populations (Barry et al., 2011). The base of adaptation is a phenotypic plasticity in a population which provides a genetically based variation (DeWitt and Schneider, 2004). Nevertheless, there are also costs and limits to phenotypic plasticity (DeWitt et al., 1998). For the adaptation process populations have to shift their distribution of phenotypes so that the fitness of the shifted phenotype is higher than that of the original distribution (Visser, 2008). There are two different ways of adapting to novel environments: using an already existing genetic variation or a new mutation. Usually a standing variation is faster than a new mutation, because the alleles are already available and start at a higher frequency (Barrett and Schuler, 2008). Up to date, only a few experiments have been carried out for a sufficient period of time to make assumptions about organisms' abilities to genetically adapt to OA changes (Royal Society, 2005). Genetic adaptation involves a structural or functional change inserted into the molecular genetic code, which is responsible for supported survival in a certain

environment. The process that generates these changes and produces new alleles is called mutation. A mutation is a single change that is found in a single cell and they are responsible for changes in allele frequencies. For evolutionary processes only changes in the germ cell line have consequences, as somatic mutations cannot be inherited (Jobling et al., 2014). Meiotic recombination can combine advantageous alleles at different loci and can therefore help to adapt to the environment (Jobling et al., 2014). Therefore, adaptation is a long process and needs several generations to distribute through a population (Piantadosi, 2003).

One of the main questions is whether species are able to adapt fast enough with the changing environment surrounding them (Visser, 2008). The fresh water green alga *Clamydomonas* is a suitable model organism for many generation experiments due to its rapid growth (doubling time, 6-8 hr) (Shimogawara et al., 1998). One study, conducted on *Clamydomonas*, showed that no adaptation took place, even after the organisms were exposed to high CO₂ concentrations for 1,000 generations (Collins and Bell, 2004). In contrast a study on the adaptive evolution of the phytoplankton *E. huxleyi* discovered a higher growth rate in individuals kept at elevated CO₂ levels for 500 generations compared to phytoplankton kept at ambient CO₂ conditions (Lohbeck et al., 2012). Form and Riebesell (2012) reported the first evidence that the cold-water coral *Lophelia pertusa* can acclimate to OA and is able to enhance its calcification rate. Of particular interest for the present thesis is the study of Calosi et al. (2013). Using *in situ* transplant experiments they investigated tolerant and sensitive polychaete species in natural CO₂ vent systems according to their ability to acclimate or genetically adapt to high CO₂ conditions. Results showed that *Platynereis dumerilii* was able to adapt both genetically and physiologically to chronic and elevated pCO₂ levels. On the other hand, *Amphiglena mediterranea* showed an acclimation response only (Calosi et al., 2013).

Overall, it is expected that some species will turn out as “winners” and others as “losers” under the expected ocean changes. In particular, the reef builders are especially supposed to be vulnerable and therefore possible “losers” (Kleypas and Yates, 2009). Species with short generation times and big population sizes such as phytoplankton and microbes are predicted to have more potential to adapt (Barry et al., 2011).

1.5 Naturally venting sites as models

To date, our knowledge of how marine organisms respond to OA are mainly based on short term experiments. Usually aquaria or mesocosm experiments are employed (Benton et al., 2007; Rodolfo-Metalpa et al., 2011). These experiments give insights into the phenotypic plasticity of the test organisms to OA conditions. Though, lasting only a few hours or a maximum of a few weeks, these studies are too short to show any evolutionary adaptation abilities. Only species with short generation times will be able to go through many generations during a short period of time to provide potential information on adaptation processes (Lohbeck et al., 2012). For the study of *in situ* long term exposure to elevated $p\text{CO}_2$ levels naturally CO_2 enriched sites are often applied. These comprise cold water CO_2 vents (Hall-Spencer et al., 2008; Dias et al., 2010), hydrothermal vents (Tunnicliffe et al., 2009; Vizzini et al., 2010), low pH coastal springs (Crook et al., 2012) and CO_2 upwelling areas (Thomsen et al., 2010). The application of such systems can provide important information of organisms’ abilities to adapt to extreme environments (Calosi et al., 2013).

In addition to studying the response to OA at the species level of biological organisation, it is also possible to observe community and ecosystem levels too (Kroeker et al., 2011). Marine CO_2 vents can be found in the Mediterranean, especially in Italy and Greece (Dando et al., 1999). The released volcanic gases often contain a small percentage

of hydrogen sulphide (Dando et al., 1999). The CO₂ gradient along the volcanic island of Vulcano (NE Sicily) is a good example for such an area (Boatta et al., 2013; Johnson et al., 2013). The rocky coast is acidified through volcanic CO₂ vent activity, producing areas with ambient CO₂ levels up to extreme levels beyond the levels expected due to OA (Boatta et al., 2013; Johnson et al., 2013). In the south bay of the CO₂ vent, sulphur has also been detected, though not in the sampling sites usually used in scientific experiments (Boatta et al., 2013; Johnson et al., 2013). However, there are also some CO₂ vents where the gases comprises no toxic sulphur compounds and therefore makes them ideal to study OA (Hall-Spencer et al., 2008). One of these CO₂ vent areas is the cold vent areas off Ischia in Italy (Tyrrhenian Sea) (Hall-Spencer et al., 2008) (Fig. 1.6).



Figure 1.6 Diverse ocean life near the island of Ischia in Italy (left picture). The CO₂ vent, which is only a few hundreds of meters away shows a decreased diversity of species (right picture). Image credit: David Liittschwager, National Geographic.

Several different low pH studies have been conducted at the Ischia vents (Cigliano et al., 2010; Dias et al., 2010; Kroeker et al., 2011; Lombardi et al., 2011a; Lombardi et al., 2011b; Lombardi et al., 2011c; Porzio et al., 2011; Rodolfo-Metalpa et al., 2011; Hahn et al., 2012; Meron et al., 2012; Ricevuto et al., 2012; Calosi et al., 2013; Porzio et al., 2013; Donnarumma et al., 2014; Garrard et al., 2014; Goodwin et al., 2014; Langer et al., 2014; Ricevuto et al., 2014). Research has focused on the settlement of benthic invertebrates,

microfauna and epibiont communities (Cigliano et al., 2010; Ricevuto et al., 2012; Porzio et al., 2013; Garrard et al., 2014; Donnarumma et al., 2014), ecosystem responses along the pH gradient (Kroeker et al., 2011), colonization of selected polychaete species (Ricevuto et al., 2014), sponge species composition and cover (Goodwin et al., 2014), coral microbial communities (Meron et al., 2012) adaptation and acclimation in marine ectotherms (Calosi et al., 2013), coral and mollusc resistance to high $p\text{CO}_2$ levels (Rodolfo-Metalpa et al., 2011), changes in foraminiferal assemblages (Dias et al., 2010), macroalgal communities (Porzio et al., 2011) marine bivalve shell geochemistry and ultrastructure (Hahn et al., 2012), shell alteration of limpets (Langer et al., 2014) and skeletal changes and polymorphism in bryozoans (Lombardi et al., 2011a; Lombardi et al., 2011b; Lombardi et al., 2011c).

However, the direct comparison to OA is limited for several reasons. The pH/ $p\text{CO}_2$ is not stable, as variations occur due to time and space (wind, currents etc.) (Kroeker et al., 2011; Ricevuto et al., 2014). Furthermore, the $p\text{CO}_2$ values are often much higher than those expected for the next century (Ricevuto et al., 2014; supplementary material), which makes a direct comparison not suitable. Many organisms are mobile or have pelagic live stages, which means that they can move between the vent and non-vent areas. It is therefore uncertain if these animals have been in the low pH zones for many generations or just migrated into the venting area.

1.6 A model organism

With the help of ‘model’ organisms investigations such as how life develops, exists and reproduces can be explored. The advantage of model organisms is that they can be grown easily, they reproduce fast, their genomes are completely sequenced and each stage of their development can be studied. Well established model organisms include

Caenorhabditis elegans, *Drosophila melanogaster*, *Danio rerio*, *Aplysia californica*, *Fugu rubripes* and *Arbacia punctulata* (Clark and Pazdernik, 2012; Knudsen et al., 2006; Aparicio et al., 2002; Dupont et al., 2010).

1.6.1 Polychaeta

The phylum annelida is usually subdivided into the two groups Polychaeta and Clitellata. Polychaetes are an important part of the diversity of marine animals. Linnaeus (1758) was the first who named them formally. There are still many unknown polychaetes that need to be documented and formally described (Rouse and Pleijel, 2001).

The most common polychaetes, often known as ragworms, are the Nereididae (Nereididae Johnston, 1865). There are about 500 nominal species. According to fossil discoveries, Nereididae could be 350 million years old. Most Nereididae live in shallow water and can be found in all kinds of substrate in the oceans. Moreover some occur in brackish water such as the genus *Hediste*. There is a variation in size from only a few centimetres (*Micronereis*) up to over a meter (*N. virens*). As well as the size, colours can be different. There are Nereididae with transparent to red-brown colour, but also other colours and pigmentation patterns exist (Rouse and Pleijel, 2001). Polychaetes are considered as an ecologically important group and several species have been used for monitoring of ecotoxicological effects of marine contaminants (Pocklington and Wells, 1992). Besides experimental studies, there are polychaete groups with economical importance. Some are used for bait as fish and some as a delicacy in south-eastern Asia (Rouse and Pleijel, 2001).

1.6.2 *Platynereis dumerilii* (Audouin & Milne-Edwards, 1933)

As a model organism for this study, a model system is needed that is easy to maintain in culture and ideally the genome is available. The polychaete, *P. dumerilii*, is a marine

model that presents both, simple establishment in lab culture and availability of the genome (PLATYpopsys, transcriptomic and genomic data base: <http://hydra.cos.uni-heidelberg.de/pps/styled-2/>) (Fig. 1.7). Gene expression studies focusing on the mRNA expression under low pH conditions are not yet studied in this species. Therefore this study can give an interesting insight into mechanistic aetiology of such biological impacts at the molecular level.



Figure 1.7 Close-up picture of *P. dumerilii* head
(source: <http://bit.ly/1ahJJsl>; accessed on 17.07.2015).

In the last couple of years, the annelid *P. dumerilli* has become increasingly popular as a marine model in several areas. It is used in research on developmental (Dorresteijn, 1990; Fischer and Dorresteijn, 2004), evolutionary (Tessmar-Raible and Arendt, 2003), neurobiological (Jékely et al., 2008), ecological and toxicological questions (Hutchinson et al., 1995; Jha et al., 1996; Hardege, 1999). In 1995a Jha et al. described the chromosomes ($2n=28$) of *P. dumerilii* for the first time. Further studies showed that the karyotype and chromosome morphology of *P. dumerilii* is appropriate for cytogenetic analysis and indicated its suitability as an ecotoxicity test species (Jha et al., 1996; Jha et al., 1997; Hutchinson et al., 1998; Hagger et al., 2002). Furthermore, a vertebrate telomeric sequence was discovered in the *P. dumerilii* chromosome by fluorescence in situ hybridization (Jha et al., 1995b). The small size and fast development of this tube

dwelling polychaete makes it ideal for laboratory cultures and allows to study the various developmental stages (Hauenschild and Fischer, 1969) (Fig. 1.8). The development of *P. dumerilii* is divided into 16 stages. It starts with a zygote and ends with the death of the mature worms after reproduction. The cleavage of the eggs follows a spiral cleavage pattern and the planktonic larvae continues growing. *P. dumerilii* has a biphasic life cycle, composed of a benthic and planctonic part. Between 5 and 7 days post fertilization the larvae changes its lifestyle from pelagic-benthic to fully benthic (Fischer et al., 2010). The three-segmented worms form spinning glands in their parapodia and generates the first mucus. They still don't form complete tubes (Fischer, 1985). Once settled, the young worms start to build their characteristic living tubes (Daly, 1973).

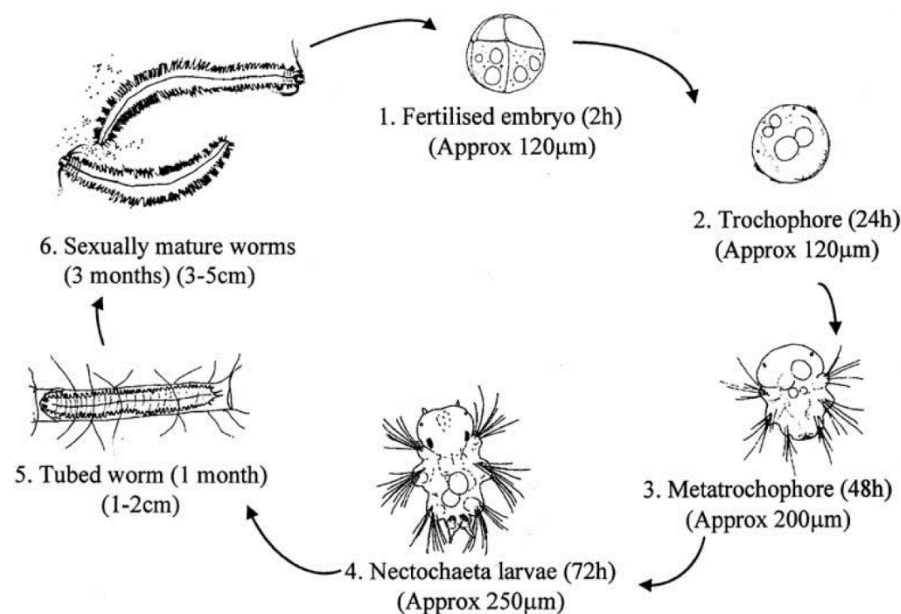


Figure 1.8 Life cycle of *P. dumerilii* (Hagger et al., 2002)

The tubes are usually built on algal substrate, which is both food and living site for the mesograzer (Hay et al., 1988). Besides feeding on algae, *P. dumerilii* is also known as a coprophagia and cannibal, consuming their own faecal and smaller fellow species (Hauenschild and Fischer, 1969). Pettibone (1963) described *P. dumerilii* as “a

cosmopolitan form with wide geographic distribution in warm seas". They can be found in "Massachusetts (Cape Cod), south of Newfoundland (surface) to Florida, Gulf of Mexico, West Indies, Brazil, Iceland, Faroes, Scandinavia to Yance, Mediterranean, Iranian Gulf, Red Sea, Indian Ocean, central Pacific (Bikini), West and South Africa"(Pettibone, 1963).

The reproductive behaviour of *P. dumerilii* is well studied. Atokous worms undergo a metamorphosis into an epitokous (Heteronereis) worm, which is controlled by the decrease of a hormone produced in the brain (Hauenschild and Fischer, 1969). Preferentially, during nightfall and midnight the specimens leave their mucous/living tubes and swim up to the water surface. At the water surface both males and females release their gametes (Hauenschild and Fischer, 1969). This manner of assembling at the water surface to reproduce takes place during the first week after new moon and is therefore suggested to be a photoperiodical effect (Hauenschild, 1956). The characteristic reproductive behaviour, known as nuptial dance, is caused by chemical stimulating releases from the partner of the opposite sex (Boilly-Marer, 1974). These chemical stimulating substances were identified as the egg release pheromone L-Ovothiol A and the sperm-release pheromone uric acid (Zeeck et al., 1998; Röhl et al., 1999).

Atokous *P. dumerilii* have a heterogeneous cephalon and a homogeneous segmented trunk. The head is composed of a prostomium and a peristomium (Fig. 1.9). The prostomium contains the supraesophageal ganglion, two paired grope-appendices (thin antennae and thick, shorter palpi) and three paired sense organs (two pairs of eyes and a nuchal organ). The peristomium has no parapodia but two pairs of moveable sensor-cirri. Parapodia are movable, paired lateral appendages extending from the body segments. The main function of the parapodia is locomotion, but their glands also play an important role in tube construction (Hauenschild and Fischer, 1969).

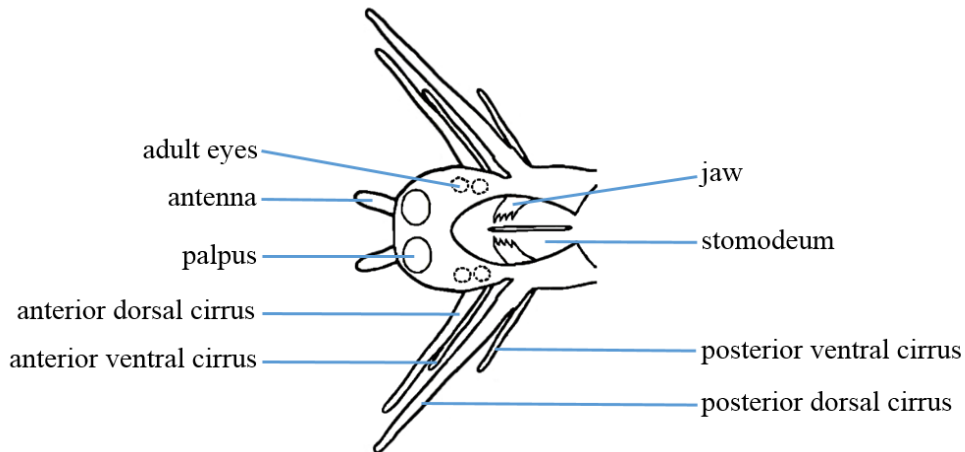


Figure 1.9 Prostomium and peristomium of small atokous *P. dumerilii*. Adapted from Fischer et al. (2010).

The trunk starts with the first segment carrying parapodia and consists of maximal 75 segments. Each segment has one pair of parapodia. The end of the trunk is formed by the pygidium including the anus (Fig. 1.10).

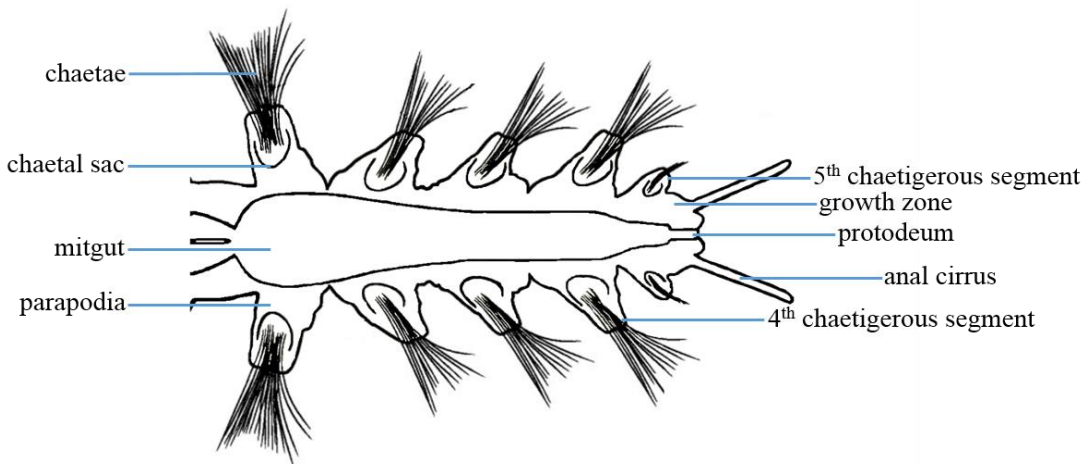


Figure 1.10 Trunk of small atokous *P. dumerilii*. Further segments are budding off from the posterior growth zone. The worm increases in diameter. The size of the anterior segments is still growing in size. Adapted from Fischer et al. (2010).

The trunk can be separated in two parts. The anterior part, comprises the first eight segments carrying the parapodia, and includes the pharynx and oesophagus, whilst in rest position, and the posterior part, which is evenly streaked by the midgut. *P. dumerilii* has a closed vascular system and due to haemoglobin the blood has a red colour (Hauenschild and Fischer, 1969).

1.7 Objectives of this thesis

The aim of this PhD project is to study the biological effects of low pH on the marine polychaete *P. dumerilii*, and, in particular, the molecular events caused by chemical changes in the seawater that could be involved in the physiological responses. The earliest signals of responses to pollutant stress within a biological system are represented by molecular level changes (Van der Oost et al., 2003). This dissertation investigates molecular responses of exposure to low pH adjusted by the mineral acid hydrochloric acid (HCl) as well as CO₂. HCl has the advantage that the pH stays relatively constant after pH adjustment. In contrast, seawater adjustments with CO₂ are less stable due to the volatile characteristic of CO₂ gas. Many OA studies address the effects as an event induced by acidification, though by only looking at CO₂ it is not clear whether the effect is caused by pH or maybe changes at the carbonate level. Therefore, the present thesis looked at both HCl and CO₂ to investigate this question.

Using a targeted approach the genes, *sodium-hydrogen antiporter* and *carbonic anhydrase*, are selected, since both are involved in pH regulation mechanisms. The third gene examined is the Ca²⁺ binding protein *calmodulin*, which is involved in the activation of several enzymes and could therefore be a likely candidate as a general marker for stress. In addition, a non-targeted approach has been used to identify other potential genes and processes involved in acid-base balance. Furthermore, a spatial gene expression experiment was conducted with larvae, one of the most vulnerable life stages. Genes involved in acid base regulation, such as *sodium-hydrogen antiporter* and *carbonic anhydrase*, are expected to be up-regulated under low pH conditions. However, potential down-regulation as an initial shock- and therefore protection response is expected. Furthermore, genes involved in general metabolism (*calmodulin*) are expected to be

down-regulated. Besides these two categories, other gene groups are assumed to be affected by the low pH exposure.

In terms of methods and samples used in this work, all laboratory and field experiments were conducted with atokous worms, a sexually immature stage of the worm, to exclude metabolic processes linked to maturation (metamorphosis) and reproduction from the metabolic processes of interest. During the metamorphosis *P. dumerilii* goes through major rearrangements of the body with substantial biochemical, morphological and physiological changes (Hauenschild and Fischer, 1969). The worms stop feeding, the gut slowly disappears, the eyes enlarge, the shape of the parapodia changes, and the body colour becomes transparent (Hauenschild and Fischer, 1969). All these changes are strongly connected to the gene expression and therefore had to be avoided.

Studies involved both laboratory cultures (EMBL, Heidelberg) and populations of *P. dumerilii* found in the Tyrrhenian Sea (Ischia, Italy). This includes populations residing in natural CO₂ vents in comparison to populations outside the vents in Italy. Both laboratory and field experiments were used to investigate potential differences in their tolerance towards pH changes.

Additionally, a phylogenetic analysis of different Mediterranean populations from Italy, France and Spain, as well as populations from Bristol Channel (England) and Arcachon (Atlantic coast, France) was conducted, in order to investigate the relatedness of different populations as well as to examine the potential adaptation to low pH of worms from CO₂ vents. When comparing vent populations with control populations different gene expression profiles are expected, due to the acclimation or potentially adaptation of worms to the low pH areas. Moreover, *P. dumerilii* from the CO₂ vents in Ischia and Vulcano are expected to be genetically different to non-vent populations.

To achieve the proposed objectives, the following aspects have been investigated:

Study of the short term effect of low pH on gene expression and expression patterns on laboratory cultured worms (Chapter 2, 3, 4, 5)

- Isolation and characterisation of the three *target* genes: *sodium-hydrogen antiporter*, *carbonic anhydrase* and *calmodulin*
- Analysis of *sodium-hydrogen antiporter*, *carbonic anhydrase* and *calmodulin* gene expression levels under low pH conditions induced by HCl
- Analysis of *sodium-hydrogen antiporter* expression location in *P. dumerilii* larvae under low pH induced by HCl (*in situ* hybridisation)
- Identification of potential genes involved in acid-base balance by suppression subtractive hybridisation (SSH)
- Analysis of *sodium-hydrogen antiporter*, *carbonic anhydrase* and *calmodulin* gene expression levels under low pH conditions induced by CO₂

Study of pH effects on the gene expression of field populations (Chapter 6)

- Analysis of the relative gene expression of different field populations (vent/ non-vent) of *P. dumerilii*
- Analysis of relative gene expression of different field populations (vent/ non-vent) after a 7 day transfer experiment in the laboratory

Phylogenetic study of different *P. dumerilii* populations including vent population (Chapter 6)

- Analysis of phylogenetic relatedness of different *P. dumerilii* populations including heteronereis based on cytochrome *c* oxidase I (COI)

Combining all results and their interpretations to form a comprehensive conclusion (Chapter 7)

2.1 Introduction

The first part of this chapter presents the isolation and characterisation of the three *target* genes *sodium hydrogen antiporter (NHE)*, *carbonic anhydrase (CA)*, and *calmodulin (CaM)*. The three *target* genes were selected based on their function and potential relevance to low pH exposure as indicated by recent transcriptomic and proteomic studies on marine organisms (Todgham et al., 2009; O'Donnell et al., 2010; Martin et al., 2011; Parker et al., 2011; Stumpp et al., 2011; Tomanek et al., 2011; Wong et al., 2011; Dineshram et al., 2012; Moya et al., 2012; Dineshram et al., 2013; Jones et al., 2013; Pespeni et al., 2013; Tseng et al., 2013; Vidal-Dupiol et al., 2013) (Fig. 2.1).

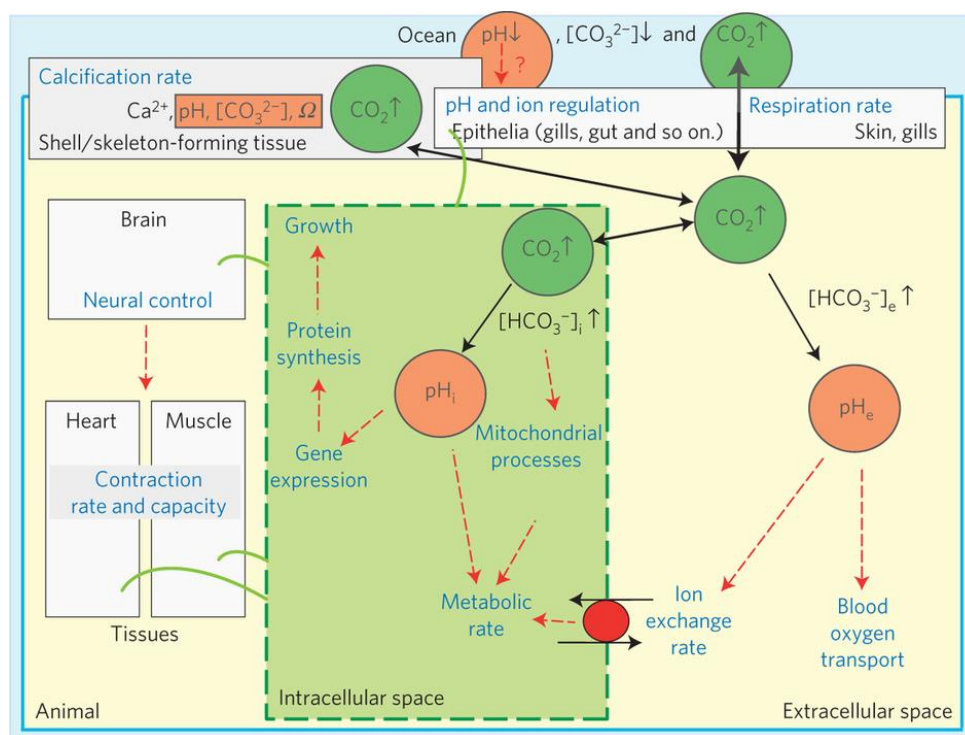


Figure 2.1 Schematic overview of effects of low pH on animal's body. Ocean pCO_2 is increasing (dark green) and decreases water pH (red). CO₂ distributes by diffusion (black arrows), causing pH disturbance in extra and intracellular compartments and influences directly or indirectly (red broken arrows) tissues, cells and their inherent processes and functions (blue) (Wittmann and Pörtner, 2013).

The altered gene and protein expression profiles collectively reveal a few common biological impacts across different marine species, including genes or proteins involved in biomineralization (O'Donnell et al., 2010; Dineshram et al., 2012; Moya et al., 2012; Pespeni et al., 2013), lipid/energy metabolism (O'Donnell et al., 2010; Wong et al., 2011; Pespeni et al., 2013; Vidal-Dupiol et al., 2013), acid-base regulation (O'Donnell et al., 2010; Moya et al., 2012) and ion transport processes (O'Donnell et al., 2010; Pespeni et al., 2013; Vidal-Dupiol et al., 2013) (Fig. 2.1). Having identified some major processes impacted, the following section gives a short introduction of the key features of the three selected *target* genes.

Sodium hydrogen antiporter

Several studies have highlighted the alteration of genes taking part in ion regulation processes under low pH exposure (O'Donnell et al., 2010; Pespeni et al., 2013; Vidal-Dupiol et al., 2013). One transporter family involved in the maintenance of intracellular pH are the NHEs. Na^+ and H^+ are important ions in cell physiological processes such as bioenergetics (Padan and Schuldiner, 1993). The transmembrane Na^+ gradient is used by many transporters to move other ions across the plasma membrane. Furthermore, the concentration of H^+ is crucial for protein functions, as many of them are pH-sensitive (Lewin et al., 2007). Therefore, the amount of ions needs to be regulated. Amongst other transporters, such as $\text{Na}^+/\text{HCO}_3^-$ -cotransporters, NHEs are fundamental in maintaining intracellular and extracellular acid-base balance (Lewin et al., 2007).

NHEs are widely used membrane proteins that exchange Na^+ for H^+ (Fig. 2.2 A). Their amino acid length varies between species as well as isoforms (Cox et al., 1997; Xu et al., 2005; Slepko et al., 2007). NHEs are found in the cytoplasmic membranes of all cells in both prokaryotes and eukaryotes (Padan et al., 2001). The most thoroughly

characterised NHEs are the mammalian NHE1 and the NhaA from *Escherichia coli* (Slepkov et al., 2007; Padan, 2009). NhaA and NHE1 show little sequence homology, however both proteins share a similar basic topology with 12 membrane-spanning segments and both C- and N-termini in the cytoplasm (Fig. 2.2 A). It has also been suggested that NhaA has a similar three-dimensional structure to the mammalian NHEs (Slepkov et al., 2007). In both cases the pH regulatory site is different from the active site, a loop takes part in the pH response and both proteins are oligomers within the membrane (Slepkov et al., 2007). Many NHE proteins are directly regulated by pH. A cellular pH sensor and the conformational change of the protein converts the pH signal into an activity change of the enzyme (Padan et al., 2004). In terms of laboratory studies focussed on NHEs, an alteration of such genes taking part in the acid-base pathway has been observed under low pH exposure (Stumpp et al., 2011; Tseng et al., 2013).

Carbonic anhydrase

As a representative for acid-base regulation processes the conserved zinc containing enzyme CA was chosen. CA catalyses the reversible hydration of CO₂:



(Tripp et al., 2001)

CAs are represented in all three life domains (Bacteria, Archaea and Eukarya). They can be found in many different tissues and cell compartments (Bertucci et al., 2013). By comparing sequences and crystal structures it was shown that mammalian and plant CA evolved independently (Tripp et al., 2001). Overall five groups of CA (α , β , γ , δ and ζ) are known. The α -class are found in vertebrates, protozoa, algae and cytoplasm of green plants, whereas the β -class are observed in higher plants, bacteria, fungi and archaea. γ -CAs can be only found in archaea and some bacteria. The δ - and ζ -class have only been

observed in diatoms (Supuran, 2011). All enzyme classes have an active site with a single zinc atom, which is crucial for catalysis (Fig. 2.2 B). It is assumed that these three classes work via a two-step isomechanism (Supuran, 2011) as follows:

1) The zinc bound hydroxide ion attacks the CO₂ nucleophilic and converts it into bicarbonate.



2) The elimination of a proton and the binding of a new water molecules regenerates the active centre.



(Tripp et al., 2001; Berg et al., 2013).

The three-dimensional structure of α -CAs of mammals is overall very similar. They appear almost in a spherical structure, apart from the amino terminal region, which is loosely connected to the rest. The active site is located in the cone-shaped cavity of the molecules, where the zinc ion is located near the bottom (Lindskog, 1997). With respect of invertebrate structure of α -CAs not much information is available. It is known from the mosquito *Aedes aegypti* that there is a high sequences homology to human CA I, however there are morphological differences which alter the surface topology and charge distribution (Fisher et al., 2006). CAs are known to be involved in important physiological processes such as respiration, transport of CO₂/HCO₃⁻, pH and CO₂ homeostasis, electrolyte secretion, biosynthetic reactions, bone resorption, calcification, tumorigenicity and a lot of other physiological and pathological processes in vertebrates (Supuran, 2011). In invertebrate species, CA is known for its involvement in the biomineralisation process in coral, *Stylophora pistillata* (Moya et al., 2008), and is also highlighted as triggered by changing HCO₃⁻ concentrations and OA stress conditions (Moya et al., 2012).

Calmodulin

Another major process affected under OA conditions are biomineralisation processes (O'Donnell et al., 2010; Dineshram et al., 2012; Moya et al., 2012; Pespeni et al., 2013). However, it should be noted that this type of research into OA is focussed mainly on calcifying organisms. CaM is a 148 amino acid protein, which is present in all eukaryotic cells. It works as a primary intracellular receptor for Ca^{2+} and takes part in the activation of several enzymes involved in various physiological processes (Means et al., 1991). These processes include secretion, cell proliferation, cellular metabolism, muscle contraction, differentiation and apoptosis (Means and Dedman, 1980; Rasmussen and Means, 1989; Chin and Means, 2000). In the pearl oyster *Pinctada fucata* CaM was identified to be involved in the regulation of calcium uptake, transport and secretion during shell formation (Li et al., 2004). There is also evidence that CaM is linked to Ca^{2+} -ATPase in the crayfish *Procambarus clarkia* during the molting process (Gao et al., 2009). Chen et al. (2012a) reported that CaM is involved in the settlement of barnacle larvae (*B. amphitrite*) and a recent study on the polychaete *Hydroides elegans* showed a similar effect (Chen et al., 2012b). The three-dimensional structure of the Ca^{2+} -calmodulin complex has been determined by Babu et al. (1985). They described the structure of the α carbon backbone as dumbbell-shaped and a pair of Ca^{2+} binding sites was discovered in the globular regions of the protein (Fig. 2.2 C). CaM is known for its role in modulating pathways influenced by intracellular messengers, whereby free Ca^{2+} activates the calmodulin-dependent pathways (MacNicol et al., 1990).

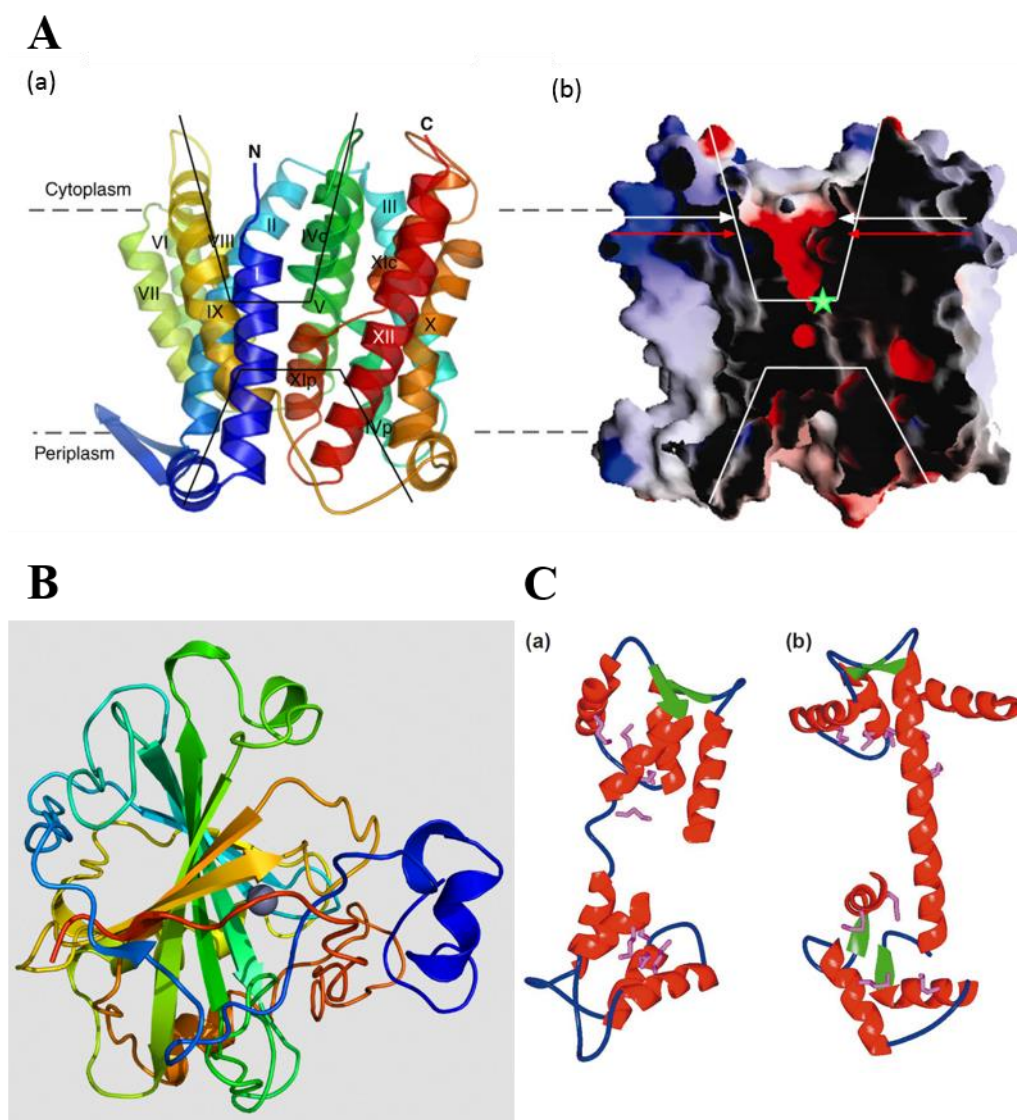


Figure 2.2 Examples for the three-dimensional protein structures of the selected *target* genes NHE, CA and CaM. **A (a)** Ribbon structure presentation of the crystal structure of NhaA of *E. coli*. Presented is a view parallel to the membrane. The 12 transmembrane segments are numbered with roman numerals. The letters C and N describe the N- and C-termini. The black lines present the cytoplasmic and periplasmic funnels. **(b)** Cross-section of the antiporter, without front part. The cytoplasmic and periplasmic funnels are marked in white. Hydrated cations can potentially access the cytoplasmic funnel down to the white arrow, whereas below the red arrow only non-hydrated Na⁺ and Li⁺ can enter. The green star indicated the ion-binding site (Padan, 2009). **B** Structure of human CA II at 2.0 Å resolution. The zinc ion is presented in the active site. From PDB 1CA2. **C** Structure of CaM during Ca²⁺-regulated conformational change. **(a)** Ca²⁺-free and **(b)** as Ca²⁺₄-CaM. Presented are the methionine side chains in purple to represent the location of potential hydrophobic pockets in both domains. Through the binding of Ca²⁺, large changes in the helices in both domains are triggered and result in an exposure of several hydrophobic residues (Chin and Means, 2000).

Having identified and selected three *target* genes the next step is to develop a quantitative assay of their gene expression using real-time PCR (qPCR) in order to conduct an mRNA expression analysis of normal tissue and acid stressed tissues in *P. dumerilii*.

Proteins are encoded by genetic information contained within the nucleus, and accomplish most of the functional roles in cells. The information for the synthesis of proteins resides in the genomic DNA. During a process called ‘transcription’ the genetic information is copied from DNA into mRNA. In the ribosome such information can then be translated into proteins (Berg et al., 2013). A very common method used to evaluate the expression levels of individual genes (more specifically the amount of mRNA presented at the sampling time) is qPCR (Dale et al., 2012). The technique of monitoring the whole reaction allows the quantification of RNA concentrations, which was not possible with RNase protection assays, or with gel-based end-point detections (Wang and Brown, 1999).

There are two different fluorescent chemistries called DNA-binding dyes and fluorescently labelled sequence-specific primers/probes that can be applied for the process. In both cases, fluorescence is emitted upon binding with double-stranded DNA so the amount of amplified product in each cycle is proportional to the amount of measured fluorescence. The most commonly used chemistries are the DNA-binding dye SYBR Green and the TaqMan hydrolysis probes. In the present study, the DNA binding dye SYBR Green (SYBR Green Master Rox, Roche) was applied. SYBR Green is suitable for singleplex reactions and has the advantage of easy assay design, fast set up and is initially more cost-effective. SYBR Green binds non-specifically to double-stranded DNA (dsDNA). Free in solution it exhibits only little fluorescence, but when it binds to dsDNA its fluorescence increases up to 1,000-fold (Bio-Rad Laboratories, 2006). A drawback of DNA-binding dyes is the lack of specificity, as DNA-binding dyes bind

to any dsDNA (Bio-Rad Laboratories, 2006). Therefore, nonspecific products can contribute to the overall fluorescence signal. To identify nonspecific products a melt-curve analysis needs to be performed. A distinct peak presenting the amplicon's melting temperature makes it distinguishable from other products such as primer dimers, which melt at a different temperature. Target gene expression can be measured either as absolute (the amount of nucleic acid, using an external standard) or relative (presenting the ratio between a *target* and a *reference* gene). For the following chapters the relative quantification method was applied to analyse the gene expression data for the *target* genes of interest.

This chapter describes the isolation and identification of the three *target* genes *NHE*, *CA*, and *CaM*, as well as the subsequent method development, using qPCR, in order to measure and compare gene expression levels in normal worms and worms exposed to different pH conditions.

2.2 Material and Methods

2.2.1 Animals

P. dumerilii used were from the laboratory culture from the European Molecular Biology Laboratory Heidelberg (EMBL, Germany). The worms were originally collected from a shallow depth in the Mediterranean Sea (Ischia, Italy) and Atlantic Ocean (Roscoff, France) (Simakov, 2013). Worms were kept in filtered natural seawater in culture tanks (2000cm³; approximately 50 individuals per tank) at a light regime of 16 h light/ 8 h dark in a temperature controlled room at 18 °C. Up to the adult stage, worms were separated by age groups, as larger worms eat smaller fellow species. Twice a week, they were fed with either organic spinach or a fish food-microalgae-mix (e.g. *Tetraselmis marinus* or *Isochrysis galbana*) following a culture method developed by Hauenschild (1951). The

fish food was ground to a powder. Larvae were fed with microalgae (e.g. *Tetraselmis marinus* or *Isochrysis galbana*) only. On occasion, the adult worms were fed additionally with *Artemia*. A complete water change was conducted every fortnight or earlier if the water quality did not meet the standard. No additional oxygen was bubbled into the tanks, as the shallow water allows enough oxygen to diffuse into the water and bubbling of oxygen would cause evaporation and therefore salinity changes. Worms were transferred into RNAlater solution (Sigma-Aldrich Company Ltd., Gillingham, UK), then sent on dry ice to the University of Hull, where they were stored at -80°C until further molecular processing. An overview of the molecular method is described in Figure 2.3.

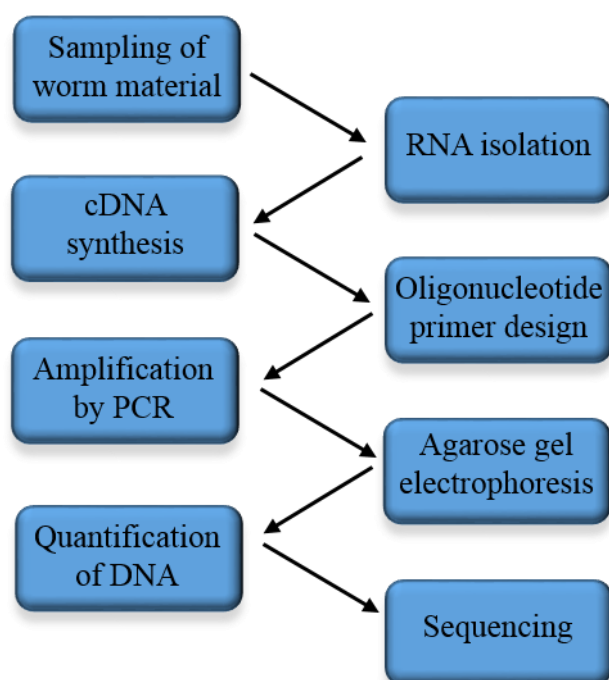


Figure 2.3 Overview of methodical approach for gene isolation.

2.2.2 Total RNA isolation and purification from worm tissue

Total RNA was extracted from each individual worm using High Pure RNA Tissue Kit reagents and protocol (Roche, Burgess Hill, UK). Approximately 10 mg of tissue was cut up in a 2 ml Eppendorf tube using a rotor homogeniser containing 400 µl Lysis/Binding

Buffer (4.5 M guanidine-HCl, 100 mM sodium phosphate, pH 6.6). The lysate was centrifuged at $14,500\times g$ for 2 min and the supernatant transferred into a new 1.5 ml tube. To get appropriate binding conditions 200 μ l of ethanol 100 % was added and the sample was transferred into a High Pure filter tube (polypropylene tube with two layers of glass fibre fleece) and centrifuged for 30 s at $13,000\times g$ to dry the glass fleece. The flow-through was discarded. To digest residual contaminating DNA, 90 μ l DNase Incubation Buffer (1 M NaCl, 20 mM Tris-HCl, 10 mM $MnCl_2$, pH 7.0) mixed with 10 μ l DNase I (10 kU) working solution were added to the column and left for 15 min incubation at room temperature ($\sim 22^\circ C$). Subsequently 500 μ l Wash Buffer I (5 M guanidine-HCl, 20 mM Tris-HCl, pH 6.6) was added to the column and centrifuged at $8,000\times g$ for 15 s. Again, the flow-through was discarded. The column was returned and the same step was repeated with 500 μ l Wash Buffer II (20 mM NaCl, 2 mM Tris-HCl, pH 7.5). Then 300 μ l Wash Buffer II were added and spun at $13,000\times g$ for 2 min. The column was transferred to a new 1.5 ml tube and a 100 μ l Elution Buffer (Nuclease-free, sterile, double distilled water) was added to the column. The column was centrifuged at $8000\times g$ for 1 min and the pure RNA stored at $-20^\circ C$ until further processing. The integrity of total RNA was analysed on a denaturing TAE agarose gel stained with ethidium bromide (Life Technologies, Paisley, UK). The gel contained 1.2 g agarose and 10 ml $10\times$ buffer FA (200 mM 3-[N-morpholino] propanesulfonic acid, 50 mM sodium acetate, 10 mM ethylenediaminetetraacetic acid, pH 7.0) in a total volume of 100 ml molecular graded water. The mixture was heated and, after cooling down to $65^\circ C$, 1.8 ml of 37 % (12.3 M) formaldehyde and 1.8 μ l of ethidium bromide (10 mg/ml) were added, mixed and poured into the gel support. The gel was equilibrated in $1\times$ FA gel running buffer for 30 min. 10 μ l (approximately 10 μ g/ml) of RNA samples were mixed with 3 μ l RNA loading dye (16 μ l saturated bromophenol blue solution, 80 μ l 500 mM ethylenediaminetetraacetic

acid (pH 8.0), 720 μ l 37 % (12.3 M) formaldehyde, 2 ml 100% glycerol, 3.084 ml formamide, 4 ml 10 \times FA gel buffer, add RNase-free H₂O to 10 ml) and heated at 65 °C for 3-5 min. Subsequently the samples were chilled on ice and loaded onto the gel. A 1 kb molecular weight ladder (Thermo Fisher Scientific, Loughborough, UK) was loaded to identify the approximate sizes. The electrophoresis was run in 1 \times FA buffer (100 ml 10 \times FA gel buffer, 20 ml 37 % (12.3 M) formaldehyde, 880 μ l RNase-free water) for ~40 min at 90 V.

2.2.3 Synthesis of cDNA

Using the SuperScript VILO cDNA Synthesis Kit (Life Technologies, Paisley, UK) cDNA was synthesised from total RNA. 4 μ l 5 \times VILOTM Reaction Mix, 2 μ l 10 \times SuperScript[®] Enzyme Mix were gently mixed with up to 0.5 μ g total RNA and incubated at 25 °C for 10 min, followed by 60 min at 42 °C and 5 min at 85 °C. After cooling to 4 °C, 1 μ l of RNase H (5 U/ μ l) (Thermo Scientific, Loughborough, UK) and 2 μ l of 10 \times Buffer (200 mM Tris-HCl (pH 7.8), 400 mM KCl, 80 mM MgCl₂, 10 mM DTT) were added and incubated at 37 °C for 45 min to degrade remaining RNA template.

2.2.4 Oligonucleotide primer design

Nucleotide sequences for the two *reference* genes *18S rRNA* (*18S*) and *α -Tubulin* (*α -TUB*) and the three *target* genes *NHE*, *CA*, and *CaM* were obtained from GenBank (<http://blast.ncbi.nlm.nih.gov/Blast.cgi>) and Blasted on the worm database PLATYpopsys (<http://hydra.cos.uni-heidelberg.de/pps/>) from the EMBL, Heidelberg. Matched sequences were counterchecked by ReBlast against GenBank. PLATYpopsys is a database with transcriptomic and genomic data specifically for *P. dumerilii*. The use of the database enables the identification of sequences from the experimental species, which

are not available on GenBank and therefore allowed the design of species-specific primers. Primers were designed with a product length between 101 bp and 239 bp (Table 2.1) and the primer self-complementarity was checked using Oligo Calc: (www.basic.northwestern.edu/biotools/OligoCalc.html).

Table 2.1 Oligonucleotide primer sequences for the two *reference* (*18S* and *α -TUB*), and the three *target* genes (*NHE*, *CA* and *CaM*) and their amplicon size in bp.

<i>Target gene</i>	Forward primer (5'-3')	Reverse primer (5'-3')	Amplicon size (bp)
<i>18S</i>	GCGCATTATCAGCACAAGA	CTTGGATGTGGTAGCCGTTT	239
<i>α-TUB</i>	CTTCAAGGTCGGCATCAACT	TGGCAGTGGTATTGCTCAAC	101
<i>NHE</i>	CGCTCTGTTGCTGTCTTGAG	TGGCTACTAAGGCGAATGCT	130
<i>CA</i>	TAACCACCTCAACCGGAGAC	ATGGTGTGCTCTGAGCCTTT	118
<i>CaM</i>	AAGCTTCCGAGTGTTTCGAC	CCTCTTCGTCCGTCAATTC	102

The oligonucleotide primers were synthesised by IDT (Integrated DNA Technologies, Leuven, Belgium) and delivered in lyophilised form. The primers were then resuspended in molecular grade water to a concentration of 100 pmol/ μ l. For the PCR the primers were further diluted with water in a ratio of 1/10 to give a final concentration of 10 pmol/ μ l.

2.2.5 Amplification of DNA by the Polymerase Chain Reaction (PCR)

For all PCRs, autoclaved tubes and pipette tips were used to prevent contamination of the sample with other, contaminating, DNA. In order to avoid degradation of the reagents by repeated defrosting, small volumes of each were aliquoted into tubes. For the generation of *NHE*, *CA* and *CaM* PCR products, 1 μ l of cDNA was combined with 0.5 μ l of 10 pmol/ μ l forward and reverse primer (Table 2.1), 0.25 μ l of Herculase cDNA polymerase (Agilent Technologies, Wokingham, UK), 5 μ l 5 \times PCR buffer (Agilent Technologies, Wokingham, UK), 0.5 μ L 40 mM dNTP mix (Thermo Fisher Scientific,

Loughborough, UK), 0.5 μ L DMSO (Agilent Technologies, Wokingham, UK), 0.5 μ L 25 mM $MgCl_2$ (Thermo Fisher Scientific, Loughborough, UK) and 16.25 μ L sterile nuclease-free water (Thermo Fisher Scientific, Loughborough, UK) to prepare a total reaction volume of 25 μ L. For the PCR conditions an initial denaturation at 94 °C for 30 s was used, followed by 35 cycles of denaturation at 94 °C for 30 s, annealing at 60 °C for 30 s and extension at 72 °C for 30 s, finishing with a final extension of 72 °C for 2 min. For each PCR reaction a positive and negative control was carried out. Both controls were based on the *18S* gene (Table 2.1). The negative control included all components of the PCR reactions but replaced template DNA with molecular grade water. The negative control was performed to monitor that no contamination took place and the positive control to ensure that the reaction has worked.

2.2.6 Agarose gel electrophoresis of DNA

The PCR products were separated and visualised by agarose gel electrophoresis to confirm the presence of a single, correctly-sized band. For every 0.1 g agarose (Thermo Fisher Scientific, Loughborough, UK) 10 ml 1 \times TBE-buffer (89 mM Tris Base, 89 mM Boric acid and 2 mM EDTA (pH 8.3 \pm 0.1)) (Thermo Fisher Scientific, Loughborough, UK) and 1 μ l gel stain SYBR Safe DNA gel stain (Life Technologies, Paisley, UK) was used to produce a 1 % gel. The gel was placed in a gel electrophoresis tank with 1 \times TBE-buffer (89 mM Tris Base, 89 mM Boric acid and 2 mM EDTA (pH 8.3 \pm 0.1)) and the comb removed. Prior to loading on the gel, 10 μ l of the sample was mixed with 2 μ l loading dye (Gel loading dye blue (6 \times) New England Biolabs, Hitchin, UK). To be able to determine the size of the DNA fragments a 100 bp DNA Ladder (New England Biolabs, Hitchin, UK) was loaded next to the samples. The gel was run using a current of 70 V for between approximately 45 min. Finally the gel was analysed under UV-

transillumination and photographed using a Gel DocTM EZ Imager (Bio-Rad, Hemel Hempstead, UK).

2.2.7 Quantification of DNA

The DNA concentration of the samples was measured with a QubitTM fluorometer (Life Technologies, Paisley, UK). The QubitTM fluorometer is standardised by two standard solutions from which the machine generates the concentration data using a curve fitting algorithm. Through the use of dye that becomes fluorescent when binding to nucleic acid DNA and RNA concentrations can be measured. To achieve the maximum fluorescence level, the sample mixed with working solution needs to be incubated for 2 min at room temperature (~22 °C). It is important that the buffer (QubitTM RNA Buffer, Life Technologies, Paisley, UK) and the dye (QubitTM RNA Reagent, Life Technologies, Paisley, UK) are stored at room temperature (~22 °C) as temperature fluctuations can influence the readings.

The readings of the QubitTM fluorometer correspond to the concentration of the sample after dilution. The actual sample concentration is calculated with the following equation:

$$\text{Sample concentration} = \text{QF value} \times (200/x)$$

The QF value stands for the value given by the QubitTM fluorometer and the x for the number of microliters of sample that were added to the assay tube.

2.2.8 Sequencing the potential gene

PCR products within the concentration range of approximately 10 µg/ml and 20.1 µg/ml were sequenced directly, using the EZ-Seq Service (Macrogen Europe, Amsterdam, Netherlands). For the sequencing process the corresponding PCR primers were used as sequencing primers. All sequences were checked and edited using BioEdit (Version

7.0.9.0). Sequencing identities were verified using a BLAST search (<http://blast.ncbi.nlm.nih.gov/Blast.cgi>) to complete nucleotide comparisons (blastn), and to compare the translated nucleotide sequence against the protein database (blastx). Additionally, the sequences were investigated on the worm database PLATYpopsys (<http://hydra.cos.uni-heidelberg.de/pps/>) using nucleotide sequence comparison (blastn) and comparison of the translated nucleotide sequence against the protein database (blastx).

2.2.9 Phylogenetic analysis

In order to analyse the phylogenetic relationships of the sequences (*NHE*, *CA* and *CaM*) used for primer design phylogenetic trees were constructed as follows.

2.2.9.1 *NHE*

The original *NHE* sequence used for primer design (PLATYpopsys: FARO denovo 101100021518) was aligned with sequences obtained from NCBI. With Jalview 2.8.0b1 (<http://www.jalview.org/>) the amino acid sequences in Table 2.2 were aligned.

Table 2.2 Amino acid sequences for *NHE* obtained from NCBI used for the alignment and following phylogenetic analyses. The sequence for the outgroup is marked with an asterisk (*).

GenBank Accession number	Gene name	Species name	Common name
AAF80554.1	NHE	<i>A. aegypti</i>	yellow fever mosquito
AAO34131.1	alkali metal ion/proton exchanger 3	<i>Anopheles gambiae</i>	mosquito
XP_002430244.1	NHE	<i>Pediculus humanus corporis</i>	body louse
XP_004931663.1	Predicted: NHE 5-like	<i>Bombyx mori</i>	silkworm
XP_003699746.1	Predicted: NHE 3-like	<i>Megachile rotundata</i>	alfalfa leafcutter bee
XP_002741674.2	Predicted: NHE 3-like	<i>Saccoglossus kowalevskii</i>	acorn worm
EGI71052.1	NHE 3	<i>Acromyrmex echinator</i>	New World ant
NP_001137847.1	NHE 2	<i>D. melanogaster</i>	fruit fly
EFN63440.1	NHE 3	<i>Camponotus floridanus</i>	ant
XP_002811759.1	Predicted: NHE 2	<i>Pongo abelii</i>	Sumatran orang-utan
XP_004031583.1	Predicted: NHE 2	<i>Gorilla gorilla gorilla</i>	western lowland gorilla
P13607.3*	Na ⁺ /K ⁺ ATPase alpha subunit*	<i>D. melanogaster</i> *	fruit fly*

The aligned data was then imported into Mega6 (Tamura et al., 2013), which was used to conduct the phylogenetic analysis on the partial-gene amino acid sequences. A Maximum Likelihood Analysis with the Nearest Neighbor Interchange method (1000 bootstrap replicates) was performed. The tree was rooted to the outgroup.

2.2.9.2 CA

Similarly to the procedure in 2.2.9.1 the CA sequence (PLATYpopsys: TUEB denovo 100100001529) was aligned with the amino acid sequences in Table 2.3.

Table 2.3 Amino acid sequences for CA obtained from NCBI used for the alignment and following phylogenetic analyses. The sequence for the outgroup is marked with an asterisk (*).

GenBank Accession number	Gene name	Species name	Common name
AAZ03744.1	CA 4	<i>Squalus acanthias</i>	spiny dogfish
XP_005460906.1	Predicted: CA 4-like	<i>Oreochromis niloticus</i>	Nile tilapia
XP_002195938.2	Predicted: CA 15-like	<i>Taeniopygia guttata</i>	zebra finch
XP_005524458.1	Predicted: CA 15-like	<i>Pseudopodoces humilis</i>	ground tit
XP_003225153.1	Predicted: CA 15-like	<i>Anolis carolinensis</i>	Carolina anole
XP_006021613.1	Predicted: CA 15-like	<i>Alligator sinensis</i>	Chinese alligator
XP_415218.3	Predicted: CA 15-like	<i>Gallus gallus</i>	red junglefowl
XP_002759086.1	CA 2	<i>Callithrix jacchus</i>	common marmoset
DAA22514.1	CA 2	<i>Bos taurus</i>	cattle
ERG79841.1*	beta carbonic anhydrase 1*	<i>Ascaris suum</i> *	large roundworm of pigs*

The aligned data was then imported into Mega6 (Tamura et al., 2013), which was used to conduct the phylogenetic analysis on the partial-gene amino acid sequences. A Maximum Likelihood Analysis with the Nearest Neighbor Interchange method (1000 bootstrap replicates) was performed. The tree was rooted to the outgroup. For details of phylogenetic analysis on the partial-gene amino acid sequences see 2.2.9.1.

2.2.9.3 *CaM*

The *CaM* sequence used for primer design (PLATYpopsys: HEIDELBERG denovo 100500002325) was aligned with the amino acid sequences in Table 2.4.

Table 2.4 Amino acid sequences for *CaM* obtained from NCBI used for the alignment and following phylogenetic analyses. The sequence for the outgroup is marked with an asterisk (*).

GenBank Accession number	Gene name	Species name	Common name
AEK21539.1	CaM A	<i>Litopenaeus vannamei</i>	whiteleg shrimp
EZA53913.1	CaM	<i>Cerapachys biroi</i>	clonal raider ant
O96081.3	CaM B	<i>Halocynthia roretzi</i>	sea pineapple
NP_001734.1	CaM	<i>Homo sapiens</i>	modern human
EHB00855.1	CaM	<i>Heterocephalus glaber</i>	naked mole-rat
P02594.2	CaM	<i>Electrophorus electricus</i>	electric eel
NP_001159980.1	CaM	<i>B. taurus</i>	cattle
ACO13793.1	CaM	<i>Esox lucius</i>	northern pike
ABM53481.1	CaM 1b	<i>Branchiostoma belcheri tsingtauense</i>	Belcher's Lancelet
NP_001177086.1*	parvalbumin*	<i>Sus scrofa</i> *	wild boar*

For details of phylogenetic analysis on the partial-gene amino acid sequences see 2.2.9.1.

2.2.10 Determination of gene expression levels

2.2.10.1 Primer optimization and assay performance

The *target* gene specific primers were generated as described in 2.2.4. qPCR assays require optimisation in order to ensure that the efficient and accurate quantification of the target template takes place. To this end, the MIQE guidelines were adopted (Bustin et al., 2009). The first step was required to find the optimal primer concentration. For this five concentrations with equimolar amounts of each primer were tested: 500 nM, 300 nM, 100 nM, 80 nM and 50 nM. Each reaction had 1 µl of template added. The primer pair concentration with the lowest C_q (threshold cycle) value and a melt curve showing only a single distinct product was chosen. The C_q describes the cycle number during the exponential phase at which enough amplified product accumulated to give a detectable

fluorescent signal. A robust and precise qPCR assay generally corresponds to a high PCR efficiency. To determine the efficiency of the assay, a serial dilution of a template was run. For the serial dilution the template was used in the following concentrations: 1:1, 1:10, 1:100, 1:1000 and 1:10000 or 1:1, 1:4, 1:16, 1:64 and 1:256. The result was analysed by standard curve. For this, the log of the dilution factor was plotted against the C_q . The equation of the regression line and the coefficient of determination (R^2), were used to assess the qPCR assay. An efficiency of 1.00 (or 100 %) indicates that the amount of product doubles with each cycle. Generally C_q values above 40 are assumed to be due to low efficiency and according to the MIQE guidelines (Bustin et al., 2009) these values should not be recorded.

2.2.10.2 Amplification using qPCR

For the qPCR reactions a final volume of 20 μ l containing 10 μ l of qPCR FastStart SYBR Green Master Rox (Roche, Burgess Hill, UK), 1 μ l of cDNA and 2 μ l of primers with a concentration of 50 nM for *18S* and 100 nM for *α -TUB*, *NHE*, *CA* and *CaM* in the final reaction (Table 2.1) and 7 μ l molecular grade water (Thermo Fisher Scientific, Loughborough, UK) was used. To determine the target cDNA amplification specificity, a control lacking cDNA template was included in the qPCR analysis. A CFX96 Real Time PCR Detection System (Bio-Rad, Hemel Hempstead, UK) was used to detect amplification and the CFX Manager™ software (Bio-Rad, Hemel Hempstead, UK) applied to evaluate the generated amplification plots and melt peaks. Initially all reactions were denatured at 95 °C for 2 min. This was followed by 45 cycles of denaturation at 95 °C for 10 s, annealing at 60 °C for 1 min and an extension step at 72 °C for 1 min. To generate the melt curve, a heating step gradient from 5 s at 60 °C to 5 s at 95 °C, was added to the end of the PCR run. Two *reference* genes with different roles in

cellular processes were utilised: *18S*, involved in ribosomal structure and *α -TUB*, taking part in cytoskeletal structure. *18S* has previously been established as a *reference* gene for *Nereis* species (Won et al., 2011; Zheng et al., 2011). To show the gene expression stability of *18S* and *α -TUB* under experimental conditions, the geometric mean for both control and treatment C_q values measured were validated by an analysis of variance (ANOVA).

2.2.10.3 Analysis of qPCR products

For the verification of the target mRNAs, melting curves, melt peak and gel pictures were analysed to check for amplification specificity and absence of primer dimers. For the melt curve generation the qPCR product is gradually heated from 60 °C to 95 °C and fluorescence is measured. In the beginning the dsDNA is bound to SYBR green and a high fluorescent signal is measured. When the qPCR product is heated it reaches the point where it forms two DNA strands and the SYBR green is released. Therefore, the fluorescence signal will suddenly drop. The same data can also be presented as rate-of-change-of-fluorescence. The sudden change in fluorescence is presented as a sharp peak. The melt-curve analysis should show a single peak, as the qPCR product ought to consist of similar sequences that melt at the same time. The negative control should show neither a melt curve nor a melt peak to confirm the absence of primer dimers and contamination. The gel analysis of the qPCR products should show one distinct band to confirm the presence of only one product and the negative controls should show no band.

2.2.10.4 Quantification of *target* gene expression

To analyse the gene expression a relative quantification method was applied. For both the test sample and the calibrator sample the C_q (previously known as C_T , see MIQE guidelines, Bustin et al., 2009) values were normalised to that of the *reference* genes (*18S* and *α -TUB*). The relative gene expression level of each gene was calculated. For this the $2^{-\Delta\Delta CT}$ (Livak) method was used (Livak and Schmittgen, 2001).

Normalisation to the reference (ref) gene:

$$\Delta C_{T(\text{test})} = C_{T(\text{target, test})} - C_{T(\text{ref, test})}$$

$$\Delta C_{T(\text{calibrator})} = C_{T(\text{target, calibrator})} - C_{T(\text{ref, calibrator})}$$

Normalisation to the the calibrator:

$$\Delta\Delta C_T = \Delta C_{T(\text{test})} - \Delta C_{T(\text{calibrator})}$$

Expression ratio:

$$2^{-\Delta\Delta CT} = \text{Normalized expression ratio}$$

(Bio-Rad Laboratories, 2006)

2.3 Results

2.3.1 Target gene isolation and characterisation

2.3.1.1 Isolation of a partial *NHE-like* cDNA sequence from *P. dumerilii*

A 110 bp PCR product was sequenced from *P. dumerilii*, with a Blastx search showing highest similarity to a solute carrier family 9, subfamily A (NHE2, cation antiporter 2) from the sperm whale *Physeter catodon* (**XM_007108520.1**); rat *Rattus norvegicus* (**NM_012653.2**); and a Na/H ion exchanger mRNA of another rat species *Rattus* sp. (**L11236.1**) with 78% similarity in each case. Aligning the original *NHE* amino acid sequence used for primer design (**FARO denovo 101100021518**) with *NHE* sequences from the yellow fever mosquito *A. aegypti* (**AAF80554.1**) and common fruit fly *D. melanogaster* (**NP_001137847.1**) showed a partial coverage of the Na/H exchanger domain (Fig. 2.4), and 45.6% similarity between the three sequences. The phylogenetic analysis separates the sequences into two main branches, whereby the *P. dumerilii* sequence clusters with the acorn worm *S. kowalevskii* and two mammalian sequences (Fig. 2.5).

```

A.aegypti_NHE      MVAHSLQQEVNLSRRACRIPKWPLSGAQEQEENDEEVLEEQLLNGANQSPASEVAAFRLG 60
D.melanogaster_NHE2 ---MSIRTEQDYDS-----ATPALAQQMN-----LARRACWRIKSYSSSESLFKTYA 43
P.dumerilii_NHE    -----MLVPVN-----RALLICVICLSCTK----- 20
                                     *                               * :.

A.aegypti_NHE      PVHSENSPGGIDEDPLSFRNRRMHDGRMGSVVDFSCDLVAHVFLLVKALVMGVLRFDLTS 120
D.melanogaster_NHE2 SVITDTSANEIDA EAPP PPRDKTKT-----RIEQI 74
P.dumerilii_NHE    LVYSGTTPGDVTPDSVTVDG-----LVVNL 45
* : :. . . : :. .

A.aegypti_NHE      PKRASSSSSSSSSYGSQFSKNLVKWTWAIVLSVLLANHGGFVLARPKNGVVTADGVDA 180
D.melanogaster_NHE2 APAKRNSCTSSDWRGMFSKRTLLICALALILGSAQARPNTSAVGVAPR-KVSQDIVDAV 133
P.dumerilii_NHE    TTAAPHSVTSQTDHGNNTN-----GHKHSNMSG-----DAHTDDAH 82
. * :. . . :. : . . . . . **

A.aegypti_NHE      SVASGQWELLTPQPVSSDGAGGQISGSLSSVKQDDQSHGGELGDASHGEGHEVERYPV 240
D.melanogaster_NHE2 TQLN----LGQSAPIDAVDVG----LDPTPSARVPRPEPLKSGDE-NAKGDEGHKEMERYPL 185
P.dumerilii_NHE    SDDN-----HSGQGHDSQGG-----HAGGQGHSDGGQGHSGDDHDSHGPFERFPV 129
: . . . . * : : * : : * : : * : : * : : * : : * : : * : : * : : * : : * : :
                                     Na_H_Exchange

A.aegypti_NHE      AQVEFSRVETPFVIGVWILSASIAKIGFHMTPKLSKIFPESCLLIVGVVIGVLLRYATN 300
D.melanogaster_NHE2 SSVDFARVKT PFIIGI WILSASIAKIGFHMTPKLHLIFPESCLLIVGVVIGVLLYFCTD 245
P.dumerilii_NHE    AYLKWHHVMYPYIPFLWII IACIARLAL EYNP NLTEYMP EGCYMVILGVLIGICLWFS-K 188
: : : : * * : : * : : * : : * : : * : : * : : * : : * : : * : : * : : * : :

A.aegypti_NHE      LHVSP LTPNTFFFYMLPPIILDAGYFMPNRMFFDNIGTILLMAVIGTIFNIATIGVSLWA 360
D.melanogaster_NHE2 VAVSP LTPNTFFFYMLPPIILDAGYFMPNRLFFDNLGTILLMAVVG TIFNIATIGGSLYA 305
P.dumerilii_NHE    ISQESLNSEHFFIFLLPPIIEAGYFMPKRAFFDQIGTILWYAI VSTLFSTFAIGFSLWG 248
: . . * : : * : : * : : * : : * : : * : : * : : * : : * : : * : : * : :

```

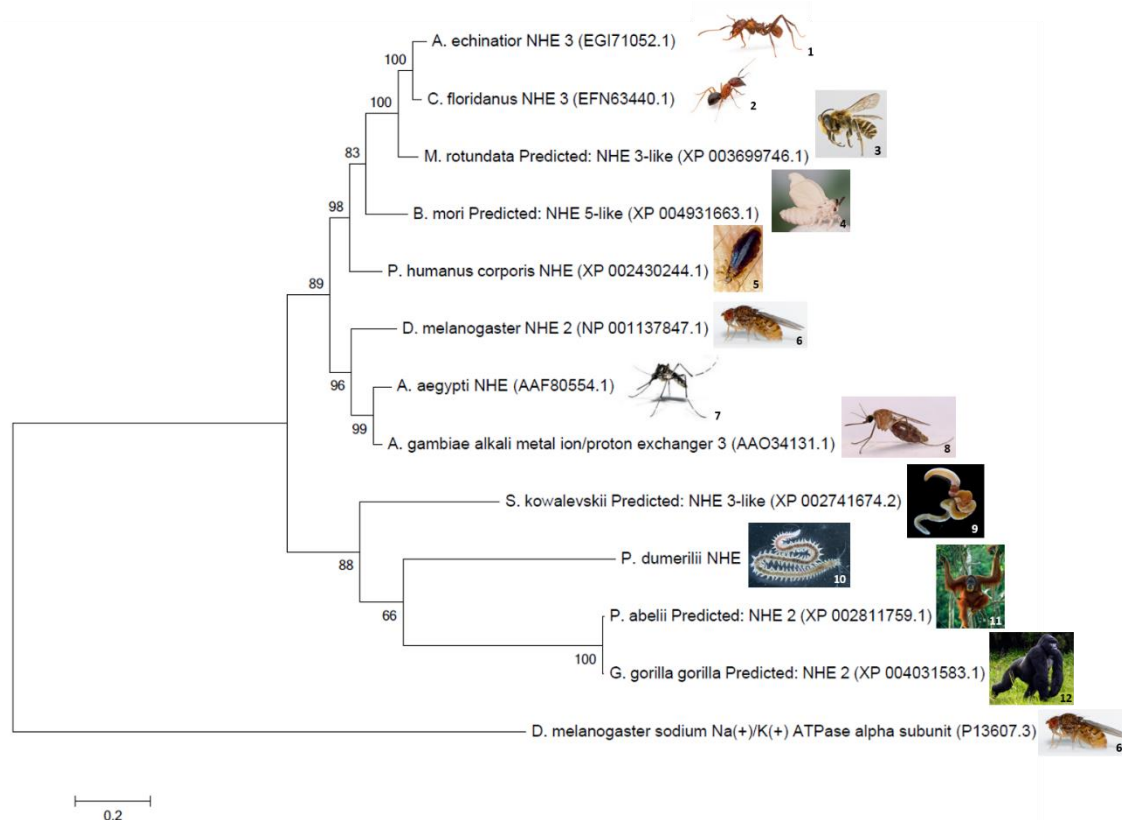



Figure 2.5 Phylogeny of predicted partial amino acid sequences for *NHE*, using an amino acid sequence with gaps. Sequences were aligned and edited in Jalview 2.8.0b1 and for the Maximum likelihood analysis Mega6 was used. The Jones-Taylor-Thornton (JTT) model was applied and for the heuristic search the Nearest Neighbour Interchange (NNI) method was performed. The numbers in the nodes represent bootstrap probabilities with 1000 replicates.

2.3.1.2 Isolation of a partial *CA* cDNA sequence from *P. dumerilii*

A partial sequence for the *CA* gene (113 bp) was obtained by PCR from *P. dumerilii* cDNA. The Blastx search showed 76 % and 62 % similarity of the translated nucleotide sequence with *carbonic anhydrase 9-like* sequence and *carbonic anhydrase 1-like* sequence, both from *S. kowalevskii* (**XP_006811134.1** and **XP_006822732.1** respectively). An alignment of the original *CA* amino acid sequence (**TUEB denovo 100100001529**) used for primer design with *CA* sequences from common limpet *Patella vulgata* (**CCJ09594.1**) and the starlet sea anemone *Nematostella vectensis* (**DAA06053.1**) showed a partial coverage of the conserved alpha-*CA* domain (Fig. 2.6),

with a similarity of 31.07%. The phylogenetic analysis showed clustering of the sequence with other alpha-CA sequences (Fig. 2.7).

```

P.dumerilii_CA    --METS LVFIACILLS-----ATQAADWSYK GANGPSNWKNDYSTCGGSKQSPIN 48
P.vulgata_CA     -MAKISLMFLLSLMRQQD-----PSHKAQNYHWSYLGTEG PSSWQKH YEHCAGKRQSPIN 54
N.vectensis_CA   MSLVCRFLFFFC L I V F I L G A L E R V E A A D P M G D W S Y D E A T G P S T W P N H F P H C G K M Q S P I N 60
                  :::  :::                               .*** : **.* :: : *. * . *****

                                alpha_CA
P.dumerilii_CA   IVSGDVVKDENLANIKVSASYSTKPSGS---WSIKNNGHSVGVTTSTGDYTLSEGG-LGA 104
P.vulgata_CA    IDTNTVVYDETLQDFDLSEFHLLRGSQHPMIVNVTNNGHSASARVP-GEIHCSSGGG-LSG 112
N.vectensis_CA  INTEEAKYDGS L T D L D I K Y P N T T -----D V L L V N H H G H A I E A D I L S S E P F V A T G A D L S S 114
                  * : . * . * : : : : . : : : * : . : : : * . * .

                                # # #
P.dumerilii_CA   TYKLAQFHFHWGSTD SKGSEHTMDGKEYPLEIHFVHYNSKYADLTTAIDKSDGLAVLGFF 164
P.vulgata_CA    AYRTAEFHFHWGSI DNRGSEH G I N G R V Y P L E M H V V Q Y A V K Y S L A K A K T K P D G L A V L G T M 172
N.vectensis_CA  RYRLAQFHFHWGSSDIQGS E H H I H G V K Y P L E M H L V H Y N D K Y P N A S S A Q G L L D G L A V I S V L 174
                  *: *.***** ** * :***** :.* *****.*.* * * . :.* *****:. :

P.dumerilii_CA   FEVDGSDNAAMQPIVDK LSSVTNKDDTATIDP M I L L D L M G G D A A T F S E F Y R Y S G S L T T P G 224
P.vulgata_CA    YEISEQDNPSFEPVVAALKNIKHEGNEDSITNLDLRNLLPKDS---SKFYRYEGSLTTPP 229
N.vectensis_CA  FESSSTDNPALNEIIDNLQNASYKDEEITVQNVVPGKI IPTDT---EKFYRYNGSLTTPP 231
                  :* . **::: : : * . . . : : : : : : : * : . :*****.*****

P.dumerilii_CA   CYESVTWTVFEKTVKISS----- 242
P.vulgata_CA    CFESVIWTVFAIPQKISAPQLAVLRSLFLEAHGDAGLKPTDGHSHTVNVQSQPGSSTNS 289
N.vectensis_CA  CFETVKWIVLKKTASISEKQLRQFRSVFSTSR--QATKPNS----- 270
                  *:.* * * * : . . * *

P.dumerilii_CA   ----- 349
P.vulgata_CA    VKYLVDNFRPFQVLNGRVVKKSFKELHPISNTAPTTS L T Q A D I K Q V N T A M E S S H P V G S S P 349
N.vectensis_CA  ---LVDNFRPTQSLNGRIIRKNFGKLLKYIY----- 299

P.dumerilii_CA   ----- 409
P.vulgata_CA    SNNIGNFNLENGHK T I L S G A N A V P G F N A A S D T K A A A T R T Q I S V P E Q Q L T S I K L G S A N E A I 409
N.vectensis_CA  -----

```

Figure 2.6 Alignment of partial *P. dumerilii* CA (TUEB *denovo* 100100001529), *P. vulgata* CA (CCJ09594.1) and *N. vectensis* CA1 (DAA06053.1) predicted amino acid sequences. Dashes represent alignment gaps and asterisks represent homology. Colons represent sites with conserved amino acid substitutions and dots represent semi-conserved amino acid substitutions (similar shape). Light grey shaded regions represent functional protein domains. Dark grey shaded regions represent active sites on the conserved domain and the hash sign the zinc binding sites.

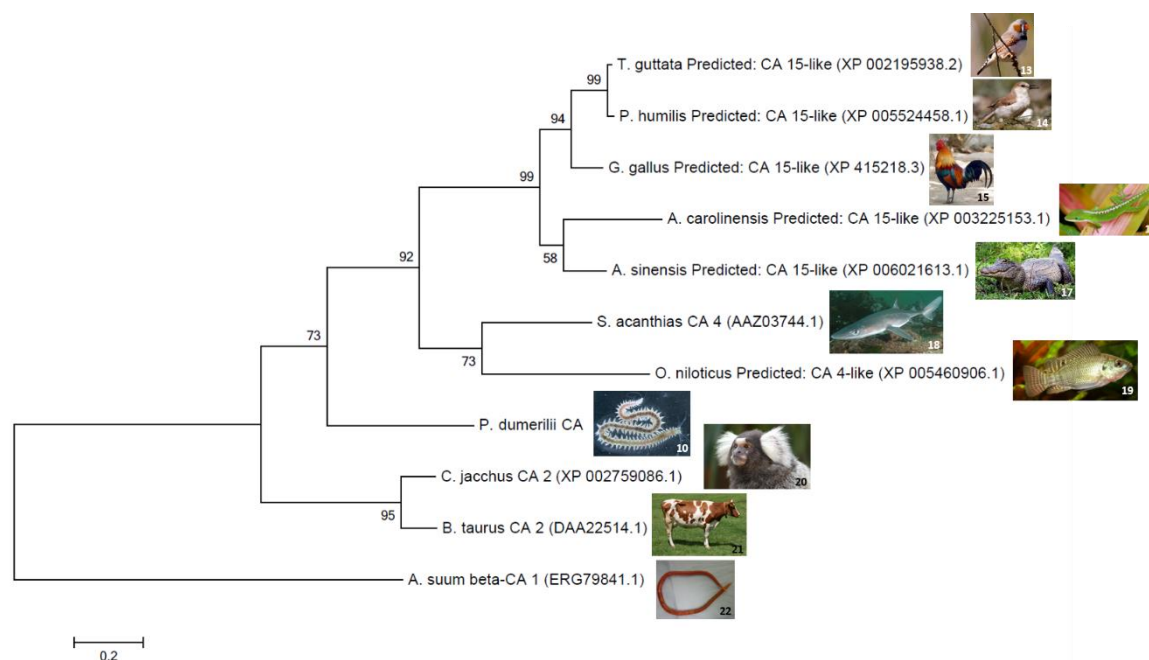


Figure 2.7 Phylogeny of partial amino acid sequences for *CA*, using an amino acid sequence with gaps. Sequences were aligned and edited in Jalview and for the Maximum likelihood analysis Mega6 was used. The Jones-Taylor-Thornton (JTT) model was applied and for the heuristic search the Nearest Neighbour Interchange (NNI) method was performed. The numbers in the nodes represent bootstrap probabilities with 1000 replicates.

2.3.1.3 Isolation of a partial *CaM* cDNA sequence from *P. dumerilii*

A 57 bp *CaM* PCR product was isolated from *P. dumerilii* matching to CaMs from the purple sea urchin *S. purpuratus* (P05934.1), the hermit crab hydroid *Hydractinia symbiolongicarpus* (AGB14582.1) and *Clytia gracilis* (AAZ23122.1). Blastn searches revealed the highest similarity for the nucleotide sequence with calmodulin-1 of the nematode parasite *Trichinella spiralis* (XM_003379512.1) with 93 %, followed by the CaM of the African cotton leafworm *Spodoptera littoralis* (HM445737.1) with 91 % and GM21351 of the fruit fly *D. sechellia* (XM_002033477.1) likewise with 91 %, all indicating that the isolated *P. dumerilii* cDNA fragment could be identified as a partial *CaM* sequence. An alignment of the original *CaM* amino acid sequence (HEIDELBERG denovo 100500002325) used for primer design with *CaM*

sequences from the whiteleg shrimp *L. vannamei* (**AEK21539.1**) and cattle *B. taurus* (**NP_001159980.1**) showed conserved features of two EF-hand domains with Ca²⁺ binding sites (Fig. 2.8). The two conserved EF-hand domains showed 96% similarity between the three sequences. The phylogenetic analysis showed that *P. dumerilii* clusters with other invertebrate *CaM* sequences (Fig. 2.9).

```

                                     EF-hand
P.dumerilii_CaM      MADQLTEEQIAEFKEAFSLFDKDGDTITTKELGTVMRS LGQNPTAEELQDMINEVDADG 60
L.vannamei_CaM      MADQLTEEQIAEFKEAFSLFDKDGNGTITTKELGTVMRS LGQNPTAEELQDMINEVDADG 60
B.taurus_CaM        MADQLTEEQIAEFQEAFLFDKDGDTITTKELGTVMRS LGQNPTAEELQDMINEVDADG 60
*****:*****:*****

                                     EF-hand
P.dumerilii_CaM      NGTIDFPEFLTMMARKMKD TDSEEEIREAFRVFDKDGNGFISAAELRHVMTNLGEKLTDE 120
L.vannamei_CaM      NGTIDFPEFLTMMARKMKD TDSEEEIREAFRVFDKDGNGFISAAELRHVMTNLGEKLTDE 120
B.taurus_CaM        NGTIDFPEFLTMMARKMKD TDSEEEIREAFRVFDKDGNGYISAAELRHVMTNLGEKLTDE 120
*****:*****

P.dumerilii_CaM      EVDEMIREADIDGGQVNYEEFVTMMTSK 149
L.vannamei_CaM      EVDEMIREADIDGGQVNYEEFVTMMTSK 149
B.taurus_CaM        EVDEMIREADIDGGQVNYEEFVHMMTAK 149
***** **:*

```

Figure 2.8 Alignment of partial *P. dumerilii* *CaM* (**HEIDELBERG denovo 100500002325**), *L. vannamei* *CaM* A (**AEK21539.1**) and *B. taurus* *CaM* (**NP_001159980.1**) predicted amino acid sequences. Dashes represent alignment gaps and asterisks represent homology. Colons represent sites with conserved amino acid substitutions and dots represent semi-conserved amino acid substitutions (similar shape). Light grey shaded regions represent functional protein domains. Dark grey shaded regions represent Ca²⁺ binding site on a conserved domain. The EF hand is a calcium-binding motif, which is the most common calcium-binding motif found in proteins. It usually has a helix-loop-helix motif (Lewit-Bentley and Réty, 2000).

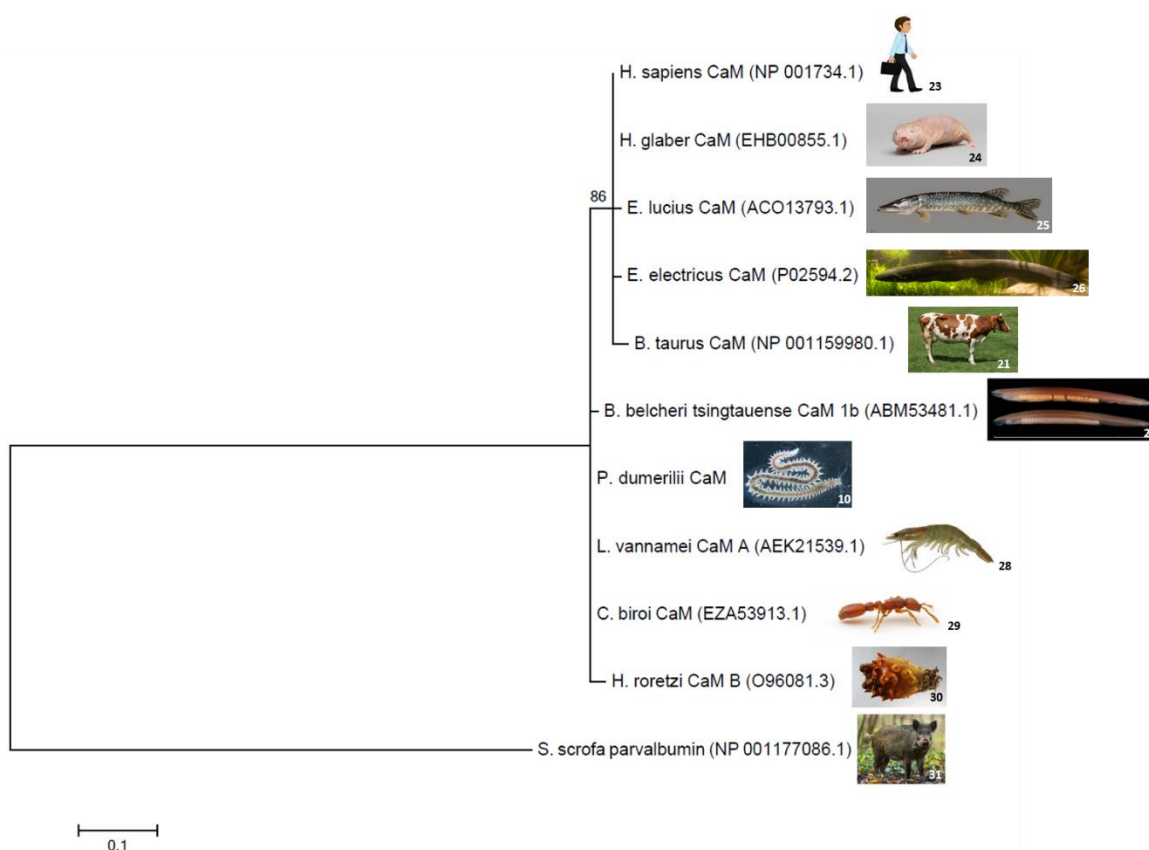


Figure 2.9 Phylogeny of partial amino acid sequences for *CaM*, using an amino acid sequence with gaps. Sequences were aligned and edited in Jalview 2.8.0b1 and for the Maximum likelihood analysis Mega6 was used. The Jones-Taylor-Thornton (JTT) model was applied and for the heuristic search the Nearest Neighbour Interchange (NNI) method was performed. The numbers in the nodes represent bootstrap probabilities with 1000 replicates.

2.3.2 Quantitative qPCR analysis of *NHE*, *CA* and *CaM* mRNA expression

2.3.2.1 Real-time amplification

After the detection of the optimal primer concentration (*18S* 50 nM, *α-TUB* 100 nM, *NHE* 100 nM, *CA* 100 nM, and *CaM* 100 nM) a real-time amplification with *P. dumerilii* cDNA from the experimental sample set was performed. The amplifications of the *reference* and *target* genes generated products with different melting temperatures (Table 2.5), based on the length of the amplicon size. The melt-curve analysis showed for all genes a distinct peak, indicating the presence of a single qPCR product (Fig. 2.11). All negative controls did not record any amplification for both *target* and genes of interest.

The 1% agarose gel electrophoresis picture of the qPCR products showed distinct band for all genes confirming the presence of only one product (Fig. 2.10).

Table 2.5 Primer concentrations for qPCR in nM, melting temperature in °C, efficiency of amplification in % and amplification of the oligonucleotide primers for *18S*, *α-TUB*, *NHE*, *CA* and *CaM*.

<i>Target gene</i>	Primer concentration (nM)	Melting temperature (°C)	Efficiency of amplification (%)
<i>18S</i>	50	84.5	107.95
<i>α-TUB</i>	100	80	98.92
<i>NHE</i>	100	78.5	92.5
<i>CA</i>	100	80	90.42
<i>CaM</i>	100	81	104.12

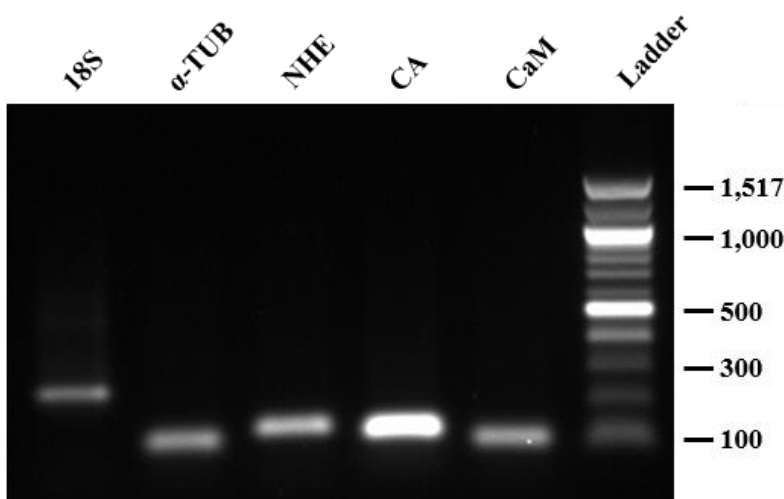


Figure 2.10 qPCR products derived from *18S*, *α-Tub*, *NHE*, *CA* and *CaM* primers sets were separated using a 1% agarose gel in TBE buffer stained with SYBR Safe DNA gel stain. A 100 bp DNA Ladder was loaded to the right of the samples.

The two *reference* genes, *18S* and *α-TUB*, showed a stable expression across both treatments. Several C_q values ($n=77$) measured for the two *reference* genes were validated by an ANOVA using GraphPad InStat v3 (GraphPad Software Inc., La Jolla, U.S.A.), as data confirmed normal distribution with the Kolmogorov-Smirnov test. No significant difference between the pH treatment and/or time points could be detected [$F(3, 73) = 0.923$, $p=0.4341$].

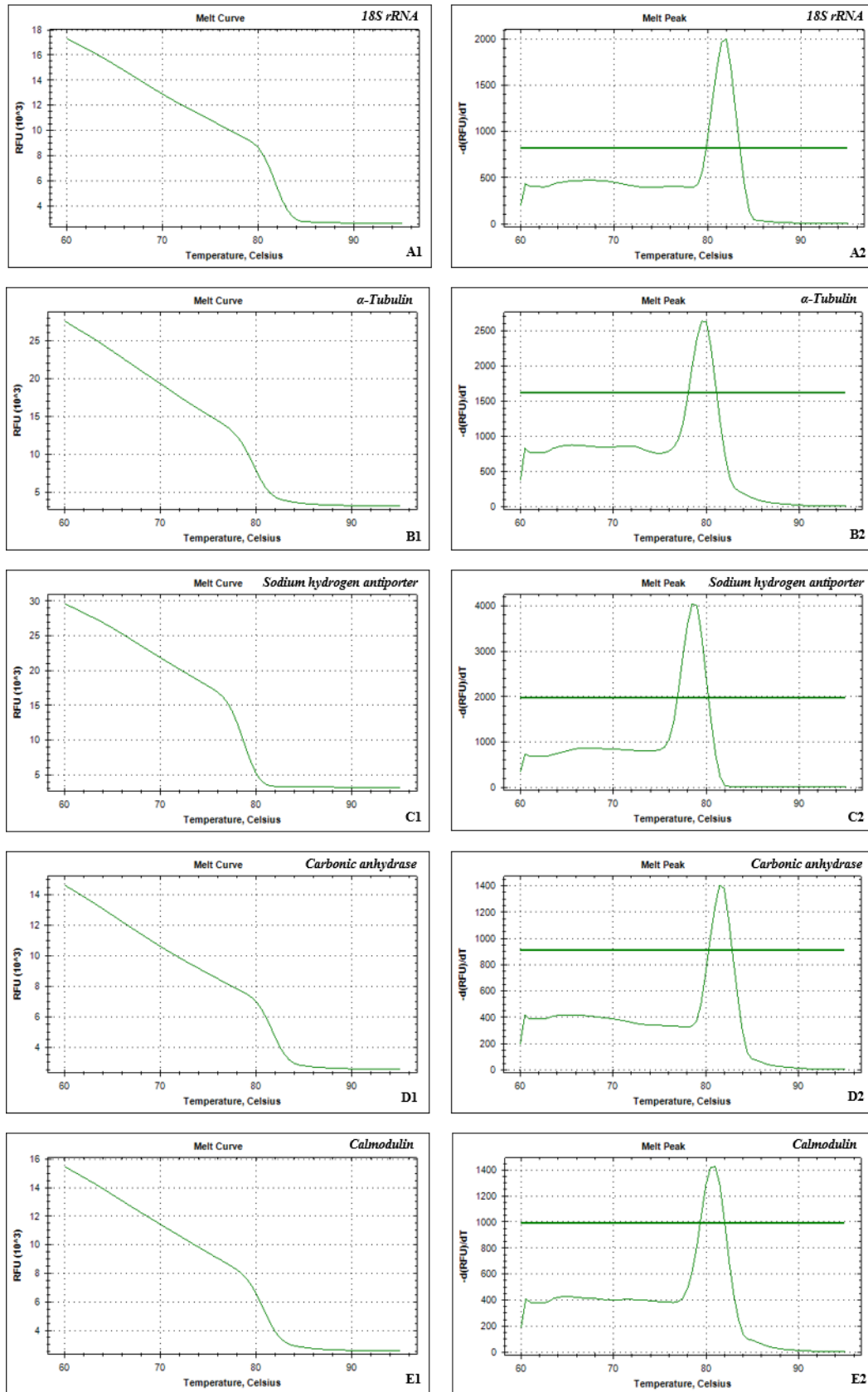


Figure 2.11 Melt curve and melt peak of the real-time amplification of *P. dumerilii* 18S (A1, A2), α -TUB (B1, B2), NHE (C1, C2), CA (D1, D2) and CaM (E1, E2).

2.3.2.2 Assay performance

For each gene a standard curve was generated to evaluate the overall amplification performance. The serial dilution of *I8S* generated a standard curve (Fig. 2.12) with an efficiency of amplification of 107.95%. The efficiency of the reaction is defined by the slope of the line of best fit. The equation is $E = 10^{(-1/\text{slope})} - 1$. The linearity of the assay is expressed by R squared (R^2). *I8S* showed an R^2 of 0.98. The efficiency of the reaction is consistent at different template concentrations if the value is close to 1 and shows therefore a linear range. For the α -*TUB* cDNA serial dilution, the amplification showed linearity with a regression coefficient of 0.99 (Fig. 2.12) and an amplification efficiency of 98.92%. For the *NHE* cDNA serial dilution, the amplification was linear with a regression coefficient of 0.97 (Fig. 2.12) and an amplification efficiency of 92.5%. The *CA* cDNA serial dilution revealed a linear amplification with a regression coefficient of 0.99 (Fig. 2.12) and amplification efficiency of 90.42%. The serial dilution of *CaM* showed linearity with a regression coefficient of 0.97 (Fig. 2.12) and an amplification efficiency of 104.12%.

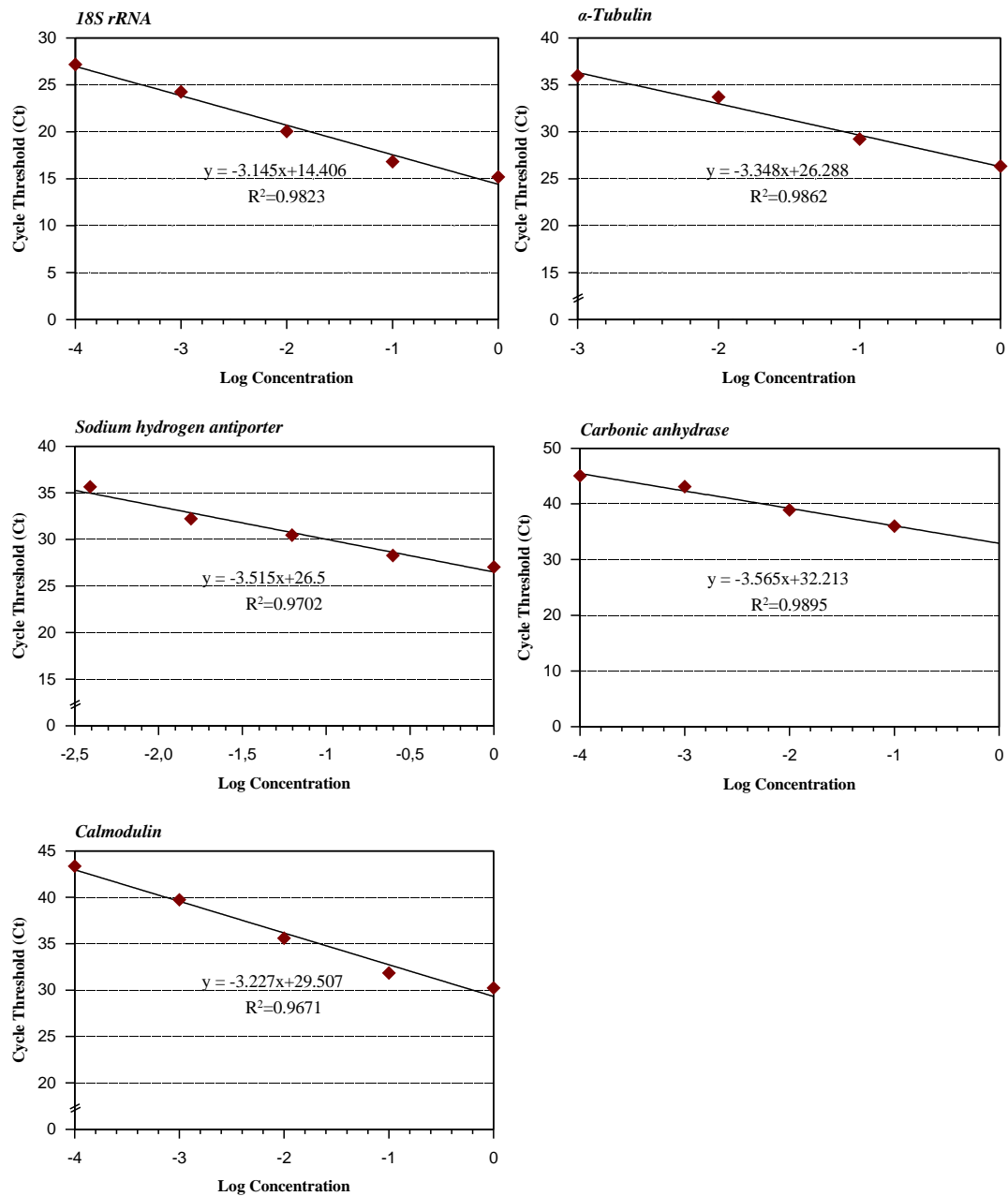


Figure 2.12 qPCR standard curves generated from *18S rRNA*, *α-TUB*, *NHE*, *CA* and *CaM* amplification data. The slope, y-intercept and correlation coefficient (R^2) of the calibration curve are presented. This is the minimum information needed for real-time PCR experiment publications stated by Bustin et al. (2009). Graphs were designed with XACT 8.03 (SciLab, Germany).

2.4 Discussion

The aim of this chapter was to isolate and characterise the three selected *target* genes *NHE*, *CA* and *CaM* from the marine polychaete *P. dumerilii*, as well as to develop and validate a quantitative assay of their expression. The primers trialled and adopted (in Table 2.1) amplified *P. dumerilii* partial *NHE*, *CA* and *CaM* cDNA sequences, which showed clear similarities with sequences available on GenBank as follows.

The potential isolated *NHE* fragment share 78% similarity with NHE2 in sperm whale *P. catodon*, rat *R. norvegicus* and a Na/H ion exchanger mRNA of another rat species *Rattus* sp.. The functional NaH exchanger domain was identified with a sequence alignment (Fig. 2.4). The obtained *CA* sequences showed the greatest similarity (76%) with a *carbonic anhydrase 9-like* sequence from the acorn worm *S. kowalevskii*. Furthermore, the functional alpha-CA domain with zinc binding sites was characterised with a sequence alignment (Fig. 2.6). Finally, the BLAST algorithm confirmed the identity of the isolated *CaM* fragment. It shared 93 % similarity with calmodulin-1 of the nematode parasite *T. spiralis*. With the help of an alignment, the EF hand, a conserved functional protein domain, could be identified (Fig. 2.8). The EF hand is a calcium-binding motif, which usually has a helix-loop-helix motif (Lewit-Bentley and Réty, 2000).

The phylogenetic analysis of the three different genes placed all sequences used for primer design within the tree of the desired gene confirming their identity (Fig. 2.5, 2.7, 2.9). The phylogeny of partial amino acid sequences for NHE, rooted to the Na⁺/K⁺ ATPase alpha subunit, showed two main branches. The first branch grouped NHEs from Insecta together, whereas the second branch included NHEs of Mammalia as well as the acorn worm and the target sequence of *P. dumerilii*. The phylogenetic tree of partial CA amino acid sequences showed two main branches one composing Mammalia and a second branch comprising several other classes of vertebrates. The β-CA 1

sequences, used as outgroup, showed a clear difference to the α -CA sequences in the tree. Using the structurally related protein sequence of parvalbumin as outgroup for the phylogenetic analysis of CaM, the clear conserved feature of the gene could be shown. Several different classes, such as Insecta, Ascidiacea and Polychaeta clustered together.

The second aim of this chapter was to develop a quantitative assay of each gene expression for the use with worms from differing exposure histories. qPCR is an advanced form of the PCR and has become a key method in modern molecular biology. It is a common method to characterise *target* gene expression patterns in different organisms. Real-time PCR is a simple method that has a high sensitivity and specificity. Therefore, it is a powerful technique to quantify a number of mRNA expression levels at the same time. As the name already describes the reaction is monitored as it occurs, hence observed and as such analysed at “real-time” (Primerdesign, 2008).

The present chapter describes the development of a quantitative method to measure the expression levels of *NHE*, *CA* and *CaM* in *P. dumerilii* using the qPCR technique. In the following chapters the method is then applied to study the putative *NHE*, *CA* and *CaM* mRNA expression levels in worms that were experimentally- and/or environmentally- exposed to different pH levels. Breaking the assay development down into individual steps and optimisations carried out, a crucial step for generating reliable gene expression profiles is the template preparation where pure, high quality RNA is needed. Therefore, a DNase treatment and DNase removal step is performed to eliminate all potential gDNA contamination of the RNA. In the present work the DNase I digestion was performed as a standard step within the RNA extraction using the High Pure RNA Tissue Kit (2.2.2). Moreover, the integrity of 18S and 28S ribosomal RNA was checked on an agarose gel stained with ethidium bromide (2.2.2). Good quality RNA will show two distinct bands (18S and 28S) whilst degraded RNA will show a smear on the gel. For

the reverse transcription a kit based on the random priming strategy was applied. Random primers have the advantage to bind to both ribosomal, as well as messenger RNA, in contrast to oligo dT primers which only bind to the polyA tail of mRNA. Random primers are particularly important in the present project, because the 18S ribosomal RNA was chosen as one of the *reference* genes (2.2.10.2).

For the normalization of qPCR reactions at least two *reference* genes should be used (Bustin et al., 2009). The present work utilised two established *reference* genes with different roles in cellular processes: *18S*, involved in ribosomal structure and α -*TUB*, taking part in cytoskeletal structure. *18S* has previously been established as a *reference* gene for *Nereis* species (Won et al., 2011; Zheng et al., 2011). The mitochondrial 18S rRNA gene is highly conserved and inherited independently from the nuclear rRNA genes (Garey et al., 1998). α -*TUB* has been validated as particularly stable in different organisms (Spanier et al., 2010; Zhai et al., 2014). It is one of the three highly conserved subfamilies of the tubulin family, and is one of the main components of microtubules, which are important for eukaryotic flagella, cilia, mitotic spindles and cytoskeleton (Keeling and Doolittle, 1996). An ANOVA based on experimental measured C_q values for the following chapter showed that the two *reference* genes *18S* and α -*TUB* showed no significant difference between pH treatments and time points, confirming their stable expression [$F(3, 73) = 0.923, p=0.4341$].

For the detection of the fluorescence signal, an intercalating dye, SYBR Green, was chosen. This dye allows the real-time PCR machine to monitor the reaction by detecting a fluorescence signal caused by the intercalation of the dye into dsDNA. During this process the structure of the dye changes and the fluorescence signal increases (PrimerDesign, 2008). The advantage of this method is that the same dye can be used with any primers and any *target*. On the other hand, intercalating dyes are nonspecific,

which means that they will bind to any dsDNA that is amplified during the reaction. Therefore, additional analyses are necessary to verify the results. Nonspecific products can be identified by performing a melt curve analysis. A specific amplification is confirmed by a single homogenous melt peak, as the melting temperature of a product is sequence specific. All chosen primers for the *target* and *reference* genes amplified a specific product and single homogenous melt peaks were produced (Fig. 2.11). Additionally, the concentration of the primers appeared to be important. High primer concentrations are likely to increase the formation of nonspecific products and primer-dimers. On the other hand, low primer concentrations could limit the reaction. Accordingly, different primer concentrations were tested to identify the concentration with best specific amplification and no primer-dimer formation. For the primer design an amplicon size between 101-239 bp and a primer length of 20 bp was chosen (Table 2.1). The primer concentrations in the final reaction with 50 nM for *18S* and 100 nM for *α-TUB*, *NHE*, *CA* and *CaM* gave the best amplification and showed no primer-dimer formation. (Table 2.5). To prevent self-complementarity and G/C clamps, too many G's and C's at the 5' and 3' ends should be avoided. The online self-complementarity check using Oligo Calc showed no potential hairpin formation or self-complementarity for any of the present primers. For the amplification of *18S*, *α-TUB*, *NHE*, *CA* and *CaM* *P. dumerilii* cDNA a single product formation was achieved.

The primer efficiencies of the genes of interest as well as the *reference* genes are highly important for the accuracy of the real-time PCR analysis. The ideal efficiency for a set of primers would be 100 %. An efficiency of 100 % means that with each cycle the amount of template is doubled. An accepted efficiency lies between 90 % and 110 % (Taylor et al., 2010) and the efficiency is calculated by a template serial dilution. The dilution is plotted against the C_q values and the slope of the graph is converted into a

percentage efficiency. A slope of -3.3 indicates an efficiency of 100 %. The efficiencies of *18S*, *α -TUB*, *NHE*, *CA* and *CaM* resided between 90.42 % and 107.95 % (Table 2.5, Fig. 2.12). Hence, all genes were suitably for the comparative C_T method.

Real-time PCR quantifications can be qualitative (presence or absence) or quantitative (copy number of DNA). For the absolute quantification the C_q value of a test sample is compared to a standard curve. The analysis shows the quantity of nucleic acid (copy number, μg) per given amount of sample (per cell, per μg of total RNA). The relative quantification analysis shows changes in gene expression in a given sample relative to a reference sample (e.g. untreated control) (Bio-Rad Laboratories, 2006). Therefore, in a relative quantification experiment, changes in gene expression are normalised to reference genes. There are different methods to determine the expression level of the *target* gene in the test sample relative to the calibrator sample (Bio-Rad Laboratories, 2006). The ΔC_T method is based on the difference between reference and target C_T values for each sample (Livak and Schmittgen, 2001). A disadvantage of the ΔC_T method is that it is based on the assumption that with every cycle the PCR product doubles. Hence, the efficiencies have to be equal, as demonstrated to be the case in the present work (Table 2.5). A method for amplicons with efficiencies that are not similar has been developed by Pfaffl (2001). Nevertheless, it is recommended to design primers with a good efficiency rather than fixing poor primers with mathematical corrections (Primerdesign, 2008).

In summary, this chapter focused on the isolation and characterization of partial sequences of *NHE*, *CA* and *CaM* cDNA from *P. dumerilii* and the designed primers were optimized for the expression analysis with qPCR. The sequences are used to develop assays of mRNA expression to examine their role in response to different pH exposures, which will be examined in the following chapter.

3.1 Introduction

The regulation of the acid-base balance in cells is essential for cellular homeostasis. In order to maintain a normal pH range, H^+ are often regulated in body fluids (Siggaard-Andersen, 2005). Most cellular processes have a small pH range within they will function, since protein conformations are altered by H^+ , and therefore their biochemical activity may be modulated (Petsko and Ringe, 2004). The activity of an enzyme decreases outside the optimum pH range and greater changes can lead to denaturation (Ochei and Kolhatkar, 2000). There are other consequences of acid-base imbalance, such as metabolic suppression (Guppy and Withers, 1999), altered oxygen binding (Jensen, 2004), muscle malfunctions (Orchard and Kentish, 1990) and impaired synaptic transmission, neurotransmitter function and receptor binding (Ahn and Klinman, 1983; Ryu et al., 2003; Sinning and Hübner, 2013). Acid-base regulation also requires energy and can therefore cause changes in the energy budget depending on the function of the tissue (Pörtner et al., 2000).

Encountering a low pH environment can therefore potentially lead to acidification of bodily fluids unless cellular mechanisms, such as ion transporting or binding proteins, are able to maintain homeostasis (Michaelidis et al., 2005). To maintain the acid-base balance, ionic transporters are required to carry the excess ions out of the body (Walsh and Milligan, 1989), and these include the cell membrane NHEs (Pörtner et al., 2000). NHEs are conserved throughout evolution, maintain pH and Na^+ homeostasis, and provide an adaptation mechanism to extreme pH environments (Hunte et al., 2005). Relevantly, NHE activities have been reported as inhibited at low pH (7.5) in the marine worm *Sipunculus nudus* relative to worms kept at pH 7.9 conditions (Pörtner et al., 2000).

CA encodes a zinc-containing enzyme that catalyses the reversible hydration of CO_2 to HCO_3^- ($\text{CO}_2 + \text{H}_2\text{O} \rightleftharpoons \text{HCO}_3^- + \text{H}^+$) (Tripp et al., 2001), regulating H^+ and HCO_3^- levels in marine organisms such as the blue crab, *Callinectes sapidus* (Henry and Cameron, 1983). The function of *CA* is well known in vertebrates, with roles in respiration, transport of $\text{CO}_2/\text{HCO}_3^-$, pH and inorganic carbon homeostasis and calcification (Bertucci et al., 2013). In the invertebrate species, *S. pistillata*, *CA* was discovered to be involved in the biomineralisation process (Moya et al., 2008) and is also influenced by HCO_3^- concentrations (Moya et al., 2012). In contrast, *CaM* is a multifunction Ca^{2+} binding protein, found in all eukaryotic cells, that triggers activation of more than 20 enzymes, and is essential in the regulation of cell proliferation and several stages of the cell cycle. Research suggests that Ca^{2+} -*CaM* is involved in the G_1/S , G_2/M and mitotic metaphase in the cell cycle (Means et al., 1991). *CaM* is considered to have functions in the larval settlement and metamorphosis of the polychaete *H. elegans*, as both processes were inhibited by the *CaM* inhibitor W7 in unsettled larvae (Chen et al., 2012b). Importantly, down-regulation of *CaM* gene expression has been detected in oysters exposed to low pH seawater induced by CO_2 perturbations (Dineshram et al., 2012). The roles that *NHE*, *CA*, and *CaM* play in maintaining acid-base balance has yet to be determined in many marine invertebrates, including Polychaeta.

The marine polychaete worm *P. dumerilii* is a model organism used for the study of molecular development (Dorresteijn, 1990; Fischer and Dorresteijn, 2004), evolution (Tessmar-Raible and Arendt, 2003), neurobiology (Jékely et al., 2008), ecology and toxicology (Hutchinson et al., 1995; Jha et al., 1996; Hardege, 1999) and, relevantly, can be found in, and perhaps adapted to, naturally occurring acidified habitats such as CO_2 vents (Cigliano et al., 2010; Calosi et al., 2013). Literature suggests that *NHE*, *CA* and *CaM* could be suitable markers of OA, due to their mechanistic involvement in other

aquatic species (Pörtner et al., 2000; Moya et al., 2008; Dineshram et al., 2012). The use of both qPCR and *in situ* hybridization can potentially provide a better understanding of acid-base regulation mechanisms in *P. dumerilii*, under experimentally altered pH environmental conditions. This chapter of work therefore investigates the gene expression of the potential acid-base regulation players, *NHE*, *CA* and *CaM*, from a non-calcifying invertebrate, *P. dumerilii*, in low pH (7.8) relative to control conditions (pH 8.2) following a 1 h and 7 d experimental exposure. *NHE* and *CA* are expected to be initially down-regulated and subsequently up-regulated under the low pH exposure regime. *CaM* is expected to show a down-regulation at both time points. Furthermore, a potential change in the expression location of *NHE* is expected under low pH conditions in *P. dumerilii* larvae.

3.2 Material and Methods

3.2.1 Animals and experimental exposure

P. dumerilii (mean mass \pm SEM: pH 8.2 worms 1 h: 13.18 ± 1.63 mg, n=10; pH 7.8 worms 1h 11.32 ± 2.06 mg, n=10; pH 8.2 worms 7 d: 12.68 ± 1.65 mg, n=10; pH 7.8 worms 7 d: 10.47 ± 1.89 mg, n=10) used were from the laboratory culture originating from the EMBL Heidelberg (Germany). All exposure experiments were conducted at the EMBL Heidelberg. The gene isolation and temporal expression experiments were accomplished with adult, yet sexually immature atokous worms to reduce metabolic variation resulting from physiological processes linked to reproduction and metamorphosis. The worm body mass was determined before the molecular analysis. For this the worms were transferred onto filter paper to remove excess of RNALater and subsequently the wet mass was measured using an analytical balance. The spatial gene expression experiments were conducted using three-segmented larvae. Before the

experiment, all specimens were kept in filtered natural seawater (~pH 8.2) at a light regime of 16 h light/ 8 h dark in a temperature controlled room at 18 °C. 20 worms were transferred into plastic containers (2000 cm³) with approximately 800 ml filtered natural seawater (salinity 35 ppt) of pH 8.2 (control) and another 20 worms were transferred into plastic containers (2000 cm³) with approximately 800 ml filtered natural seawater of pH 7.8 (treatment) kept at the same light regime and temperature. The pH was adjusted using HCl (1M) and sodium hydroxide (NaOH) (1M), and the whole water was changed every 24 h to ensure that the desired pH was maintained. After 1 h, 10 individuals from each treatment were transferred into RNALater solution (Sigma-Aldrich Company Ltd., Gillingham, UK). The remaining worms were kept for 7 d in the containers at the two controlled pH levels and then transferred into RNALater. Samples were stored at -80 °C until further processing. The two time points were selected to represent the initial stress response (1 h) and the acclimation response (at 7 d). The exposure length of 7 days has been used in a previous OA study on the sea urchin *S. purpuratus* (Stumpp et al., 2011). The very short term exposures of 1 h has not been reported in previous studies, only an exposure length of 3 h has been used (Kim et al., 2013). However, the exposure time of 1 h was chosen to ensure to monitor the initial expression response only.

For the *in situ* hybridisation investigation of gene expression localisation, 1 d post fertilized *P. dumerilii* larvae (trochophora stage) were separated from their jelly and transferred into plastic containers (100 cm³) with approximately 80 ml filtered natural seawater at a pH of 7.8 or 8.2 for 7 d at 18 °C. The light regime, pH maintenance, and water change were the same as described for the adults. *P. dumerilii* larvae were then fixed in 4 % PFA for 2 h and stored in 100 % methanol at -20 °C until hybridisation.

3.2.2 Total RNA isolation and purification from worm tissue

From each worm total RNA was extracted using the High Pure RNA Tissue Kit (Roche, Burgess Hill, UK), as described in section 2.2.2. The integrity of total RNA was analysed on denaturing TAE agarose gel stained with ethidium bromide (see section 2.2.2.). The pure RNA was stored at -20 °C until further processing.

3.2.3 Synthesis of cDNA

Using the SuperScript VILO cDNA Synthesis Kit (Life Technologies, Paisley, UK) cDNA was synthesised from total RNA. 4 µl 5× VILO™ Reaction Mix, 2 µl 10× SuperScript® Enzyme Mix were gently mixed with 14 µl of RNA (pH 8.2 1 h: 0.52 ± 0.077 µg, pH 7.8 1 h: 0.51 ± 0.077 µg; pH 8.2 7 d: 0.46 ± 0.069 µg, pH 7.8 7 d: 0.41 ± 0.060 µg) and incubated at 25 °C for 10 min, followed by 60 min at 42 °C and 5 min at 85 °C. To degrade remaining RNA template RNase H (5 U/µl) (Thermo Scientific, Loughborough, UK) was used as described in section 2.2.2.

3.2.4 Target gene isolation and characterisation

The characterised primer sequences for *18S*, *α-TUB*, *NHE*, *CA* and *CaM* described in section 2.2.4 were used in this experiment. To amplify *NHE*, *CA* and *CaM* cDNA all *target* genes were run in a PCR. The PCR products were visualised on an agarose gel to confirm a single, correctly-sized band. The DNA concentration of the samples was measured with a Qubit™ fluorometer (Life Technologies, Paisley, UK) and the PCR products were sequenced directly (Macrogen Europe, the Netherlands). For more detail see Chapter 2.

3.2.5 Amplification using qPCR

For the qPCR reactions a CFX96 Real Time PCR Detection System (Bio-Rad, Hemel Hempstead, UK) was used to detect amplification. To amplify the cDNA 10 μ l of qPCR Fast Start SYBR Green Master Rox (Roche, Burgess Hill, UK), 1 μ l of cDNA and 2 μ l of primers (*18S* 50 nM; α -*TUB*, *NHE*, *CA*, *CaM* 100 nM) (Table 2.1) and 7 μ l molecular grade water (Thermo Fisher Scientific, Loughborough, UK) were used to make up a final reaction volume of 20 μ l. For each gene a control lacking reaction was included to determine the target cDNA amplification specificity. After an initial denaturation at 95 °C for 2 min all reactions were carried out in the following 45 cycles: Denaturation at 95 °C for 10 s, annealing at 60 °C for 1 min and an extension step at 72 °C for 1 min. In order to create the melt curve, a temperature gradient was created from 60 °C to 95 °C. As described in the previous chapter, *18S* and α -*TUB* were used as *reference* genes.

3.2.6 Statistical analyses

Statistical analyses were conducted using GraphPad InStat v3 (GraphPad Software Inc., La Jolla, U.S.A.). Significance for relative gene expression was tested using an unpaired *t*-test, as the data showed a normal distribution with the Kolmogorov-Smirnov test. Outliers were identified, and removed, if they differed by more than twice the standard deviation of the mean. For each *NHE* (pH 7.8; 1 h) and for *CA* (pH 8.2; 1 h, 1 w) one value was identified as an outlier and excluded from the statistical analysis. For all analyses, statistical significance was accepted at $p < 0.05$. Values are presented as means \pm SE. All graphs were designed with XACT 8.03 (SciLab, Germany).

3.2.7 *In situ* hybridisation of *NHE*

3.2.7.1 Experimental animals

1 dpf *P. dumerilii* larvae were separated from their jelly and transferred into plastic containers (100 cm³) with approximately 80 ml filtered natural seawater (salinity 35 ppt) at a pH of 7.8 or 8.2 for 7 d at 18 °C. The light regime, pH maintenance, and water change were the same as described for the adults (see section 3.2.1).

3.2.7.2 Probe synthesis

3.2.7.2.1 Oligonucleotide primer design

Following the procedure described in section 2.2.4 primers for the *NHE_{Probe}* were designed with a product length of 803 bp (Table 3.1).

Table 3.1 Oligonucleotide primer of *NHE_{Probe}* for *in situ* hybridisation with sequence and amplicon size in bp.

<i>Target gene</i>	Forward primer (5'-3')	Reverse primer (5'-3')	Amplicon size (bp)
<i>NHE_{Probe}</i>	TCATGACAGCCATGGTCCTA	ACGTCAGGTATCCGAAGGTG	803

The oligonucleotide primers were synthesised by Sigma-Aldrich (Seelze, Germany) and delivered in lyophilised form. The primers were then resuspended in molecular grade water to a concentration of 100 pmol/μl. For the PCR the primers were further dilute with water in a ratio of 1/10 to give a final concentration of 10 pmol/μl.

3.2.7.2.2 Amplification of DNA by PCR

For the generation of *NHE_{Probe}* PCR products, 1 μl of cDNA (representing a mixture of different stages of *P. dumerilii*) was combined with 1 μl of 10 pmol/μl forward and reverse primer (Table 3.1), 0.12 μl (5 U/μl) of HotStar Taq Polymrerase (Qiagen, Hilden,

Germany), 1.2 µl 10× PCR buffer (Qiagen, Hilden, Germany), 0.5 µl 40 mM dNTP mix (Thermo Fisher Scientific, Schwerte, Germany), 0.5 µl 25 mM MgCl₂ (Thermo Fisher Scientific, Germany) and 17.68 µl sterile nuclease-free water (Thermo Fisher Scientific, Schwerte, Germany) with a total reaction volume of 25 µl. The following PCR conditions were used: initial denaturation at 95 °C for 15 s, followed by 35 cycles of denaturation at 95 °C for 30 s, annealing at 50 °C for 30 s and extension at 72 °C for 1 min, finishing with a final extension of 72 °C for 10 min.

3.2.7.2.3 Agarose gel electrophoresis of DNA

To visualise the PCR product an agarose gel electrophoresis was conducted as described in section 2.2.6. The gel was run using a current of 110 V for 45 min.

3.2.7.2.4 Purification of PCR product

To purify the PCR product the QIAquick PCR Purification kit (Qiagen, Hilden, Germany) was used. 100 µl of buffer PB that contains a high concentration of guanidine hydrochloride and isopropanol (exact composition is confidential and therefore not provided by Qiagen) was added to 20 µl of PCR product and mixed. The sample was then applied to the QIAquick column and centrifuged for 30 s at 17,900× *g*. The flow-through was discarded and then 750 µl Buffer PE (the composition of Buffer PE is confidential) added to the column and centrifuged for 30 s. The flow-through was discarded and the column spun again. Afterwards the column was placed in a clean 1.5 ml microcentrifuge tube and the DNA was eluted with 30 µl of water by centrifugation at 17,900× *g* for 1 min.

3.2.7.2.5 TOPO[®] TA Cloning reaction –Ligation and Transformation

In order to sub clone PCR products TOPO[®] TA Cloning[®] Kit reagents and protocol (Invitrogen, Life Technologies, Germany) were used. 4 µl of the purified PCR product was mixed with 1 µl salt solution (1.2 M NaCl, 0.06 M MgCl₂) and 0.25 µl (25 ng/µl in 10 mM Tris-HCl, 1 mM EDTA, pH 8) TOPO[®] vector (pCR[®]2.1). After 30 min incubation at room temperature (~22 °C), 2 µl of the TOPO[®] cloning reaction was added to One Shot[®]Top10 competent *E. coli* cells (ElectrocompTM). The cells were then incubated for 30 min on ice and subsequently heat-shocked for 30 s at 42 °C and then immediately transferred on ice. 250 µl of LB medium (10 g tryptone, 5 g yeast extract, 10 g NaCl in 950 ml deionized water) was added to the cells. This was followed by horizontally shaking for 37 °C for 1 h. Finally, 40 µl of bacteria was added to LB-plates containing kanamycin (25 mg/ml using 2 µl per 1ml media) and X-Gal (20 mg/ml using 40 µl per 25 ml LB agar plate). The bacteria were spread on the plates by shaking with solid, glass beads.

3.2.7.2.6 Overnight culture

White colonies, indicating inserts, were picked from the LB-plates using aseptic technique and each colony was inoculated into 5 ml LB medium (10 g tryptone, 5 g yeast extract, 10 g NaCl in 950 ml deionized water) with ampicillin (50 mg/ml). The LB medium was then left to shake at 37 °C overnight.

3.2.7.2.7 Plasmid DNA isolation

5 ml of the overnight bacteria culture was transferred into an Eppendorf tube and centrifuged for 1 min at 13,000× g. The supernatant was removed and 300 µl of buffer P1 (50 mM Tris pH 8.0, 10 mM EDTA, 100 µg/ml RNase A) was used to resuspend the

pellet. Next, 300 μl of lysis buffer P2 (200 mM NaOH, 1 % SDS) was added, the tube inverted 5 \times and then incubated for 3 min at room temperature ($\sim 22\text{ }^{\circ}\text{C}$). 300 μl of neutralization Buffer P3 (3.0 M potassium acetate, pH 5.5) was added and the tube inverted 5 \times . The mixture was centrifuged at maximum speed for 10 min, the supernatant transferred to a new Eppendorf and 550 μl of isopropanol added. Everything was mixed by inversion. The contents were centrifuged at 13,000 $\times g$ and the supernatant removed. This was followed by a washing step with 500 μl of 80 % ethanol and centrifugation at maximum speed for 3 min. Then the supernatant was removed and the pellet air dried. Finally the pellet was resuspended in 50 μl H₂O.

3.2.7.2.8 Quantification of DNA

The concentrations of the plasmid DNA was measured with a NanoDrop 3300 Fluorospectrometer (Thermo Scientific, Schwerte, Germany), giving a concentration of 956.1 ng/ μl .

3.2.7.2.9 Sequencing

50 ng/ μl sample with the associated primer in a total amount of 20 μl was sent to GATC Biotech (Konstanz, Germany). Depending on the concentration H₂O was added to the sample. The sequence was checked and edited as described in section 2.2.8.

3.2.7.2.10 Vector opening and clean up from enzymatic reaction

20 μl of the plasmid (14.12 ng of DNA) was mixed with 4 μl *NotI* restriction enzyme (5 U/ μl) (Thermo Fisher Scientific, Schwerte, Germany), 5 μl of 1 \times Buffer O (50 mM Tris-HCl (pH 7.5 at 37 $^{\circ}\text{C}$), 10 mM MgCl₂, 100 mM NaCl, 0.1 mg/mL BSA) and 11 μl H₂O and left at 37 $^{\circ}\text{C}$ overnight. For the cleanup of impurities from the DNA the

QIAquick[®] Nucleotide Removal Kit (Qiagen, Hilden, Germany) was used. 200 μ l of Buffer PNI (the composition of Buffer PNI is confidential) was mixed with 40 μ l of the sample and applied to the QIAquick spin column. The column was centrifuged at 6.000 rpm for 1 min and the flow-through discarded. In the next step, 750 μ l of Buffer PE (the composition of Buffer PE is confidential) was added and the column centrifuged at 6000 rpm. Once again the flow-through was discarded and the column centrifuged for another min. Then the column was placed in a new 1.5 ml microcentrifuge tube and eluted twice with 20 μ l of pre-warmed H₂O. The concentration was measured as described in section 3.3.2.8.

3.2.7.2.11 RNA-probe preparation

1 μ g of DNA was mixed with 2 μ l 100 mM dithiothreitol (DTT), 1.3 μ l NTP mix (15.4 mM each ATP, CTP, GTP, and 10 mM UTP), 0.7 μ l 10 mM DIG-UTP, 0.5 μ l RNase inhibitor (4 U/ μ l), 1 μ l of Polymerase T7/SP6 (20 U/ μ l) and 2 μ l 10 \times transcription buffer. Everything was adjusted to a total volume of 20 μ l and incubated at 37 °C for 6 h. After the incubation 1 μ l DNase I (1 U/ μ l) was added to the sample and incubated at 37 °C for 1 h. The next step was the purification with the RNeasy Mini Kit reagents and protocol (Qiagen, Hilden, Germany). 80 μ l of H₂O, 350 μ l Buffer RLT (high concentration of guanidine isothiocyanate, exact composition is confidential) and 250 μ l of ethanol (96 %) were added. The solution was transferred to an RNeasy spin column and centrifuge for 20 s at 14,000 rpm. The flow-through was discarded. After centrifugation 700 μ l of buffer RW1 (guanidine salt and ethanol, exact composition is confidential) was added and the column centrifuged at 14,000 rpm. After the flow-through was discarded, 500 μ l of RPE Buffer (composition of Buffer RPE is confidential) was added and the column centrifuged at 14,000 rpm. In the final step, the RNA was

eluted twice in 20 µl of RNase free water and the success of the cleaning was checked by measuring the concentration on a spectrophotometer at 260 nm and also by using an agarose gel.

3.2.7.3 Preparation of larvae and fixation

Larvae were passed through a filter (nylon netting with 100 µm mesh diameter) for collection and washed with filtered natural seawater. Afterwards they were passed into MgCl₂ (7.5 %) and filtered natural seawater in a 50 %/50 % concentration for 1 min. Directly after the larvae were transferred into a well-plate prepared with PFA 4 %. The plate was left on a rocking plate for 2 h. This was followed by 3 washes with PTW (phosphate-buffered saline (PBS) with 0.1 % Tween[®] 20) and the transfer of the animals into a 1.5 ml Eppendorf tubes. The PTW was replaced by methanol and shaken for 20 min. Afterwards the animals were left to sink to the bottom and the upper phase was removed and more methanol was added. This step was repeated 3×. The embryos were stored in methanol at -20 °C until further processing.

3.2.7.4 Rehydration and ProtK digestion

The fixation was followed by the rehydration of the animals in different methanol/1× PTW (PBS with 0.1% Tween[®] 20) dilutions (25 % PTW, 50 % PTW, 75 % PTW, and 2× 100 % PTW). The next step was the ProteinaseK (100 µg/ml) digestion in PTW for 2 min, followed by two rinses with glycine in PTW and a 5 min wash in 1 % triethanolamine. After that a 5 min wash in 1 % triethanolamine with 0.5 % acetic anhydride and two 5 min washes in PTW were performed. Then the animals were fixed in 4 % PFA/PTW for 20 min and washing in PTW 5× for 5 min each.

3.2.7.5 Hybridisation

Animals were transferred into a new 1.5 ml Eppendorf tubes and prehybridised in hybridisation mixture (50% formamide (Fluka, ultra pure), 5× standard saline citrate (SSC) (0.75 M NaCl, 0.075 M Sodium citrate, pH 7.0), 50 µg/ml heparin, 0.1% Tween[®] 20, 5 mg/ml *Torula* RNA (Sigma, St. Louis, MO, U.S.A.)) for 1 h at 65 °C. The probe was denatured at 80 °C for 10 min in hybridisation mixture. Finally the hybridisation was carried out at 65 °C overnight. The next step was to wash the specimens at 65 °C, twice in 50 % formamide/ 2× SSCT (standard saline citrate (SSC) containing 0.1% Tween[®] 20) for 30 min, once in 2× SSCT for 15 min, and twice in 0.2× SSCT for 30 min.

3.2.7.6 Primary Staining

After the hybridisation washes, larvae were blocked for 1 h with 5 % sheep serum in PTW at room temperature (~22 °C) on a rocking plate. After adding pre-absorbed anti-DIG-AP F_{ab} (in 5 % Sheep Serum/PTW) at a 1:2000 dilution and anti-acetylated tubulin at 1:250 dilution, the specimens were incubated at 4 °C overnight. Specimens were washed by shaking in PTW 6× and equilibrated 2× 5 min in staining buffer (100 mM TrisCl, pH 9.5, 100 mM NaCl, 50 mM MgCl₂, 0.1 % Tween20) while shaking. Larvae were transferred into a well plate and NBT/BCIP (337.5 µg/ml NBT and 175 µg/ml BCIP; Boehringer Ingelheim) staining buffer was added. The staining was carried out in the dark and the staining process was monitored frequently under a microscope. Finally, the specimens were washed in PTW 3× for 5 min.

3.2.7.7 Analysis of staining

Bright field images were taken with a Zeiss Axiophot microscope (Carl Zeiss, Jena, Germany) and a 200-fold magnification was used.

3.3 Results

3.3.1 qPCR analysis of *NHE*, *CA* and *CaM* mRNA expression

The expression level of each target mRNA was analysed in worms maintained in normal or low pH conditions using qPCR (Fig. 3.1). *NHE* was significantly down-regulated at the $p < 0.05$ level after 1 h ($t(17) = 2.154$; $p = 0.0459$), but subsequently up-regulated after 7 d ($t(18) = 2.122$; $p = 0.0480$) of treatment (Fig. 3.1 a). *CA* mRNA expression showed a down-regulated trend ($t(17) = 1.759$; $p = 0.0966$) after 1 h treatment, yet no clear trend was detected after 7 d of treatment ($t(17) = 0.271$; $p = 0.7896$) (Fig. 3.1 b). *CaM* gene expression showed no statistically significant difference between pH treatments at any of the two time-points (1h: $t(18) = 1.007$; $p = 0.3273$ and 7d: $t(18) = 0.4709$; $p = 0.6434$) (Fig. 3.1 c).

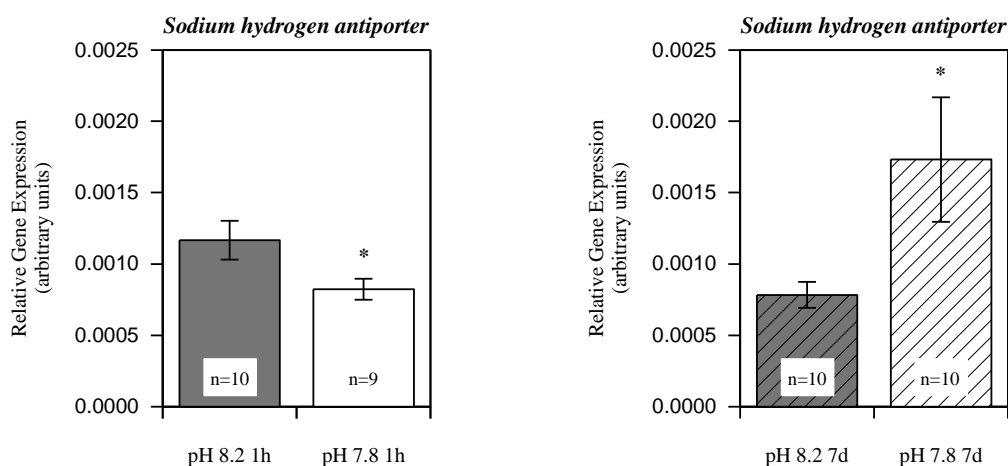
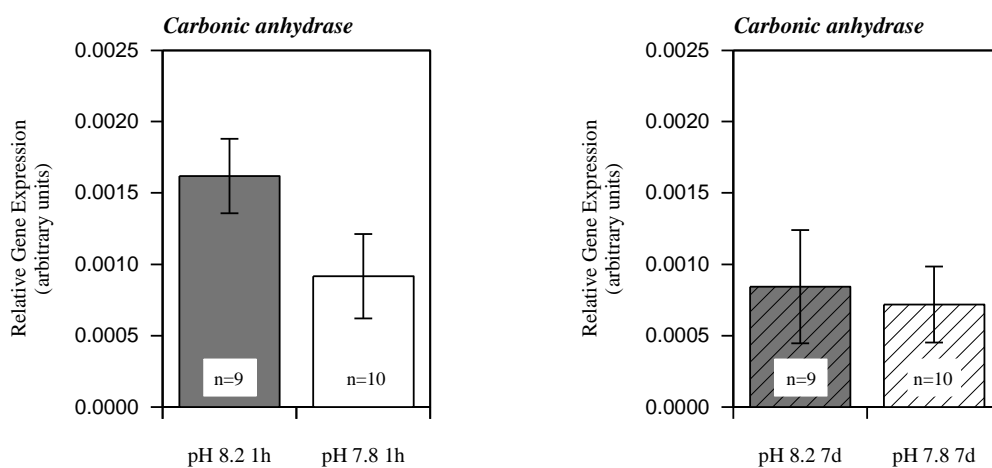
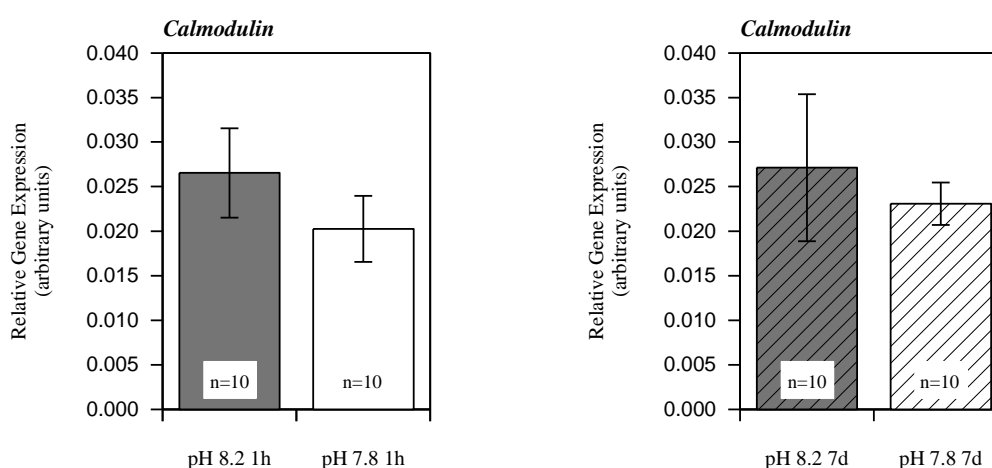
a) *NHE*b) *CA*c) *CaM*

Figure 3.1 Normalised average relative mRNA transcription \pm standard error of the mean in *P. dumerilii* for (a) *NHE* (b) *CA* and (c) *CaM* after 1 h and after 7 d in seawater with pH 8.2 and pH 7.8. Analysis was performed by unpaired *t*-test. * indicates significant differences ($p < 0.05$) of mRNA transcription between pH 8.2 and pH 7.8.

3.3.2 *In situ* hybridisation of *NHE*

The *NHE* transcript was localised via *in situ* hybridisation in 7 dpf old larvae kept at pH 8.2 and pH 7.8 (Fig. 3.2). Figure 3.2 shows the *in situ* hybridisation results obtained with the 803 bp *NHE*-specific probe. 13 out of 16 (81.25 %) larvae kept at pH 8.2 (Fig. 3.2 a and b) displayed a signal in the parapodia, as well as areas of the antennae and palpi. Pictures c and d (Fig. 3.2) shows the hybridisation with the same probe after 7 d in pH 7.8. 14 out of 16 (87.5 %) larvae showed the following pattern: Similar to samples of pH 8.2, parapodia displayed a signal along with the antennae and palpi, though the stained area is bigger. Additionally there could be a signal detected in the area of the protodeum.

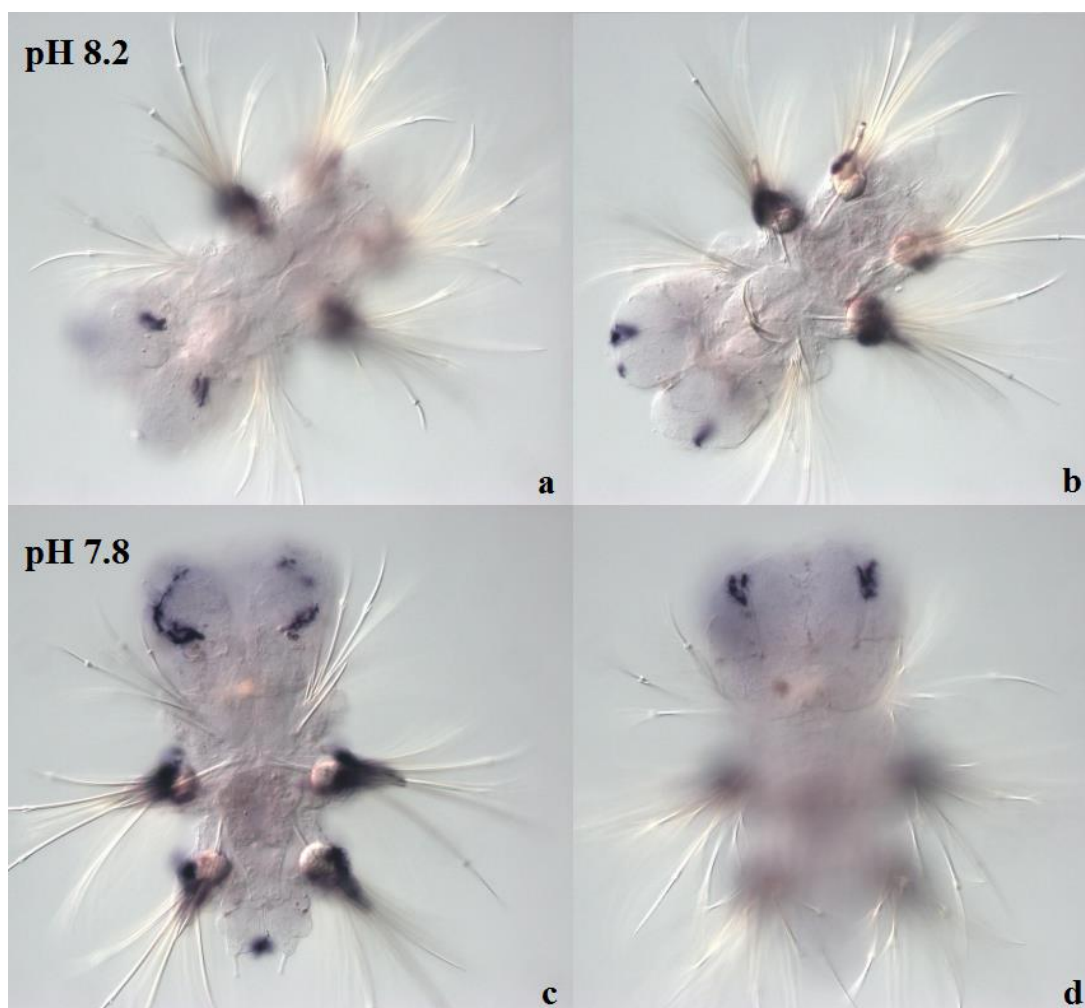


Figure 3.2 Localized *NHE* expression in 7 dpf larvae maintained at pH 8.2 (a and b) and pH 7.8 (c and d). Bright-field images were taken using a Zeiss Axiophot microscope with a 200× magnification (Carl Zeiss, Jena, Germany).

3.4 Discussion

The present chapter examined selected molecular-level biological effects of acidified seawater (pH 7.8) on adult, atokus marine polychaete, *P. dumerilii*. *NHE*, *CA*, and *CaM* partial sequences were isolated and their mRNA expression analysed in worms kept at acidified and normal pH seawater. These *target* genes represent several of the four general coping mechanisms for changing CO₂ and H⁺ concentrations: namely passive intra- and extracellular fluids buffering; ion exchange and transport; transport of CO₂ in the blood if respiratory pigments exist; and change to a stage of metabolic suppression lasting until normal environmental conditions are restored (Fabry et al., 2008). Each of the partial sequences isolated from *P. dumerilii* (see: PLATYpopsys database: <http://hydra.cos.uni-heidelberg.de/pps/>) showed similarity to a range of other species counterparts, as well as conserved domains, confirming their likely identities.

The expression of each gene was investigated in *P. dumerilii* kept at normal (8.2) and at low (7.8) pH, at two time points of 1 hour and 7 days. The seawater low pH treatment was achieved using acid adjustment, to gain a better general understanding of mechanisms involved in internal pH regulation. Following this simulated low pH exposure regime, *NHE* expression showed a significant initial down-regulation at 1 hour, followed by a subsequent up-regulation at 7 days. *CA* and *CaM* showed no statistically significant changes at either time point relative to the control pH samples (Fig. 3.1 b and c).

The significant up-regulation of the NHE transport protein after 7 days suggests that the activity of existing protein levels were insufficient to regulate the pH under low pH conditions, and that an increase in *NHE* was required to maintain the acid-base balance. Stumpp et al. (2011) report *NHE3* expression level changes in sea urchin, *S. purpuratus*, pluteus larvae, kept at pH 7.7 for 2, 4 and 7 days post-fertilization (Stumpp et al., 2011).

After 2 days an up-regulation in *NHE3* was detected followed by a down-regulation of 45 % after 4 days (Stumpp et al., 2011). In contrast, a different study conducted on the same species showed no change in NHE expression under acidified conditions (pH 7.88-7.96) within <72 hours (Todgham and Hofmann, 2009). In line with our result, the gene expression of *NHE* in the Japanese medaka fish, *O. latipes*, showed an up-regulation in different ontogenetic stages (embryos, hatchlings, adults) as well as different tissue (gill, intestine) (pH 7.1-7.6) (Tseng et al., 2013). Each of these *NHE* expression studies discussed were, however, conducted using CO₂ modulated pH and the molecular level changes observed may have been triggered through different acid-base balance mechanisms compared with the acid modulated pH change used in the present study.

Perhaps surprisingly, neither gene expression of *CaM* nor *CA* changed significantly at altered pH in the worms studied, although *CA* mRNA expression did show an initial down-regulated trend ($p=0.0966$) after 1 hour treatment (Fig. 3.1 b). This agrees with a study using the coral *A. millepora*, using CO₂ altered pH conditions, where membrane associated and secreted *CA* were expressed at lower levels in elevated $p\text{CO}_2$ conditions after 3 days (Moya et al., 2012). Furthermore, a recent study on the polychaete *Sabella spallanzanii* showed a decrease in the *CA* concentration after a 5 day low pH exposure in a CO₂ vent (Turner et al., 2015). In contrast, *CA* expression in a second coral species, *P. damicornis*, was found to be up-regulated at pH 7.8 and 7.4 after a significantly longer exposure time of 3 weeks using CO₂ driven pH changes (Vidal-Dupiol et al., 2013).

That no significant changes in *CaM* expression were detected is in contrast to a number of other studies using calcifying organisms, such as oyster and coral. *CaM* expression has been previously reported as down-regulated in Pacific oyster (*C. gigas*) larvae and coral (*A. millepora*), in response to low pH seawater exposure induced using

CO₂ (*C. gigas*: pH ~7.5 for 6 days; *A. millepora*: pH 7.8-7.9 and 7.6-7.77 for 10 days) (Dineshram et al., 2012; Kaniewska et al., 2012). In the commercial oyster, *C. hongkongensis*, CaM was discovered to be significantly down-regulated at moderate low pH (7.9) and slightly up-regulated at low pH (7.6) (Dineshram et al., 2013). The comparison between the calcifying species, *C. gigas*, *A. millepora* and *C. hongkongensis* and *P. dumerilii*, a non calcifying species, may suggest that the expression of *CaM* under low pH conditions is more important for calcification / biomineralisation processes rather than any other stages in the cell cycle. Alternatively, the CO₂ driven pH change may trigger a change in *CaM* expression, via hypercapnia induced cellular processes, that are not responsive to the acid manipulated pH changes used in this study.

Possible explanations for a lack of significant changes in *CaM* or *CA* expression herein may relate to tolerance towards exposure to a relatively acidified environment and relative ion regulatory capacity or isoform differences. There is some evidence to indicate that *P. dumerilii* is more tolerant to low pH than calcifying species based on its occurrence in CO₂ vents in the Tyrrhenian Sea (Cigliano et al., 2010; Calosi et al., 2013). It has been shown that the species reside in naturally low pH environments, although it remains unclear whether they spend their entire life cycle in these areas or just inhabit them for a period of time. Another relevant factor is that adaptability towards environmental changes may vary according to different life stages, whereby many studies focus on early life history stage (O'Donnell et al., 2010; Zippay and Hofmann, 2010; Wong et al., 2011). In cuttlefish *Sepia officinalis*, early life stages were affected by elevated *p*CO₂ and Hu et al. (2011) hypothesize that 'hypercapnia' causes metabolic depression, diverting energy towards ion regulation processes, and diverting it from embryonic growth (Hu et al., 2011). Thus, it is possible that *P. dumerilii* larvae may respond differently to low pH compared to adults, as such further studies using atokous stages are needed to clarify such

questions. A field investigation would also clarify whether acid-base impacts observed in the aquaria-reared worms are similar in worms sampled directly from the environment. Further studies would also be required to establish whether different isoforms of each gene exist in this, and other species, and any subsequent account for differing activities. The localization of transcripts via *in situ* hybridisation contributes to a better understanding of their potential molecular mechanisms of action (Dale et al., 2012; Moya et al., 2012). This study examined the expression patterns of *NHE* in 7 dpf old larvae using the same pH treatment (pH 8.2 and pH 7.8) regime, indicating differences in the *NHE* expression localization (Fig. 3.2). A pH-induced localization change, of glutamate decarboxylase, has previously been reported in the bacterium *E. coli* (Capitani et al., 2003). The novel *NHE* expression detected in larvae kept at low pH near the anus area (Fig. 3.2 c) is interesting since the anal papillae from *A. aegypti* larvae take up Na^+ and Cl^- ions by Na^+/H^+ and $\text{Cl}^-/\text{HCO}_3^-$ exchange (Stobbart, 1971). Studies using the teleost fish (*Opsanus beta*) showed that the intestinal epithelium plays a major role in acid-base relevant ion transport (Grosell and Genz, 2006; Grosell et al., 2009a, Grosell et al., 2009b; Wilson et al., 2009). It thus appears that such additional changes take place around the protodeum area in *P. dumerilii*. It would be interesting to examine if the expression pattern is changing with the different larvae stages, however, due to lack of time and resources it was not possible to investigate this question within the present project.

The molecular underpinning mechanisms of internal pH regulation are largely uncharacterised in many marine organisms. Herein, *NHE*, *CA* and *CaM* partial cDNA sequences from *P. dumerilii* were isolated and their expression in worms kept at normal and low seawater pH examined. After 7 days, *NHE* expression was higher, and localized in different tissues, in worms kept at low pH levels compared to worms at normal pH levels. This indicates that under low pH conditions at least one active proton-ion transport

mechanism is affected presumably in order to cope with the environmental changes taking place. These results reinforce the previous hypothesis that *NHE* is initially down-regulated and subsequently up-regulated (see page 89), and that the expression location is changed in the worm larvae. However, the hypothesis could not be proved for *CA* and *CaM*. This chapter provides a first insight into the molecular mechanisms of action involved in seawater acidification in the non-calcifying marine model organism *P. dumerilii*.

3.5 Conclusions

The effects of short-term low pH, mainly induced by CO₂ gas, have been studied in a wide range of aquatic species, primarily focusing on calcifying organisms, yet the molecular underpinning mechanisms are still uncharacterised. In this chapter the mRNA expression of *NHE*, *CA* and *CaM* was examined in *P. dumerilii* kept at normal and low (acid-induced) seawater pH. After 7 days, *NHE* expression was significantly higher in worms kept at low pH levels compared to worms at normal pH levels. This indicates that under low pH conditions at least one active proton-ion transport mechanism is affected in order to cope with the environmental changes taking place. Furthermore, a trend in the relative gene expression of *CA* could be shown after 1 hour. The down-regulation of the gene indicates a change in the interconversion of CO₂ and HCO₃⁻. Further investigation is required to understand the importance of *CA* in *P. dumerilii*. The relative gene expression of *CaM* showed no significant result or changing trend with the pH treatment. Further experiments are needed to interpret these findings. Additionally to the relative gene expression of *NHE*, its expression location was studied in larvae kept at low and normal pH conditions. The results show that not only the expression levels are altered but also its expression location is changed in acidified seawater. This suggests that more

changes, other than just the quantity of gene transcripts, take place. However, further investigation is required to gain a clearer understanding of the molecular genetic mechanisms involved in acidification. This chapter provides a first step to understand acid-base regulation in the marine worm *P. dumerilii* and could potentially be used as a starting point to continue examining acid-base regulation processes in marine Polychaeta.

4.1 Introduction

The regulation of the acid-base status is an essential task for animals in order to maintain homeostasis. Deviation from normal pH values can reduce the metabolic performance, due to optimum pH requirements of metabolic pathways (Heisler, 1988). The everyday production of H⁺ or OH⁻ ions in animals' body fluids, is regulated by excretory organs to keep the pH of body compartments in the required pH range (Heisler, 1984). Monitoring acid-base mechanisms in animals can help to understand their ability to maintain homeostasis under environmental altered pH conditions.

The mechanisms involved in acid-base regulation in vertebrates follow the same principle, however the use of such processes can greatly vary in their extent (Heisler, 1988). The balancing of ion exchange with the environment across epithelia of the integument, gut and excretory organs is essential for any animal (Barnhart, 1992). The regulation of the blood pH is very important in humans (Emminger, 2005). For this different metabolic mechanism can be applied: H⁺ excretion, bicarbonate reabsorption and production of ammonia in the kidney. Furthermore, the respiratory regulation is important for a stable pH in the organism (Emminger, 2005). In fish and crustaceans this exchange mainly takes part via the gills (Barnhart, 1992). Up to date, there is very little knowledge about the mechanism of acid-base regulation in polychaetes. In contrast, the ion and acid-base regulation mechanisms in fish are well studied (Heisler, 1988; Goss et al., 1992; Claiborne et al., 2002; Perry et al., 2003). In the rainbow trout, *Oncorhynchus mykiss*, and brown bullhead, *Ictalurus nebulosus*, acid base regulation is maintained by adjustment of Na⁺ and Cl⁻ net fluxed across the gills (Goss et al., 1992).

For this three different branchial mechanisms are used: 1) Changes in the Na^+ and Cl^- effluxes, whereby the flux rates are determined by external ion concentration (Na^+ , Cl^-), as well as the internal counterion (H^+ , HCO_3^-) providing an automatic negative feedback, 2) Alteration of internal substrate (H^+ , HCO_3^-) availability, 3) Adjustment of the morphology of the gill epithelia such as changing the availability of $\text{Cl}^-/\text{HCO}_3^-$ exchange mechanism by physical covering/ uncovering of certain areas (Goss et al., 1992). Furthermore, NHE and vacuolar-type H^+ -ATPase were highlighted as transporters involved in the acid-base ion transfer (H^+) from fish into the environment (Claiborne et al., 2002). Crustaceans, a large group of arthropods, use both intracellular buffering and transmembrane exchange of acidic/base equivalents including $\text{Na}^+/\text{H}^+/\text{HCO}_3^-/\text{Cl}^-$ mechanisms and Na^+/H^- exchanger as compensatory strategy (Wheatly and Henry, 1992). Aquatic crustacean species use mainly electro-neutral ion exchangers (Na^+/Cl^-) at the branchial epithelium. Species that produce urine use also the renal tubule (Wheatly and Henry, 1992).

The impact of changing pH in the environment on acid-base regulation in polychaetes is not known. A study on cuttlefish *S. officinalis* exposed to low pH induced by CO_2 gas flow reported a fast increase in HCO_3^- concentration in blood achieved by active ion-transport processes in order to compensate the respiratory acidosis. Only a minor increase in intracellular pH could be observed, indicating an efficient pH regulation (Gutowska et al., 2010). In contrast, the coelomic fluid of the sea cucumber *Holothuria scabra* and *H. parva* was negatively affected by reduced seawater pH and led to extracellular acidosis. Such an uncompensated acid-base balance could have negative impacts on both species (Collard et al., 2014). In fish, effects on the gills have been reported as follows. An increase in number and turnover of ion-transporting cells, elevating mucus production and recruiting leukocytes have been observed (Kwong et al.,

2014). Furthermore, a breakdown in gill structure and suffocation through mucus accumulation could be shown in the brook trout *Salvelinus fontinalis* (Packer and Dunson, 1972). Yet, the main effect of acid exposure is the inhibition of active Na⁺ uptake and an increase in passive losses (Kwong et al., 2014).

The suppression subtractive hybridization (SSH) technique used in the present chapter can highlight genes encoding proteins involved in pathways that are changed under different pH conditions and may allow a better understanding of the underlying mechanisms of acid-base regulation in annelid worms. The SSH technique has previously been used in *P. dumerilii* to selectively amplify cDNAs of differentially expressed genes potentially involved in immune responses (Altincicek and Vilcinskas, 2007). Another study using SSH, on a hydrothermal vent annelid *Paralvinella pandorae irlandei*, investigated the effects of temperature to gain an understanding of the physiological processes involved at high temperatures (Boutet et al., 2009). Furthermore, the SSH technique has been applied in other marine invertebrates such as Mollusca (*Bathymodiolus thermophilus*, *C. gigas*, *M. edulis*, *Scrobicularia plana*, *Venerupis philippinarum*, *Ruditapes philippinarum*) (Boutet et al., 2009; Collin et al., 2010; Ciocan et al., 2011; Ciocan et al., 2012, Zhang et al., 2013; Miao et al., 2014) Arthropoda (*Scylla paramamosain*, *Calanus helgolandicus*) (Zeng et al., 2011; Carotenuto et al., 2014;) and Cnidaria (*Acropora microphthalma*, *Erythropodium caribaeorum*, *S. pistillata*) (Starcevic et al., 2010; Lopez et al., 2011; Chen et al., 2012c).

In summary, in order to understand the molecular-level impacts of acidic pH exposure on the polychaeta species, *P. dumerilii*, this chapter of the thesis provides an exploratory approach to isolate and identify differentially - regulated pH-specific mRNA transcripts from worms maintained at control (8.2) and acidified (7.8) pH levels. This

approach works on the hypothesis to find and identify novel molecular responses, from changes that are predicted to occur at the level of gene expression to compensate potential molecular damage or cellular dysfunctions. The knowledge gained will help determine the molecular mechanisms involved in acid-base regulation in polychaete worms.

4.2 Material and Methods

4.2.1 Animals and experimental exposure

P. dumerilii (mean mass \pm SEM: pH 8.2 worms 7 d: 13 ± 1.55 mg, n=8; pH 7.8 worms 7 d: 10.94 ± 1.76 mg, n=8) from the laboratory culture supplied by EMBL Heidelberg (Germany) were used for the experiment. All exposure experiments were conducted at the EMBL Heidelberg. Atokus worms, a sexually immature stage of the worm, were used to reduce natural variation linked to maturation, reproduction and sex. Specimens were raised in filtered natural seawater (~pH 8.2). For the low pH exposure regime, 8 worms were kept in closed plastic containers (2000 cm³) with approximately 800 ml filtered natural seawater of pH 7.8 (salinity 35 ppt) at a light regime of 16 h light/ 8 h dark at 18 °C simulating summer conditions. A further 8 worms were kept at pH 8.2 and in the same experimental conditions as for controls. A complete water change was conducted each day. HCl (1M) and NaOH (1M) were used to maintain pH levels. After 7 d, chosen to reflect an acclimation time point, each single worm was immediately immersed in 800 μ l of RNALater solution (Sigma-Aldrich Company Ltd., Gillingham, UK) and stored at - 80°C until molecular analysis. To determine the body mass, worms were transferred onto filter paper to remove any excess of RNALater solution. Afterwards the wet weight was measured using an analytical balance.

4.2.2 Total RNA isolation and purification from worm tissue

Total RNA was extracted from worms kept at normal and low pH using High Pure RNA Tissue Kit (Roche, Burgess Hill, UK) as described in the manufacture's procedures. For detailed description see section 2.2.2. The RNA concentration was measured using a Qubit® Fluorometer (Life Technologies, Paisley, UK).

4.2.3 RNA Integrity

The integrity of the RNA was checked using a standard ethidium bromide stained 1% formaldehyde agarose gel (see section 2.2.2).

4.2.4 RNA Precipitation

To concentrate the RNA and remove salt, a precipitation was performed. The RNA was mixed with 1/10 of sodium acetate (NaOAc, 3 M, pH 5.3) and 2 volumes of cold (4 °C) ethanol (EtOH) absolute and incubated at -80 °C for 30 min. Afterwards the RNA was centrifuged for 20 min at maximum speed and subsequently the supernatant removed. The remaining pellet was then air-dried and 3.5 µl of sterile water was added. 0.2 µl of the RNA was quantified with a Qubit® fluorometer (Life Technologies, Paisley, UK) to confirm a minimum concentration of at least 50 ng/µl.

4.2.5 cDNA synthesis and Amplification by LD PCR

For the cDNA synthesis the samples were pooled with equal amounts of RNA from each worm (8 worms / group) with a total RNA concentration of 2.5 µg for each pool. Only high quality RNA, showing two distinct bands (18S and 28S ribosomal RNA), was used for cDNA synthesis. The SMARTer™ PCR cDNA Synthesis Kit (Clontech, Saint-Germain-en-Laye, France) was applied according to the manufacturer's protocol. 2.5 µg

of RNA, 1 μ l 3' SMART CDS Primer II A (12 μ M) and 0.5 μ l deionized water were combined, mixed and incubated for 3 min at 72 °C and 2 min at 42 °C. To each tube a Master Mix containing 2 μ l 5 \times First Strand Buffer, 0.25 μ l DTT (100 mM), 1 μ l dNTP Mix (10 mM), 1 μ l SMATer II A Oligonucleotide (12 μ M), 0.25 μ l RNase Inhibitor and 1 μ l SMARTScribe Reverse Transcriptase (100 U) was added. Afterwards the tubes were incubated at 42 °C for 1 h 30 min and the reaction terminated by heating the tubes to 70 °C for 10 min. Finally 40 μ l of TE buffer (10 mM Tris (pH 8.0), 0.1 mM EDTA) was added to the first-strand reaction product and the tubes were stored at -20 °C until further processing.

For the generation of ds cDNA the first-strand cDNA was amplified by LD PCR (Long-Distance Polymerase Chain Reaction). 10 μ l first-strand cDNA was mixed with 74 μ l deionised H₂O, 10 μ l 10 \times Advantage 2 PCR Buffer, 2 μ l 50 \times dNTP Mix (10 mM), 2 μ l 5' PCR Primer II A (12 μ M) and 2 μ l 50 \times Advantage 2 Polymerase Mix. The tubes were placed in a preheated thermal cycler. To define the optimal numbers of cycles, a range of cycles: 15, 18, 21, 24, 27, 30, 33, 36, were performed. For the PCR conditions, an initial denaturation at 95 °C for 1 min was used, followed by X cycles of denaturation at 95 °C for 15 s, annealing at 65 °C for 30 s and extension at 68 °C for 3 min. Each cycle stages was counterchecked by an aliquot on a 1.2 % agarose/EtBr gel in 1 \times TAE buffer in order to ascertain the optimal number of cycles. The best number of cycles for the ds cDNA from low pH samples was after 29 cycles and for normal pH samples after 18 cycles.

Subsequently the cDNA was purified after the PCRs. The PCR product was mixed with 200 μ l of phenol-chloroform and centrifuged for 5 min. Afterwards the supernatant was mixed with 80 μ l NH₄OAc (4 M) and 600 μ l cold ethanol (abs.) and centrifuged for 20 min. The supernatant was removed and the pellet dried. Afterwards the pellet was

resuspended in 50 μ l of sterile H₂O. The purified samples were checked on an agarose gel.

4.2.6 Rsa I Digestion

The Rsa I digest was performed to produce shorter, blunt-ended ds cDNA fragments. These are necessary for adaptor ligation and best for subtraction. The ds cDNA was mixed with 10 \times Rsa I Restriction Buffer and Rsa I (10 U/ μ l) and incubated for 3 h at 37 °C. This was followed by a purification using the NucleoSpin[®] Gel and PCR clean-up kit (Macherey Nagel, from Fisher Scientific, Loughborough, UK). 1 volume of cDNA was mixed with 2 volumes of Buffer NTI (contains chaotropic salts; exact composition is confidential), loaded onto the NucleoSpin[®] Column and centrifuged for 30 s at 11,000 \times g. 700 μ l of Buffer NT3 (composition is confidential) were added and again the column was centrifuges for 30 s at 11,000 \times g. The flow-through was discarded and the column centrifuged twice for 1 min at 11,000 \times g to remove all Buffer NT3. The column was placed in a new 1.5 ml microcentrifuge tube and eluted with 15 μ l Buffer NE (5 mM Tris/HCl, pH 8.5) after 1 min incubation at room temperature (~22 °C) at 11,000 \times g for 1 min.

4.2.7 Adapter Ligation

For the adapter ligation three separate ligations were conducted for the forward (pH 7.8), reverse (pH 8.2) and control subtraction (skeletal muscle) (Fig. 4.1). The protocol of the PCR-Select[™] cDNA Substraction Kit (Clontech, Saint-Germain-en-Laye, France) was applied. Each cDNA was separated into two tubes and ligated with Adaptor 1 (Tester 1-1, 2-1, 3-1) and the second with Adaptor R2 (Tester 1-2, 2-2 and 3-2) (Fig. 4.1). For this, 2 μ l diluted cDNA (3 μ l cDNA with 3 μ l H₂O) was mixed with 2 μ l of Adaptor 1 or 2R

and 6 μl Master Mix containing 3 μl sterile H_2O , 2 μl 5 \times Ligation Buffer and 1 μl T4 DNA Ligase (400 units/ μl). Afterwards 2 μl of each adaptor ligated tester (e.g. 1-1 and 1-2) were combined and incubated at 16 $^\circ\text{C}$ overnight. In order to stop the ligation reaction 1 μl of EDTA/Glycogen Mix was added and the samples was heated at 72 $^\circ\text{C}$ to inactivate the ligase. The sample was stored at -20 $^\circ\text{C}$ until further processing.

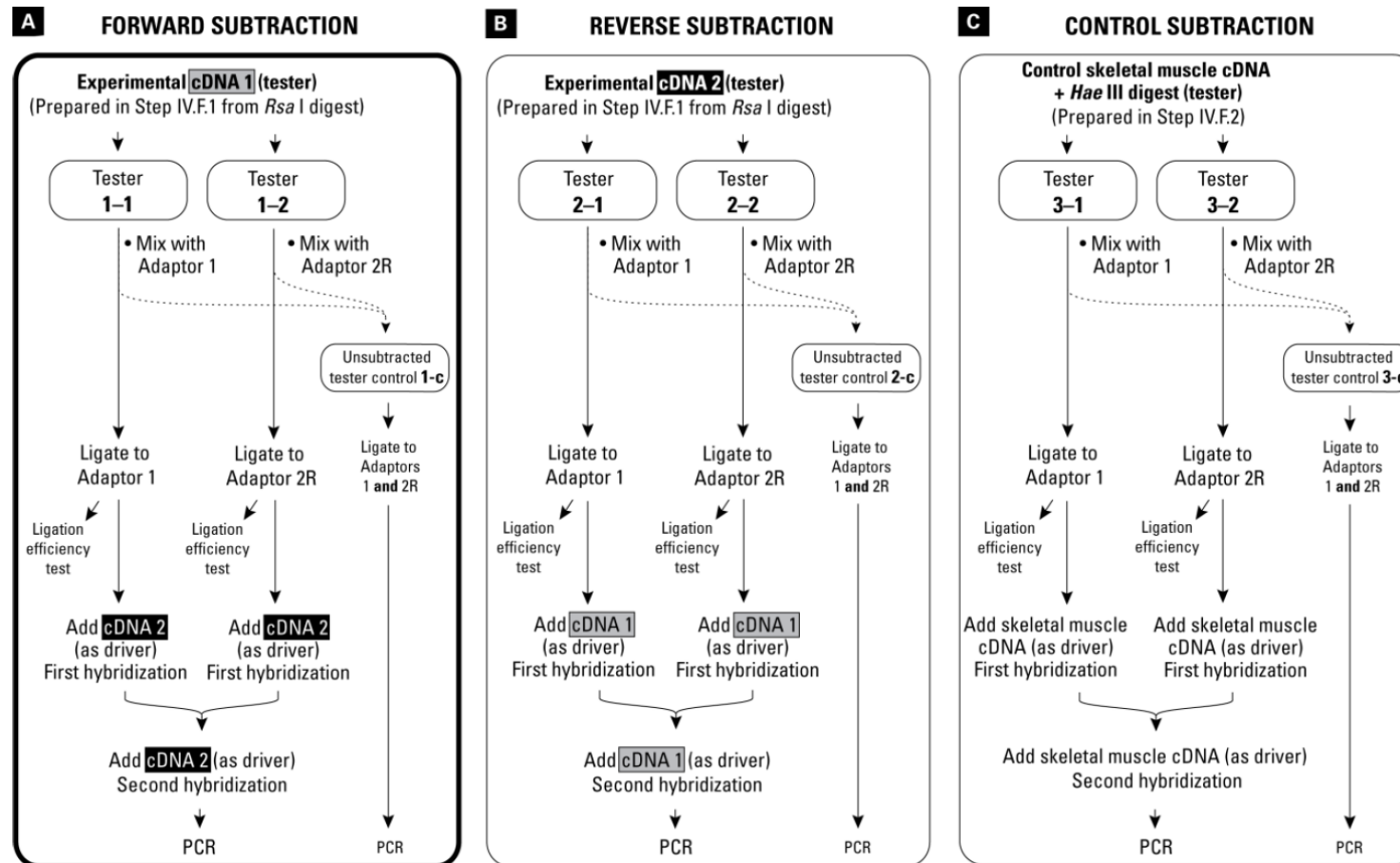


Figure 4.1 Scheme of the preparation of adaptor-ligated tester cDNAs for hybridisation and PCR. Each tester cDNA is ligated to the appropriate adaptor. **A** The forward subtraction represents the intended experiment. **B** The reverse subtraction is required for differential screening of the subtracted cDNA library. **C** A control subtraction is performed with skeletal cDNA (Scheme taken from the Select™ cDNA Subtraction Kit User Manual, Clontech).

4.2.8 Suppression subtractive hybridisation

4.2.8.1 First hybridisation

The SSH technique was used to isolate and enrich differentially-expressed genes between *P. dumerilii* kept at normal pH and *P. dumerilii* kept at low pH conditions using PCR-selected cDNA subtraction reagents and protocol (Clontech, Saint-Germain-en-Laye, France). For each subtraction 1.5 µl Rsa I-digested Driver cDNA, 1.5 µl Adaptor 1-ligated Tester 1-1 or Adaptor 2R-ligated Tester 1-2 and 1 µl 4× Hybridization Buffer were combined and incubated at 98°C for 1.5 min, followed by 68 °C for 10 h. The same was carried out for Tester 2-1 and 2-2, 3-1 and 3-2.

4.2.8.2 Second hybridisation

For the second hybridisation, 1 µl Driver cDNA, 1 µl 4× Hybridisation Buffer and 2 µl of sterile H₂O were mixed and incubated at 98 °C for 1.5 min in a thermal cycler. The denatured driver is then simultaneously mixed with hybridisation samples 1 and 2 to make sure that the hybridised samples are only mixed in presents of freshly denatured driver. This was followed by an incubation step at 68 °C overnight. Finally 200 µl of dilution buffer was added and the mixture heated at 68 °C for 7 min. The sample was stored at -20 °C until further processing.

4.2.9 PCR amplification

After the hybridisation the subtracted cDNAs were amplified by PCR using 12 cycles for low pH and 17 cycles for normal pH cDNA in the primary PCR. For the PCR reaction 1 µl of the diluted cDNA (1 µl of the subtracted samples in 1 ml H₂O) was mixed with 19.5 µl sterile H₂O, 2.5 µl 10× PCR reaction buffer, 0.5 µl dNTP Mix (10 mM), 1 µl PCR Primer 1 (10 µM) and 0.5 µl 50× Advantage cDNA Polymerase Mix. To extend the adaptors, the reaction mix got incubated at 75 °C for 5 min. For the PCR conditions an

initial denaturation at 94 °C for 25 s was used, followed by X cycles of denaturation at 94 °C for 10 s, annealing at 66 °C for 30 s and extension at 72 °C for 1.5 min. After 12 cycles an aliquot was analysed on a 1.5 % agarose/EtBr gel in 1× TAE buffer. For low pH samples 5 additional cycles were run.

For the second PCR 1 µl diluted primary PCR product (3 µl in 27 µl H₂O) was mixed with 18.5 µl sterile H₂O, 2.5 µl 10× PCR reaction buffer, 1 µl Nested PCR primer 1 (10 µM), 1 µl Nested PCR primer 2R (10 µM), 0.5 µl dNTP Mix (10 mM) and 0.5 µl 50× Advantage cDNA Polymerase Mix. The PCR was run for 12 cycles using 94 °C for 10 s for the denaturation, 68 °C for 30 s for annealing and 72 °C for 1.5 min as an extension period. An 8 µl aliquot was analysed on a 1.5 % agarose/EtBr gel in 1× TAE buffer and the PCR product bands were cut from the gel under UV-light. The gel bands were then purified using the High Pure PCR Cleanup Micro reagents and protocol (Roche, Burgess Hill, UK). For this, Binding Buffer (300 µl for 100 mg agarose) was added to the excised gel band and heated at ~50 °C until completely dissolved. The sample was then transferred onto a filter tube and centrifuged at 8,000× g for 60 s. The flow-through was discarded and 400 µl of Wash Buffer were added. After centrifuged at 8,000× g for 60 s the flow-through was discarded and 300 µl of Wash Buffer were added and the filter tubed centrifuged for 60 s at maximum speed. The filter tube is transferred into a clean 1.5 ml tube and 10 µl of Elution Buffer was added. A final centrifugation step at 8,000× g for 60 s was carried out. The last step was repeated to end up with a final volume of 20 µl. The eluted sample was stored at -20 °C until further processing.

4.2.10 Cloning of PCR generated fragments

In order to produce large amounts of DNA fragments and to be able to sequence them, the cloning technique was performed using TA Cloning[®] Kit, with pCR[™]2.1 Vector (Life

Technologies, Paisley, UK). An overview of the cloning method is described in Figure 4.2.

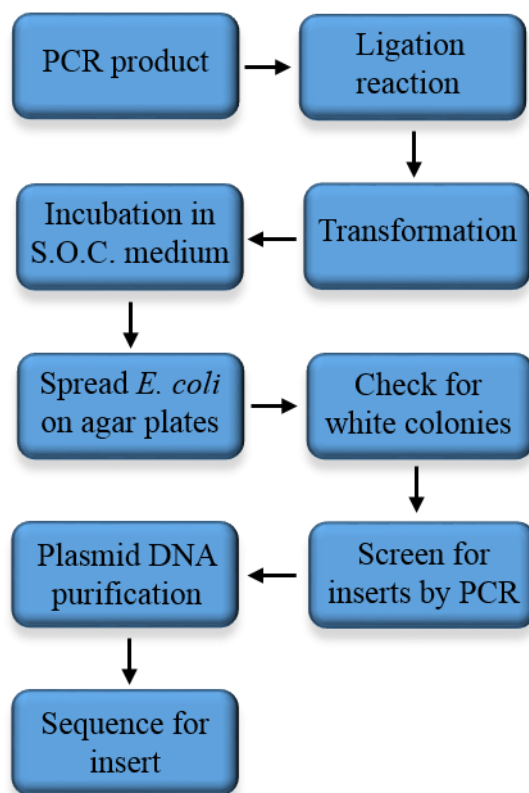


Figure 4.2 Overview of the main steps employed for the subcloning procedure.

For this, the DNA was inserted into a plasmid vector. The plasmid is linearised, has single 3'-thymidine (T) overhangs, and contains the resistance genes to kanamycin and ampicillin as well as a *LacZ α* gene. The DNA fragment is inserted into the middle of the *LacZ α* gene, enabled through the added 3'-deoxyadenosine (A) ends. For the ligation reaction 1.5 μ l of the PCR product, 0.5 μ l (25 ng/ μ l in 10 mM Tris-HCl, 1 mM EDTA, pH 8) TOPO[®] vector (pCR[®]2.1), 0.5 μ l T4 DNA Ligase (4.0 Weiss units) and 0.5 μ l 10 \times Ligation buffer were mixed and incubated at 14 $^{\circ}$ C overnight. The prepared vectors were then transformed into DH10B-T *E. coli* (Life Technologies, Paisley, UK) cells. For the transformation, 50 μ l of frozen competent cells (DH10B-T) were mixed with 2 μ l of the ligation reaction and incubated on ice for 30 min. After the incubation the cell mixture

was heat shocked in a water bath for exactly 75 s at 42 °C and immediately transferred back on ice. 250 µl of S.O.C. medium (2 % tryptone, 0.5 % yeast extract, 10 mM NaCl, 2.5 mM KCl, 10 mM MgCl₂, 10 mM MgSO₄, 20 mM glucose (dextrose)) was added to the solution at room temperature (~22 °C) and then incubated shaking (225 rpm) at 37 °C for 1 h. After incubation, the *E. coli* cells were spread on pre-warmed LB-Agar plates (LB Agar Miller, Fisher Scientific, UK) containing kanamycin (50 µg/ml) and X-Gal (40 µg/ml). The plates were left in an incubator at 37 °C overnight. Plates were checked for single white colonies, indicating a plasmid containing an insert. Two hundred randomly selected colonies from each subtracted library were inoculated in 5 ml LB broth (Lennox, Fisher Scientific, UK) and 10 µl of 25 mg/ml stock kanamycin was added. Cell cultures were grown in a shaking incubator (225 rpm) at 37 °C overnight. The colonies were screened for inserts using the vector-based primers M13 (M13 Reverse: CAGGAAACAGCTATGAC and M13 Forward GTAAAACGACGGCCAG) and a conventional PCR cycling protocol. Samples containing inserts were purified using the Plasmid DNA purification reagents and protocol (Macherey-Nagel, from Fisher Scientific, Loughborough, UK). 5 ml of *E. coli* LB culture was pelleted by centrifugation at 11,000× *g* for 30 s. The pellet was resuspended in 250 µl of Buffer A1 (composition is confidential) and 250 µl of Buffer A2 (composition is confidential) were added and the tube inverted 6×. This cell lysis step was followed by a 5 min incubation until the lysate appeared clear. 300 µl of Buffer A3 (composition is confidential) were added and mixed by inverting the tube 6×. The mixture was centrifuged at 11,000× *g* for 5 min and the supernatant was transferred onto a column. The column was centrifuged at 11,000× *g* for 1 min to bind the DNA. The flow-through got discarded and the column placed back into the collection tube. To wash the silican membrane 600 µl Buffer A4 (composition is confidential) were added to the column and centrifuged at 11,000× *g* for 1 min.

Subsequently, the column was placed into a new collection tube and after centrifugation at $11,000\times g$ for 2 min the collection tubes was discarded. To elute the DNA the column was placed in a 1.5 ml microcentrifuge tube and 50 μ l Buffer AE (5 mM Tris/ HCl, pH 8.5) was added. This was followed by a 1 min incubation and a centrifugation step at $11,000\times g$ for 1 min. Afterwards, the concentrations were determined with a Qubit[®] fluorometer (Life Technologies, Paisley, UK) and the required sample concentration sent for sequencing of the insert (Macrogen Europe, the Netherlands).

4.2.11 Bioinformatics

Fifty-two colonies were sequenced and their identities were determined by BLAST searches (<http://blast.ncbi.nlm.nih.gov/Blast.cgi>) against the NCBI nucleic acid and protein databases, as well as the PLATYpopsys database (<http://hydra.cos.uni-heidelberg.de/pps/>). BLAST sequence reads with E -value $<10^{-5}$ were selected. Hits only matching with PLATYpopsys database are labelled with an asterics (*) in Table 4.2.

4.2.12 qPCR validation

Target mRNAs, identified using SSH, were selected for validation using qPCR according to MIQE guidelines (Bustin et al., 2009). Total RNA was isolated from 8 individual worm tissues per exposure group using High Pure RNA Tissue Kit reagents (Roche, Burgess Hill, UK). Template RNA was then removed using RNase H enzyme and 10 \times buffer (Thermo Fisher Scientific, Loughborough, UK) with a 45 min incubation at 37 °C. The RNA concentrations were measured with the Quant-iT RNA assay kit and Qubit[®] fluorometer (Life Technologies, Paisley, UK). Reverse transcription of 140 ng of total RNA from each individual worm sample (based on the typical yield from each RNA extraction) was carried out using SuperScript VILO cDNA Synthesis reagents (Life

Technologies, Paisley, UK) and following the manufacturer's instructions. All qPCR reactions were performed in duplicate, in a final volume of 20 μ l containing 10 μ l of qPCR Fast Start SYBR Green Master Rox (Roche, Burgess Hill, UK). 1 μ l of cDNA and the corresponding primers (Table 4.1) were used. Amplifications were performed in a CFX96 Real Time PCR Detection System (Bio-Rad, Hemel Hempstead, UK) and using the following conditions: after 2 min at 95 °C, 45 cycles at 95 °C for 10 s, 60 °C for 1 min and 72 °C for 1 min. To generate the melt curve, a heating step gradient from 5 s at 60 °C to 5 s at 95 °C, was added to the end of the qPCR run. For each of the *target* mRNAs, the melting curve, gel picture and sequences were analysed in order to verify the specificity of the amplified products. The amplification efficiency of each primer pair was calculated using a ten times dilution series of cDNA. The detected efficiency recided between 94.4 % and 101.7 %. Additionally, the C_q was detected for each *target* mRNA and normalised to the *reference* genes α -*TUB*, and *18S* (Zheng et al., 2011; Won et al., 2011).

Table 4.1 *Target* and *reference* gene primer sequences, amplicon sizes and primer concentrations used for qPCR.

<i>Target gene</i>	Primer sequence (5'-3')	Amplicon size (bp)	Primer concentration (nM)
<i>18S</i>	F: GCGCATTTATCAGCACAAGA R: CTTGGATGTGGTAGCCGTTT	239	50
α - <i>TUB</i>	F: CTTCAAGGTCGGCATCAACT R: TGGCAGTGGTATTGCTCAAC	101	100
<i>Calponin</i>	F: GGAGCCAGTGTGCTTGGT R: AGCCTGTCCAGACTTGCCA	126	100
<i>Paramyosin</i>	F: AGAACGCTGAGGGTGAATTG R: CGAGCTGGAGCCTGTCGGCA	183	80
<i>Cytochrome c oxidase</i>	F: GCGCAGATGTTTCGTATGCTA R: GAGCCTACTCGGCATCTGTC	197	100
<i>NADH dehydrogenase</i>	F: CGAACCGGATTATGGCTTTG R: GGGAATTTGTCCCGTCTGCA	147	100

4.2.13 Statistical analyses

Statistical analyses were conducted using GraphPad InStat v3 (GraphPad Software Inc., La Jolla, U.S.A.). All data were tested for normality and homogeneity of variances. Significance for relative gene expression was tested using an unpaired *t*-test. Outliers were identified, and removed, if they differed by more than twice the standard deviation of the mean. For *paramyosin* (pH 8.2), *cytochrome c oxidase* (pH 7.8) and *NADH dehydrogenase* (pH 7.8) one value was identified as an outlier and excluded from the statistical analysis. For all analyses, statistical significance was accepted at $p < 0.05$. Values are presented as means \pm SEM. All graphs were designed with XACT 8.03 (SciLab, Germany).

4.3 Results

4.3.1 SSH analysis

A total of fifty-two differentially expressed mRNA sequences were isolated and then compared with sequences in the NCBI GenBank database and PLATYpopsys database (<http://hydra.cos.uni-heidelberg.de/pops/styled-2/>) using the blastn and blastx algorithms. 32% of the sequences libraries matched to genes from different categories (Fig. 4.3 and 4.4) and organisms, predominantly invertebrates (Table 4.2). The remaining sequences showed either similarity to unidentified hypothetical proteins or showed no similarity with the sequences available on the database.

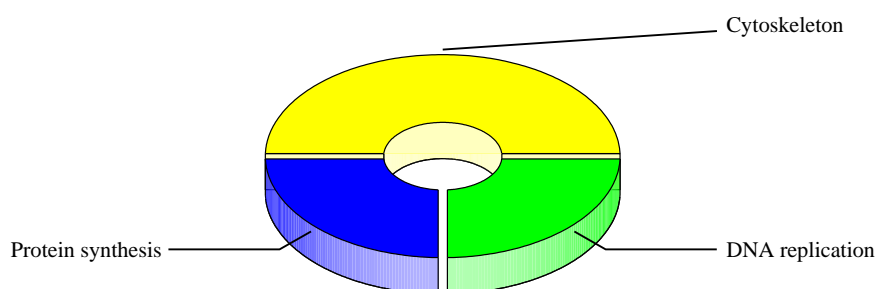


Figure 4.3 Pie chart presenting the three different groups identified as up-regulated mRNA transcripts in *P. dumerilii* kept at low pH seawater conditions relative to normal pH conditions.

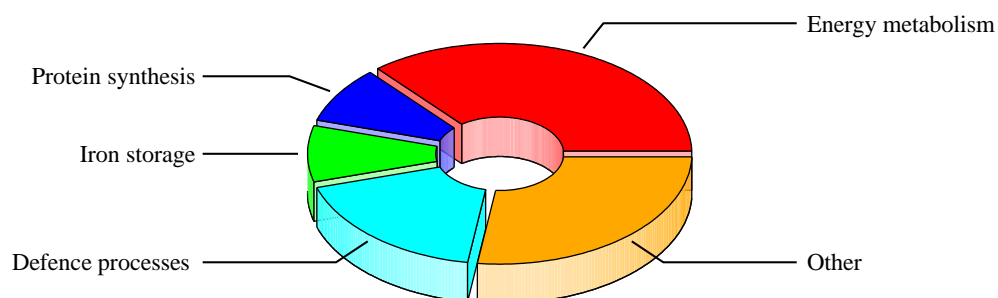


Figure 4.4 Pie chart presenting the different groups identified as down-regulated mRNA transcripts in *P. dumerilii* kept at low pH seawater conditions relative to normal pH conditions.

4.3.2 Validation of differential mRNA transcriptions

Four *target* mRNAs were selected to validate the SSH differential transcription results by qPCR (Fig. 4.5). *Calponin* and *paramyosin*, were significantly ($t(14) = 2.214$; $p=0.044$ and $t(13) = 2.301$; $p=0.0386$) up-regulated in worms kept at low pH compared with worms kept at normal pH (Fig. 4.5 a, b). *Cytochrome c oxidase* and *NADH dehydrogenase* were down-regulated in worms kept at pH 7.8 compared with worms kept at pH 8.2 (Fig. 4.5 c, d), though the results were not significant ($t(13) = 1.174$; $p=0.2615$ and $t(13) = 1.138$; $p=0.2757$).

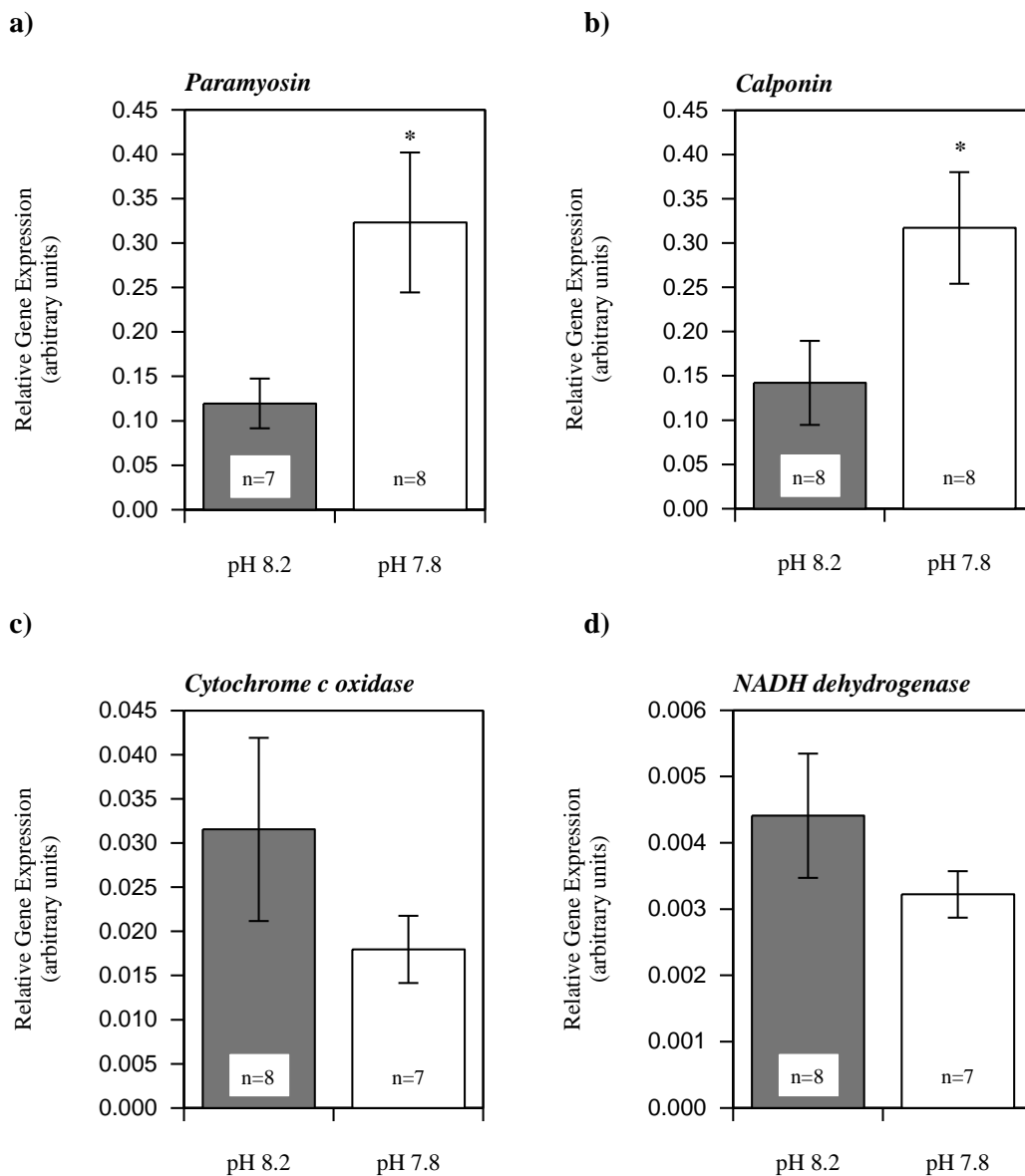


Figure 4.5 qPCR analysis of selected transcripts (a) *paramyosin* (b) *calponin* (c) *cytochrome c oxidase* (d) *NADH dehydrogenase* identified by SSH as differentially expressed in worms maintained at low pH seawater conditions relative to normal pH conditions. * $p < 0.05$.

Table 4.2 Differentially expressed (subtracted) mRNAs identified in *P. dumerilii* maintained at low pH conditions. For each identified gene the corresponding accession number and nucleotide base pair length of the transcript is presented, as well as the homologues species match including E-value and GenBank accession number. Furthermore the functional category with small explanation and reference is presented. * indicates hits with PLATYpopsys database only and corresponding E-value represents the re-blast result of the matched sequence.

Clone accession no.	Category and gene identity	Length (bp)	Homolog species	E-value	GenBank accession no.	Functional category	Function	Reference
Up-regulated in pH 7.8:								
JZ820677	Paramyosin*	380	<i>M. galloprovincialis</i>	0.0	O96064.1	Cytoskeleton	-Involved in the length and stability of muscle filaments -Involved in the modulation of host's immune systems under parasitic infestations	Mackenzie and Epstein, 1980 Zhao et al., 2007
No accession number available	Calponin*	50	<i>Echinococcus granulosus</i>	$4E^{-143}$	CDJ18009.1	Cytoskeleton	-Involved in control of smooth muscle contraction activity -Inhibits actin-activated myosin MgATPase activity	Takahashi and Nadal-Ginard, 1991 Abe et al., 1990
KP640621	ribosomal protein L34 (Rpl34)	230	<i>Cerebratulus lacteus</i>	$1E^{-15}$	KJ526218.1	Protein synthesis	-RNA binding	http://www.uniprot.org/uniprot/P49207 (20.03.2015)
JZ820678	DNA replication complex GINS protein PSF3	765	<i>S. kowalevskii</i>	$5E^{-13}$	NM_001184840.1	DNA replication	-Component of the eukaryotic DNA replication machinery -Required for the initiation of chromosome replication and normal progression of DNA replication forks	Takayama et al., 2003 Kubota et al., 2003

Down-regulated in pH 7.8:								
JZ820679	PREDICTED: NADH dehydrogenase [ubiquinone] 1 beta subcomplex subunit 7-like	292	<i>Ceratititis capitata</i>	$9E^{-8}$	XM_004520945.1	Energy metabolism	-Enzyme of the mitochondrial electron transport chain	Weiss et al., 1991
JZ820680	PREDICTED: Cytochrome c oxidase subunit 6A	489	<i>Poecilia formosa</i>	$3E^{-14}$	XM_007557010.1	Energy metabolism	-Part of the last enzyme in the respiratory electron transport chain	Capaldi, 1990
JZ820681	2-Oxoglutarate dehydrogenase*	316	<i>P. humilis</i>	0.0	XP_005532951.1	Energy metabolism	-Enzyme complex found in TCA cycle	Bittar and Bittar, 1995
JZ820682	ATP synthase F chain	350	<i>Ixodes scapularis</i>	$3E^{-6}$	XM_002399310.1	Energy metabolism	-Enzyme that provides energy through the synthesis of ATP	Stock et al., 2000
KP640622	16S ribosomal RNA*	500	<i>Hediste diadroma</i>	$5E^{-150}$	AB703100.1	Protein synthesis	-Involved in base-pairing role of termination and initiation of protein synthesis	Shine and Dalgarno, 1974
JZ820683	PREDICTED: serine protease 55*	168	<i>Pteropus lecto</i>	$2E^{-22}$	XP_006906396.1	Hydrolysis of peptide bonds	-In mammalian cells: involved in angiogenesis, apoptosis, differentiation, immune response, matrix remodelling and protein activation	Ekici et al., 2008
JZ820684	ferritin	571	<i>Periserrula leucophryna</i>	$7E^{-124}$	DQ207752.1	Iron storage	-Iron storage in a soluble, bioavailable and nontoxic form -involvement in immune response	Andrew et al.,1992 Beck et al., 2001

JZ820685	WNK lysine deficient protein kinase 1 (WNK1)	234	<i>H. sapiens</i>	0.003	NG_007984.2	Ion transport	-A serine-threonine kinase that phosphorylates synaptotagmin 2 -WNK1 activates SGK1 leading to activation of the epithelial sodium channel	Lee et al., 2004 Xu et al. 2005
JZ820686	PREDICTED: calcium-binding and coiled-coil domain-containing protein 2	363	<i>Peromyscus maniculatus bairdii</i>	1E ⁻⁶	XP_006971971.1	Immunity	Human: gene encodes a protein which functions as a receptor for ubiquitin-coated bacteria and plays a role in innate immunity by mediating macroautophagy	http://l.usa.gov/1DMjFrH (13.02.2015)
JZ820687	IQ and ubiquitin-like domain-containing protein	711	<i>S. purpuratus</i>	5E ⁻⁶⁴	XM_789342.3	Predicted: cilia formation	-Putative cilia protein	Lai et al., 2011
JZ820688	fucolectin-1	323	<i>Anguilla japonica</i>	1E ⁻⁰⁴	AB037867.1	Immune defense	-Involved in host defence	Honda et al., 2000
JZ820689	Paneth cell-specific alpha-defensin	366	<i>Equus caballus</i>	3E ⁻⁵	NM_001166074.1	Host defence	-Well-established antimicrobial proteins and peptides	Ouellette and Bevins, 2001

4.4 Discussion

Using the SSH approach, libraries enriched for genes that vary between normal pH (8.2) and simulated acidification (7.8) conditions were generated from the marine polychaete worm *P. dumerilii*. In the subtractions reported in this chapter two separate libraries were constructed using: a) cDNA from worms exposed to normal pH for one week as driver (reverse library), and b) cDNA from worms exposed to acidified pH conditions for one week as tester (forward library). From these libraries, 32% of the sequences obtained were identified, which is comparable to similar studies using invertebrates (6-44%, Boutet et al., 2008; Craft et al., 2010; Ciocan et al., 2011; Ciocan et al., 2012).

Several mRNA transcripts were identified and validated as up-regulated in *P. dumerilii* kept under low pH seawater conditions (Table 4.2; Fig. 4.3, 4.4, 4.5). Amongst these transcripts were proteins involved in cytoskeleton function (paramyosin and calponin), protein synthesis (Ribosomal protein L34 and 16S ribosomal RNA) and DNA replication (GINS protein Psf3) functions. These represent inter-linked processes as the cytoskeleton plays a major role in cell division. Tubulin subunits are organised into mitotic spindle, which are necessary for the orderly distribution of chromosomes during cell division (Solomon et al., 2011). Furthermore, a ring of actin associated with myosin constricts cells to form two daughter cells (Solomon et al., 2011). For calponin, the sequence isolated is short (at 50 bp) and, as such, only a tentative identity can be assumed. Further work would yield full gene sequence lengths and additional functional protein studies but was beyond the scope of this project.

Changes to metabolic rates have often been observed in organisms under stress conditions (Djawdan et al., 1997; Langenbuch and Pörtner, 2004). Down-regulation of *2-oxoglutarate dehydrogenase*, *NADH-dehydrogenase*, *cytochrome c oxidase*, and *ATP synthase*, collectively representing genes involved in the Krebs cycle and the

mitochondrial electron transport chain, indicate a reduction in oxidative metabolism and capacity to generate ATP and NADPH. Similar down-regulation of such metabolism-related genes has been reported in coral (*A. millepora*) and sea urchin (*S. purpuratus*) larvae after 28 days high $p\text{CO}_2$ exposure and 40 hours post hatching with medium level CO_2 exposure treatment respectively (Todgham and Hoffmann, 2009; Kaniewska et al., 2012). In a study using the scleractinian coral, *P. damicornis*, *2-oxoglutarate dehydrogenase* was observed to be slightly up-regulated at pH 7.8 and subsequently down-regulated at pH 7.4 (Vidal-Dupiol et al., 2013). Also, in contrast to our findings, Vidal-Dupiol et al. (2013) reported an enrichment of genes involved in oxidative phosphorylation (among them NADH dehydrogenase) at pH 7.8 and 7.2 in coral. Oyster (*C. hongkongensis*) and sea urchin (*L. pictus*) larvae behaved similarly to the worms however, with an apparent down regulation of *cytochrome c oxidase* and *NADH dehydrogenase* at low pH (O'Donnell et al., 2010; Dineshram et al., 2013). Yet, the discussed studies used CO_2 for pH modulation and different acid-base balance mechanisms might be involved in comparison to the mineral acid used in the present chapter.

Of the cytoskeleton function transcripts identified, *paramyosin* is primarily a muscle thick filament protein that is common in invertebrate species (Hooper et al., 2008). Unusually, *paramyosin* has roles in both muscle contraction as well as immunoregulation (Gobert and McManus, 2005). Nematode muscles consist of a contractile part made up of fibres with myosin, actin, tropomyosin and *paramyosin*, and a non-contractile part supplying energy requirements (Hooper et al., 2008). Related to this is another of the isolated transcripts, *calponin*. *Calponin* (calcium- and calmodulin-binding troponin T-like protein) is a calcium-binding protein that inhibits ATPase activity of myosin in smooth muscle (Castagnone-Sereno et al., 2001). An up-regulation of *paramyosin* and

calponin transcripts following acidic pH seawater exposure is consistent with other investigations reported in the literature. Adult oysters (*C. virginica*) and oyster larvae (*C. hongkongensis*) exposed to pH 7.9 - pH 7.5, induced by CO₂ bubbling, displayed increased calponin-2 and myosin (light chain) expression respectively (Tomanek et al., 2011; Dineshram et al., 2013).

In addition to muscle microfilament up-regulation, there was also an apparent increase in protein synthesis related (ribosomal protein L34) and DNA replication (GINS protein Psf3) processes (Table 4.2). Such changes are common following stress conditions and consistent with findings for other invertebrate species, including oysters (*C. virginica*) exposed to CO₂ driven low pH (Tomanek et al., 2011). Specifically, Psf3, is a protein from the Psf family, involved in cell cycle, and has been observed herein as up-regulated in worms kept at low pH (7.8) similarly to the *Psf2* transcript identified in sea urchin (*S. purpuratus*) larvae kept under a moderate level of acidified seawater aerated with CO₂ gas (Todgham and Hofmann, 2009). Besides the up-regulated transcripts several other transcripts showed a down-regulation in the worms kept in acidified seawater conditions.

Down-regulation of the immune-related transcripts *fuclectin* and *paneth cell-specific alpha defensin* was observed in worms kept at low pH conditions (Table 4.2). Fuclectins are fucose binding proteins that have a pathogen recognition role in fish (Honda et al., 2000), while alpha defensins are microbiocidal and cytotoxic peptides involved in host defence (Szyk et al., 2006). Defensins have previously been isolated from invertebrate species such as the horseshoe crab (*Tachypleus tridentatus*, Kawabata, 2010) and oyster (*C. gigas*, Rosa et al., 2011), but, based on current literature, this study seems to represent the first isolation from a polychaete species (Smith et al., 2010). Immunosuppression upon contaminant exposure is well documented for marine

vertebrates (De Swart et al., 1996). To what extent pH changes will impact the immune system of invertebrates is less extensively studied. Bibby et al. (2008) reported that several components of mussel (*M. edulis*) immune response, including suppressed phagocytosis, were modulated following (32 day) exposure to acidified seawater. A similar trend in immune suppression has also been reported in the starfish *Asterias rubens* (Hernroth et al., 2011). Calcium ion concentrations have been suggested as the mechanism by which acidification causes suppression of the immune system (Bibby et al., 2008). However, those studies used CO₂ to induce low pH conditions, which might underlie different acid-base balance mechanisms compared to direct pH changes by acid.

The other down-regulated genes in worms exposed to low pH include IQ ubiquitin-like domain-containing protein (IQUB), ferritin and WNK1 (Table 4.2). IQUB is a putative cilia protein (Lai et al., 2011) previously observed as down-regulated in larvae hatched from gastropod egg masses that had been co-exposed to temperature and UVB stresses (Fischer and Phillips, 2014). Ferritin stores iron and protects cells from iron-induced redox damage while also controlling its release for different enzymatic reactions (Theil, 1987). In an investigation of the interactive effects of acidification (using elevated CO₂ levels for a duration of 4 to 5 weeks) and metal exposure in oysters (*C. virginica*), Götze et al. (2014) reported *p*CO₂ potentiation of metal-induced ferritin expression. WNK1 down-regulation in worms exposed to low pH is also interesting in that WNK1 in vertebrates is a serine-threonine kinase, which is expressed in different tissue including kidneys, and phosphorylates synaptotagmin 2. This phosphorylation process is suggested to regulate vesicle trafficking and fusion (Lee et al., 2004; Xu et al., 2005). Furthermore, WNK1 activates the serum- and glucocorticoid-inducible protein kinase SGK1, which leads to the activation of the epithelial sodium channel (Xu et al., 2005). WNK1 might also be involved in the regulation of ROMK1, an ATP dependent

potassium channel (Lee et al., 2004; Xu et al., 2005). The observed differential expression of the WNK1 gene is therefore interesting because no common sodium, calcium nor carbonate transporter protein transcripts are among those differentially expressed in the worms kept at low pH in this study, and as such WNK1 may represent an alternative mechanism of ion transport and balance in this worm relative to other species.

4.5 Conclusions

Using an SSH transcriptomic approach, differentially expressed genes were identified in worms kept at low pH seawater conditions. Such worms represent a non-calcifying marine species. Particularly novel findings are differentially regulated transcripts involved in cytoskeleton processes and the immune system, supporting the hypothesis of finding and identifying novel molecular responses under low pH exposure. The present findings demonstrate that the gene expression of *P. dumerilii* is altered under low pH conditions modulated by mineral acid. The experiment demonstrated that many different processes are changed in worms kept in a low pH environment. However, the group of acid-base transporters, highlighted in previous studies on marine organisms, was not amongst the identified expressed sequence tags (EST). Yet, a potential indirect alteration of a sodium transporter through the down-regulation of WNK1 could be observed.

The present chapter identified potential novel molecular responses involved in acid-base regulation and could be used as a starting point to continue investigating acid-base mechanisms in marine polychaetes. Alternative methods to the SSH technique could be the whole genome/ or transcriptome sequencing methods, however they are much more expensive (Badapanda, 2013).

5.1 Introduction

Due to the increasing fossil fuel emissions and changes in net land use the atmospheric CO₂ concentration is rising faster than ever recorded in the last 800 000 years (Lüthi et al., 2008). While CO₂ levels do not usually reach toxic concentrations, once dissolved in sea water it can lead to a decrease in seawater pH. The ocean's surface pH has dropped by 0.1 pH-units, which is equivalent to a 26 % increase in H⁺ ion concentration (IPCC, 2013), leading to a current average pH of ocean surface water at around pH 8.1 (IGBP, 2013). Furthermore, global ocean surface pH is predicted to decrease to ~7.8 by 2100 (IPCC, 2013). As a result of these unprecedented fast present-day changes, more adaptation pressure is expected to act on marine species (Hoegh-Guldberg et al., 2007), especially on organisms' physiological processes such as acid-base regulation, growth and reproduction (Kurihara et al., 2004; Kurihara and Shirayama, 2004; Miles et al., 2007; Sewell et al., 2014). A recent OA study showed that, even when the whole organism response is very small, numerous compensatory responses at the cellular level occur (Pan et al., 2015). Furthermore, another study showed that OA conditions can increase the toxicity of other stressors such as copper (Campbell et al., 2014).

Predicting how OA will biologically impact organisms relies to a large extent upon understanding and characterising the underpinning molecular level changes of such physiological processes. Recently a number of transcriptomic and proteomic studies have been conducted using marine organisms exposed to experimental OA conditions (Todgham and Hofmann, 2009; O'Donnell et al., 2010; Martin et al., 2011; Parker et al., 2011; Stumpp et al., 2011; Tomanek et al., 2011; Wong et al., 2011; Dineshram et al., 2012; Moya et al., 2012; Dineshram et al., 2013; Jones et al., 2013; Pespeni et al., 2013;

Tseng et al., 2013; Vidal-Dupiol et al., 2013). Previous studies included an analysis of differential gene and protein expression in sea urchins (*S. purpuratus*, *L. pictus* and *P. lividus*) (Todgham and Hofmann, 2009; Stumpp et al., 2011; Pespeni et al., 2013; O'Donnell et al., 2010; Martin et al., 2011), coral (*A. millepora* and *P. damicornis*) (Moya et al., 2012; Vidal-Dupiol et al., 2013), barnacle (*B. amphitrite*) (Wong et al., 2011), oysters (*S. glomerata*, *C. virginica*, *C. gigas* and *C. hongkongensis*) (Parker et al., 2011; Tomanek et al., 2011; Dineshram et al., 2012; Dineshram et al., 2013), fish (*O. latipes*) (Tseng et al., 2013) and the coccolithophore (*E. huxleyi*) (Jones et al., 2013) kept at pH 7.0-7.96 or 540-1340 ppm CO₂ concentrations for various exposure durations and at different life stages.

Although the species used in these studies mainly represent calcifying organisms and the main focus has been on biomineralisation processes, the effects on acid-base regulation (O'Donnell et al., 2010; Moya et al., 2012), ion transport (O'Donnell et al., 2010; Pespeni et al., 2013; Vidal-Dupiol et al., 2013) and energy metabolism (O'Donnell et al., 2010; Wong et al., 2011; Pespeni et al., 2013; Vidal-Dupiol et al., 2013) have also been observed besides biomineralisation processes (O'Donnell et al., 2010; Dineshram et al., 2012; Moya et al., 2012; Pespeni et al., 2013). For instance, a down-regulation of metabolic genes, such as succinyl-CoA synthetases, ATP synthase and succinate dehydrogenase has been observed in sea urchin larvae (O'Donnell et al., 2010; Todgham and Hoffmann, 2009). Also, a down-regulation of genes involved in metabolic pathways in oyster larvae, primary coral polyps, adult corals and developing fish have been reported (Dineshram et al., 2012; Kaniewska et al., 2012; Moya et al., 2012; Tseng et al., 2013). However, a different study using sea urchin larvae (*S. purpuratus*) observed an up-regulation of metabolic genes (Stumpp et al., 2011). The latter studies assume that the increase in metabolic rate related genes is caused by higher energetic demands to support

other processes functioning in ion homeostasis and calcification processes (Stumpp et al., 2011). This is also consistent with another study on the blue mussel *M. edulis*, where increasing seawater $p\text{CO}_2$ leads to an up-regulation of metabolism (Thomsen and Melzner, 2010). Nevertheless, there are also calcifying species, such as the marine coccolithophore, *E. huxleyi*, that did not show any changes in key metabolic processes (Jones et al., 2013). In addition to changes in metabolic processes, ion regulation and acid-base pathways have been reported as impacted. In the sea urchin larvae *L. pictus* both pathways were up-regulated (O'Donnell et al., 2010), whereas a different sea urchin species (*S. purpuratus*) showed both up- regulation (NHE3, Na^+/K^+ -ATPase, SERCA, VSOP) and down-regulation (V-type H^+ -ATPase, NHE3) of ion regulation genes (Stumpp et al., 2011). Also cytoskeleton related genes were altered in commercial, pacific and eastern oysters (e.g. several actin isoforms, superoxide dismutase, several peroxiredoxins, thioredoxin-related nucleoredoxin, tektin and myosin light chain) (Tomanek et al., 2011; Dineshram et al., 2012; Dineshram et al., 2013). Another affected group of comprised genes reported in the literature are those involved in apoptosis. In the coral *A. millepora* an increase of ATPase, MALT1 and API-5 could be observed (Kaniewska et al., 2012) whereas in the sea urchin larvae *S. purpuratus* a down-regulation was reported (e.g. Tnfrsf-like1, HVEM, Troy and TRAF3) (Todgham and Hofmann, 2009). Taken together, these studies show that responses to low pH/ high $p\text{CO}_2$ are highly species specific and that many cellular processes, in addition to calcification, can be affected in marine organisms.

To date, few studies have investigated the molecular mechanisms that underlie the responses of non-calcifying species to future CO_2 scenarios. The present chapter investigates if transcripts of genes involved in biomineralisation, ion transport, acid-base regulation and energy metabolism in the polychaete *P. dumerilii* are affected, by the projected future seawater pH levels, after short term exposure (1 hour and 7 days).

Furthermore, it explores the hypothesis that it is the pH change that causes the gene expression changes and therefore that the same responses as induced by HCl (Chapter 3) are expected. Information on non-calcifying species could help to gain a greater understanding of effects of OA on different organisms as well as potential effects on ecosystems.

5.2 Material and Methods

5.2.1 Animals and experimental exposure

P. dumerilii (mean body mass \pm SEM: pH 8.2 worms 1 h: 24.22 ± 2.43 mg, n=10; pH 7.8 worms 1h 21.86 ± 3.19 mg, n=10; pH 8.2 worms 7 d: 31.34 ± 4.80 mg, n=10; pH 7.8 worms 7 d: 30.33 ± 3.34 mg, n=10) were used from the laboratory culture obtained from the EMBL Heidelberg (Germany). All exposure experiments were conducted at the EMBL Heidelberg. The gene isolation and temporal expression experiments were conducted with adult, but sexually immature, atokous worms to reduce natural variation associated with metabolic processes linked to reproduction and metamorphosis. Before the experiment, all specimens were kept in filtered natural seawater (\sim pH 8.2) at a light regime of 16 h light/ 8 h dark in a temperature controlled room at 18 °C. 20 worms were transferred into plastic containers (2000 cm³) with approximately 800 ml filtered natural seawater (salinity 33.23 ± 0.21 ppt; temperature 17.81 ± 0.13 °C) of pH 8.2 (control) and another 20 worms were transferred into plastic containers (2000 cm³) with approximately 800 ml filtered natural seawater (salinity 33.19 ± 0.22 ppt; temperature 17.81 ± 0.13 °C) of pH 7.8 (treatment) kept at the same light regime and temperature. The pH was adjusted by addition of CO₂ gas into the water, and a complete water change was conducted every 24 h to ensure that the desired pH was maintained. For the pH adjustment CO₂ gas was bubbled into the seawater for approximately 20 s from a gas cylinder, whilst mixing the

water allowing the gas to spread. The pH of the water was checked again after ~20 min to assure that the desired pH was reached. After 1 h, 10 individuals from each treatment were transferred into RNALater solution (Sigma-Aldrich Company Ltd., Gillingham, UK). The remaining worms were kept for 7 d in the different pH seawater and then transferred into RNALater. Samples were stored at -80 °C until further processing. To determine the body mass, worms were transferred onto filter paper to remove any excess of RNALater solution. Subsequently the wet mass was measured on an analytical balance. The two selected time points were chosen to investigate an initial stress response (1 h) and an acclimation response (7 d).

5.2.2 Total RNA isolation and purification from worm tissue

Total RNA was extracted from each worm using High Pure RNA Tissue Kit reagents and protocol (Roche, Burgess Hill, UK), as described in section 2.2.2. The integrity of total RNA was analysed on denaturing TAE agarose gel stained with ethidium bromide (see section 2.2.2.). The pure RNA was stored at -20 °C until further processing.

5.2.3 Synthesis of cDNA

cDNA was synthesised from total RNA using the SuperScript VILO cDNA Synthesis Kit reagents and protocol (Life Technologies, Paisley, UK). 4 µl 5× VILO™ Reaction Mix, 2 µl 10× SuperScript® Enzyme Mix were gently mixed with approximately 300 ng of RNA and incubated at 25 °C for 10 min, followed by 60 min at 42 °C and 5 min at 85 °C. To degrade remaining RNA template RNase H (5 U/µl) (Thermo Scientific, Loughborough, UK) was used as described in section 2.2.3.

5.2.4 Target gene isolation and characterisation

The characterised primer sequences for *18S*, *NHE*, *CA* and *CaM* described in Chapter 2 were used in this experiment. However, the previously characterised primers for α -*TUB* did not show the desired efficiency with this worm sample set, therefore a new primer pair was used (Table 5.1). To amplify *NHE*, *CA* and *CaM* cDNA all *target* genes were run in a PCR (as described in section 2.2.5). The PCR products were visualised on an agarose gel to confirm a single, correctly-sized band (as described in section 2.2.6). The DNA concentration of the samples was measured with a QubitTM fluorometer (Life Technologies, Paisley, UK) (as described in section 2.2.7) and the PCR products were sequenced directly (Macrogen Europe, the Netherlands) (as described in section 2.2.8).

5.2.5 Amplification using qPCR

For each qPCR reaction, a CFX96 Real Time PCR Detection System (Bio-Rad, Hemel Hempstead, UK) was used to detect amplification. To amplify the cDNA, 10 μ l of qPCR Fast Start SYBR Green Master Rox (Roche, Burgess Hill, UK), 1 μ l of cDNA and 2 μ l of primers (*18S* 50 nM; α -*TUB*₂ 700 nM; *NHE*, *CA*, *CaM* 100 nM) (Table 5.1) and 7 μ l molecular grade water (Thermo Fisher Scientific, Loughborough, UK) were used to make up a final reaction volume of 20 μ l. For each gene, a control reaction lacking template was included to determine the target cDNA amplification specificity. After an initial denaturation at 95 °C for 2 min all reactions were carried out in the following 45 cycles: Denaturation at 95 °C for 10 s, annealing at 60 °C for 1 min and an extension step at 72 °C for 1 min. In order to create the melt curve a temperature gradient was created from 60 °C to 95 °C. As described in section 2.2.10.2, *18S* and α -*TUB* were used as *reference* genes.

Table 5.1 Oligonucleotide primer sequences for the *18S*, *NHE*, *CA* and *CaM*, as well as the new primer pair for the second *reference* gene *α-TUB₂*. For all *target* and *reference* genes the amplicon size in base pairs (bp) are presented.

<i>Target gene</i>	Primer sequence (5'- 3')	Amplicon size (bp)	Primer concentration (nM)
<i>18S</i>	F: GCGCATTATCAGCACAAGA R: CTTGGATGTGGTAGCCGTTT	239	50
<i>α-TUB₂</i>	F: TTGCTGTCTACCCAGCTCCT R: AGATGGCCTCATTGTCAACC	123	700
<i>NHE</i>	F: CGCTCTGTTGCTGTCTTGAG R: TGGCTACTAAGGCGAATGCT	130	100
<i>CA</i>	F: TAACCACCTCAACCGGAGAC R: ATGGTGTGCTCTGAGCCTTT	118	100
<i>CaM</i>	F: AAGCTTTCCGAGTGTTTCGAC R: CCTCTTCGTCCGTC AATTTC	102	100

5.2.6 Statistical analyses

Statistical analysis were conducted using IBM[®] SPSS[®] Statistics 22.0 (Armonk, NY: IBM Corp.). All data were tested for normality and homogeneity of variances. Significance for relative gene expression was tested using a two-way ANOVA. Outliers were identified, and removed, if they differed by more than twice the standard deviation of the mean. For *NHE* one value of each treatment was identified as an outlier. For *CA* one value for pH 8.2, 1 h; two values of pH 7.8, 1 h and two values for pH 7.8, 7 d were identified as outliers and excluded from the statistical analysis. For all analyses, statistical significance was accepted at $p < 0.05$. Values are presented as means \pm SE. All graphs were designed with XACT 8.03 (SciLab, Germany). Additionally a two-way ANOVA was conducted on the weight of the worms. The data was log transformed in order to fulfil the condition of normal distribution.

5.3 Results

5.3.1 qPCR analysis of *NHE*, *CA* and *CaM* mRNA expression

The expression level of each target mRNA was analysed in worms maintained in normal or low pH conditions using qPCR (Fig. 5.1). For *NHE* expression, both time [F(1, 32) = 2.448; p=0.128] and pH [F(1, 32) = 3.528; p=0.069] showed no significant change on the relative gene expression and there was also no significant interaction [F(1, 32) = 0.00; p=1.000]. However, pH did show a clear trend. As shown in Figure 5.1 a, the relative *NHE* gene expression at pH 7.8 in the group after 7 d showed a down-regulation trend. *CA* mRNA expression showed no significant effect of time [F(1, 31) = 0.00; p=1.000], but a significant effect of pH [F(1, 31) = 9.045; p=0.005] (Fig. 5.1 b). *CA* was significantly up-regulated at pH 7.8 in comparison to pH 8.2 (Fig. 5.1 b). There was no significant interaction between time and pH [F(1, 31) = 0.019; p=0.892]. For *CaM* both time [F(1, 36) = 0.812; p=0.374] and pH [F(1, 36) = 0.061; p=0.806], as well as the interaction [F(1, 36) = 0.279; p=0.601] between the two showed no significant relative gene expression change (Fig. 5.1 c).

5.3.2 Analysis of weight differences

The weight of the four worm groups was analysed for differences. No significant effect of pH [F(1, 36) = 0.281; p=0.599] could be observed, however, time showed a significant effect [F(1, 36) = 4.966; p=0.032]. There was no significant interaction between time and pH [F(1, 36) = 0.445; p=0.509].

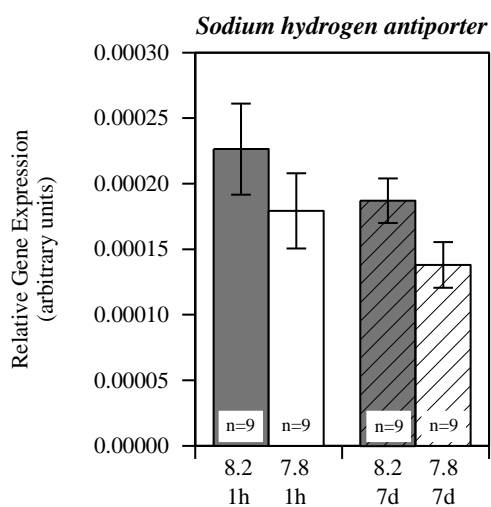
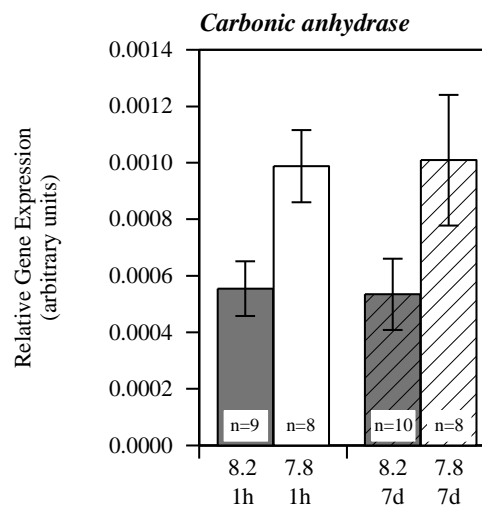
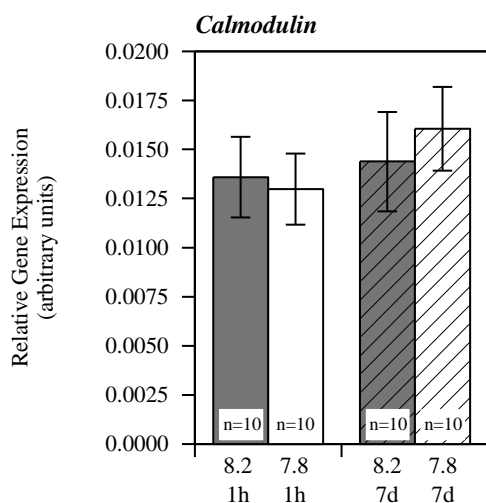
a) *NHE*b) *CA*c) *CaM*

Figure 5.1 Normalised average relative mRNA transcription \pm standard error of the mean in *P. dumerilii* for (a) *NHE* (b) *CA* and (c) *CaM* after 1 h and after 7 d in seawater with pH 8.2 and pH 7.8. Analysis was performed by two-way ANOVA. *NHE* showed a clear trend ($p=0.069$) for the effect of pH, and *CA* a significant effect ($p=0.005$). Both did not show a significant effect of time ($p=0.128$; $p=1.000$). *CaM* did not show a significant effect for pH ($p=0.806$) or time ($p=0.374$). Graphs were designed with XACT 8.03 (SciLab, Germany).

5.4 Discussion

The present chapter examined the relative gene expression of a selected number of genes, including *NHE*, *CA* and *CaM*, in response to acidified seawater (7.8) on adult, atokous *P. dumerilii*. Partial sequences were isolated and their mRNA expression analysed in worms kept at acidified seawater in comparison to worms kept at normal pH seawater (8.2). The chosen values reflect the pH values predicted for the year 2100 (pH 7.79) (Gattuso and Lavigne, 2009) at two time points of 1 hour and 7 days. The low pH seawater treatment was achieved by aeration with CO₂ gas, to mimic the predicted low pH value as well as to imitate the additional changes expected in dissolved inorganic carbons (DIC) through OA. This is a standard method to manipulate the carbonate chemistry in OA experiments described by Gattuso et al. (2010). The selected *target* genes, already introduced in Chapter 2 and Chapter 3, are involved in passive intra- and extracellular fluids buffering, ion exchange and transport, transport of CO₂ in blood, biomineralisation and metabolic processes (Fabry et al., 2008). The identities of each partial sequence isolated were confirmed showing similarity to other species counterparts.

Simulating the pH conditions expected for 2100, the *NHE* expression showed no significant change after 1 hour and also not after 7 days ($p=0.128$), yet a down-regulation trend ($p=0.069$) in the worm group kept at low pH for 7 days could be observed (Fig. 5.1 a). However, it should be noted that there is a significant difference in the size of the worms from the different time groups, which could have also affected gene expression. The *CA* expression showed a statistically significant change for the effect of pH ($p=0.005$) but no difference between the two time points ($p=1.000$). *CaM* showed no statistically significant changes at either time point relative to the control group.

In contrast to the present results, the study on sea urchin larvae, *S. purpuratus*, of Stumpp et al. (2011) showed an up-regulation of *NHE3* after 2 days in low pH (7.7)

conditions and a 45% down-regulation after 4 days. They assume that the down-regulation could be based on the “energy-turnover” model (Reipschläger and Pörtner, 1996), which suggests that there is an activation of energetically more favourable transporters instead of NHE. The observed lack of significant changes in the *NHE* expression herein may suggest that the activity of existing protein levels were sufficient to regulate the pH under low pH conditions, and that a costly increase in *NHE* was not required to maintain the acid-base balance. However, the clear trend of down-regulation would support the “energy-turnover” model proposed by Reipschläger and Pörtner (1996). In line with the present results, another study conducted on the *S. purpuratus* showed no significant change in *NHE* expression under acidified conditions (pH 7.88-7.96) within <72 hours (Todgham and Hofmann, 2009). Contrary to the present study, the Japanese medaka fish, *O. latipes*, showed an up-regulation in *NHE* in different ontogenetic stages as well as different tissue exposed to pH 7.6 and 7.1 (Tseng et al., 2013). *NHE* expression thus appears to differ according to the species used and the pH exposure regime adopted.

The mRNA expression of *CA* showed a significant up-regulation ($p=0.005$) under low pH conditions in both groups (1 hour and 7 days) in comparison to worms kept at control pH conditions (Fig. 5.1 b). On the other hand, no effect of time ($p=1.000$) and no significant interaction ($p=0.892$) between time and pH could be observed. In contrast to the present findings, a study on the sea urchin larvae *S. purpuratus* kept at pH 7.7 for 2, 4 and 7 days could not find a significant effect on CA15 as well as on the CA related protein (CA10) (Stumpp et al., 2011). Another study on sea urchin larvae *S. purpuratus* found five *CA* mRNA transcripts altered under high CO₂ conditions (Todgham and Hofmann, 2009). The study highlights the importance of CAs for biomineralisation processes and found *CA-7 like A* transcript levels up-regulated (Todgham and Hofmann, 2009). The remaining four *CA* transcripts were down-regulated (Todgham and Hofmann,

2009). The study of Moya et al. (2012) using the coral *A. millepora*, also showed a down-regulation of several *CA* transcripts after 3 days under elevated $p\text{CO}_2$ conditions. Some of these *CAs* were already suggested to be associated with calcification processes (Moya et al., 2012). In *M. edulis* the protein activity of *CA* was reported to be reduced after a six months exposure to high $p\text{CO}_2$ conditions mimicking future OA conditions (Fitzer et al., 2014). In line with the present results, *CA* expression in another coral species, *P. damicornis*, was found to be up-regulated under low pH (7.8 and 7.4) after a longer exposure time of 3 weeks (Vidal-Dupiol et al., 2013).

The different expressions of the *CAs* are likely caused by functional differences of the isoforms as well as different requirements in the above mentioned calcifying species in contrast to the non-calcifying polychaete *P. dumerilii* used in the present study. In calcifying species the importance of *CAs* in biomineralisation processes were highlighted (Todgham and Hofmann, 2009; Moya et al., 2012), but these will only play a minor role in the non-calcifying species *P. dumerilii*. However, biomineralisation processes cannot be completely excluded as jaw and chaetae formation might apply similar mechanisms (George and Southward, 1973; Colbath, 1986). The up-regulation in *P. dumerilii* under high $p\text{CO}_2$ concentrations could suggest an increased need of *CA* to maintain the acid-base balance in the blood and other tissues and to help to transport CO_2 out of the tissues. Additional studies are needed to gain better knowledge of the function of individual isoforms of *CA* to understand the exact processes.

The gene expression of *CaM* was not altered under low pH conditions ($p=0.806$) and also no significant change over time ($p=0.374$) or an interaction between both could be observed ($p=0.601$). The present findings are in contrast to other studies using a range of species. For example, a study on the coral *A. millepora* showed a down-regulation of *CaM* in response to high CO_2 stress (pH 7.6-7.7) after 28 days (Kaniewska et al., 2012).

Kaniewska et al. (2012) assume that the down-regulation of *CaM* together with other proteins could indicate a disruption in the cell calcium homeostasis. Also in the Pacific oyster (*C. gigas*) larvae *CaM* was down-regulated after low pH (~7.5) exposure for 6 days (Dineshram et al., 2012). On the other hand, the commercial oyster *C. hongkongensis* showed a significant down-regulation at moderate low pH (7.9) and a small up-regulation at low pH (7.6) (Dineshram et al., 2013). However, *A. millepora*, *C. gigas* and *C. hongkongensis* represent calcifying species unlike the present study using a non-calcifying polychaete. Calcification is considered to be one of the most vulnerable physiological processes towards OA (Doney et al., 2009). It is therefore possible that the *CaM* is more important for calcification / biomineralisation processes than other physiological processes, as indicated by the present results. Another relevant factor that needs to be considered is the life stage of the animals. Many of the studies available in the literature solely focus on the early life history stages (O'Donnell et al., 2010; Zippay and Hofmann, 2010; Wong et al., 2011). In contrast, the present data was collected from adult specimens. *P. dumerilii* larvae are likely to respond differently to the same exposure regime. Therefore, further studies are needed to make predictions for different life stages. To date, several studies have investigated the effects of short term high $p\text{CO}_2$ exposure on different aquatic species. In most cases, such studies focus on calcifying organisms, and correspondingly little is known about the effects on non-calcifying species. Moreover, the molecular mechanisms triggered during low pH exposure still need to be characterised. This chapter presents relative gene expression data for three *target* genes *NHE*, *CA* and *CaM* of *P. dumerilii* kept at normal seawater pH levels and pH levels predicted for 2100. Only the expression of *CA* was significantly altered under low pH conditions. An up-regulation could be observed in both groups kept under low pH conditions for 1 hour and for 7 days. Both, *NHE* and *CaM* did not show a significant change. However, a down-

regulation trend could be observed in *NHE*. When comparing the present gene expression data to the data of animals exposed to low pH induced by HCl (Chapter 3) the results do not correspond with each other, which suggests that it is not necessarily the pH change that induces the gene expression changes. Nevertheless, these results indicate that also non-calcifying species can be affected by the seawater pH changes expected within this century. The present chapter provides a first insight into such potential affected mechanisms in the non-calcifying marine worm *P. dumerilii*.

5.5 Conclusions

The present chapter demonstrates that low pH seawater, induced by CO₂ gas, effects the gene expression in *P. dumerilii*. The relative expression of *CA* in adult, yet sexually immature, worms was significantly up-regulated under low pH conditions. Being affected by high *pCO*₂ levels and also showing significant changes in other species such as *S. purpuratus*, *A. millepora*, *M. edulis* and *P. damicornis*, *CA* could potentially be developed into a molecular biomarker for *OA* (Todgham and Hofmann, 2009; Moya et al., 2012; Fitzner et al., 2014 and Vidal-Dupirol et al., 2013). However, further studies and optimization procedures are needed to evaluate the validity of *CA* as a biomarker. The two other genes analysed (*NHE* and *CaM*) were not significantly altered, though a higher sample number for *NHE* might have yield in a significant result. Showing no significant effect for both HCl (Chapter 3) and CO₂, *CaM* does not seem to be a good candidate to investigate *OA* stress in marine polychaeta. Future work could look at other candidate genes such as those identified with the SSH approach (Chapter 4).

Overall, these findings show that those species previously considered more tolerant towards *OA* may be affected by acidified seawater. However, further studies are needed to understand the involved mechanisms in more detail and to investigate the resulting consequences on *P. dumerilii*.

6.1 Introduction

Predominantly, due to anthropogenic activities atmospheric CO₂ levels have increased to over 380 ppm in comparison to 280 ppm at pre-industrial times. Without oceans these levels would have been even higher because oceans have taken up about one third of the CO₂ from the atmosphere (Feely et al., 2004). However, this slowing down of global warming by the uptake of CO₂ leads to another substantial problem, namely OA (IPCC, 2014). In recent years OA has become a main focus of research and numerous experiments have examined the effects of changing seawater conditions on marine organisms (Gattuso and Hansson, 2011). Since the pre-industrial times to the 1990s the ocean surface pH has decreased from 8.2 to 8.07 (Gattuso and Lavigne, 2009) and the “business-as-usual” RCP8.5 model predicts a mean surface pH change of -0.33 (± 0.003) pH units in the 2090s relative to the 1990s (Bopp et al., 2013). Most organisms inhabit areas near the surface, where the highest pH changes are expected (Caldeira and Wickett, 2003). Such changes may cause a reduction in ecosystem function due to the loss of stress-intolerant species (Fischlin et al., 2007). To make predictions of how OA will affect organisms it is essential to understand and characterise the molecular level changes of any physiological processes affected. Knowing that calcifying organisms are highly vulnerable to acidification (Hofmann et al., 2010) it would be informative to know if these processes are similarly altered in other types of organisms. Interestingly, Calosi et al. (2013) have shown that the polychaete worm *P. dumerilii*, which is present in natural, existing CO₂ vent areas in Ischia, Italy, was able to adapt physiologically to chronic and elevated levels of *p*CO₂. A colonization experiment performed along the CO₂ gradient in

the Ischia vents (Tyrrhenian Sea, Italy) showed the abundant occurrence of *P. dumerilii* in highly acidified areas (Ricevuto et al., 2014). The experiment indicates the species tolerance for low and variable pH. Furthermore, it has been shown that volcanic CO₂ vents can be useful to investigate long-term effects of OA on benthic biota and sea-floor ecosystems (Hall-Spencer et al., 2008). The study addresses the problem that the natural venting sites are not exactly similar to global OA but that the systems can still provide important information about high CO₂ effects on spatial and temporal scales.

The CO₂ vents of Ischia (Bay of Naples, Italy) have been used in many studies to explore the effects of low pH/ high *p*CO₂ on marine communities in order to make predictions about responses of marine organisms/ ecosystems to OA (Hall-Spencer et al., 2008; Cigliano et al., 2010; Kroeker et al., 2011). Experiments conducted on the Ischia vents have reported an effect of the settlement of different benthic organisms with increasing CO₂ levels (Cigliano et al., 2010; Kroeker et al., 2011). Only one syllid polychaete *Syllis prolifera* showed a high occurrence at the very low pH zone (Cigliano et al., 2010). The study of Kroeker et al. (2011) observed fewer taxa, reduced taxonomic evenness and lower biomass in the very low pH areas of the Ischia vent. Further experiments showed that the sponge (*Phorbas tenacior*, *Petrosia ficiformis*, *Chondrilla nucula* and *Hemimycale columella*) percentage cover was significantly lower in low pH areas of the vent than in the normal pH parts (Goodwin et al., 2014). Similarly, the sponge species composition also changed under the different *p*CO₂ conditions (Goodwin et al., 2014). On the other hand, a study on coral microbial communities was not significantly impacted by pH (Meron et al., 2012). As well as the vents around Ischia, the natural CO₂ gradients off the island of Vulcano (North of Sicily, Italy) have also been used to study biogeochemical processes related to CO₂ release and OA (Arnold et al., 2012; Boatta et al., 2013; Johnson et al., 2013; Kerfahi et al., 2014).

Phylogenetic studies are often applied in addition to physiological, biochemical, morphological and behaviour studies, in order to interpret evolutionary adaptation (Garland et al., 2005). Calosi et al. (2013) used a putatively neutral molecular marker, cytochrome c oxidase subunit I (COI), to investigate the relatedness and phylogeographic pattern in *P. dumerilii* and *A. mediterranea* populations from different areas including the Ischia CO₂ vent area. The “universal” DNA primers used in the study code for a 710 bp fragment of the mitochondrial COI gene and are described as primers that generate informative sequences for phylogenetic analyses for investigations at species as well as higher taxonomic levels (Folmer et al., 1994). Mitochondrial COI genes are supposed to be very conserved protein-coding genes (Folmer et al., 1994) and have been used in insect phylogeny for many years (Lunt et al., 1996; Jamnongluk et al., 2003; Bacci et al., 2009). The phylogenetic analysis of Calosi et al. (2013) showed that *P. dumerilii* from the vent population are genetically different from the nearby populations although also showing the existence of normal “typical” *P. dumerilii* in the vent system. In contrast *A. mediterranea* showed no difference between vent and non-vent individuals.

The present chapter examines gene expression changes of a selected number of genes, representing energy metabolism (*NADH dehydrogenase*), ion exchange and transport (*NHE*), acid-base regulation (*CA*) and cytoskeleton (*paramyosin*) processes, of the non-calcifying marine invertebrate, *P. dumerilii*, collected from the CO₂ vent and from non-vent areas around Ischia within their own habitat, as well as after a low/ high pH laboratory exposure experiments. Vent populations are expected to have a different gene expression of the *target* genes in comparison to non-vent populations, due to potential low pH adaptation mechanisms. Also a further molecular approach, using a restriction enzyme digest, was used to determine whether the individuals collected inside the vent area were part of the vent population or decent from the populations nearby. Additionally,

a group of swimming, reproducing heteronereids was collected directly over the vent and a phylogenetic approach based on COI was used to determine their origin as this could provide useful information on reproduction behaviour of the vent/ non-vent populations. Furthermore, different populations of *P. dumerilii* collected at various places in the Mediterranean including CO₂ venting sites at Vulcano (Sicily) and Ischia (Napels), as well as worms from France and England were included in the analysis, in order to investigate the phylogeographic pattern of different populations including potential low pH adapted ones. *P. dumerilii* from the CO₂ vents in Ischia and Vulcano are expected to be genetically different to non-vent populations.

6.2 Material and Methods

6.2.1 Study area

Ischia is a small island located in the bay of Naples (Tyrrhenian Sea, Italy). The studied CO₂ vents of the island occur on the north and south sides of the Castello Aragonese (40°43'54.00"N 13°57'48.45"E) (Fig. 6.2), a small islet of volcanic origin connected to the main Island of Ischia by an artificial road. Gas emissions occur in shallow waters in the area around the island (Tedesco, 1996) (Fig. 6.1). It has been estimated that the subsurface gas emissions have occurred locally for approximately 1800-1900 years (Lombardi et al., 2011b). The gas of the vent area is almost entirely composed of CO₂ and no toxic compounds are detected as follows: 90.1-95.3 % CO₂, 3.2-6.6 % N₂, 0.6-0.8 % O₂, 0.08-0.1 % Ar and 0.2-0.8 % CH₄ (Hall-Spencer et al., 2008). At the south site of the vent the gas is released in an area of approximately 3,000 m² at 1.4 × 10⁶ litre day⁻¹; at the north side at 0.7 × 10⁶ litre day⁻¹ in an area of about 2,000 m² (Hall-Spencer et al., 2008). In the study of Kroeker et al. (2011) the pH values ranged between 8.07 and 6.51. Furthermore, pH monitoring showed high variability with daily fluctuations (Kroeker et

al., 2011). According to the study of Hall-Spencer et al. (2008) the water salinity (38 ‰) and the total alkalinity (2.5 mequiv.kg⁻¹) are similar in all survey stations and the temperature undergoes seasonal fluctuations between 13 and 25 °C.

The reference site is located around the Sant'Anna islets (40°43'35.76"N 13°57'36.95"E) (Fig. 6.2), which are approximately 600 m south of the CO₂ vents. At that study site venting activities are absent. *P. dumerilii* were associated with the same algae as described for the sampling site around Castello and additionally could be found in *Corallina* sp. (Calosi et al., 2013).

6.2.2 Animal collection

P. dumerilii (size range shown in Table 6.5) were collected by snorkelling (at 1-2 m depth) within their associated macro-algae (mainly *Dictyota* spp., *Halopteris scoparia* and *Cladophora prolifera*) in the two CO₂ vents as well as control area at the north-east side of the island Ischia (Tyrrhenian Sea, Italy) (Fig. 6.2).

The first sampling area, called 'Castello N3' was characterised by a rocky reef on the north side of the Castello Aragonese, Ischia, Naples (40°43'55.00"N, 13°57'48.82"E) (Fig. 6.2), which low pH conditions of 7.14 ± 0.40 (Ricevuto et al., 2014). The second vent sampling site, named Castello S3, was a rocky reef on the south side of the Castello Aragonese, Ischia, Naples (40°43'51.18"N, 13°57'47.45"E) (Fig. 6.2), characterised by acidified conditions of pH 7.37 ± 0.37 (Ricevuto et al., 2014). The reference site, named 'S. Anna', was located besides the Sant'Anna islets, and was approximately 600 m distance from the vents. Venting activities are absent in this area and pH values represent low *p*CO₂ conditions (mean pH 8.05 ± 0.001 (late spring) and 8.11 ± 0.001 (autumn)) (Ricevuto et al., 2015).

At each sampling site worms were transferred straight into RNALater solution (Sigma-Aldrich Company Ltd., Gillingham, UK) (Castello N3 n=21; Castello S3 n=25; S. Anna n=15). For this and all other experiments atokus worms, a sexually immature stage of the worm, were used to reduce expression differences based on reproduction. Swimming heteronereids were collected over the south vent of Castello Aragonese using light to attract the worms (Haunenschild, 1955; Hardege et al., 1990). Specimens were immediately transferred into RNALater solution (Sigma-Aldrich Company Ltd., Gillingham, UK) and stored at -20 °C.



Figure 6.1 CO₂ vent around the island of Ischia (Italy). The picture was provided by Jason Hall-Spencer (Plymouth University). Image credit: David Liittschwager, National Geographic (2010).

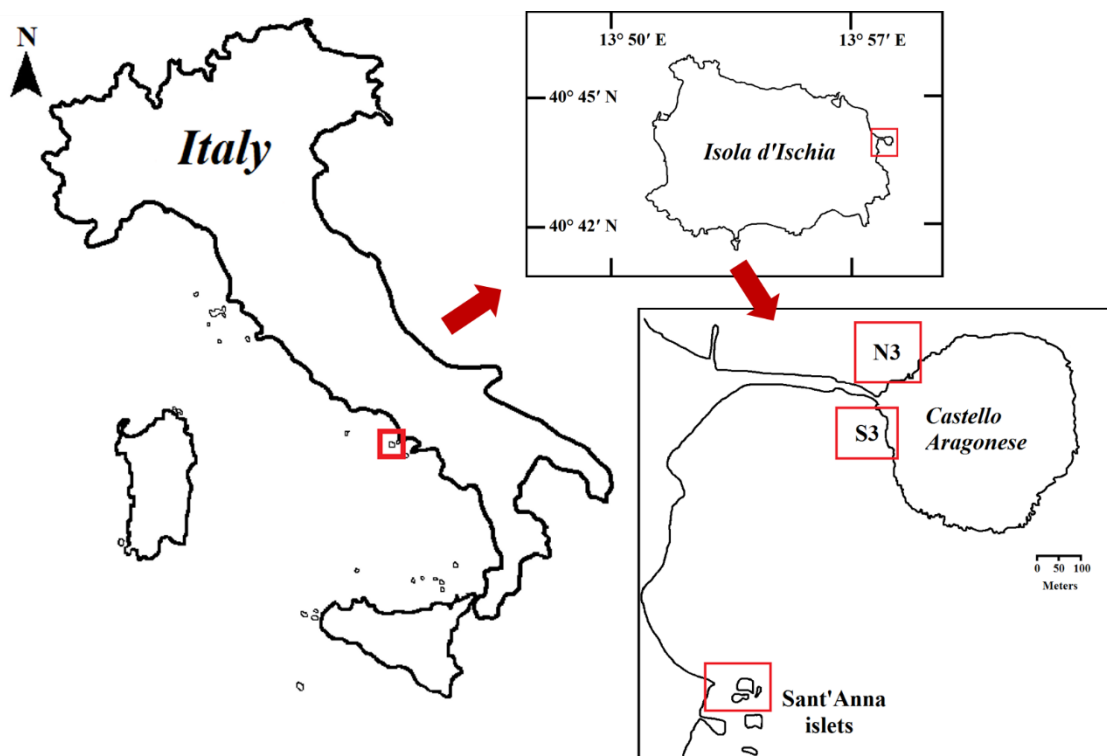


Figure 6.2 Map of the sampling site in Italy on the island Ischia around Castello Aragonese and the S. Anna islets, highlighted with red rectangles.

6.2.3 Laboratory exposure experiment

6.2.3.1 S. Anna - reference site worms

Additional *P. dumerilii*, (n=24) sampled from the S. Anna reference site, were used for a 7 d laboratory exposure experiment in parallel to the field sample analysis. The exposure length was chosen to reflect a potential acclimation time point. This is similar time frame (5-7 d) used in previous studies (Stumpff et al., 2011; Dineshram et al., 2012; Calosi et al., 2013). For the exposure regime, worms were kept in closed glass bowls (approx. 8 individuals per bowl), each containing 300 ml of filtered (HAWP 0.45 μm , Merck Millipore) natural seawater at their original seawater pH/ $p\text{CO}_2$ (pH \sim 8.00) at a light regime of 12 h light/ 12 h dark in a temperature controlled room at 19 $^{\circ}\text{C}$ as a control group ('non-acidified C-C'). Another group of worms (n=24) collected from the S. Anna site were exposed to low pH (7.7) at the same light regime and temperature (now referred

to as ‘acidified C-A’). The pH was adjusted by bubbling CO₂ into the seawater (KitCO₂ Energy Professional, Ferplast, Castelgomberto, Italy).

6.2.3.2 Castello S3 – vent worms

A similar exposure regime was used for worms collected at the vent sampling site ‘Castello S3’. One group (n=20) of worms were kept in closed glass bowls in filtered natural seawater at pH 7.7 as a control group (‘acidified A-A’). The same light regime and temperature condition was used as described for the S. Anna. A second group of Castello S3 vent worms (n=20) were kept in natural seawater with a pH of 8.00 (now referred to as ‘non-acidified A-C’) as treatment. For both exposure experiments the pH of the water was measured every day (for mean \pm SEM see Table 6.4). A whole water changed was carried out on a daily basis. Worms were fed with spinach every 2 d. After 7 d worms were transferred into approximately 800 μ l of RNALater (Sigma-Aldrich Company Ltd., Gillingham, UK) and stored at -20°C until molecular analysis.

6.2.4 Total RNA isolation and cDNA synthesis

Total RNA was extracted from each individual worm using High Pure RNA Tissue Kit reagents and the manufacturers protocol (Roche, Burgess Hill, UK). For detailed protocol see section 2.2.2. cDNA was synthesised from approximately 250 ng of total RNA using SuperScript VILO cDNA Synthesis Kit reagents (Life Technologies, Paisley, UK) following the protocol described in section 2.2.3 and stored at -20°C.

6.2.5 Target gene isolation and characterisation

Target genes were selected based on previous chapters. *NADH dehydrogenase* was selected to represent energy metabolism processes. *NHE* and *CA* were chosen as

representatives for acid base regulation and *paramyosin* for cytoskeleton functions. For qPCR analysis *18S* and *α -TUB* were chosen as *reference* genes. The designed primers were synthesised by IDT (Integrated DNA Technologies, Leuven, Belgium) and resuspended in molecular grade water to a concentration of 10 pmol/ μ l.

Nucleotide sequences for all *target* and *reference* genes were obtained from GenBank (<http://blast.ncbi.nlm.nih.gov/Blast.cgi>) and Blasted against the worm database PLATYpopsys (<http://hydra.cos.uni-heidelberg.de/ppp/styled-2/>) from the EMBL, Heidelberg. PCR products were sequenced directly (Macrogen Europe, Amsterdam, the Netherlands) and the sequence identities were verified using BLAST search (<http://blast.ncbi.nlm.nih.gov/Blast.cgi>).

6.2.6 Amplification using qPCR

For the qPCR amplification all reactions were performed in duplicates. The reagents volumes and cycling conditions were exactly the same as described in section 2.2.10.2. For primer concentrations and assay performance see Table 6.1 and Table 6.2.

Table 6.1 Oligonucleotide primers for the four *target* genes and the two *reference* genes with forward and reverse sequence, amplicon size in bp and primer concentration used in nM.

<i>Target gene</i>	Primer sequence (5'-3')	Amplicon size (bp)	Primer concentration used (nM)
<i>18S</i>	F GCGCATTTATCAGCACAAGA R CTTGGATGTGGTAGCCGTTT	239	50
<i>α-TUB₂</i>	F TTGCTGTCTACCCAGCTCCT R AGATGGCCTCATTGTCAACC	123	700
<i>NADH dehydrogenase</i>	F CGAACCGGATTATGGCTTTG R GGAATTTGTCCCGTCTGCA	153	100
<i>NHE</i>	F CCTACCTCAAGTGGCACCAT R GGCATGTACTCCGTCAGGTT	115	500
<i>CA</i>	F GCAAGCAGAGCCCTATCAAC R TTTGTAGGTGGCTCCAGTC	197	100
<i>Paramyosin</i>	F AGAACGCTGAGGGTGAATTG R CGAGCTGGAGCCTGTCGGCA	183	80

Table 6.2 Melting temperature (°C) and efficiency of amplification (%) of the oligonucleotide primers for *18S rRNA*, *α-TUB₂*, *NHE*, *CA*, *NADH dehydrogenase* and *paramyosin*.

<i>Target gene</i>	Melting temperature (°C)	Efficiency of amplification (%)
<i>18S rRNA</i>	82	103.54
<i>α-TUB₂</i>	81	102.78
<i>NADH dehydrogenase</i>	77.5	98.03
<i>NHE</i>	78	100.96
<i>CA</i>	78.5	90.60
<i>Paramyosin</i>	84	96.84

6.2.7 Restriction enzyme analysis to determine species

Previously, phylogenetic analysis based on cytochrome c oxidase I (COI) by Calosi et al. (2013), showed that *P. dumerilii* from the vent sampling site Castello S3 are genetically different to *P. dumerilii* from the reference site S. Anna. Available sequences on GenBank were used to create a sequence alignment in order to find nucleotide differences between the two populations (Fig. 6.6). Based on the alignment, an enzyme restriction site (BstZ17I) was located that is only present in vent worms sampled at Castello S3 but not in reference S. Anna worms. Therefore, the restriction enzyme BstZ17I can be used to confirm that the worms collected at Castello S3 actually represent specimens from the vent population rather than worms that had travelled into the area.

6.2.7.1 Generation of COI PCR product

To generate the COI PCR products, 1 µl of cDNA was combined with 0.5 µl of 10 pmol/µl universal primers LCO1490 (5'-GGTCAACAAATCATAAAGATATTGG-3') and HCO2198 (5'-TAAACTTCAGGGTGACCAAAAAATCA-3') from Folmer et al. (1994).

0.25 µl of Herculase cDNA polymerase (Agilent Technologies, Wokingham, UK), 5 µl 5× PCR buffer (Agilent Technologies, Wokingham, UK), 0.5 µL 40 mM dNTP mix (Thermo Fisher Scientific, Loughborough, UK), 0.5 µL DMSO (Agilent Technologies, Wokingham, UK), 0.5 µL 25 mM MgCl₂ (Thermo Fisher Scientific, Loughborough, UK) and 16.25 µL sterile nuclease-free water (Thermo Fisher Scientific, Loughborough, UK) to prepare a total reaction volume of 25 µL. For the PCR, a ‘touch-up’ protocol was used. The PCR conditions were as follows: 2 min at 94 °C; then 4 cycles of 94 °C for 30 s, 48 °C for 50 s, and 68 °C for 1 min, followed by 4 cycles of 92 °C for 30 s, 50 °C for 50 s, and 70 °C for 1 min, followed by 24 cycles of 92 °C for 30 s, 52 °C for 50 s, and 72 °C for 1 min, followed by 72 °C for 5 min. The negative control included all components of the PCR reactions but replaced template DNA with molecular grade water.

6.2.7.2 BstZ17I restriction digest

5 µl of COI PCR product, 1 µl (10 U) restriction enzyme and 2 µl of the corresponding 1× Buffer 0 (Thermo Fisher Scientific, Loughborough, UK) were mixed and incubated at 37°C for 3 h. The restriction digested PCR products were analysed on a 1 % agarose gel, stained with SYBR Safe DNA gel stain (Life Technologies, Paisley, UK). For more details of the gel preparation see section 2.2.6.

6.2.8. Phylogenetic analyses

The molecular phylogenetic analyses were conducted on specimens collected at S. Anna (Ischia, Italy), S. Pietro (Ischia, Italy), Forio (Ischia, Italy), Castello N3 (Ischia, Italy), Castello S3 (Ischia, Italy), Vulcano (Baia di Levante, Italy), S. Catarina (Italy), Nisida (Italy), Palinuro (Italy), Stareso (Italy), Ustica (Italy), Blanes (Spain), Arcachon (France) and Bristol (England) (Fig. 6.3), including sequences previously published in Calosi et al.

(2013), sequences newly generated for this study and the COI sequence from the complete mitochondrial genome of *P. dumerilii* (Boore and Brown (2000), GenBank accession number AF178678). For each population individuals (n= 3-15) were collected for genetic analyses and preserved in 95% ethanol. Total DNA was extracted from each individual worm using the DNeasy Blood & Tissue Kit (Qiagen, Manchester, UK) following the manufacturer's instructions. The gene region of the mitochondrial COI was amplified using the established primers described by Folmer et al. (1994). PCR products were sequenced directly (Macrogen Europe, Amsterdam, the Netherlands) and the sequence identities were verified using BLAST search (<http://blast.ncbi.nlm.nih.gov/Blast.cgi>). All sequences were submitted to GenBank under accession numbers KT124668 through KT124738.

The following paragraph shows the data analysis conducted by Dr Anja Schulze (Marine Biology Department, Texas A&M University). The sequences were aligned using the ClustalW algorithm in MEGA 6 (Tamura et al., 2013). The final alignment length was: 568 bp. A phylogenetic analysis was conducted using Bayesian Inference in MrBayes 3.2.1 (Ronquist et al., 2012) through the CIPRES Science Gateway v 3.3 (Miller et al., 2010), using two runs with four Metropolis Coupled Markov Chains Monte Carlo (MCMCMC) each for 5,000,000 generations under a General Time Reversible Model plus Gamma, with the first 1,000,000 generations discarded as burn-in. Trees were sampled every 100 generations from the posterior distribution after the burn-in period and a 50% majority rule consensus tree was generated. *Nereis pelagica* (GenBank accession GU672554) was chosen as the outgroup and *N. zonata* (HQ024403) was included additionally.

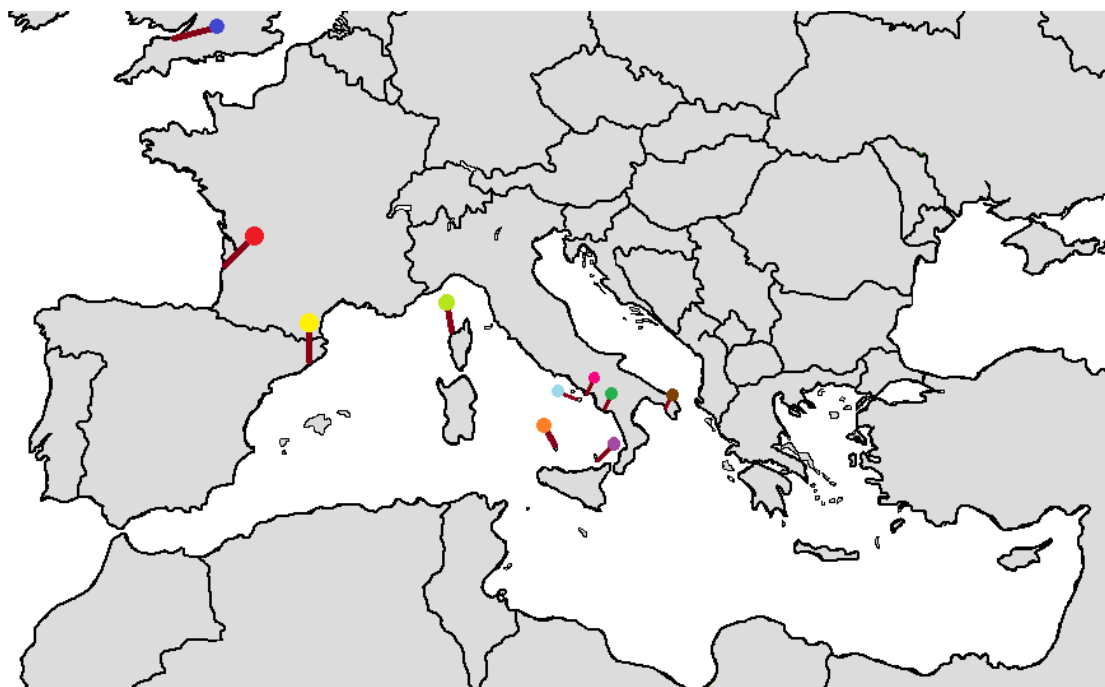


Figure 6.3 Map of the sampling sites used for the phylogenetic analysis around the Mediterranean Sea, Atlantic Ocean and Bristol Channel. Approximate sampling locations are highlighted with pins (blue-Bristol, red-Arcachon, yellow-Blanes, light green-Stareso, light blue-Ischia, pink-Nisida, dark green-Palinuro, orange-Ustica, purple-Vulcano, brown-S. Catarina).

6.3 Statistical analyses

Statistical analysis was performed using Minitab 16 (Minitab Inc., State College, PA). Since normality (Shapiro-Wilk) and independence assumptions were not fulfilled and log transformation was not successful, the significant variations in gene expression levels were determined using the nonparametric Kruskal-Wallis test ($p < 0.05$). In case of significance a Mann-Whitney U test was used to evaluate significant differences between data. For all analyses, statistical significance was accepted at $p < 0.05$. Significant effects are labelled with asterisks (* $p < 0.05$; ** $p < 0.01$; *** $p < 0.001$). Non-significant results are labelled with ns. Values are presented as means \pm SE. All graphs were designed with XACT 8.03 (SciLab, Germany).

6.4 Results

6.4.1 Experimental parameters

6.4.1.1 Seawater pH during exposure experiment

The seawater pH of the normal pH condition, pumped straight from the sea next to the Villa Dohrn (Ischia) showed a pH of around 8.0 (Table 6.3). The low pH exposure condition was approximately 7.7 with small variations (Table 6.3).

Table 6.3 Seawater pH (mean \pm SEM) in *P. dumerilii* holding glass bowls during 7 d exposure experiment.

Treatment	pH measured	
	S. Anna	Castello S3
8.0	8.00 \pm 0.011	7.99 \pm 0.014
7.7	7.68 \pm 0.038	7.70 \pm 0.032

6.4.1.2 Punctual value records of sample collection sides

Salinity and temperature measurements showed relative stable values with only small fluctuations between the three sample stations at the measured time points (Table 6.4). The measured pH showed greater fluctuations and also larger differences between the two vent sampling sites (Castello S3 and Castello N3) (Table 6.4).

Table 6.4 Average punctual value records (n=13) and SEM of salinity, temperature and pH at the three sampling station Sant'Anna, Castello S3 and Castello N3 in June 2014.

Station	Sant'Anna	Castello S3	Castello N3
Salinity (PSU)	38.50 \pm 0.29	38.00 \pm 0.00	38.00 \pm 0.00
Temperature ($^{\circ}$ C)	23.86 \pm 0.27	23.98 \pm 0.30	23.8 \pm 0.22
pH	8.13 \pm 0.02	7.42 \pm 0.10	7.91 \pm 0.08

6.4.1.3 Body mass differences from the three sampling sites

The worms collected from the two vent sampling areas (Castello S3 and Castello N3) and the reference site (S. Anna) showed no significant difference in their body weight (one-way ANOVA, $p=0.7938$) (Table 6.5; Fig. 6.4).

Table 6.5 Body mass (mean \pm SEM) in mg of *P. dumerilii* direct field samples from the three sampling station S. Anna, Castello S3 and Castello N3 as well as for the individuals used in the transplant experiment (C-C, C-A and A-A, A-C).

Station	Body mass (mg)
S. Anna	2.86 \pm 0.38
Castello S3	2.96 \pm 0.58
Castello N3	2.78 \pm 0.55
S. Anna C-C	2.77 \pm 0.74
S. Anna C-A	2.12 \pm 0.31
Castello S3 A-A	2.26 \pm 0.22
Castello S3 A-C	3.48 \pm 0.84

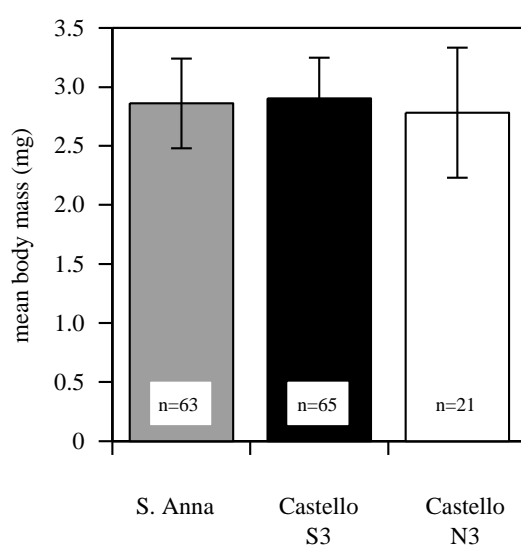


Figure 6.4 Body mass of all *P. dumerilii* collected from S. Anna in low $p\text{CO}_2$ environment and within the two CO_2 vents (Castello S3 and N3) with elevated $p\text{CO}_2$ conditions.

6.4.2 qPCR analysis of *target* gene mRNA expression

The expression levels of the four *target* genes were analysed for *P. dumerilii* from their original locations (S. Anna, Castello S3 and Castello N3), as well as for worms maintained in the laboratory at normal and low pH conditions (S. Anna C-C, C-A and Castello S3 A-A, A-C) for 7 d (Fig. 6.5 a-d). The results are summarised as follows:

Field investigation of relative *target* gene expression

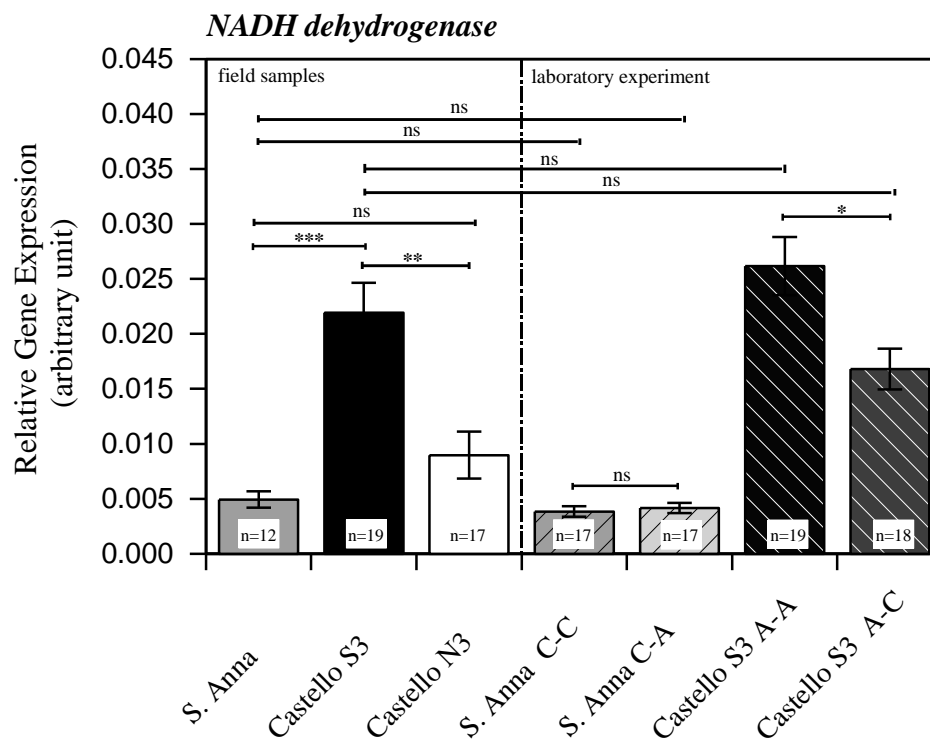
NADH dehydrogenase mRNA expression in *P. dumerilii* collected from the field was significantly lower ($p < 0.001$) in S. Anna worms in comparison to vent (Castello S3) worms, yet no significant difference ($p = 0.674$) was observed between S. Anna and the Castello N3 vent individuals (Fig. 6.5 a). The *NADH dehydrogenase* mRNA expression in worms sampled at the Castello S3 vent was significantly higher ($p = 0.0019$) in comparison to that for worms sampled at Castello N3 (Fig. 6.5 a). The relative gene expression of *NHE* was significantly increased ($p < 0.001$) at the reference sampling site S. Anna in comparison to the vent sampling sites Castello S3 and Castello N3. No significant difference ($p = 0.1165$) was detected between the two vent populations Castello S3 and Castello N3 (Fig. 6.5 b). The primers designed for *CA* failed to amplify using worms from S. Anna and most Castello N3, therefore, only the gene expression of Castello N3 (small sample number) and S3 were analysed. No significant gene expression differences on any of the field populations or treatments could be observed, however a clear trend could be observed (P-value of Kruskal-Wallis $p = 0.051$) (Fig. 6.5 c). *Paramyosin* mRNA expression was significantly higher in worms from S. Anna in comparison to the vent sites Castello S3 ($p = 0.0145$) and Castello N3 ($p < 0.001$) (Fig. 6.5 d). There was no significant difference between Castello N3 and Castello S3 ($p = 0.0536$) (Fig. 6.5 d).

Experimental exposure and impact of translocation on *target* gene expression

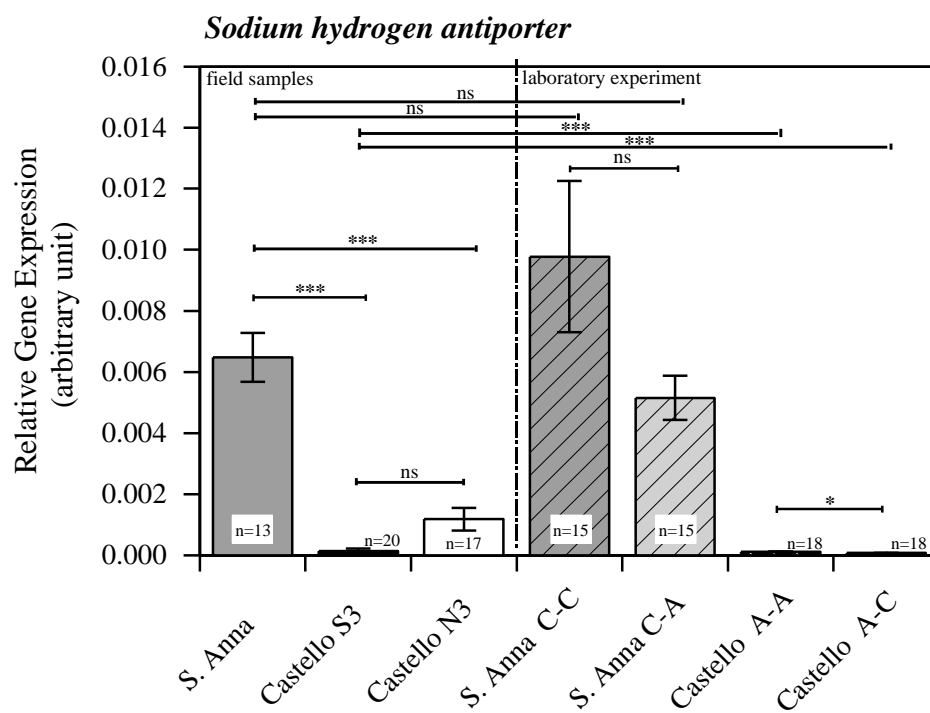
The 7 d normal pH exposure (A-C) of worms sampled from Castello S3 showed a significant down regulation ($p=0.0171$) of *NADH dehydrogenase* in comparison to Castello S3 kept at low pH (7.7). In contrast, the worms from S. Anna, which were transferred from normal to low pH conditions, showed no significant ($p=0.5353$) gene expression difference in *NADH dehydrogenase* after 7 d (Fig. 6.5 a). No significant effect on the relative gene expression of *NADH dehydrogenase* could be observed when comparing individuals from the 7 d transfer experiment to direct field samples from the control site S. Anna (C-C: $p=0.3191$; C-A: $p=0.6420$) and the vent site Castello S3 (A-A: $p=0.3972$; A-C: $p=0.3087$) (Fig. 6.5 a). The 7 d low pH exposure (C-A) of worms sampled from S. Anna showed no significant effect ($p=0.229$) on the relative gene expression of *NHE* (Fig. 6.5 b). Comparing the expression of *NHE* from worms of the laboratory experiment to the worms sampled straight from the field, no difference could be detected (C-C: $p=0.7822$; C-A: $p=0.2495$). In contrast to S. Anna, worms from Castello S3 that were transferred to normal pH (8.0; A-C) showed a significant ($p=0.0169$) down regulation in *NHE* in comparison to Castello S3 kept at low pH (7.7). Also the transfer to the laboratory led to significant down-regulation in *NHE* (A-A: $p<0.001$; A-C: $p<0.001$) (Fig. 6.5 b). The relative gene expression of *CA* of worms from Castello S3, which were transferred to normal pH (A-C), showed no significant change (Fig. 6.5 c). The relative gene expression of *paramyosin* of worms from S. Anna transferred to low pH (7.7; C-A) for 7 d showed no significant ($p=0.5284$) difference. However, the transfer to the laboratory led to a significant down-regulation of *paramyosin* (C-C: $p<0.001$; C-A: $p<0.001$) when comparing to the S. Anna field investigation. Worms from the Castello S3 vent transferred to normal pH conditions (A-C) showed no significant difference ($p=0.2750$) in the relative gene expression of *paramyosin* (Fig. 6.5 d), but the transfer to

the laboratory showed a significant ($p < 0.001$; $p < 0.001$) down-regulation in comparison to the field samples of Castello S3.

a



b



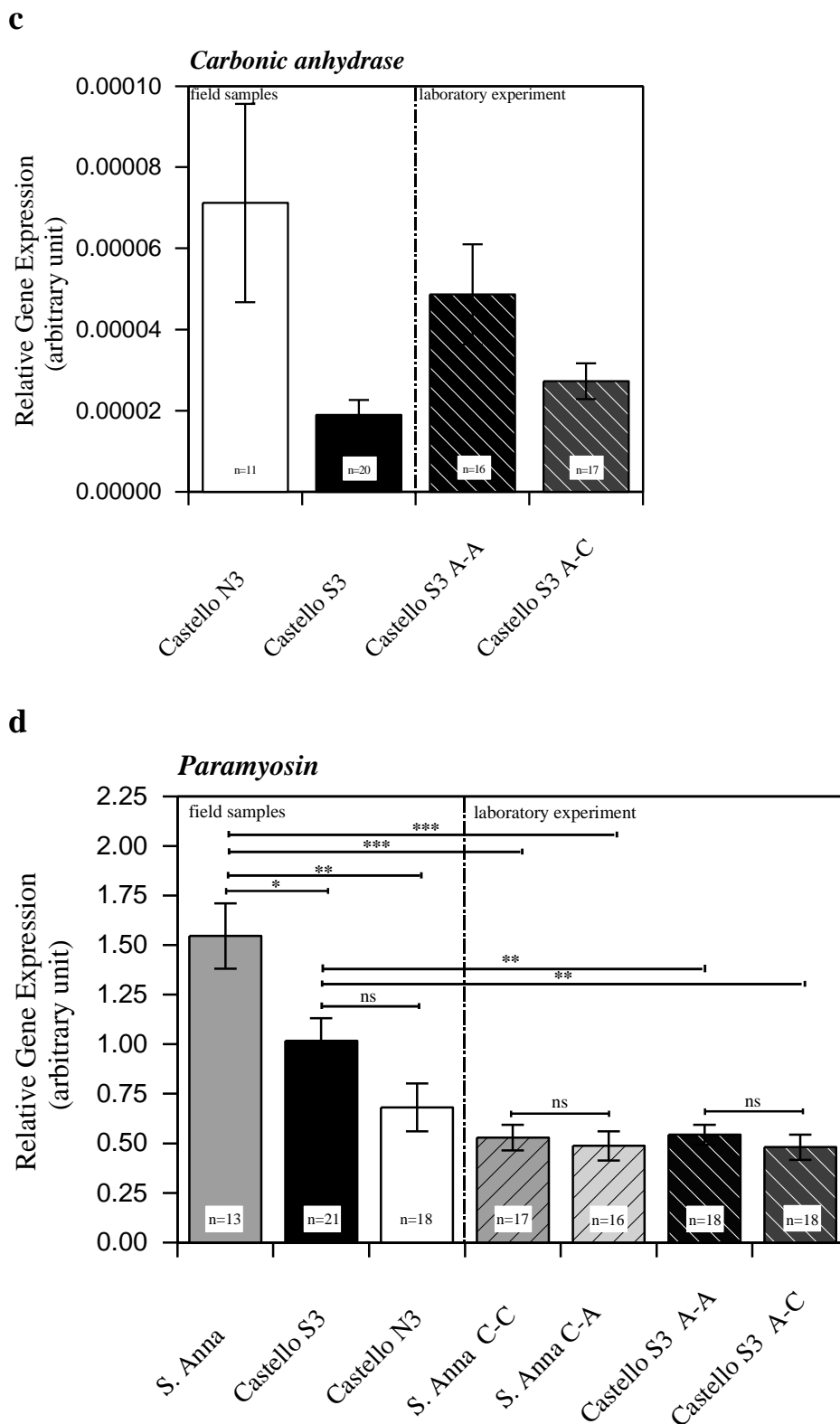


Figure 6.5 Normalised average relative mRNA transcription \pm SEM in *P. dumerilii* for *NADH dehydrogenase* (a), *NHE* (b), *CA* (c) and *paramyosin* (d) in field samples (S. Anna, Castello S3, Castello N3) and after 7 d in sea water with pH 8.0 (C-C, control and A-C, treatment) and pH 7.7 (C-A, treatment and A-A, control). Analysis was performed by nonparametric Kruskal-Wallis test ($p < 0.05$). In case of significance a Mann-Whitney U test was used to evaluate

significance. For all analyses, statistical significance was accepted at $p < 0.05$. Significant effects are labelled with asterisks (* $p < 0.05$; ** $p < 0.01$; *** $p < 0.001$). Non-significant results are labelled with ns.

6.4.3 Restriction enzyme analysis of Castello S3 and N3

All *P. dumerilii* from Castello S3 and N3 used for qPCR analysis were analysed by a restriction digest with BstZ17I (Fig.6.6; Fig. 6.7). 95.2 % of the *P. dumerilii* collected in the CO₂ vents Castello S3 and N3 could be restriction digested. Only 4.8 % of the COI were not digested.

```

S3_10_COI      CCGGATCACTACTGGGAAGGGATCAACTATATAATAACAATCGTTACAGCCCATGCCTTCT 60
S3_8_COI       CCGGATCACTACTGGGAAGGGATCAACTATATAATAACAATCGTTACAGCCCATGCCTTCT 60
S3_12_COI      CCGGATCACTACTGGGAAGGGATCAACTATATAATAACAATCGTTACAGCCCATGCCTTCT 60
S.Anna_29_COI  CCGGATCGCTACTCGGGAGAGACCAACTATATAATAACTATTGTTACAGCCCACGCATTCC 60
S.Anna_26_COI  CCGGATCGCTACTCGGGAGAGACCAACTATATAATAACTATTGTTACAGCCCACGCATTCC 60
S.Anna_22_COI  CCGGATCGCTACTCGGGAGAGACCAACTATATAATAACTATTGTTACAGCCCACGCATTCC 60
*****.***** **.*.*** *****;*** ***** **.*.***

S3_10_COI      TAATAATCTTTTTTCTCGTTATACCTGTAATAATGGAGGATTGGTAATTGACTAGTAC 120
S3_8_COI       TAATAATCTTTTTTCTCGTTATACCTGTAATAATGGAGGATTGGTAATTGACTAGTAC 120
S3_12_COI      TAATAATCTTTTTTCTCGTTATACCTGTAATAATGGAGGATTGGTAATTGACTAGTAC 120
S.Anna_29_COI  TAATAATTTTTTCTTAGTTATACCCGTAATAATCGGAGGGTTGGCAATTGATTGGTGC 120
S.Anna_26_COI  TAATAATTTTTTCTTAGTTATACCCGTAATAATCGGAGGGTTGGCAATTGATTGGTGC 120
S.Anna_22_COI  TAATAATTTTTTCTTAGTTATACCCGTAATAATCGGAGGGTTGGCAATTGATTGGTGC 120
*****.***** *.***** ***** *****.***** ***** **.*.***

S3_10_COI      CTCTAATATTAGGGGCACCGGACATAGCCTTTCTCGATTAATAATATAAGGTTTTGAT 180
S3_8_COI       CTCTAATATTAGGGGCACCGGACATAGCCTTTCTCGATTAATAATATAAGGTTTTGAT 180
S3_12_COI      CTCTAATATTAGGGGCACCGGACATAGCCTTTCTCGATTAATAATATAAGGTTTTGAT 180
S.Anna_29_COI  CTTTAATATTAGGGGCCCGAGATATAGCATTCCCCGATTAATAACATAAGCTTCTGAC 180
S.Anna_26_COI  CTTTAATATTAGGGGCCCGAGATATAGCATTCCCCGATTAATAACATAAGCTTCTGAC 180
S.Anna_22_COI  CTTTAATATTAGGGGCCCGAGATATAGCATTCCCCGATTAATAACATAAGCTTCTGAC 180
** *****.***.*** *****.*** ** ***** ***** ***** **.*.***

S3_10_COI      TACTCCCCCATCATTAAACCTTCTCTTATCTAGGGCCGAGTAGAAAAGGGAGTCGGCA 240
S3_8_COI       TACTCCCCCATCATTAAACCTTCTCTTATCTAGGGCCGAGTAGAAAAGGGAGTCGGCA 240
S3_12_COI      TACTCCCCCATCATTAAACCTTCTCTTATCTAGGGCCGAGTAGAAAAGGGAGTCGGCA 240
S.Anna_29_COI  TTCTTCCCCCTCTCTGACTCTTCTTCTTTCTAGGGCAGCAGTAGAAAAGGGAGTGGGTA 240
S.Anna_26_COI  TTCTTCCCCCTCTCTGACTCTTCTTCTTTCTAGGGCAGCAGTAGAAAAGGGAGTGGGTA 240
S.Anna_22_COI  TTCTTCCCCCTCTCTGACTCTTCTTCTTTCTAGGGCAGCAGTAGAAAAGGGAGTGGGTA 240
*:* *****.***.*** *****.*** *****.*****.*****.***** **.*.***

S3_10_COI      CTGGTTGAACAGTATACCCGCCATTAGCAAGTAATATTGCACACGCTGGCCCCCTCAGTAG 300
S3_8_COI       CTGGTTGAACAGTATACCCGCCATTAGCAAGTAATATTGCACACGCTGGCCCCCTCAGTAG 300
S3_12_COI      CTGGTTGAACAGTATACCCGCCATTAGCAAGTAATATTGCACACGCTGGCCCCCTCAGTAG 300
S.Anna_29_COI  CCGGCTGAACAGTCTATCCTCCTTTATCCAGTAATATTGCTCATGCTGGCCCCCTCAGTAG 300
S.Anna_26_COI  CCGGCTGAACAGTCTATCCTCCTTTATCCAGTAATATTGCTCATGCTGGCCCCCTCAGTAG 300
S.Anna_22_COI  CCGGCTGAACAGTCTATCCTCCTTTATCCAGTAATATTGCTCATGCTGGCCCCCTCAGTAG 300
* ** *****.*** ** **.*.*** *.*****.*****.***** *****

S3_10_COI      ATTTAGCTATTTTCTCCCTCCATCTAGCAGGGGTCTCCTCTATTATAGGAGCCCTAAAT 360
S3_8_COI       ATTTAGCTATTTTCTCCCTCCATCTAGCAGGGGTCTCCTCTATTATAGGAGCCCTAAAT 360
S3_12_COI      ATTTAGCTATTTTCTCCCTCCATCTAGCAGGGGTCTCCTCTATTATAGGAGCCCTAAAT 360
S.Anna_29_COI  ACCTGGCAATCTTTTCTCTTACCTAGCGGGGTGTCTCTATTATAGGGCCCTAAAT 360
S.Anna_26_COI  ACCTGGCAATCTTTTCTCTTACCTAGCGGGGTGTCTCTATTATAGGGCCCTAAAT 360
S.Anna_22_COI  ACCTGGCAATCTTTTCTCTTACCTAGCGGGGTGTCTCTATTATAGGGCCCTAAAT 360
* **.*.*** **.*.*** **.*.*** *****.***** ***** ***** **.*.***

S3_10_COI      TTATCACAACAGTCATCAATATACGATCAAAAAGGACTAAAATAGAACGCGTTCCTTTAT 420
S3_8_COI       TTATCACAACAGTCATCAATATACGATCAAAAAGGACTAAAATAGAACGCGTTCCTTTAT 420
S3_12_COI      TTATCACAACAGTCATCAATATACGATCAAAAAGGACTAAAATAGAACGCGTTCCTTTAT 420
S.Anna_29_COI  TTATTACCACAGTTATCAATATACGCTCAAAAAGGACTAAAATAGAACGCTGTCCCTTTAT 420
S.Anna_26_COI  TTATTACCACAGTTATCAATATACGCTCAAAAAGGACTAAAATAGAACGCTGTCCCTTTAT 420
S.Anna_22_COI  TTATTACCACAGTTATCAATATACGCTCAAAAAGGACTAAAATAGAACGCTGTCCCTTTAT 420
***** **.*.*** *****.***** ***** ***** **.*.***

```

```

S3_10_COI          TTGTATGATCTGTAGTAATTACAGCAGTACTTCTTCTTTTAAGATTGCCAGTACTAGCAG 480
S3_8_COI           TTGTATGATCTGTAGTAATTACAGCAGTACTTCTTCTTTTAAGATTGCCAGTACTAGCAG 480
S3_12_COI          TTGTATGATCTGTAGTAATTACAGCAGTACTTCTTCTTTTAAGATTGCCAGTACTAGCAG 480
S.Anna_29_COI      TTGTATGATCTGTAGTAATTACAGCGGTTCTTCTACTATTAAGGCTTCCAGTGTAGCGG 480
S.Anna_26_COI      TTGTATGATCTGTAGTAATTACAGCGGTTCTTCTACTATTAAGGCTTCCAGTGTAGCGG 480
S.Anna_22_COI      TTGTATGATCTGTAGTAATTACAGCGGTTCTTCTACTATTAAGGCTTCCAGTGTAGCGG 480
*****.***.*****.***.*****.***.*****. * *****. *****.*

S3_10_COI          GAGCTATTACTATGTTATTAACAGACCGCAACCTAAATACTGCGTTTTTTGATCCTGCAG 540
S3_8_COI           GAGCTATTACTATGTTATTAACAGACCGCAACCTAAATACTGCGTTTTTTGATCCTGCAG 540
S3_12_COI          GAGCTATTACTATGTTATTAACAGACCGCAACCTAAATACTGCGTTTTTTGATCCTGCAG 540
S.Anna_29_COI      GTGCTATCACAATATTATTAACAGACCGAAACCTAAACACTGCGTTCTTTGATCCTGCTG 540
S.Anna_26_COI      GTGCTATCACAATATTATTAACAGACCGAAACCTAAACACTGCGTTCTTTGATCCTGCTG 540
S.Anna_22_COI      GTGCTATCACAATATTATTAACAGACCGAAACCTAAACACTGCGTTCTTTGATCCTGCTG 540
*.***** **.*.*****.*****.***** ***** *****

S3_10_COI          GAGGAGGGGACCCCATTTTATACCAACA 568
S3_8_COI           GAGGAGGGGACCCCATTTTATACCAACA 568
S3_12_COI          GAGGAGGGGACCCCATTTTATACCAACA 568
S.Anna_29_COI      GAGGGGGAGACCCAATCCTATACCAGCA 568
S.Anna_26_COI      GAGGGGGAGACCCAATCCTATACCAGCA 568
S.Anna_22_COI      GAGGGGGAGACCCAATCCTATACCAGCA 568
****.*.*****.* *****.*

```

Figure 6.6 Alignment of selected *S. Anna* and *Castello S3* COI sequences from GenBank. Regions showing homology are indicated by an asterisk. Grey shaded region shows restriction site for *BstZ17I* in *Castello S3*. Red arrow indicates cutting position. GenBank accession numbers for sequences are: *S3_10* (KC591836.1), *S3_8* (KC591834.1), *S3_12* (KC591838.1), *S. Anna_29* (KC591867.1), *S. Anna_26* (KC591865.1) and *S. Anna_22* (KC591864.1).

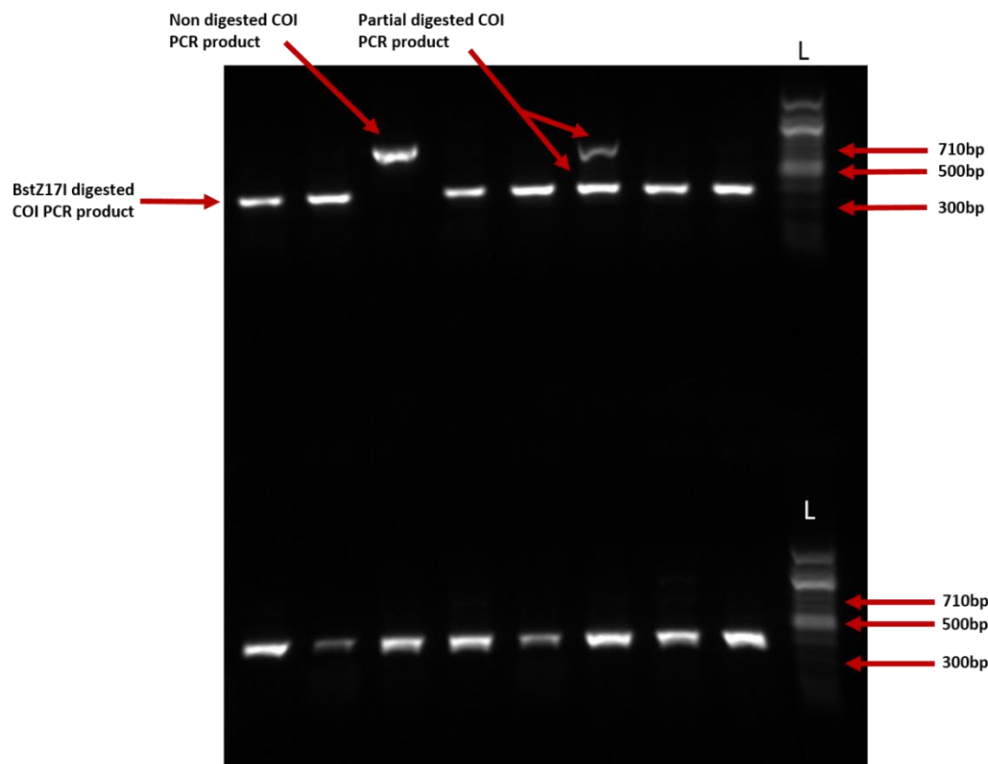


Figure 6.7 Image of a 1% GelRed-stained (Biotium, Cambridge Bioscience, Cambridge, UK) agarose-gel of *BstZ17I* digested COI PCR products from *Castello S3* and *N3* worms used in qPCR analysis. A 100 bp ladder (L) (undiluted) (New England BioLabs, Hitchin, UK) was run to the right of the sample wells.

6.4.4 Re-analysis of qPCR data (taking restriction enzyme analysis into account)

After the restriction digest with BstZ17I, four worms (three worms from Castello N3 and one worm from Castello S3) out of 83 were identified as non-vent worms even though they were collected inside the vent. To check if those four worms had a significant influence on the data, the qPCR statistical analysis was repeated. No significant change that would alter the conclusions from the data was observed.

6.4.5 Phylogenetic analyses of different populations and heteronereids

The phylogenetic tree (Fig. 6.8) shows that the *Platynereis* spp. sequences form four distinct clades. Clade 1 comprises most of the Ischia vent samples as well as samples from three control sites (San Pietro, Santa Catarina and Blanes). Clade 2 consists mainly of the Vulcano vent samples, plus one sample from the Ischia vents. Clade 3 includes samples from three control locations (Folio, S. Anna and Stareso) and one heteronereid from the Ischia vents. Clade 4 comprises the largest number of sequences, all collected from non-vent sites, except for the heteronereids that were caught swarming above the vents. It also includes the COI sequence for *P. dumerilii*, Clade 4 is referred to as *P. dumerilii*.

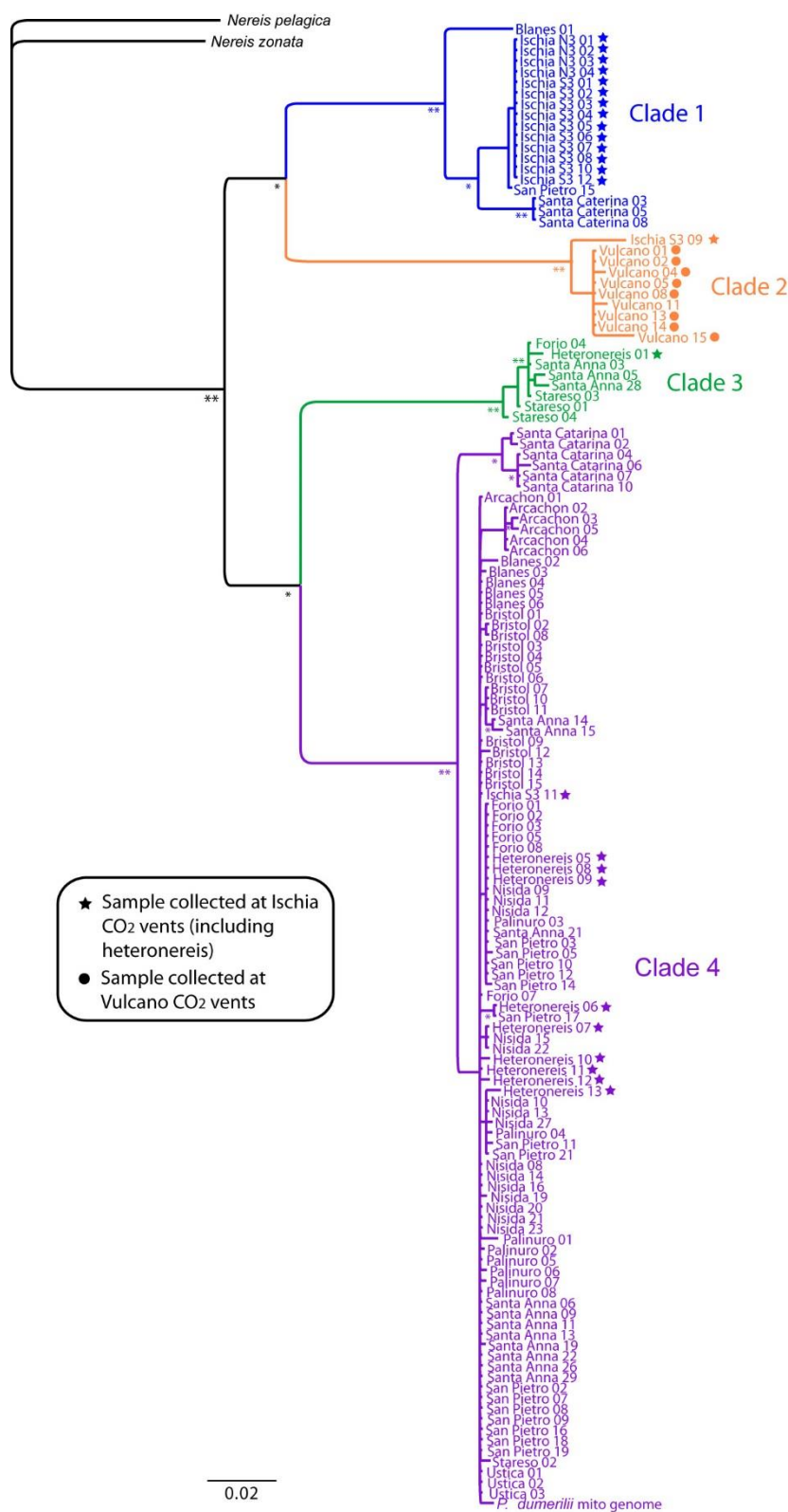


Figure 6.8 50% majority rules consensus tree resulting from Bayesian Inference analysis of 139 sequences of *Platynereis* spp. (including pelagic heteronereis) from CO₂ vents in Ischia and Vulcano and from 12 control locations. Double asterisks (**) at nodes indicate branch support of 100% posterior probability; single asterisks indicate branch support of $\geq 95\%$ posterior probability. The figure was produced by Dr Anja Schulze (Texas A&M University).

6.5 Discussion

The present chapter shows that a selected number of *target* genes are significantly differentially regulated in adult, atokous *P. dumerilii* residing in natural low pH environments in comparisons to individuals from a control population nearby (Fig. 6.5 a, b, d). These results reinforce the constructed hypothesis, that acclimation or potentially adaptation mechanisms occur in *P. dumerilii* residing in CO₂ vents. Only one gene, *NADH dehydrogenase*, was significantly changed (up-regulated) when comparing the south vent populations to the north vent populations (Fig. 6.5 a). This supports previous theories based on physiology and phylogenetics that described *P. dumerilii* in the Ischia vents to be adapted to chronic and elevated levels of *p*CO₂ (Calosi et al., 2013; Ricevuto et al., 2014). The laboratory transfer experiment of worms from a non-vent population (S. Anna), originally residing in ambient CO₂ conditions, to elevated *p*CO₂ conditions (pH 7.7) showed no significant effects on the gene expression on any of the selected genes. In contrast, two genes (*NADH dehydrogenase* and *NHE*) showed a significant down-regulation in *P. dumerilii* from the Castello S3 vent area transferred to non-vent conditions (pH 8.0) (Fig. 6.5 a and b).

A disadvantage of natural vent systems is that vents are usually small, open systems enabling mobile species such as polychaetes to move in and out of these. As such, it is for example unclear, whether individuals found at a vent at a particular time spend their entire life in such low pH conditions or alternatively sustain key functional traits including feeding and reproduction under normal seawater conditions near to, but outside a vent. Collecting specimens in a vent does therefore not guarantee that this individual is a long-term resident of this extreme environment potentially impacting physiological and ecological studies undertaken with those individuals (Calosi et al., 2013). Unlike previous studies on vents (Hall-Spencer et al., 2008; Calosi et al., 2013) this chapter therefore

included a study to examine the origin (vent type or not) of all test individuals. The digestion of the COI PCR products of each individual with BstZ17I showed that 4.8 % of the worms collected inside the vents were not from the vent populations. However, the gene expression analysis showed only small, but no significant difference in the relative gene expression when excluding these worms from the analysis. Furthermore, different *P. dumerilii* populations were collected throughout the Mediterranean Sea as well as in the Atlantic Ocean and Bristol Channel, to study the relatedness of different populations as already started by Calosi et al. (2013). Additionally, swimming heteronereids were sampled during the reproductive spawning above the Ischia vent and their population origin investigated.

For this chapter a targeted approach was used. A selected number of different genes involved in energy metabolism (*NADH dehydrogenase*), ion exchange and transport (*NHE*), pH regulation (*CA*) and cytoskeleton function (*Paramyosin*) were examined to look at the molecular-level effects of acidification. *NADH dehydrogenase*, is involved in the mitochondrial electron transport chain (Weiss et al., 1991) and therefore indirectly in the capacity to generate ATP. In worms collected at S. Anna *NADH dehydrogenase* showed significantly lower levels of gene expression compared to the vent population Castello S3. This coincides with a study that looked at the metabolic rate (MO_2) in vent and non-vent worms in Ischia, which found that the metabolic rate in vent specimens is constantly maintained at high levels (Calosi et al., 2013). Living under acidified conditions is potentially energetically costly, including physiological regulations such as intracellular pH maintenance. Therefore, the overall energy needed is likely to be higher in vent worms. Calosi et al. (2013) suggested that the MO_2 is potentially higher to compensate chronic $p\text{CO}_2$ -induced hypoxaemia. A study on the brittle star, *Ophiura ophiura*, provided similar findings, as Wood et al. (2010) reported an up-

regulation in the metabolism under low pH treatments (pH 7.3) and low temperature. Widdicombe and Spicer (2008) predicted that there is a trade-off between metabolism and cost elsewhere, such as growth.

In contrast to the study on *P. dumerilii* from Calosi et al. (2013) there was no significant difference in the mean weight between the two vent populations and the non-vent population (Table 6.5; Fig. 6.4), but this is maybe due to patchiness when sampling from a mixture of macroalgae, seagrass and epiphytes (Ricevuto et al., 2014) or is potentially based on seasonal differences. The relative gene expression encoding for *NADH dehydrogenase* in the Castello N3 vent worms was significantly down-regulated in comparison to the Castello S3 individuals (Fig. 6.5 a). A possible explanation for this could be the locations of the vents. The north vent is much more exposed to wind, waves and shade than the sunny, sheltered south vent (Ricevuto et al., 2014; Ricevuto et al., 2015), and could therefore effect the gene expression of the worms in a different way. The transfer of worms from the control site S. Anna (C-C) to low pH conditions (C-A) showed no significant effect on the gene expression of *NADH dehydrogenase* (Fig. 6.5 a), which indicated that *P. dumerilii* maintained their pre-exposure metabolic condition as shown by Calosi et al. (2013) measuring the MO_2 . In contrast, during the transfer of *P. dumerilii* from Castello S3 to lower pCO_2 conditions (A-C) a significant down regulation of *NADH dehydrogenase* was observed (Fig. 6.5 a). A possible explanation could be that the pH change to less acidic conditions leads to a reduction in metabolic processes, as less energy might be needed for processes such as internal pH regulation.

This alternate explanation is supported by the mRNA expression observed for *NHE* (Fig. 6.5 b). With the transfer of worms from Castello S3 to normal pCO_2 conditions (A-C) a significant lower relative gene expression of the acid-base transporter was observed (Fig. 6.5 b). The relative gene expression of *NHE* in worms collected at S. Anna

in control conditions is much higher than in both vent populations. This could be explained by the metabolic expense of the *NHE*, which is considered as a particular costly antiporter (Pörtner et al., 2000). As living in extreme environmental conditions, such as CO₂ vents, already incurs a significant cost, this could explain the lower expression of this antiporter in vent populations.

Surprisingly, the primers designed for *CA*, a zinc-containing enzyme that catalyses the hydration of CO₂ to HCO₃⁻ (Tripp et al., 2001), failed to amplify using worms from S. Anna and most of the Castello N3 worms. This indicates that the sequences of *CA* of different *P. dumerilii* populations are distinguished from each other. The primers do not appear to be specific enough to amplify the template, which resulted either in mispriming or no amplification of the target. This may be due to differences in the third codon position which will not affect the amino acid sequence but the function of the primer. Therefore, only the expression of Castello S3 and a small sample number of Castello N3 could be analysed. The gene expression of *CA* did not show a significant change in the different vent populations and in the transfer experiment (Fig. 6.5 c). However, the p-value of 0.051 in the Kruskal-Wallis-Test indicates a clear trend. The transfer of worms from Castello S3 to ambient pH conditions showed a down-regulation trend in the relative gene expression of *CA*. Potentially a lower activity is needed due to the lower concentrations of CO₂ in the seawater. Other studies reported significant up-regulation at pH 7.8 and 7.4 in the coral species, *P. damicornis*, after low pH exposure of 3 weeks (Vidal-Dupiol et al., 2013). Another study on coral, using *A. millepora*, showed a down-regulation after 3 days under elevated pCO₂ (Moya et al., 2012). These data would support the theory that *CA* is up-regulated under low pH conditions and down-regulated under normal pH conditions as shown for *P. dumerilii* in this chapter. Another interesting fact is that the *CA* primers did not amplify *P. dumerilii* cDNA from the control

site S. Anna and quite a few from Castello N3, indicating that the two populations are more different as their morphological identical appearance indicates.

The gene expression of *paramyosin*, involved in muscle contraction and immunoregulation (Gobert and McManus, 2005), was significantly up-regulated in worms collected at S. Anna compared to the two vent populations (Fig. 6.5 d). Furthermore, the transfer to the laboratory led to a down-regulation of *paramyosin* in both S. Anna and Castello S3 individuals, indicating a stress response potentially induced through the transport and changing environment. A study on *C. elegans* showed that loss-of-function mutants have disorganised body-wall muscle and are severely paralysed (Riddle et al., 1997) demonstrating the importance of the gene for movement. Studies showed that *paramyosin* content increase with the length of thick filaments and it is hypothesised that it improves the stability of muscles and therefore indirectly helps to increase the force (Hooper et al., 2008). The synthesis of *paramyosin* is potentially energetically costly and therefore maybe reduced under extreme environments. Broadcast spawning in *P. dumerilii* is based on an energetically very costly metamorphosis into the epitokous heteronereis (Hauenschild and Fischer, 1969). *Paramyosin* could potentially play an indirect role in upkeep of muscle contraction essential during the reproduction process of fast swimming and spawning of gametes.

Based on physiological studies and a phylogenetic tree, Calosi et al. (2013) suggested that the south vent population could be a cryptic species. The present data suggests that worms collected in the most acidified area (~pH 7.49; Johnson et al., 2013) of the Baia di Levante (Vulcano Island, Italy) differed in the COI sequence to those in the Ischia vents and to the *P. dumerilii* found elsewhere in Europe, suggesting that radiation pressures at the vents do exist. Furthermore, it supports the hypothesis that *P. dumerilii* can adapt to such localised environmental pressure. Non-calcifying polychaetes living in

the CO₂ vents seem to show a high phenotypic plasticity making them less vulnerable to environmental changes and potentially a “winner” towards OA (Ricevuto et al., 2015). *P. dumerilii* has been extensively studied in the Gulf of Naples over centuries and a sibling species *P. massiliensis* (Moquin-Tandon 1869) has been described in the Ischia region (Hauenschild, 1951). These two species are morphologically indistinguishable as mature adults but differ in their maturation and morphologically different gametes (Schneider et al., 1992; Fischer, 1999). In contrast to spawning *P. dumerilii*, *P. massiliensis* is laying large eggs in their complex structured living tubes and exhibit parental care (Schneider et al., 1992). A recent study of Lucey et al. (2015, in press) suggests that the worms in the vents are *P. massiliensis*, however no reference *P. massiliensis* were used from a different sampling site in the study.

With all heteronereids collected from the water body over the vent originating from outside the vent (Fig. 6.8) it is feasible to assume that the vent populations could potentially use a different reproductive strategy, as suggested by Lucey et al. (2015, in press). However, future phylogenetic studies including reference individuals of *P. massiliensis*, for example from Banyuls-sur-Mer (France) combined with life history studies of worms from the vent are required to fully elucidate the question if it is really the polychaete species *P. massiliensis* in the vents.

To date, there are no studies confirming that marine invertebrates complete their entire lifecycle and recruit successfully in oceanic vent areas. Until this significant gap in OA research is closed it remains unclear whether the communities described from such vents (Hall-Spencer et al., 2008) do in fact resemble those that may exist under OA conditions in the future.

6.6 Conclusion

The present chapter shows that the relative gene expression between individuals collected from vents and the reference site differs. As already shown by the work of Calosi et al. (2013) the phylogenetic analysis revealed distinct differences between the south vent population in Ischia to other non-vent populations. Combined with the published data, this may suggest that the north vent population in Ischia is similar to the south vent population. However, the individuals collected in the CO₂ vent in Vulcano (Sicily) formed a completely new clade. Together, the results suggest that the extreme conditions in vents generate substantial pressure to adapt, and that those at Ischia have resulted potentially in the presence of an adapted, or cryptic species. Further life history studies are required to fully understand the *P. dumerilii* species complex inhabiting CO₂ vents. As the transfer experiments of atokous non-vent worms did not show expression changes in any of the selected genes, this indicates that the worms may be relatively tolerant towards pH changes. More experiments are needed to see how other life stages of *P. dumerilii* are affected by different pH conditions. However, looking at CO₂ vent systems and the abundance of Polychaeta this may suggest that *P. dumerilii* and other Nereidae are likely to be so called “winners” in respect of the expected ocean changes. The present phylogenetic analysis suggested that there is a great potential for evolutionary radiation in *P. dumerilii* resulting in cryptic species.

Human activity has led to a significant increase in atmospheric CO₂ levels (IPCC, 2014). The combination of industrial and agricultural activities caused an increase from 280 to 387 ppm of atmospheric CO₂ concentrations, where half of the increase took place in the past three decades (Feely et al., 2009). Approximately 30% of the CO₂ has been taken up by the oceans, which causes changes in the seawater carbonate chemistry and lowers the pH (Feely et al., 2004). This process, known as OA, has lately moved more into the focus of the scientific community, policymakers and media (Gattuso and Hansson, 2011). Depending on the emission scenario, CO₂ concentrations of up to 936 ppm are predicted by 2100 (IPCC, 2013). These fast changes are expected to have severe effects on marine biota, with most effects likely to be negative for the organisms (for detailed review see Fabry et al., 2008). Nevertheless, there are still many knowledge gaps about how individual species and especially how marine ecosystems will be affected by these seawater chemistry changes.

To date, research has mainly focused on calcifying organisms and only little is known about non-calcifying species (Dupont and Thorndyke, 2009). Studies have revealed that the ability of marine organisms to produce calcareous skeletal structures and maintain their acid-base balance are especially likely to be affected (Fabry et al., 2008). To maintain a normal acid-base status in the body fluids, the concentration of H⁺ needs to be regulated. This is a process which is essential for cellular homeostasis (Siggaard-Andersen, 2005). Currently, very little is known about the acid-base regulation in Polychaeta. The focus of research resides on effects induced through oxygen and temperature (Toulmond and Tchernigovtzeff, 1984; Sommer et al., 1997). One well established polychaete model species is *P. dumerilii*, which has been used in many different research areas such as developmental biology (Dorresteijn, 1990;

Fischer and Dorresteijn, 2004), chemical ecology (Hutchinson et al. 1995; Hardege, 1999), toxicology (Hutchinson et al., 1995; Jha et al., 1996) and evolution (Tessmar-Raible and Arendt, 2003). Research using *P. dumerilii* also includes OA studies (example studies: Cigliano et al., 2010; Calosi et al., 2013; Davidson, 2013; Ricevuto et al., 2015), however the basic mechanisms involved in acid-base balance are still unknown, and are the main focus of this thesis.

Summary of the main findings of this work

The present dissertation contributes to an advance in our understanding of the impact of low pH on acid-base regulation on the marine polychaete *P. dumerilii*. To begin to understand the mechanistic change involved in acid-base regulation, *target* and *reference* genes were first isolated and characterized prior to development as a quantitative tool with which to then investigate changes in exposed worms (Chapters 2, 3, 5 and 6). Building on that foundation, experiments using acidified conditions simulated with both CO₂ and HCl were used to investigate the question whether it is the pH change or other chemical alterations that induces the expression changes under the exposure conditions (Chapter 3 and 5). As *P. dumerilii* is one of the species that occurs in natural CO₂ vents, this dissertation also looks at field populations collected inside two vent areas off the island Ischia (Italy) and a reference site close by (Chapter 6). The use of such natural CO₂ vents in the Mediterranean could potentially provide information on how OA could affect benthic systems (Hall-Spencer et al., 2008). These model environments show how community composition changes with changing seawater conditions and may help to identify and understand mechanisms that are responsible for specimens that are able to tolerate the low pH conditions. Furthermore, a transfer of vent populations to “normal”

pH and a transfer of field populations to low pH has been conducted in order to see how worms from the field respond to changing seawater conditions.

Selecting *target* genes potentially relevant to regulatory mechanisms involved in acid-base regulation or the overall physiological performance of an animal, can improve understanding of the molecular mechanisms induced through low pH exposure. Based on recent literature, several processes were highlighted as likely to be changed under low pH conditions in marine organisms. *NHE* and *CA* were known to be involved in maintenance of pH and CO₂ homeostasis in many organisms (Padan et al., 2001; Supuran, 2011), and are therefore likely to be good candidates to investigate the effects of acidification events on *P. dumerilii*. Also *CaM* has been highlighted in previous OA studies (Dineshram et al., 2012; Kaniewska et al., 2012; Dineshram et al., 2013). *CaM* is a Ca²⁺-binding protein that is involved in secretion, cell proliferation, cellular metabolism, muscle contraction, differentiation and apoptosis (Means and Dedman, 1980; Rasmussen and Means, 1989; Chin and Means, 2000). A recent study also revealed that *CaM* has an important function in larval settlement and metamorphosis in the polychaete *H. elegans* (Chen et al., 2012b). These genes therefore comprised a targeted mechanistic approach to studying OA impacts in worms.

Combining this targeted approach with a global approach can provide a better understanding of the molecular events taking place. Using the exploratory SSH method to isolate and identify differentially regulated pH-specific mRNA transcripts helped to highlight potential pathways that are changed in laboratory cultured *P. dumerilii* kept under low pH conditions. Both the targeted and the global experimental approach, following a simulated low pH exposure regime using acid adjustment, highlighted different molecular level biological effects, such as the up-regulation of an active proton-transport mechanism and the down-regulation of metabolism related genes (Chapter

3 and 4). Dupont and Thorndyke (2009) reported that OA can induce physiological stress through the decrease in pH. The present work discovered processes involved in energy metabolism and defence processes to be down-regulated in *P. dumerilii* under low pH conditions induced by HCl. Immune-related transcripts such as *fuclectin* and *paneth cell-specific alpha defensin* were expressed at a lower level (Table 4.2). Together with the down-regulation of *2-oxoglutarate dehydrogenase*, *NADH-dehydrogenase*, *cytochrome c oxidase*, and *ATP synthase*, representing genes involved in the Krebs cycle and the mitochondrial electron transport chain, the results may indicate vulnerability towards low pH environments and could suggest substantial pressure on the marine polychaete in process such as maintenance (Fig. 7.1). In addition to the down-regulations, transcripts involved in cytoskeleton function (*paramyosin* and *calponin*), protein synthesis related (*ribosomal protein L34*) and DNA replication (*GINS protein Psf3*) processes were up-regulated, potentially showing that the worms try to compensate at the cellular level.

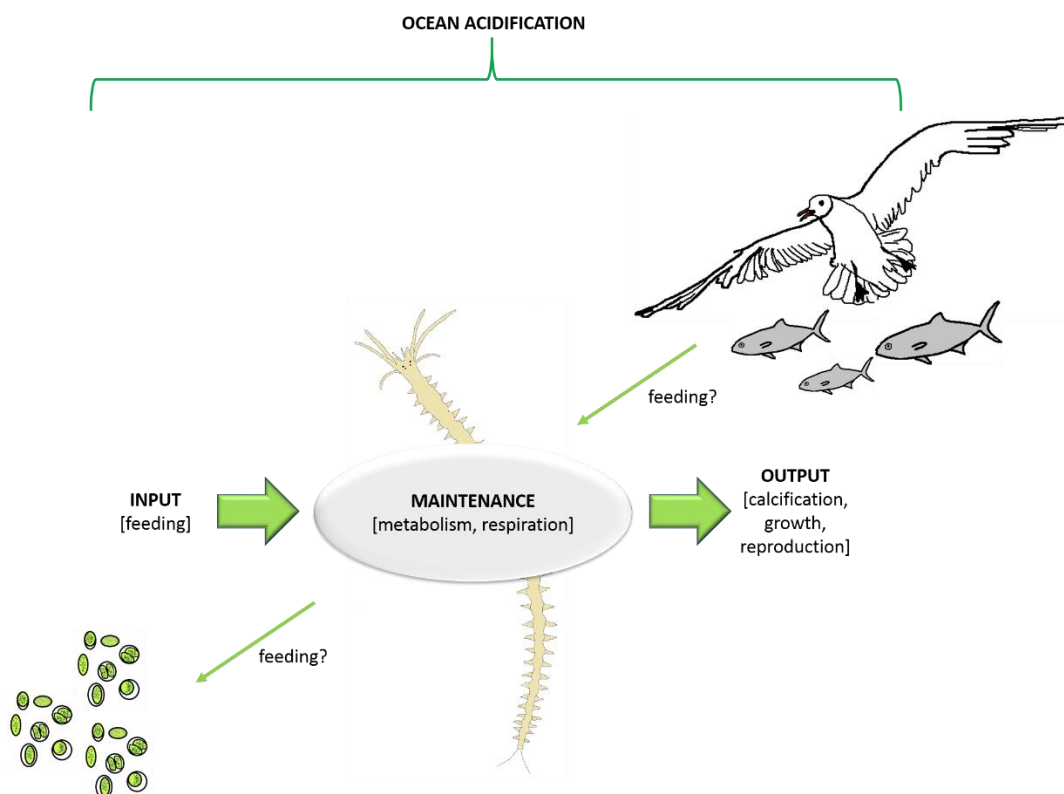


Fig. 7.1 OA has direct and indirect effects on many physiological processes which, in turn, can have consequences on the fitness of an organism (adapted from Dupont and Thorndyke (2009).

Surprisingly, the global approach did not reveal any direct ion-transport processes, which were discovered as one of the processes changed under low pH conditions in previous studies (O'Donnell et al., 2010; Vidal-Dupiol et al., 2013; Pespeni et al., 2013). Only the serine-threonine kinase WNK1, which was down-regulated, is indirectly involved in ion transport through the activation of the serum- and glucocorticoid-inducible protein kinase SGK1, which subsequently activates an epithelial sodium channel (Xu et al., 2005).

Since the sequencing of isolated clones from the SSH approach only identified 32 % of the sequences, processes including acid-base transport could be simply missed out. This is due to the limitation of sequences available on the NCBI database, and many sequences being unidentified not matching to any of the provided nucleotide or protein sequences. However, the results from the global approach were based on using acids (HCl) to modulate pH experiments, and the molecular changes observed may have been triggered through different acid-base mechanism compared to CO₂ modulated pH changes in OA studies. Using the parallel targeted approach, one acid-base relevant ion-transport mechanism was observed to be changed (Fig. 3.1 a). The *NHE* exchanger showed an initial down regulation after 1 hour low pH exposure and an up-regulation after 7 days, demonstrating that ion-transport processes are altered (Fig. 3.1 a). The exposure time of 1 hour shows that the initial stress response is different to the mRNA expression after an acclimation period of 7 days. Presumably this could be interpreted as a protective response to reduce energetic costs and alleviate the impact of the environmental change.

P. dumerilii larvae may respond differently to the same exposure regime as at this life stage energy is mainly invested into growth, whilst in adults, energy is directed towards maturation. Therefore, it would be useful for future work to investigate other life

stages of *P. dumerilii*. Localising the expression of *NHE* in *P. dumerilii* larvae generated spatial information about the expression under normal and low pH conditions. Under both pH conditions *NHE* expression in the parapodia, antennae and palpi could be observed (Fig. 3.2). Additionally under low pH conditions *NHE* expression in the anus area was detected (Chapter 3). The results indicate that *P. dumerilii* larvae compensate the low pH exposure with additional ion-exchange in this area. In the literature, it has also been documented that *A. aegypti* larvae exchange Na^+ and Cl^- in the anal papillae by using a *NHE* and also teleost fish exchange acid-base relevant ions in the intestinal epithelium (Stobbart, 1971; Grosell and Genz, 2006; Wilson et al., 2009; Grosell et al., 2009a, Grosell et al., 2009b).

Taking a closer look at the word OA, clearly this expression stresses the fact that the process of taking up CO_2 from the atmosphere by the oceans leads to a lower pH of the seawater (Gattuso and Hansson, 2011). In addition to pH change, the dissolved CO_2 in seawater causes several changes such as the alteration in carbonate chemistry. For example, the concentrations of HCO_3^- and H^+ ions are increased with CO_2 being absorbed in the seawater (Gattuso and Hansson, 2011). Almost all OA studies alter the pH with CO_2 , as this is deemed appropriate to demonstrate the expected environmental changes, yet many studies address the effect as an event induced by acidification of the seawater (e.g. Bibby et al., 2008; Hernroth et al., 2011; Dineshram et al., 2013). However, when focusing only on CO_2 for the experimental exposure it is difficult to assess whether the observed changes (e.g. immune response and responses of larval proteome) are causally linked to pH or are induced by the changes at the carbonate level. Therefore, the present dissertation looked at both approaches, using CO_2 and HCl , to change the pH.

The two methods of controlling pH cause two additional changes to the species in solution that are unique to the method chosen. Because of these interconnectivity of the

various species in equilibrium, by Le Châtelier's principle, any disturbance to one will have a cascading effect upon all the other species in the equilibrium. CO₂ dissolved in seawater changes the inorganic carbon (DIC) and keeps the total alkalinity (A_T) at a constant level (see equation 1, Chapter 1), while mineral acid (HCl) changes the A_T but not the concentration of DIC. A_T is comprised of $[\text{HCO}_3^-] + 2[\text{CO}_3^{2-}] + [\text{B}(\text{OH})_4^-] + [\text{OH}^-] - [\text{H}^+] + \text{minor components}$ (Gattuso et al., 2010). The present experiments were chosen to control for pH and allow for the second factors of DIC and A_T to be explored. This work sought to investigate the possibility that these other factors (DIC or A_T) also had an influence on gene expression besides strict pH.

The experimental data (comprising Chapters 3 and 5) revealed that two of the *target* genes investigated showed different, and in one case opposite results when using a CO₂ exposure regime in contrast to pH changes adjusted with an acid. *CA* was significantly up-regulated in *P. dumerilii* under low pH conditions induced by CO₂ in both groups (1 hour and 7 days). By contrast, worms exposed to low pH using HCl reported a down-regulation trend of *CA* after 1 hour and no effect could be observed after 7 days (for summary, see Table 7.1). The higher concentration of CO₂ in the seawater increased the quantity of *CA* mRNA, presumably required to keep up the catalytic reaction of the interconversion of CO₂ and water to HCO₃⁻ and H⁺, whereas this effect could not be observed when changing only the A_T of the water. Also, *NHE* appeared to be differentially expressed under the two exposure regimes (Fig. 3.1 a and 5.1 a). In *P. dumerilii* kept in acidified conditions induced by CO₂ no effect could be observed in the 1 hour group and only a down-regulation trend could be detected for the group of 7 days (Fig. 5.1 a). Worms exposed to HCl showed a significant down-regulation after 1 hour and a significant up-regulation after 7 days (Fig. 3.1 a), suggesting that an increase of *NHE* was required to maintain the acid-base balance. These results clearly show that manipulating

the DIC or A_T results in a different expression of the two *target* genes, indicating that it is not only the pH change leading to the expression change. In contrast to *CA* and *NHE*, the third *target* gene *CaM* did not show any significant expression changes with either CO_2 or HCl.

Based on these results, and as already suggested by Gattuso and Hansson (2011), a better name for describing the event of uptake of CO_2 from the atmosphere by oceans could be the expression of ‘carbonation’, as it is a change in the DIC that takes place. The present work clearly showed that it is not necessarily the pH change that induces the changes in mRNA expression and should be considered also in the discussions of other OA work.

Table 7.1 Summary of the responses of *P. dumerilii* to low pH induced by HCl and CO₂ of long term laboratory cultured worms labelled with * and field populations called non-vent, vent S3 and vent N3. All expressions are relative to normal pH conditions (~pH 8.2/ 8.0). Only, the relative expression of Vent S3 is relative to low pH (~pH 7.7). The second part of the table is a comparison of the relative expression of the non-vent population to the vent S3 and N3 population. ↑ indicates an up-regulation, ↓ indicates a down-regulation, ↔ indicates no significant change, F indicates a failed amplification, - stands for not investigated. All * next to the arrows present significant results.

	<i>NHE</i>	<i>CA</i>	<i>CaM</i>	<i>Para</i>	<i>Calpo</i>	<i>Cyto</i>	<i>NADH</i>
Laboratory exposure:							
<i>P. dumerilii</i> * 1h HCl pH 7.8	↓*	↓	↔	-	-	-	-
<i>P. dumerilii</i> * 7d HCl pH 7.8	↑*	↔	↔	↑*	↑*	↓	↓
<i>P. dumerilii</i> * 1h CO ₂ pH 7.8	↔	↑*	↔	-	-	-	-
<i>P. dumerilii</i> * 7d CO ₂ pH 7.8	↓	↑*	↔	-	-	-	-
<i>P. dumerilii</i> Non-vent 7d CO ₂ pH 7.8	↔	F	-	↔	-	-	↔
<i>P. dumerilii</i> Vent S3 7d CO ₂ pH 8.0	↓*	↔	-	↔	-	-	↓*
Direct field samples:							
<i>P. dumerilii</i> Non-vent	↑*	F	-	↑*	-	-	↓*
<i>P. dumerilii</i> Vent S3	↓*	-	-	↓*	-	-	↑*
<i>P. dumerilii</i> Vent N3	↓*	-	-	↓*	-	-	↔

In terms of the seawater parameters, all the pH values used in the present work represent values expected for 2100 following the RCP8.5 scenario (IPCC, 2014). The review of Dupont and Thorndyke (2008) stressed that many OA studies use unrealistic pH values, making comparisons and realistic predictions difficult. Therefore, it was important for the present study to select pH values with ecological relevance. Monitoring the pH of the exposure experiments showed small fluctuations. This can be explained by small gas exchanges between the water surface and the surrounding air. As pH fluctuations have been observed in the field (Kroeker et al., 2011), daily fluctuations are considered a natural event. A recent study on the Kiel Fjord showed that upwelling of hypoxic water causes also a high variability of the $p\text{CO}_2$, which today already reaches values much higher than those expected for 2100 (Melzner et al., 2013). Yet, to keep the pH levels of the present study relatively constant during the experimental exposure a complete water change was conducted every 24 hours to keep all water parameters as similar as possible.

To gain a better understanding on how field populations of worms react to low pH conditions, additional experiments were conducted off the island Ischia in Italy. This field site has the advantages that on the north-east side of the island two natural CO_2 gradients, ranging from ambient to low pH conditions, are present (Hall-Spencer et al., 2008). In contrast to laboratory exposure experiments, naturally acidified environments include information on trophic and ecosystem interactions as well as potential adaptation (Gazeau et al., 2011). Therefore, these vents provided a perfect opportunity to investigate the effects of potential long term low pH exposure on *P. dumerilii*, which has been recorded to be present in all pH zones (Ricevuto et al., 2014). However, there is the limitation that mobile species such as *P. dumerilii* might escape from the low pH zone or migrate in and

out of the vent and as such only partially reside in these open vents (Hall-Spencer et al., 2008).

The present dissertation investigated the mRNA expression of two of the *target* genes (*NHE* and *CA*) as well as two of the genes (*NADH dehydrogenase* and *paramyosin*) identified by the SSH approach (Chapter 4). The mRNA expression of all *target* genes was investigated at two vent sites and a control site (S. Anna) close by (for details see Chapter 6). Worms collected at S. Anna had significantly higher expression of *NHE* in comparison to the two vent populations (Castello S3 and N3) (Fig. 6.5 b). An explanation for the expression difference could be the energetic cost of the antiporter, which has been considered to be very high (Pörtner et al., 2000). *NADH dehydrogenase* showed a lower significant expression in S. Anna in comparison to Castello S3. Also for worms in S. Anna, the *NADH dehydrogenase* expression was lower, yet not significantly so, in comparison to Castello N3 worms (Fig. 6.5 a). These results are similar to another vent study conducted in Ischia showing that the metabolic rate, measured as oxygen consumption rate (MO_2), was constantly maintained at high levels (Calosi et al., 2013). The present comparison of the field populations from two vent areas and one non vent area could show that there are differences in the expression of target genes potentially indicating that the different water conditions led to acclimation events in the vents.

In addition to using animals collected in the field directly, laboratory transfer experiments were also conducted in Ischia. In contrast to the experiments conducted on long term laboratory cultured worms in Heidelberg (Chapter 3, 4 and 5), the worms from S. Anna, kept at low pH conditions (~ 7.7) for 7 days showed no significant *target* gene expression changes (Chapter 6). These results suggest that worms from the field are much more resilient towards pH changes in comparison to laboratory reared worms, which are acclimated to constant environmental conditions. The resistance towards the low pH

conditions can be explained by the worms being used to daily and seasonal pH changes (Kroeker et al., 2011; Ricevuto et al., 2014; Ricevuto et al., 2015).

On the other hand, the vent worms from Castello S3 transferred to normal pH conditions (~8.0) showed a down-regulation in both *NHE* and *NADH dehydrogenase*, indicating that there are differences between the tolerances towards pH changes between those two populations. It should also be noticed that the overall expression of *NHE* is lower when comparing the transferred control group (Castello S3 A-A) with the direct field samples Castello S3 (Fig. 6.5 b). Therefore, there might be a bias that the observed reaction is not due to the different pH conditions but also to experimental stress. As Widdicombe and Spicer (2008) reported, it is difficult to distinguish whether an organism is stressed due to the movement from its original habitat and if it is still functioning normally after a transfer. Hence, such data should always interpreted with care. Furthermore, the studies on the long term cultured laboratory worms and the field worms show very different effects on the expression of the investigated genes. For instance, the expression of *NHE* in long term laboratory reared worms under low pH conditions for 7 days showed a down regulation trend (Fig. 5.1 a), whereas the worms from S. Anna showed no effect at all (Fig. 6.5 b). Therefore, drawing any conclusions regarding effects of OA on natural populations based on laboratory populations should be carried out with caution.

Lab to environment extrapolation

A further criticism is that laboratory studies substantially present simplified models of natural systems usually without inclusion of effects such as predation, food availability, temperature fluctuations, currents and many other parameters (Widdicombe and Spicer, 2008). To date, most laboratory experiments focused on single species aimed at specific

responses and physiological mechanisms, however these types of experimental setup represent an artificial situation as many of the above mentioned biological interactions are missing (Dupont and Thorndyke, 2009; Widdicombe et al., 2010). Consequently, scientists tried to approach OA studies with different methods. One popular approach uses mesocosm experiments, where outdoor semi-enclosed tanks are used to try to mimic natural conditions and where $p\text{CO}_2$ concentrations can be altered (Engel et al., 2005; Andersson et al., 2009; Hicks et al., 2011). In these type of experiments organisms are less likely to get stressed than in laboratory experiments. However, interactions between the benthic and pelagic environment are often missing and a weakness of the method (Widdicombe et al., 2010).

Subsequently, so called Free Ocean CO_2 Enrichment (FOCE) systems have been developed (Kirkwood et al., 2005; Kline et al., 2012; Gattuso et al., 2014). These systems consider effects such as interspecific relationships and food webs and allow relatively long experiments with intact communities (Gattuso et al., 2014). Hofmann et al. (2010) reported that many ecosystems experience month-long pH variability with pH changes ranging between 0.024 to 1.430 pH units. Depending on the habitat there are also diel or semi-diurnal changes. An experiment in the Great Barrier Reef used a so called Coral-Proto Free Ocean Enrichment System (CP-FOCE), which maintained the pH with an incorporating natural diel and seasonal pH cycles (Kline et al., 2012). Variations in DIC, pH, alkalinity and dissolved oxygen were introduced and followed approximately the light intensity/ dark cycle with the addition of the tidal cycle (Kline et al., 2012). Such CO_2 manipulation experiments help to reflect the actual natural conditions in a much better way than conventional laboratory experiments and represent a better approach to make OA studies more applicable.

As *P. dumerilii* is residing in relatively complex habitats within different algal communities (Hay et al., 1988; Calosi et al., 2013) at the benthic zone of the sea, the FOCE experiment may provide a good approach to study OA effects on the worms within their natural habitat. Therefore, this could be an additional step to build upon the present work, however a disadvantage of this experimental method is the high cost and thus the limitations of experimental replication (Gattuso et al., 2014). Table 7.2 shows a comparison of the different approaches used to study OA.

Table 7.2 Comparison of five main approaches used to investigate the effects of OA. Five stages were used for the ranking: very high, high, medium, low and very low (Gattuso et al., 2014).

Approach	Cost	Replicability	Ecological relevance
Laboratory experiments	Very low	Very high	Very low
Field observations (monitoring)	Medium	Very low	Very high
CO ₂ vents	Low	Very low	Very high
Laboratory mesocosms	Medium	Medium	Medium
FOCE	High	Medium	High

Combinations of multiple stressors

OA is not the only stressor for marine organisms, increasing CO₂ can also cause warmer oceans through climate change (Bindoff et al., 2007; Solomon et al., 2009). A study on the Sydney rock oyster *S. glomerata* investigated the effect of OA and temperature (Parker et al., 2009). Deviations from the optimal temperature (26 °C) led to a decrease in the fertilization rate and embryo development (Parker et al., 2009). Another study looked at the effects of OA and temperature at the community level and discovered that the Mollusca abundance decreased with both pH and temperature, whilst Annelida abundance and diversity was reduced by low pH and increased at warmer temperature (Hale et al., 2011). Moreover, organisms are also simultaneously exposed to pollutants, such as metals (Förstner and Wittmann, 1981). A study of Millero et al. (2009)

investigated the effects of OA on thermodynamics and kinetics of metals in seawater and concluded that the changes in the metals due to the low pH will affect the interaction and influence of the metals. In the polychaete *A. marina*, experiments revealed that there is a synergistic increase of copper toxicity with OA on sperm DNA damage and early larval survivorship (Campbell et al., 2014). Therefore, the combined effect of high $p\text{CO}_2$ and changing temperature, or addition of pollutants, could have very different impacts on *P. dumerilii* and is something which should be considered for future work.

Life cycle stage considerations

Linking the molecular findings of the present dissertation to life cycle stages may reveal a better understanding on the effects of changing seawater conditions on *P. dumerilii*. *P. dumerilii* cultured under low pH (7.8) for 90 days revealed a lower survival rate (Davidson, 2013). As the molecular data based on mineral acid showed a decrease in metabolic related transcripts, the lower survival rate could be linked to the increased metabolic cost, which potentially were not maintained under low pH conditions. In the Ischia CO_2 vent *P. dumerilii* also showed constant high metabolic rates (Calosi et al., 2013), which coincides with the data on the CO_2 vents of the present study. Potentially the energy needed to be allocated to different processes. Furthermore, a higher number of mature individuals were observed in normal pH conditions (8.2) than in low pH (7.8) and female *P. dumerilii* produced a smaller number of eggs in low pH seawater in contrast to normal pH (Davidson, 2013).

Therefore, both the molecular, as well as the life cycle data, suggests that OA may have significant impacts on the overall performance of *P. dumerilii* including adult stages as well as fertilisation and larval development. Besides the differences in the metabolic rate, Calosi et al. (2013) also found a difference in the size of the worms. *P. dumerilii*

collected inside the CO₂ vent (~3 mg) were significantly smaller than worms from the reference site (~13 mg) (Calosi et al., 2013). In contrast, the present work did not find any differences in the size of the *P. dumerilii* (Table 6.4), which could be down to patchiness (Ricevuto et al., 2014) or seasonal differences. The molecular data based on HCl exposure also suggests that some compensating processes take place in the atokous *P. dumerilii*, such as increasing amounts of transcripts involved in cytoskeleton function, protein synthesis and DNA replication (Table 4.2). *P. dumerilii* larvae seem to involve additional ion transport in the anus area to maintain acid-base homeostasis (Fig. 3.2).

Similar life cycle experiments were conducted for the semelparous polychaete *N. succinea* (Hartley, 2013). *N. succinea* cultured from the juvenile stage onwards under OA conditions (pH 7.8) showed that worms needed an increased time to reach the matured heteronereid stage, but the overall maturation success (percentage of total individuals that developed to the heteronereid stage) did not change (Hartley, 2013). *N. succinea* lives in benthic sediment and behavioural experiments on the burrow activity revealed that worms raised under control conditions (pH 8.2) exhibited a reduced time to dig into the sediment in low pH seawater conditions in comparison to control (pH 8.2) conditions (Hartley, 2013). Hartley (2013) suggested that this affinity to burrowing might be an avoidance behaviour, to escape from the low pH water. As *P. dumerilii* does not burrow in sediment this could not be a feasible strategy for this species. However, a microfluidics study showed that *P. dumerilii* larvae accumulate at a certain pH range and actively avoid extreme pH conditions and that the late nectochaete stage has a broader comfort zone (Ramanathan et al., 2013). This could suggest that the sensitive life stages of *P. dumerilii* larvae will avoid extreme low pH zones during their development, but further research is needed to see how atokous *P. dumerilii* respond.

Winners and losers

Studies have shown that increasing CO₂ levels will have different impacts on marine biota and will lead to both so called “winners” and “losers” (Doney et al., 2009). Ricevuto et al. (2015) suggested that non-calcifying polychaetes occurring in the CO₂ vents in Ischia are potential “winners” under the expected OA conditions. However, Dupont and Thorndyke (2009) highlighted that impacts of OA are rather species-specific. An OA study on the marine polychaete *S. spallanzanii* showed an increase in energy metabolism and a decrease in CA (Turner et al., 2015). This is in contrast to the findings of the present work where an up-regulation of CA was observed in the polychaete *P. dumerilii* exposed to low pH induced by CO₂ (Fig. 5.1 b). Inter-specific variations were also reported for other species as follows. In the two closely related sea urchins *Echinus esculentus* and *Strongylocentrotus droebachiensis* for example low pH had a negative effect on mortality in *E. esculentus*, but in *S. droebachiensis* it led to an enhancement of the developmental success (Dupont and Thorndyke, 2009).

It is known that calcification is one of the main processes under threat due to OA (Hendriks et al., 2010). However, not all calcifying marine organisms will react in the same way. The study of Ries et al. (2009) showed that responses vary and are complex. Ten out of eighteen species had a reduced rate of net calcification under elevated *p*CO₂, seven species showed an increase in the net calcification and one species did not respond at all. This indicates that OA effects are species-specific and that not all calcifying organisms are necessarily vulnerable at the same level. A study on the Atlantic herring (*Clupea harengus* L.) showed that these fish can compensate their acid-base status actively due to efficient regulatory machinery, however embryonic stages lack these mechanisms. Nevertheless, the study revealed that the eggs could cope with the increasing

$p\text{CO}_2$ conditions, suggesting that higher organisms may be more robust to ocean changes (Franke and Clemmesen, 2011).

Besides species-specific effects, OA will also have impacts on marine communities and ecosystems (Fabry et al., 2008). However, it is still not clear how OA and climate change will influence species interactions, community dynamics and ecosystem functioning (Godbold and Calosi, 2013). Rossoll et al. (2012) investigated the effect of OA on food web interactions. The laboratory experiment revealed that OA has an effect on the algae (*Thalassiosira pseudonana*) fatty acid composition, which led to a decline in the essential fatty acids in the copepods that feed on the algae (Rossoll et al., 2012). This demonstrates that OA can have an impact on the ocean food webs by changes at the primary producer level. The nereidid polychaete *Alitta virens* provides important ecosystem services with bioturbation of sand and consequently the nutrient availability (Herringshaw et al., 2010). A study on OA and warming showed that growth and behaviour of *A. virens* were changed which may have knock-on effects on the whole ecosystem (Godbold and Solan, 2013). The decrease of the pH in the seawater is also suggested to have impacts on the functionality of the chemical sensory system in marine organisms (Gerlach and Atema, 2012). This can have a major impact on marine organisms as chemical signals influence spatial/ temporal distribution, predation, courtship behaviour, mating, aggregation, school formation and habitat selection (Zimmer and Butman, 2000). It has been suggested that the disruption is caused through the conformational change in the cue induced through the low pH or an alteration in the charge distribution on the odour receptor cells (Tierney and Atema, 1988; Hardege et al., 2011; De la Haye et al., 2012). Experiments showed that low pH negatively affected the detection of food and predators in *P. dumerilii* (Davidson, 2013) and both the feeding and the escape responses were reduced in low pH seawater (pH 7.8).

Moreover, OA will not have the same effects across the globe, but will occur with distinct regional patterns (Bopp et al., 2013). Changes in the surface pH are expected to be larger in the Arctic Ocean as the ocean basin is storing 23 % of the global oceanic anthropogenic CO₂, whereas the Southern Ocean contains only 9 % (Sabine et al., 2004). The study of Melzner et al. (2013) also showed that hypoxic zones in the Baltic Sea already experience significantly high *p*CO₂ levels (maximum values 1,700-3,200 μatm), which will be further exacerbated by OA and therefore exceeding the predicted values for 2100 tremendously.

Evolutionary adaptation

Most of our knowledge on OA is based on short-term perturbation experiments, which are too short to investigate potential evolutionary adaptation (Gattuso and Hansson, 2011). To investigate the physiological adaptation of different *P. dumerilii* populations, including populations occurring in a CO₂ vent Calosi et al. (2013) looked at the putatively neutral molecular marker COI. The phylogenetic tree showed a distinct clade for *P. dumerilii* collected in the acidified vent site off Ischia. Together with the experiment on the metabolic rate, the data suggests that *P. dumerilii* are physiologically adapted to elevated *p*CO₂ and potentially represent a cryptic species. This dissertation added 50 more sequences to the previously published data by Calosi et al. (2013) to improve our understanding of different *P. dumerilii* populations and the occurrence of potential cryptic species (Fig. 6.8). In addition to the sequences from Italy and England, sequences from France and Spain were included. Furthermore, two more CO₂ vents (Castello N3 and Vulcano) were added. As already shown in the previous tree, *P. dumerilii* collected at different sites show different clades indicating a complex of potentially cryptic species (Fig 6.8). In particular, the vent strains appeared genetically distinct from all other tested

populations and the specimens collected inside the Ischia vents showed great differences to the Vulcano vent system. This suggests that genetic variations within the existing populations led to speciation at these CO₂ vents systems.

There is evidence that anthropogenic habitat disturbance can lead to a rapid evolution of environmental tolerance in the copepod *Leptodiaptomus minutus*, which also showed the ability to reverse evolutionary response after the stressor was removed (Derry and Arnott, 2007). Potentially, a similar event could have occurred in these young CO₂ vents (Arnold et al., 2012; Boatta et al., 2013). Within polychaeta, cryptic species are a common phenomenon (Westheide and Hass-Cordes, 2001; Audzijonyte et al., 2008; Barroso et al., 2010). The study on *Eurythoe complanata*, indicated the existence of at least three cryptic species (Barroso et al., 2010). On the Seychelles (Indian Ocean), the polychaete *Petitia* sp. phenotypically belongs to *P. amphophthalma*, however genotypically the population forms a distinct taxonomic entity, showing great genetic difference to other sites (Westheide and Hass-Cordes, 2001).

H. diversicolor also appears as two cryptic species in the Baltic Sea (Audzijonyte et al., 2008) and *N. acuminata* samples at different locations in the U.S., Mexico and Europe represent genetically distinct groups (Reish et al., 2014). *N. diversicolor*, *N. japonica* and *N. limnicola* are three species which are very hard to distinguish morphologically and which live all in very similar habitats, brackish water and muddy sand (Bartels-Hardege, 1993). However, their reproduction strategies are very different (Dales, 1950; Smith, 1958). *N. japonica* is moving up in the water column for spawning and produces planktonic larvae (Smith, 1958), whereas in *N. diversicolor* the fertilisation and development of the eggs is taking place in the living tubes. *N. diversicolor* larvae are benthic living (Dales, 1950; Smith, 1958). On the other hand, *N. limnicola* is reproducing as a viviparous hermaphrodite (Smith, 1958).

Furthermore, the tolerance of salinity is different in these three species (Oglesby, 1968; Wu et al., 1984; Scaps, 2002). *N. japonica* can tolerate very low salinity, however for the reproduction the worms migrate to regions with higher salinity (Wu et al., 1984). *N. diversicolor* can tolerate high salinity differences ranging from almost fresh water to at least 200 % of normal seawater, but they cannot reproduce in salinities below ~10 % due to the larvae not developing under these low salinity concentrations (Scaps, 2002). The effects of low salinity on the osmoregulation of *N. diversicolor* and/ or reproduction was already suggested by Smith (1955). *N. limnicola* experiences seasonal changes in the salinity ranging from nearly fresh water to 85 % seawater (Oglesby, 1968). It is feasible that the different tolerances in salinity could have led to the development of the diverse reproductive strategies in these *Nereis* species.

With *P. dumerilii* belonging to the same family of Nereidae, the concept of different reproduction strategies under different pH condition arises. The present dissertation investigated the relatedness of swimming heteronereis collected above the south vent in Ischia in comparison to other populations (Chapter 6). The results showed that all worms belonged to the clade of “normal” *P. dumerilii* (Clade 4, see Fig. 6.8), with the exception of one worm, which clustered with clade 3, a mixture of worms from different non-vent sites. This may indicate that the worms inside the vent have a different strategy of reproduction as none of the collected heteronereis clustered with any of the vent clades. However, research on the life history of worms collected inside the CO₂ vent is needed to answer this question. Besides *P. dumerilii*, the mature morphologically indistinguishable polychaete *P. massiliensis* has been described in the Ischia region (Hauenschild, 1951), which is known to reproduce by laying large eggs in its living tubes (Schneider et al., 1992).

Future research

The present work focused on the gene expression at the mRNA level, yet this does not predict its actual protein levels. Future experiments could therefore focus on the protein levels of *NHE*, *CA* and *CaM*. This could be studied by so called enzyme-linked immunosorbent assays (ELISA) or Western blots, which both quantitatively measure proteins in a sample. Furthermore, it would be interesting to know if *P. dumerilii* only becomes stressed in response to low pH exposure or whether actual damage is occurring. To test DNA damage, for example, the so called comet assay (single-cell gel electrophoresis) could be used to look at DNA strand breakage (Dixon et al., 2002).

Another interesting approach is to examine changes in gene function that are mitotically and/or meiotically heritable but are not based on changes in the DNA sequence. This process is known as epigenetics (Armstrong, 2014). A recent study highlighted that environmental epigenetics could potentially be a suitable tool for next-generation pollution biomonitoring in marine invertebrates (Suarez-Ulloa et al., 2015). The study emphasises that epigenetic modifications are important in environmental responses and adaptation processes (Suarez-Ulloa et al., 2015). Since the present study only focused on short term exposure experiments it would be interesting for future work to see how low pH affects *P. dumerilii* over several generations. Is there any genetic or epigenetic adaptation occurring? *P. dumerilii* could be a good model organism for this, in light of its short generation time which would allow multiple generations to be studied in a laboratory setup.

The present thesis examined effects of pH changes in the laboratory only, where interactions of the benthic and pelagic environment are missing (Widdicombe et al., 2010). *P. dumerilii* is part of a complex marine food web where OA can have both direct and indirect effects (see Figure 7.1). Different species such as fish, crustaceans and sea birds

feed on the polychaetes, whilst the polychaetes themselves feed on algae. Any disturbance can cause changes at a different level of the trophic system. Therefore, additional work should focus on the interoperation of this missing link. For this the FOCE experiment could be used. This approach could add parts of the complex habitat of *P. dumerilii* such as algal communities and other organisms to the study. However, this approach can only reflect the ecosystem to a certain degree as the chamber can only hold a limited volume of water and the link to predation of birds is missing. Furthermore, the FOCE experiment is very costly (Gattuso et al., 2014).

Different life stages are expected to vary in their vulnerability towards environmental changes. Many OA studies focus on early life history stage (O'Donnell et al., 2010; Zippay and Hofmann, 2010; Wong et al., 2011). The study of Havenhand et al. (2008) showed that OA conditions reduce the fertilization success of the sea urchin *Heliocidaris erythrogramma* and the authors suggest that these findings could be relevant for other broadcast spawning marine species. Therefore, the experiments of the present thesis should be repeated with different life stages to investigate the overall vulnerability of the marine polychaete.

Calosi et al. (2013) showed that the *P. dumerilii* collected in the South vent off Ischia are genetically different to other *P. dumerilii* populations collected outside vents. The present work showed that the North vent population off Ischia forms one clade with the South vent population and that the vent population from Vulcano (Sicily) forms another genetically distinct clade. Studies on the reproductive mode on the South vent populations concluded that the populations represent *P. massiliensis* (Lucey et al., 2015). However, comparative sequence data for *P. massiliensis* from its type, such as from Banyuls-sur-mer (France), would be desirable to further examine this species complex of brooding *Platynereis*.

Finally, future work should link the molecular work represented in the present thesis to life trade end-points, such as feeding, weight, survival rate and oxygen consumption to allow linking molecular data to whole animal consequences of low pH exposure.

Conclusions

The present dissertation shows that low pH seawater altered through both HCl and CO₂ both change the relative gene expression of a number of genes in *P. dumerilii*. The exposure experiments using HCl showed that, in particular, genes involved in general metabolism and defence processes are down-regulated, indicating the potential vulnerability of *P. dumerilii* towards low pH conditions. However, possible compensation mechanisms could also be observed. *P. dumerilii* kept under low pH conditions for 7 days showed an up-regulation of the acid-base transporter *NHE* and *P. dumerilii* larvae showed an additional expression of *NHE* in the anus area after a similar exposure experiment.

Experiments using HCl and CO₂ showed differences in the mRNA expressions in two of the three selected *target* genes. This reveals that it is not necessarily solely the pH change in the seawater that induces the responses in the organisms as often assumed in OA studies.

It is known that laboratory cultures do not represent actual environmental conditions. Therefore, this dissertation looked at *P. dumerilii* collected in its natural habitat (Mediterranean Sea) including worms from CO₂ venting sites. Gene expression analysis of *target* genes showed significant differences between the worms from vent sites in comparison to non-vent sites suggesting that worms in the natural low pH areas are potentially adapted to the different seawater conditions. The transfer experiments of

the control population to high $p\text{CO}_2$ conditions showed no effect on any of the selected target genes, indicating that field populations are much more resistant to pH changes than worms cultured in the laboratory for many generations. However, two of the four genes were down-regulated in the vent worms transferred to normal pH conditions. This shows that the two field populations reacted different to the environmental changes.

Different *P. dumerilii* populations collected throughout Europe, including three CO_2 vent sites, showed that the CO_2 vent populations are genetically distinct from the other populations. The results may indicate the occurrence of so called cryptic species, which is common in polychaetes. An additional analysis looking at mature, spawning heteronereis collected over the south vent in Ischia revealed that all collected worms belong to the non-vent clade of worms, indicating that the vent populations might use a different reproductive strategy. Further research is needed to look more closely at the life history of vent worms and to elucidate the question about the reproductive mode of the vent populations, as well as to fully assess how *P. dumerilii* is affected by the expected future ocean changes.

Summary

1. Long term laboratory cultured *P. dumerilii* exposed to low pH (HCl) for 1 hour and for 7 days showed a significant gene expression difference in *NHE*. After 1 hour, *NHE* was significantly down-regulated and after 7 days significantly up-regulated. *CA* showed only a down regulation trend after 1 hour and now effect after 7 days. *CaM* was not changed at any of the time points.
2. 1 dpf *P. dumerilii* larvae exposed to low pH induced by HCl showed an additional expression of *NHE* in the anus area in comparison to “normal pH” kept worms (*in situ* hybridization).
3. Long term laboratory cultured *P. dumerilii* exposed to low pH (HCl) for 7 days showed many changes in different transcripts. Genes involved in metabolism and defence processes were down-regulated. Transcripts involved in cytoskeleton function, protein synthesis and DNA replication were up-regulated.
4. Long term laboratory cultured *P. dumerilii* exposed to low pH induced by CO₂ for 1 hour and for 7 days showed a significant up-regulation of *CA* at both time points. *NHE* showed an almost a significant down-regulation after the 7 day exposure experiment. *CaM* was not changed at any of the time points.
5. *P. dumerilii* obtained from the Ischia CO₂ vents and a nearby control site showed significant mRNA expression differences.
6. *P. dumerilii* collected in the control area S. Anna transferred to high *p*CO₂ conditions showed no significant differences in the mRNA expression of any of the target genes. *P. dumerilii* obtained from the Ischia south vent transferred to “normal” *p*CO₂ conditions showed a decrease in *NADH dehydrogenase* and *NHE* expression, but no change in *CA* and *paramyosin* expression, after the transfer.
7. *P. dumerilii* collected in three CO₂ vents (Ischia, Naples and Vulcano, Sicily) formed two clades distinct from the other worm populations sampled throughout Europe (COI analysis).
8. Swimming heteronereis obtained over the south vent in Ischia belonged to the genetic lineages that includes the non vent populations.

APPENDICES

Table 1. Sequence ID's for individual specimens, sample location and GenBank accession numbers for the COI sequences.

Sequence ID	Location	GenBank Accession Number
BankIt1831557 Seq01	Arcachon	KT124668
BankIt1831557 Seq02	Arcachon	KT124669
BankIt1831557 Seq03	Arcachon	KT124670
BankIt1831557 Seq04	Arcachon	KT124671
BankIt1831557 Seq05	Arcachon	KT124672
BankIt1831557 Seq06	Arcachon	KT124673
BankIt1831557 Seq07	Blanes	KT124674
BankIt1831557 Seq08	Blanes	KT124675
BankIt1831557 Seq09	Blanes	KT124676
BankIt1831557 Seq10	Blanes	KT124677
BankIt1831557 Seq11	Blanes	KT124678
BankIt1831557 Seq12	Blanes	KT124679
BankIt1831557 Seq13	Ischia_N3	KT124680
BankIt1831557 Seq14	Ischia_N3	KT124681
BankIt1831557 Seq15	Ischia_N3	KT124682
BankIt1831557 Seq16	Ischia_N3	KT124683
BankIt1831557 Seq17	Heteronereis_Ischia_S3	KT124684
BankIt1831557Seq18	Heteronereis_Ischia_S3	KT124685
BankIt1831557 Seq19	Heteronereis_Ischia_S3	KT124686
BankIt1831557 Seq20	Heteronereis_Ischia_S3	KT124687
BankIt1831557 Seq21	Heteronereis_Ischia_S3	KT124688
BankIt1831557 Seq22	Heteronereis_Ischia_S3	KT124689
BankIt1831557 Seq23	Heteronereis_Ischia_S3	KT124690
BankIt1831557 Seq24	Heteronereis_Ischia_S3	KT124691
BankIt1831557 Seq25	Heteronereis_Ischia_S3	KT124692
BankIt1831557 Seq26	Heteronereis_Ischia_S3	KT124693
BankIt1831557 Seq27	Palinuro	KT124694
BankIt1831557 Seq28	Palinuro	KT124695
BankIt1831557 Seq29	Palinuro	KT124696
BankIt1831557 Seq30	Palinuro	KT124697
BankIt1831557 Seq31	Palinuro	KT124698
BankIt1831557 Seq32	Palinuro	KT124699
BankIt1831557 Seq33	Palinuro	KT124700
BankIt1831557 Seq34	Palinuro	KT124701
BankIt1831557 Seq35	Stareso	KT124702
BankIt1831557 Seq36	Stareso	KT124703
BankIt1831557 Seq37	Stareso	KT124704
BankIt1831557 Seq38	Stareso	KT124705
BankIt1831557 Seq39	Ustica	KT124706
BankIt1831557 Seq40	Ustica	KT124707
BankIt1831557 Seq41	Ustica	KT124708
BankIt1831557 Seq42	Vulcano	KT124709
BankIt1831557 Seq43	Vulcano	KT124710
BankIt1831557 Seq44	Vulcano	KT124711
BankIt1831557 Seq45	Vulcano	KT124712

BankIt1831557 Seq46	Vulcano	KT124713
BankIt1831557 Seq47	Vulcano	KT124714
BankIt1831557 Seq48	Vulcano	KT124715
BankIt1831557 Seq49	Vulcano	KT124716
BankIt1831557 Seq50	Vulcano	KT124717

Table 2. Photo credits for the pictures used in the phylogenetic trees (Fig. 2.5, 2.7 and 2.9).

Figure	Photo	Web link	Accessed on
2.5	1	http://m9.i.pbase.com/o1/44/660044/1/139231079.6sdoeFeL_MG_4911Edit.jpg	17.07.2015
2.5	2	https://myrmecos.files.wordpress.com/2009/06/floridanus2.jpg	17.07.2015
2.5	3	http://www.discoverlife.org/IM/I_SD/0112/320/Megachile_centuncularis,_male_PaDIL,I_SD11243.jpg	17.07.2015
2.5	4	https://c2.staticflickr.com/4/3239/5832979089_25f1d9e33b_z.jpg	17.07.2015
2.5	5	http://fotos01.laopinion.es/2009/03/31/646x260/2009-03-31_IMG_2009-03-31_1238519529634_efe_20090330_171420.jpg	17.07.2015
2.5	6	http://images.fotocommunity.de/bilder/insekten/fliegen-muecken-schnaken/drosophila-melanogaster-fruchfliege-5e15f2b5-d673-4174-9092-84cc140ee818.jpg	17.07.2015
2.5	7	http://www.sintmaartengov.org/PressReleases/PublishingImages/aedes%5B1%5D.jpg	17.07.2015
2.5	8	http://igtrcn.org/wp-content/uploads/2014/06/Anopheles_gambiae_Mosquito.jpg	17.07.2015
2.5	9	http://www.nature.com/nature/journal/v483/n7389/images/483280a-i1.0.jpg	17.07.2015
2.5	10	http://www.embl-hamburg.de/aboutus/communication_outreach/media_relations/2007/070629_heidelberg/press29jun07_1.jpg	17.07.2015
2.5	11	http://cdn1.arkive.org/media/1A/1AC43792-60F2-4F64-8889-85478D0DE401/Presentation.Large/Immature-male-Sumatran-orangutan.jpg	17.07.2015
2.5	12	http://static.ddmcdn.com/gif/blogs/dsc-files-2011-12-gorilla-in-the-wild.jpg	17.07.2015
2.7	13	https://upload.wikimedia.org/wikipedia/commons/b/b2/Taeniopygia_guttata_-_Karratha,_Pilbara,_Western_Australia,_Australia_-_male-8_%282%29.jpg	17.07.2015
2.7	14	http://orientalbirdimages.org/images/data/humesgroundpeckerop_copy1.jpg	17.07.2015
2.7	15	http://www.fazendavisconde.com.br/images/Galo_de_Bankiva_Gallus_gallus_Fazenda_Visconde1.jpg	17.07.2015
2.7	16	http://biotropics.com/assets/images/Anolis_carolinensis_01.jpg	17.07.2015
2.7	17	http://www.clovegarden.com/ingred/img/rp_alli01g.jpg	17.07.2015
2.7	18	http://www.seafoodexport.com/nsite/components/com_virtuemart/shop_image/product/Dogfish_squalus_4addb32203df7.jpg	17.07.2015
2.7	19	http://www.biolib.cz/IMG/GAL/BIG/204152.jpg	17.07.2015
2.7	20	https://c1.staticflickr.com/1/130/329292649_c526437d5d.jpg	17.07.2015
2.7	21	https://upload.wikimedia.org/wikipedia/commons/e/ea/Bos_taurus_taurus_sideview.JPG	17.07.2015
2.7	22	http://sfghed.ucsf.edu/Education/ClinicImages/Ascaris.JPG	17.07.2015
2.9	23	http://media1.s-nbcnews.com/j/MSNBC/Components/Photo/_new/110817-HomoSapienPhoto-0345p.grid-6x2.jpg	17.07.2015
2.9	24	http://aquinas-sta.org/Raider/wp-content/uploads/2014/05/In-the-Nude_01.png	17.07.2015
2.9	25	http://gallery.nanfa.org/d/35949-3/Esox+lucius+Northern+Pike+409.JPG	17.07.2015
2.9	26	https://thegioitunhien.net/images/file/XXU8GQVD0QgBAPR/ca-chinh-dien-luon-dien-electrophorus-electricus-2.jpg	17.07.2015
2.9	27	http://www.nsc.nagoya-cu.ac.jp/~fukumoto/wwwdata/namekuji.jpg	17.07.2015
2.9	28	http://www.ictioterm.es/especies/fotos_principales/L/Penaeus_vannamei_L.jpg	17.07.2015
2.9	29	http://www.alexanderwild.com/Ants/Taxonomic-List-of-Ant-Genera/Cerapachys/i-vHFJZJH/1/XL/biroi4-XL.jpg	17.07.2015
2.9	30	http://g-tokyohumanite.jp/human/sales/2009/1120c.jpg	17.07.2015
2.9	31	http://drewbuckleyphotography.com/site/wp-content/uploads/2012/10/DBP_7244.jpg	17.07.2015

REFERENCES

- Abe, M., Takahashi, K. and Hiwada, K. (1990) Effect of calmodulin on actin-activated myosin ATPase activity. *J Biochem* 108, 835-838.
- Ahn, N. and Klinman, J.P. (1983) Mechanism of modulation of dopamine β -Monooxygenase by pH and fumarate as deduced from initial rate and primary deuterium isotope effect studies. *Biochemistry* 22, 3096-3106.
- Altincicek, B. and Vilcinskas, A. (2007) Analysis of the immune-related transcriptome of a lophotrochozoan model, the marine annelid *Platynereis dumerilii*. *Front Zool* 4: doi:10.1186/1742-9994-4-18.
- Andersson, A.J., Kuffner, I.B., Mackenzie, F.T., Jokiel, P.L., Rodgers, K. S. and Tan, A. (2009) Net loss of CaCO₃ from a subtropical calcifying community due to seawater acidification: mesocosm-scale experimental evidence. *Biogeosciences* 6, 1811-1823.
- Andrews, S.C., Arosio, P., Bottke, W., Briat, J.-F., von Darl, M., Harrison, P.M., Laulhere, J.-P., Levi, S., Lobreaux, S. and Yewdall, S.J. (1992) Structure, function, and evolution of ferritins. *J Inorg Biochem* 47, 161-174.
- Aparicio, S., Chapman, J., Stupka, E., Putnam, N., Chia, J.M., Dehal, P., Christoffels, A., Rash, S., Hoon, S., Smit, A., Sollewijn Gelpke, M.D., Roach J., Oh, T., Ho, I.Y., Wong M., Detter, C., Verhoef, F., Predki, P., Tay, A., Lucas, S., Richardson, P., Smith, S.F., Clark, M.S., Edwards, Y.J.K., Doggett, N., Zharkikh, A., Tavtigian, S.V., Pruss, D., Barnstead, M., Evans, C., Baden, H., Powell, J., Glusman, G., Rowen, L., Hood, L., Tan, Y.H., Elgar, G., Hawkins, T., Venkatesh, B., Rokhsar, D. and Brenner, S. (2002) Whole-genome shotgun assembly and analysis of the genome of *Fugu rubripes*. *Science* 297, 1301-1310.
- Arai, M.N. (2005) Predation on pelagic coelenterates: a review. *J Mar Biol Ass UK* 85, 523-536.
- Armstrong, L. (2014) Epigenetics. New York: Garland Science.
- Arnold, T., Mealey, C., Leahey, H., Miller, A.W., Hall-Spencer, J.M., Milazzo, M. and Maers, K. (2012) Ocean acidification and the loss of phenolic substances in marine plants. *PloS One* 7 e35107: doi:10.1371/journal.pone.0035107.

- Attrill, M.J., Wright, J. and Edwards, M. (2007) Climate-related increases in jellyfish frequency suggest a more gelatinous future for the North Sea. *Limnol Oceanogr* 52, 480-485.
- Audzijonyte, A., Ovcarenko, I., Bastrop, R. and Väinölä, R. (2008) Two cryptic species of the *Hediste diversicolor* group (Polychaeta, Nereididae) in the Baltic Sea, with mitochondrial signatures of different population histories. *Mar Biol* 155, 599-612.
- Babu, Y.S., Sack, J.S., Greenhough, T.J., Bugg, C.E., Means, A.R. and Cook, W.J. (1985) Three-dimensional structure of calmodulin. *Nature* 315, 37-40.
- Bacci, M., Solomon, S.E., Mueller, U.G., Martins, V.G., Carvalho, A.O., Vieira, L.G. and Silva-Pinhati, A.C.O. (2009) Phylogeny of leafcutter ants in the genus *Atta* Fabricius (Formicidae: Attini) based on mitochondrial and nuclear DNA sequences. *Mol Phylogenet Evol* 51, 427-437.
- Badapanda, C. (2013) Suppression subtractive hybridization (SSH) combined with bioinformatics method: an integrated functional annotation approach for analysis of differentially expressed immune-genes in insects. *Bioinformatics* 9, 216-221.
- Barnhart, M.C. (1992) Acid-base regulation in pulmonate molluscs. *J Exp Zool* 263, 120-126.
- Barrett, R.D.H. and Schluter, D. (2008) Adaptation from standing genetic variation. *Trends Ecol Evol* 23, 38-44.
- Barroso, R., Klautau, M., Solé-Cava, A.M. and Paiva, P.C. (2010) *Eurythoe complanata* (Polychaeta: Amphinomidae), the 'cosmopolitan' fireworm, consists of at least three cryptic species. *Mar Biol* 157, 69-80.
- Barry, J.P., Widdicombe, S. and Hall-Spencer, J.M. (2011) Effects of ocean acidification on marine biodiversity and ecosystem function. In: Gattuso, J.-P. and Hansson, L. (eds.) *Ocean acidification*. New York: Oxford University Press.
- Bartels-Hardege (1993) Zur Reproduktionsbiologie von *Nereis diversicolor* und *Nereis japonica* und der Rolle von Pheromonen bei der Steuerung des Reproduktionsverhaltens. Doktorarbeit, Universität Oldenburg.
- Battarbee, R.W., Thrush, B.A., Clymo, R.S., Le Cren, E.D., Goldsmith, P., Mellanby, K., Bradshaw, A.D., Chester, P.F., Howells, G.D. and Kerr, A. (1984) Diatom analysis and the acidification of lakes [and discussion]. *Phil Trans R Soc B* 305, 451-477.

- Beamish, R.J. (1976) Acidification of lakes in Canada by acid precipitation and the resulting effects on fishes. *Water Air Soil Poll* 6, 501-514.
- Beck, G., Ellis, T.W., Habicht, G.S., Schluter, S.F. and Marchalonis, J.J. (2001) Evolution of the acute phase response: iron release by echinoderm (*Asterias forbesi*) coelomocytes, and cloning of an echinoderm ferritin molecule. *Dev Comp Immunol* 26, 11-26.
- Benton, T.G., Solan, M., Travis, J.M.J. and Sait, S.M. (2007) Microcosm experiments can inform global ecological problems. *Trends Ecol Evol* 22, 516-521.
- Berg, J.M., Tymoczko, J.L. and Stryer, L. (2013) Stryer Biochemie, 7. Auflage. Berlin: Springer Spektrum.
- Berkner, L.V. and Marshall, L.C. (1965) On the origin and rise of oxygen concentration in the Earth's atmosphere. *J Atmos Sci* 22, 225-261.
- Bernard, C. (1878) Leçons sur les phénomènes de la vie commune aux animaux et aux végétaux. (Cours de physiologie générale du muséum d'histoire naturelle), I/II. Librairie J.-B. Baillière et files, Paris.
- Bertucci, A., Moya, A., Tambutté, S., Allemand, D., Supuran, C.T. and Zoccola, D. (2013) Carbonic anhydrases in anthozoan corals- A review. *Bioorgan Med Chem* 21, 1437-1450.
- Bibby, R., Widdicombe, S., Parry, H., Spicer, J. and Pipe, R. (2008) Effects of ocean acidification on the immune response of the blue mussel *Mytilus edulis*. *Aquat Biol* 2, 67-74.
- Biesinger, K.E. and Christensen, G.M. (1972) Effects of various metals on survival, growth, reproduction, and metabolism of *Daphnia magna*. *Journal of the Fisheries Board of Canada* 29, 1691-1700.
- Bindoff, N.L., Willebrand, J., Artale, V., Cazenave, A., Gregory, J., Gulev, S., Hanawa, K., Le Quéré, C., Levitus, S., Nojiri, Y., Shum, C.K., Talley, L.D. and Unnikrishnan, A. (2007) Observations: Oceanic Climate Change and Sea Level. In: Solomon, S., Qin, D., Manning, M., Chen, Z., Marquis, M., Averyt, K.B., Tignor, M. and Miller, H.L. (eds.) *Climate Change 2007: The Physical Science Basis. Contribution of Working Group I to the Fourth Assessment Report of the Intergovernmental Panel on Climate Change*. Cambridge: Cambridge University Press.

- Bio-Rad Laboratories, Inc. (2006) Real-Time PCR Applications Guide.
- Bittar, E.E. and Bittar, N. (1995) Principles of Medical Biology. Cellular Organelles. Greenwich: Jai Press Inc.
- Boatta, F., D'Alessandro, W., Gagliano, A.L., Liotta, M., Milazzo, M., Rodolfo-Metalpa, R., Hall-Spencer, J.M. and Parello, F. (2013) Geochemical survey of Levante Bay, Vulcano Island (Italy), a natural laboratory for the study of ocean acidification. *Mar Pollut Bull* 73, 485-494.
- Boilly-Marer, Y. (1974) Etude expérimentale du comportement nuptial de *Platynereis dumerilii* (Annelida, Polychaeta): chémoréception, émission des produits génitaux. *Mar Biol* 24, 167-169.
- Boore, J.L. and Brown, W.M. (2000) Mitochondrial genomes of *Galathealinum*, *Helobdella*, and *Platynereis*: sequence and gene arrangement comparisons indicate that Pogonophora is not a phylum and Annelida and Arthropoda are not sister taxa. *Mol Biol Evol* 17, 87-106.
- Bopp, L., Resplandy, L., Orr, J.C., Doney, S.C., Dunne, J.P., Gehlen, M., Halloran, P., Heinze, C., Ilyina, T., Séférian, R., Tjiputra, J. and Vichi, M. (2013) Multiple stressors of ocean ecosystems in the 21st century: projections with CMIP5 models. *Biogeosciences* 10, 6225-6245.
- Boutet, I., Moraga, D., Marinovic, L., Obreque, J. and Chavez-Crooker, P. (2008) Characterization of reproduction-specific genes in a marine bivalve mollusc: Influence of maturation stage and sex on mRNA expression. *Gene* 407, 130-138.
- Boutet, I., Jollivet, D., Shillito, B., Moraga, D. and Tanguy, A. (2009) Molecular identification of differentially regulated genes in the hydrothermal-vent species *Bathymodiolus thermophilus* and *Paralvinella pandorae* in response to temperature. *BMC genomics*, 10: doi:10.1186/1471-2164-10-222.
- Bustin, S.A., Benes, V., Garson, J.A., Hellems, J., Huggett, J., Kubista, M., Mueller, R., Nolan, T., Pfaffl, M.W., Shipley, G.L., Vandesompele, J. and Wittwer, C.T. (2009) The MIQE guidelines: minimum information for publication of quantitative real-time PCR experiments. *Clin Chem* 55, 611-622.
- Cai, W.-J., Hu, X., Huang, W.-J., Murrell, M.C., Lehrter, J.C., Lohrenz, S.E., Chou, W.-C., Zhai, W., Hollibaugh, J.T., Wang, Y., Zhao, P., Guo, X., Gundersen, K., Dai,

- M. and Gong, G.-C. (2011) Acidification of subsurface coastal waters enhanced by eutrophication. *Nat Geosci* 4, 766-770.
- Cajaraville, M.P., Bebianno, M.J., Blasco, J., Porte, C., Sarasquete, C. and Viarengo, A. (2000) The use of biomarkers to assess the impact of pollution in coastal environments of the Iberian Peninsula: a practical approach. *Sci Total Environ* 247, 295-311.
- Caldeira, K. and Wickett, M.E. (2003) Oceanography: anthropogenic carbon and ocean pH. *Nature* 425, 365.
- Calosi, P., Rastrick, S.P.S., Lombardi, C., de Guzman, H.J., Davidson, L., Jahnke, M., Giangrande, A., Hardege, J.D., Schulze, A., Spicer, J.I. and Gambi, M.C. (2013) Adaptation and acclimatization to ocean acidification in marine ectotherms: an *in situ* transplant experiment with polychaetes at a shallow CO₂ vent system. *Phil Trans R Soc B* 368: doi.org/10.1098/rstb.2012.0444.
- Campbell, A.L., Mangan, S., Ellis, R.P. and Lewis, C. (2014) Ocean acidification increases copper toxicity to the early life history stages of the polychaete *Arenicola marina* in artificial seawater. *Environ Sci Technol* 48, 9745-9753.
- Cannon, W.B. (1929) Organization for physiological homeostasis. *Physiol Rev* 9, 399-431.
- Capaldi, R.A. (1990) Structure and function of cytochrome c oxidase. *Annu Rev Biochem* 59, 569-596.
- Capitani, G., De Biase, D., Aurizi, C., Gut, H., Bossa, F. and Grütter, M.G. (2003) Crystal structure and functional analysis of *Escherichia coli* glutamate decarboxylase. *EMBO J* 22, 4027-4037.
- Carotenuto, Y., Dattolo, E., Lauritano, C., Pisano, F., Sanges, R., Miralto, A., Procaccini, G. and Ianora, A. (2014) Insights into the transcriptome of the marine copepod *Calanus helgolandicus* feeding on the oxylipin-producing diatom *Skeletonema marinoi*. *Harmful Algae* 31, 153-162.
- Castagnone-Sereno, P., Leroy, F. and Abad, P. (2001) cDNA cloning and expression analysis of a calponin gene from the plant-parasitic nematode *Meloidogyne incognita*. *Mol Biochem Parasit* 112, 149-152.

- Chapman, D. (ed.) (1996) Water quality assessments- A guide to the use of biota, sediments and water in environmental monitoring, 2nd Edition. Cambridge: Cambridge University Press.
- Chen, Z.-F., Wang, H., Matsumura, K. and Qian, P.-Y. (2012a). Expression of calmodulin and myosin light chain kinase during larval settlement of the barnacle *Balanus amphitrite*. *PloS one* 7: doi:10.1371/journal.pone.0031337.
- Chen, Z.-F., Wang, H. and Qian, P.-Y. (2012b) Characterization and expression of calmodulin gene during larval settlement and metamorphosis of the polychaete *Hydroides elegans*. *Comp Biochem Phys B* 162, 113-119.
- Chen, T.-H., Cheng, Y.-M., Cheng, J.-O. and Ko, F.-C. (2012c) Assessing the effects of polychlorinated biphenyls (Aroclor 1254) on a scleractinian coral (*Stylophora pistillata*) at organism, physiological, and molecular levels. *Ecotox Environ Safe* 75, 207-212.
- Chin, D. and Means, A.R. (2000) Calmodulin: a prototypical calcium sensor. *Trends Cell Biol* 10, 322-328.
- Cigliano, M., Gambi, M.C., Rodolfo-Metalpa, R., Patti, F.P. and Hall-Spencer, J.M. (2010) Effects of ocean acidification on invertebrate settlement at volcanic CO₂ vents. *Mar Biol* 157, 2489-2502.
- Ciocan, C.M., Cubero-Leon, E., Minier, C. and Rotchell, J.M. (2011) Identification of reproduction-specific genes associated with maturation and estrogen exposure in a marine bivalve *Mytilus edulis*. *PloS One* 6: doi:10.1371/journal.pone.0022326.
- Ciocan, C.M., Cubero-Leon, E., Peck, M.R., Langston, W.J., Pope, N., Minier, C. and Rotchell, J.M. (2012) Intersex in *Scrobicularia plana*: Transcriptomic analysis reveals novel genes involved in endocrine disruption. *Environ Sci Technol* 46, 12936-12942.
- Claiborne, J.B., Edwards, S.L. and Morrison-Shetlar, A.I. (2002) Acid–base regulation in fishes: cellular and molecular mechanisms. *J Exp Zool* 293, 302-319.
- Clark, D.P. and Pazdernik, N.J. (2012) Molecular Biology, 2nd Edition. Waltham: Academic Cell.
- Colbath, G.K. (1986) Jaw mineralogy in eunicean polychaetes (Annelida). *Micropaleontology* 32, 186-189.

- Collard, M., Eeckhaut, I., Dehairs, F. and Dubois, P. (2014) Acid–base physiology response to ocean acidification of two ecologically and economically important holothuroids from contrasting habitats, *Holothuria scabra* and *Holothuria parva*. *Environ Sci Pollut Res* 21, 13602-13614.
- Collin, H., Meistertzheim, A.-L., David, E., Moraga, D. and Boutet, I. (2010) Response of the Pacific oyster *Crassostrea gigas*, Thunberg 1793, to pesticide exposure under experimental conditions. *J Exp Biol* 213, 4010-4017.
- Collins, S. and Bell, G. (2004) Phenotypic consequences of 1,000 generations of selection at elevated CO₂ in a green alga. *Nature* 431, 566-569.
- Comeau, S., Gorsky, G., Jeffree, R., Teyssié, J.-L. and Gattuso, J.-P. (2009) Impact of ocean acidification on a key Arctic pelagic mollusc (*Limacina helicina*). *Biogeosciences* 6, 1877-1882.
- Cooley, D.R. and Manning, W.J. (1987) The impact of ozone on assimilate partitioning in plants: a review. *Environ Pollut* 47, 95-113.
- Cox, G.A., Lutz, C.M., Yang, C.-L., Biemesderfer, D., Bronson, R.T., Fu, A., Aronson, P.S., Noebels, J.L. and Frankel, W.N. (1997) Sodium/hydrogen exchanger gene defect in slow-wave epilepsy mutant mice. *Cell* 91, 139-148.
- Craft, J.A., Gilbert, J.A., Temperton, B., Dempsey, K.E., Ashelford, K., Tiwari, B., Hutchinson, T.H. and Chipman, J.K. (2010) Pyrosequencing of *Mytilus galloprovincialis* cDNAs: tissue specific expression patterns. *PloS One* 5: doi:10.1371/journal.pone.0008875.
- Crook, E.D., Potts, D., Rebolledo-Vieyra, M., Hernandez, L. and Paytan, A. (2012) Calcifying coral abundance near low-pH springs: implications for future ocean acidification. *Coral Reefs* 31, 239-245.
- Dale, J.W., Von Schantz, M. and Plant, N. (2012) From Genes to Genomes. Concepts and Applications of DNA Technology, 3rd Edition. Sussex: John Wiley & Sons, Ltd.
- Dales, R.P. (1950) The reproduction and larval development of *Nereis diversicolor* O.F. Müller. *J Mar Biol Ass UK* 29, 321-360.
- Daly, J.M. (1973) Behavioural and secretory activity during tube construction by *Platynereis dumerilii* Aud & M. Edw. [Polychaeta: Nereidae]. *J Mar Biol Ass UK* 53, 521-529.

- Dando, P.R., Stüben, D. and Varnavas, S.P. (1999) Hydrothermalism in the Mediterranean Sea. *Prog Oceanogr* 44, 333-367.
- Davidson, L. (2013) Ocean acidification and its effects upon fitness in nereidid polychaetes. Ph.D thesis, University of Hull, UK Available from: EThOS [10.06.2015].
- Day, T. (2006) Biomes of the Earth, Lakes and Rivers. New York: Chelsea House.
- De la Haye, K.L., Spicer, J.I., Widdicombe, S. and Briffa, M. (2012) Reduced pH sea water disrupts chemo-responsive behaviour in an intertidal crustacean. *J Exp Mar Biol Ecol* 412, 134-140.
- De Moel, H., Ganssen, G.M., Peeters, F.J.C., Jung, S.J.A., Kroon, D., Brummer, G.J.A. and Zeebe, R.E. (2009) Planktic foraminiferal shell thinning in the Arabian Sea due to anthropogenic ocean acidification? *Biogeosciences* 6, 1917-1925.
- De Swart, R.L., Ross, P.S., Vos, J.G. and Osterhaus, A.D.M.E. (1996) Impaired immunity in harbour seals (*Phoca vitulina*) exposed to bioaccumulated environmental contaminants: review of a long-term feeding study. *Environ Health Persp* 104, 823-828.
- De Witt, T.J., Sih, A. and Wilson, D.S. (1998) Costs and limits of phenotypic plasticity. *Trends Ecol Evol* 13, 77-81.
- De Witt, T.J. and Scheiner, S.M. (eds.) (2004) Phenotypic plasticity: functional and conceptual approaches. Oxford: Oxford University Press.
- Derry, A.M. and Arnott, S.E. (2007) Adaptive reversals in acid tolerance in copepods from lakes recovering from historical stress. *Ecol Appl* 17, 1116-1126.
- Dias, B.B., Hart, M.B., Smart, C.W. and Hall-Spencer, J.M. (2010) Modern seawater acidification: the response of foraminifers to high-CO₂ conditions in the Mediterranean Sea. *J Geol Soc London* 167, 843-846.
- Dineshram, R., Wong, K.K.W., Xiao, S., Yu, Z., Qian, P.Y. and Thiyagarajan, V. (2012) Analysis of Pacific oyster larval proteome and its response to high-CO₂. *Mar Pollut Bull* 64, 2160-2167.
- Dineshram, R., Thiyagarajan, V., Lane, A., Ziniu, Y., Xiao, S. and Leung, P.T.Y. (2013) Elevated CO₂ alters larval proteome and its phosphorylation status in the commercial oyster, *Crassostrea hongkongensis*. *Mar Biol* 160, 2189-2205.

- Dixon, D.R., Pruski, A.M., Dixon, L.R. and Jha, A.N. (2002) Marine invertebrate ecogenotoxicology: a methodological overview. *Mutagenesis* 17, 495-507.
- Djawdan, M., Rose, M.R. and Bradley, T.J. (1997) Does selection for stress resistance lower metabolic rate? *Ecology* 78, 828-837.
- Dockery, D.W. and Pope, C.A. (1994) Acute respiratory effects of particulate air pollution. *Annu Rev Publ Health* 15, 107-132.
- Doney, S.C., Mahowald, N., Lima, I., Feely, R.A., Mackenzie, F.T., Lamarque, J.-F. and Rasch, P.J. (2007) Impact of anthropogenic atmospheric nitrogen and sulfur deposition on ocean acidification and the inorganic carbon system. *P Natl Acad Sci USA* 104, 14580-14585.
- Doney, S.C., Fabry, V.J., Feely, R.A. and Kleypas, J.A. (2009) Ocean acidification: The other CO₂ problem. *Annu Rev Mar Sci* 1, 169-192.
- Donnarumma, L., Lombardi, C., Cocito, S. and Gambi, M.C. (2014) Settlement pattern of *Posidonia oceanica* epibionts along a gradient of ocean acidification: an approach with mimics. *Medit Mar Sci* 15, 498-509.
- Dorresteyn, A.W.C. (1990) Quantitative analysis of cellular differentiation during early embryogenesis of *Platynereis dumerilii*. *Roux Arch Dev Biol* 199, 14-30.
- Dupont, S. and Thorndyke, M.C. (2009) Impact of CO₂-driven ocean acidification on invertebrates early life-history—What we know, what we need to know and what we can do. *Biogeosciences Discussions* 6, 3109-3131.
- Dupont, S., Ortega-Martínez, O. and Thorndyke, M. (2010) Impact of near-future ocean acidification on echinoderms. *Ecotoxicology* 19, 449-462.
- Edwards, M. and Richardson, A.J. (2004) Impact of climate change on marine pelagic phenology and trophic mismatch. *Nature* 430, 881-884.
- Ekici, Ö.D., Paetzel, M. and Dalbey, R.E. (2008) Unconventional serine proteases: variations on the catalytic Ser/His/Asp triad configuration. *Protein Sci* 17, 2023-2037.
- Emminger, H. (2005) Physikum EXAKT: Das gesamte Prüfungswissen für die 1. ÄP. Stuttgart: Thieme.
- Engel, A., Zondervan, I., Aerts, K., Beaufort, L., Benthien, A., Chou, L., Delille, B., Gattuso, J.-P., Harlay, J., Heemann, C., Hoffmann, L., Jacquet, S., Nejstgaard, J.,

- Pizay, M.-D., Rochelle-Newall, E., Schneider, U., Terbrueggen, A. and Riebesell, U. (2005) Testing the direct effect of CO₂ concentration on a bloom of the coccolithophorid *Emiliana huxleyi* in mesocosm experiments. *Limnol Oceanogr* 50, 493-507.
- Fabry, V.J., Seibel, B.A., Feely, R.A. and Orr, J.C. (2008) Impacts of ocean acidification on marine fauna and ecosystem processes. *ICES J Mar Sci* 65, 414-432.
- Feely, R.A., Sabine, C.L., Lee, K., Berelson, W., Kleypas, J., Fabry, V.J. and Millero, F.J. (2004) Impact of anthropogenic CO₂ on the CaCO₃ system in the oceans. *Science* 305, 362-366.
- Feely, R.A., Doney, S.C. and Cooley, S.R. (2009) Ocean acidification: present conditions and future changes in a high-CO₂ world. *Oceanography* 22, 36-47.
- Fischer, A. (1985) Reproduction and Postembryonic Development of the Annelid *Platynereis dumerilii* (C1577) IWF Wissen und Medien gGmbH.
- Fischer, A. (1999) Reproductive and developmental phenomena in annelids: a source of exemplary research problems. *Hydrobiologia* 402, 1-20.
- Fischer, A. and Dorresteijn, A. (2004) The polychaete *Platynereis dumerilii* (Annelida): a laboratory animal with spiralian cleavage, lifelong segment proliferation and a mixed benthic/pelagic life cycle. *Bioessays* 26, 314-325.
- Fischer, A.H.L., Henrich, T. and Arendt, D. (2010) The normal development of *Platynereis dumerilii* (Nereididae, Annelida) *Front Zool* 7: doi:10.1186/1742-9994-7-31.
- Fischer, J. and Phillips, N.E. (2014) Carry-over effects of multiple stressors on benthic embryos are mediated by larval exposure to elevated UVB and temperature. *Glob Change Biol* 20, 2108-2116.
- Fischlin, A., Midgley, G.F., Price, J.T., Leemans, R., Gopal, B., Turley, C., Rounsevell, M.D.A., Dube, O.P., Tarazona, J. and Velichko, A.A. (2007) Ecosystems, their properties, goods, and services. In: Parry, M.L., Canziani, O.F., Palutikof, J.P., van der Linden, P.J. and Hanson, C.E. (eds.) *Climate Change 2007: Impacts and Vulnerability. Contribution of Working Group II to the Fourth Assessment Report of the Intergovernmental Panel on Climate Change*. Cambridge: Cambridge University Press.

- Fisher, S.Z., Tariku, I., Case, N.M., Tu, C., Seron, T., Silverman, D.N., Linser, P.J. and McKenna, R. (2006) Expression, purification, kinetic, and structural characterization of an α -class carbonic anhydrase from *Aedes aegypti* (AaCA1). *Biochimica et Biophysica Acta (BBA)-Proteins and Proteomics* 1764, 1413-1419.
- Fitzer, S.C., Phoenix, V.R., Cusack, M. and Kamenos, N.A. (2014) Ocean acidification impacts mussel control on biomineralisation. *Scientific Reports*, 4: doi:10.1038/srep06218.
- Florea, A.-M. and Büsselberg, D. (2006) Occurrence, use and potential toxic effects of metals and metal compounds. *Biometals* 19, 419-427.
- Folmer, O., Black, M., Hoeh, W., Lutz, R. and Vrijenhoek, R. (1994) DNA primers for amplification of mitochondrial cytochrome c oxidase subunit I from diverse metazoan invertebrates. *Mol Mar Biol Biotech* 3, 294-299.
- Form, A.U. and Riebesell, U. (2012) Acclimation to ocean acidification during long-term CO₂ exposure in the cold-water coral *Lophelia pertusa*. *Glob Change Biol* 18, 843-853.
- Förstner, U. and Wittmann, G.T.W. (1981) Metal pollution in the aquatic environment. 2nd Edition. Berlin: Springer-Verlag.
- Fott, J., Pražáková, M., Stuchlík, E. and Stuchliková, Z. (1994) Acidification of lakes in Šumava (Bohemia) and in the High Tatra Mountains (Slovakia). *Hydrobiologia* 274, 37-47.
- Franke, A. and Clemmesen, C. (2011) Effect of ocean acidification on early life stages of Atlantic herring (*Clupea harengus* L.). *Biogeosciences* 8, 3697-3707.
- Gao, Y., Gillen, C.M. and Wheatly, M.G. (2009) Cloning and characterization of a calmodulin gene (CaM) in crayfish *Procambarus clarkii* and expression during molting. *Comp Biochem Physiol B* 152, 216-225.
- Garey, J.R., Schmidt-Rhaesa, A., Near, T.J. and Nadler, S.A. (1998) The evolutionary relationships of rotifers and acanthocephalans. In: Wurdak, E., Wallace, R. and Segers, H. (eds.) *Developments in Hydrobiology. Rotifera VIII: A Comparative Approach*. Dordrecht: Springer Science+Business Media p 86.
- Garland, T., Bennett, A.F. and Rezende, E.L. (2005) Phylogenetic approaches in comparative physiology. *J Exp Biol* 208, 3015-3035.

- Garrard, S.L., Gambi, M.C., Scipione, M.B., Patti, F.P., Lorenti, M., Zupo, V., Paterson, D.M. and Buia, M.C. (2014) Indirect effects may buffer negative responses of seagrass invertebrate communities to ocean acidification. *J Exp Mar Biol Ecol* 461, 31-38.
- Gattuso, J.-P., Frankignoulle, M., Bourge, I., Romaine, S. and Buddemeier, R.W. (1998) Effect of calcium carbonate saturation of seawater on coral calcification. *Global Planet Change* 18, 37-46.
- Gattuso, J.-P. and Lavigne, H. (2009) Technical note: Approaches and software tools to investigate the impact of ocean acidification. *Biogeosciences* 6, 2121-2133.
- Gattuso, J.-P., Gao, K., Lee, K., Rost, B. and Schulz, K.G. (2010) Approaches and tools to manipulate the carbonate chemistry. In: Riebesell, U., Fabry, V.J., Hansson, L. and Gattuso, J.-P. (eds.) *Guide to best practices for ocean acidification research and data reporting*. Luxembourg: Publications Office of the European Union pp 41-52.
- Gattuso, J.-P. and Hansson, L. (2011) Ocean acidification: background and history. In: Gattuso, J.-P. and Hansson, L. (eds.) *Ocean acidification*. New York: Oxford University Press.
- Gattuso, J.-P., Kirkwood, W., Barry, J.P., Cox, E., Gazeau, F., Hansson, L., Hendriks, I., Kline, D.I., Mahacek, P., Martin, S., McElhany, P., Peltzer, E.T., Reeve, J., Roberts, D., Saderne, V., Tait, K., Widdicombe, S. and Brewer, P.G. (2014) Free-ocean CO₂ enrichment (FOCE) systems: present status and future developments. *Biogeosciences* 11, 4057-4075.
- Gazeau, F., Gattuso, J.-P., Dawber, C., Pronker, A.E., Peene, F., Peene, J., Heip, C.H.R. and Middelburg, J.J. (2010) Effect of ocean acidification on the early life stages of the blue mussel *Mytilus edulis*. *Biogeosciences* 7, 2051-2060.
- Gazeau, F., Martin S., Hansson L. and Gattuso J.-P. (2011) Ocean acidification in the coastal zone. In: *Land-Ocean Interactions in the Coastal Zone (LOCIZ)*, Issue 3. Geesthacht: Land-Ocean Interactions in the Coastal Zone International Project Office.
- George, J.D. and Southward, E.C. (1973) A comparative study of the setae of Pogonophora and polychaetous annelids. *J Mar Biol Ass UK* 53, 403-424.

- Gerlach, G. and Atema, J. (2012) The use of chemical cues in habitat recognition and settlement. In: Brönmark, C. and Hansson, L.-A. (eds.) *Chemical Ecology in Aquatic Systems*. New York: Oxford University Press pp 72-81.
- Gienapp, P., Teplitsky, C., Alho, J.S., Mills, J.A. and Merilä, J. (2008) Climate change and evolution: disentangling environmental and genetic responses. *Mol Ecol* 17, 167-178.
- Gobert, G.N. and McManus, D.P. (2005) Update on paramyosin in parasitic worms. *Parasitol Int* 54, 101-107.
- Godbold, J.A. and Calosi, P. (2013) Ocean acidification and climate change: advances in ecology and evolution. *Phil Trans R Soc B* 368: doi.org/10.1098/rstb.2012.0448.
- Godbold, J.A. and Solan, M. (2013) Long-term effects of warming and ocean acidification are modified by seasonal variation in species responses and environmental conditions. *Phil Trans R Soc B* 368: doi.org/10.1098/rstb.2013.0186.
- Goodwin, C., Rodolfo-Metalpa, R., Picton, B. and Hall-Spencer, J.M. (2014) Effects of ocean acidification on sponge communities. *Mar Ecol* 35, 41-49.
- Goss, G.G., Perry, S.F., Wood, C.M. and Laurent, P. (1992) Mechanisms of ion and acid-base regulation at the gills of freshwater fish. *J Exp Zool* 263, 143-159.
- Götze, S., Matoo, O.B., Beniash, E., Saborowski, R. and Sokolova, I.M. (2014) Interactive effects of CO₂ and trace metals on the proteasome activity and cellular stress response of marine bivalves *Crassostrea virginica* and *Mercenaria mercenaria*. *Aquat Toxicol* 149, 65-82.
- Grosell, M. and Genz, J. (2006) Ouabain-sensitive bicarbonate secretion and acid absorption by the marine teleost fish intestine play a role in osmoregulation. *Am J Physiol Regul Integr Comp Physiol* 291, 1145-1156.
- Grosell, M., Genz, J., Taylor, J.R., Perry, S.F. and Gilmour, K.M. (2009a) The involvement of H⁺-ATPase and carbonic anhydrase in intestinal HCO₃⁻ secretion in seawater-acclimated rainbow trout. *J Exp Biol* 212, 1940-1948.
- Grosell, M., Mager, E.M., Williams, C. and Taylor, J.R. (2009b) High rates of HCO₃⁻ secretion and Cl⁻ absorption against adverse gradients in the marine teleost intestine: the involvement of an electrogenic anion exchanger and H⁺-pump metabolon? *J Exp Biol* 212, 1684-1696.

- Guppy, M. and Withers, P. (1999) Metabolic depression in animals: physiological perspectives and biochemical generalizations. *Biol Rev Camb Philos* 74, 1–40.
- Gutowska, M.A., Melzner, F., Langenbuch, M., Bock, C., Claireaux, G. and Pörtner, H.O. (2010) Acid-base regulatory ability of the cephalopod (*Sepia officinalis*) in response to environmental hypercapnia. *J Comp Physiol B* 180, 323-335.
- Hagger, J.A., Fisher, A.S., Hill, S.J., Depledge, M.H. and Jha, A.N. (2002) Genotoxic, cytotoxic and ontogenetic effects of tri-*n*-butyltin on the marine worm, *Platynereis dumerilii* (Polychaeta: Nereidae). *Aquat Toxicol* 57, 243-255.
- Hahn, S., Rodolfo-Metalpa, R., Griesshaber, E., Schmahl, W.W., Buhl, D., Hall-Spencer, J.M., Baggini, C., Fehr, K.T. and Immenhauser, A. (2012) Marine bivalve shell geochemistry and ultrastructure from modern low pH environments: environmental effect versus experimental bias. *Biogeosciences* 9, 1897-1914.
- Hale, R., Calosi, P., McNeill, L., Mieszkowska, N. and Widdicombe, S. (2011) Predicted levels of future ocean acidification and temperature rise could alter community structure and biodiversity in marine benthic communities. *Oikos* 120, 661-674.
- Hall-Spencer, J.M., Rodolfo-Metalpa, R., Martin, S., Ransome, E., Fine, M., Turner, S.M., Rowley, S.J., Tedesco, D. and Buia, M.-C. (2008) Volcanic carbon dioxide vents show ecosystem effects of ocean acidification. *Nature* 454, 96–99.
- Hardege, J.D., Bartels-Hardege, H.D., Zeeck, E. and Grimm, F.T. (1990) Induction of spawning in *Nereis succinea*. *Mar Biol* 104, 291-295.
- Hardege, J.D. (1999). Nereidid polychaetes as model organisms for marine chemical ecology. *Hydrobiologia* 402, 145-161.
- Hardege, J.D., Rotchell, J.M., Terschak, J. and Greenway, G.M. (2011) Analytical challenges and the development of biomarkers to measure and to monitor the effects of ocean acidification. *Trac-Trend Anal Chem* 30, 1320-1326.
- Hartley, C.J. (2013) Impacts of ocean acidification on fitness and chemical communication in a model marine invertebrate, *Nereis succinea*. Msc Thesis, University of Hull, UK Available from: Hydra [10.6.2015].
- Hauenschield, C. (1951) Nachweis der sogenannten atoken Geschlechtsform des Polychaeten *Platynereis dumerilii* Aud. et M. Edw. als eigene Art auf Grund von Zuchtversuchen. *Zool Jb Anat* 63, 107-128.

- Hauenschild, C. (1955) Photoperiodizität als Ursache des von der Mondphase abhängigen Metamorphose-Rhythmus bei dem Polychaeten *Platynereis dumerilii*. *Z Naturforschg* 10b, 658-662.
- Hauenschild, C. (1956) Neue experimentelle Untersuchungen zum Problem der Lunarperiodizität. *Naturwissenschaften* 43, 361-363.
- Hauenschild, C. and Fischer, A. (1969) *Platynereis dumerilii*, Mikroskopische Anatomie, Fortpflanzung, Entwicklung. *Grosses Zoologisches Praktikum* 10b, 1-55.
- Havenhand, J.N., Buttler, F.R., Thorndyke, M.C. and Williamson, J.E. (2008) Near-future levels of ocean acidification reduce fertilization success in a sea urchin. *Current Biology* 18, 651-652.
- Hay, M.E., Renaud, P.E. and Fenical, W. (1988) Large mobile versus small sedentary herbivores and their resistance to seaweed chemical defences. *Oecologia* 75, 246-252.
- Hayashi, M., Kita, J. and Ishimatsu, A. (2004) Acid-base responses to lethal aquatic hypercapnia in three marine fishes. *Mar Biol* 144, 153-160.
- Heisler, N. (1984). Acid-Base Regulation in Fishes. In: Hoar, W.S. and Randall, D.J. *Fish physiology*. Orlando: Academic Press pp 315-401.
- Heisler, N. (1988). Acid-base regulation. In: Shuttleworth, T.J. ed *Physiology of elasmobranch fishes*. Berlin: Springer pp 215-252.
- Hendriks, I.E., Duarte, C.M. and Álvarez, M. (2010) Vulnerability of marine biodiversity to ocean acidification: a meta-analysis. *Estuar Coast Shelf S* 86, 157-164.
- Henry, R.P. and Cameron, J.N. (1983) The role of carbonic anhydrase in respiration, ion regulation and acid-base balance in the aquatic crab *Calinectes sapidus* and the terrestrial crab *Gecarcinus lateralis*. *J Exp Biol* 103, 205-223.
- Hernroth, B., Baden, S., Thorndyke, M. and Dupont, S. (2011) Immune suppression of the echinoderm *Asterias rubens* (L.) following long-term ocean acidification. *Aquat Toxicol* 103, 222-224.
- Herringshaw, L.G., Sherwood, O.A. and McIlroy, D. (2010) Ecosystem engineering by bioturbating polychaetes in event bed microcosms. *Palaios* 25, 46-58.
- Hicks, N., Bulling, M.T., Solan, M., Raffaelli, D., White, P.C.L. and Paterson, D.M. (2011) Impact of biodiversity-climate futures on primary production and

- metabolism in a model benthic estuarine system. *BMC Ecology* 11: doi:10.1186/1472-6785-11-7.
- Hillis, D.M., Sadava, D.E., Hill, R.W. and Price, M.V. (2012) Principle of Life. Sunderland: Sinauer Associates.
- Hoegh-Guldberg, O., Mumby, P.J., Hooten, A.J., Steneck, R.S., Greenfield, P., Gomez, E., Harvell, C.D., Sale, P.F., Edwards, A.J., Caldeira, K., Knowlton, N., Eakin, C.M., Iglesias-Prieto, R., Muthiga, N., Bradbury, R.H., Dubi, A. and Hatzioios, M.E. (2007) Coral reefs under rapid climate change and ocean acidification. *Science* 318, 1737-1742.
- Hofmann, G.E., Barry, J.P., Edmunds, P.J., Gates, R.D., Hutchins, D.A., Klinger, T. and Sewell, M.A. (2010) The effect of ocean acidification on calcifying organisms in marine ecosystems: an organism-to-ecosystem perspective. *Annu Rev Ecol Evol Syst* 41, 127-147.
- Honda, S., Kashiwagi, M., Miyamoto, K., Takei, Y. and Hirose, S. (2000) Multiplicity, structures, and endocrine and exocrine natures of eel fucose-binding lectins. *J Biol Chem* 275, 33151-33157.
- Hooper, S.L., Hobbs, K.H. and Thuma, J.B. (2008) Invertebrate muscles: thin and thick filament structure; molecular basis of contraction and its regulation, catch and asynchronous muscle. *Prog Neurobiol* 86, 72-127.
- Hu, M.Y., Tseng, Y.-C., Stumpp, M., Gutowska, M.A., Kiko, R., Lucassen, M. and Melzner, F. (2011) Elevated seawater PCO₂ differentially affects branchial acid-base transporters over the course of development in the cephalopod *Sepia officinalis*. *Am J Physiol Regul Integr Comp Physiol* 300, 1100-1114.
- Hunte, C., Screpanti, E., Venturi, M., Rimon, A., Padan, E. and Michel, H. (2005) Structure of Na⁺/H⁺ antiporter and insights into mechanism of action and regulation by pH. *Nature* 435, 1197-1202.
- Hutchinson, T.H., Jha, A.N. and Dixon, D.R. (1995) The polychaete *Platynereis dumerilii* (Audouin and Milne-Edwards): a new species for assessing the hazardous potential of chemicals in the marine environment. *Ecotox Environ Safe* 31, 271-281.
- Hutchinson, T.H., Jha, A.N., Mackay, J.M., Elliott, B.M. and Dixon, D.R. (1998) Assessment of developmental effects, cytotoxicity and genotoxicity in the marine

- polychaete (*Platynereis dumerilii*) exposed to disinfected municipal sewage effluent. *Mutat Res* 399, 97-108.
- IGBP, IOC, SCOR (2013) *Ocean Acidification Summary for Policymakers - Third Symposium on the Ocean in a High-CO₂ World*. International Geosphere-Biosphere Programme, Stockholm, Sweden.
- IPCC (2013) Summary for Policymakers. In: *Climate Change 2013: The Physical Science Basis. Contribution of Working Group I to the Fifth Assessment Report of the Intergovernmental Panel on Climate Change* [Stocker, T.F., Qin, D., Plattner, G.-K., Tignor, M., Allen, S.K., Boschung, J., Nauels, A., Xia, Y., Bex, V. and Midgley, P.M. (eds.)]. Cambridge University Press: Cambridge, United Kingdom and New York, NY, USA.
- IPCC (2014) *Climate Change 2014: Synthesis Report. Contribution of Working Groups I, II and III to the Fifth Assessment Report of the Intergovernmental Panel on Climate Change* [Core Writing Team, Pachauri, R.K. and Meyer, L.A. (eds.)]. IPCC: Geneva, Switzerland.
- Jamnongluk, W., Baimai, V. and Kittayapong, P. (2003) Molecular phylogeny of tephritid fruit flies in the *Bactrocera tau* complex using the mitochondrial COI sequences. *Genome* 46, 112-118.
- Jékely, G., Colombelli, J., Hausen, H., Guy, K., Stelzer, E., Nédélec, F. and Arendt, D. (2008) Mechanism of phototaxis in marine zooplankton. *Nature* 456, 395-400.
- Jensen, F.B. (2004) Red blood cell pH, the Bohr effect, and other oxygenation-linked phenomena in blood O₂ and CO₂ transport. *Acta Physiol Scand* 182, 215-227.
- Jha, A.N., Hutchinson, T.H., Mackay, J.M., Elliott, B.M., Pascoe, P.L. and Dixon, D.R. (1995a) The chromosomes of *Platynereis dumerilii* (Polychaeta: Nereidae). *J Mar Biol Ass UK* 75, 551-562.
- Jha, A.N., Dominquez, I., Balajee, A.S., Hutchinson, T.H., Dixon, D.R. and Natarajan, A.T. (1995b) Localization of a vertebrate telomeric sequence in the chromosomes of two marine worms (phylum Annelida: class polychaeta). *Chromosome Research* 3, 507-508.
- Jha, A.N., Hutchinson, T.H., Mackay, J.M., Elliot, B.M. and Dixon, D.R. (1996) Development of an in vivo genotoxicity assay using the marine worm *Platynereis dumerilii* (Polychaeta: Nereidae). *Mutat Res-Envir Muta* 359, 141-150.

- Jha, A.N., Hutchinson, T.H., Mackay, J.M., Elliott, B.M. and Dixon, D.R. (1997) Evaluation of the genotoxicity of municipal sewage effluent using the marine worm *Platynereis dumerilii* (Polychaeta: Nereidae). *Mutat Res-Gen Tox En* 391, 179-188.
- Jha, A.N. (2008) Ecotoxicological applications and significance of the comet assay. *Mutagenesis* 23, 207-221.
- Jobling, M., Hollox, E., Hurles, M., Kivisild, T., Tyler-Smith, C. (2014) Human Evolutionary Genetics. 2nd Edition. New York: Garland Science.
- Johnson, V.R., Brownlee, C., Rickaby, R.E.M., Graziano, M., Milazzo, M. and Hall-Spencer, J.M. (2013) Responses of marine benthic microalgae to elevated CO₂. *Mar Biol* 160, 1813-1824.
- Jones, B.M., Iglesias-Rodrigues, M.D., Skipp, P.J., Edwards, R.J., Greaves, M.J., Young, J.R., Elderfield, H. and O'Connor, C.D. (2013) Responses of the *Emiliana huxleyi* proteome to ocean acidification. *PloS One* 8: doi:10.1371/journal.pone.0061868.
- Kaniewska, P., Campbell, P.R., Kline, D.I., Rodriguez-Lanetty, M., Miller, D.J., Dove, S. and Hoegh-Guldberg, O. (2012) Major cellular and physiological impacts of ocean acidification on a reef building coral. *PloS One* 7: doi:10.1371/journal.pone.0034659.
- Kawabata, S.I. (2010) Immunocompetent molecules and their response network in horseshoe crabs. In: Söderhäll, K. (ed.) *Invertebrate Immunity*. New York: Springer pp 122-136.
- Keeling, P.J. and Doolittle, W.F. (1996) Alpha-tubulin from early-diverging eukaryotic lineages and the evolution of the tubulin family. *Mol Biol Evol* 13, 1297-1305.
- Kerfahi, D., Hall-Spencer, J.M., Tripathi, B.M., Milazzo, M., Lee, J. and Adams, J.M. (2014) Shallow water marine sediment bacterial community shifts along a natural CO₂ gradient in the Mediterranean Sea off Vulcano, Italy. *Microb Ecol* 67, 819-828.
- Kikkawa, T., Ishimatsu, A. and Kita, J. (2003) Acute CO₂ tolerance during the early developmental stages of four marine teleosts. *Environ Toxicol* 18: doi: 10.1002/tox.10139.

- Kikkawa, T., Kita, J. and Ishimatsu, A. (2004) Comparison of the lethal effect of CO₂ and acidification on red sea bream (*Pagrus major*) during the early developmental stages. *Mar Pollut Bull* 48, 108-110.
- Kikkawa, T., Sato, T., Kita, J. and Ishimatsu, A. (2006) Acute toxicity of temporally varying seawater CO₂ conditions on juveniles of Japanese sillago (*Sillago japonica*). *Mar Poll Bull* 52, 621-625.
- Kim, T.W., Barry, J.P. and Micheli, F. (2013) The effects of intermittent exposure to low-pH and low-oxygen conditions on survival and growth of juvenile red abalone. *Biogeosciences* 10, 7255-7262.
- Kirkwood, W., Graves, D., Conway, M., Pargett, D., Scholfield, J., Walz, P., Dunk, R., Peltzer, E., Barry, J. and Brewer, P. (2005) Engineering development of the Free Ocean CO₂ Enrichment (FOCE) experiment. Washington D.C.: *MTS/IEEE Oceans 2005*.
- Kleypas, J.A. and Yates, K.K. (2009) Coral reefs and ocean acidification. *Oceanography*, 22, 108-117.
- Kline, D.I., Teneva, L., Schneider, K., Miard, T., Chai, A., Marker, M., Headley, K., Opdyke, B., Nash, M., Valetich, M., Caves, J.K., Russell, B.D., Connell, S.D., Kirkwood, B.J., Brewer, P., Peltzer, E., Silverman, J., Caldeira, K., Dunbar, R.B., Koseff, J.R., Monismith, S.G., Mitchell, B.G., Dove S. and Hoegh-Guldberg, O. (2012) A short-term *in situ* CO₂ enrichment experiment on Heron Island (GBR). *Scientific reports* 2: doi: 10.1038/srep00413.
- Knoll, A.H. (2003) Biomineralization and evolutionary history. *Rev Mineral Geochem* 54, 329-356.
- Knudsen, B., Kohn, A.B., Nahir, B., McFadden, C.S. and Moroz, L.L. (2006) Complete DNA sequence of the mitochondrial genome of the sea-slug, *Aplysia californica*: conservation of the gene order in Euthyneura. *Mol Phylogenet Evol* 38, 459-469.
- Kroeker, K.J., Micheli, F., Gambi, M.C. and Martz, T.R. (2011) Divergent ecosystem responses within a benthic marine community to ocean acidification. *P Natl Acad Sci USA* 108, 14515-14520.
- Kubota, Y., Takase, Y., Komori, Y., Hashimoto, Y., Arata, T., Kamimura, Y., Araki, H. and Takisawa, H. (2003) A novel ring-like complex of *Xenopus* proteins essential for the initiation of DNA replication. *Gene Dev* 17, 1141-1152.

- Kurihara, H., Shimode, S. and Shirayama, Y. (2004) Effects of raised CO₂ concentration on the egg production rate and early development of two marine copepods (*Acartia steueri* and *Acartia erythraea*). *Mar Pollut Bull* 49, 721–727.
- Kurihara, H. and Shirayama, Y. (2004) Effects of increased atmospheric CO₂ on sea urchin early development. *Mar Ecol Prog Ser* 274, 161–169.
- Kwong, R.W.M., Kumai, Y. and Perry, S.F. (2014) The physiology of fish at low pH: the zebrafish as a model system. *J Exp Biol* 217, 651–662.
- Lai, C.K., Gupta, N., Wen, X., Rangell, L., Chih, B., Peterson, A.S., Bazan, J.F., Li, L. and Scales, S.J. (2011) Functional characterization of putative cilia genes by high-content analysis. *Mol Biol Cell* 22, 1104–1119.
- Langenbuch, M. and Pörtner, H.O. (2004) High sensitivity to chronically elevated CO₂ levels in a eurybathic marine sipunculid. *Aquat Toxicol* 70, 55–61.
- Langer, G., Nehrke, G., Baggini, C., Rodolfo-Metalpa, R., Hall-Spencer, J.M. and Bijma, J. (2014) Limpets counteract ocean acidification induced shell corrosion by thickening of aragonitic shell layers. *Biogeosciences Discussions* 11, 7363–7368.
- Leduc, A.O.H.C., Munday, P.L., Brown, G.E. and Ferrari, M.C.O. (2013) Effects of acidification on olfactory-mediated behaviour in freshwater and marine ecosystems: a synthesis. *Phil Trans R Soc B* 368: doi:10.1098/rstb.2012.0447.
- Lee, B.-H., Min, X., Heise, C.J., Xu, B.-E., Chen, S., Shu, H., Luby-Phelps, K., Goldsmith, E.J. and Cobb, M.H. (2004) WNK1 phosphorylates synaptotagmin 2 and modulates its membrane binding. *Mol Cell* 15, 741–751.
- Lewin, B., Cassimeris, L., Lingappa, V.R. and Plopper, G. (eds.) (2007) *Cells*. Sudbury: Jones and Bartlett Publisher.
- Lewis, C., Clemow, K. and Holt, W.V. (2013) Metal contamination increases the sensitivity of larvae but not gametes to ocean acidification in the polychaete *Pomatoceros lamarckii* (Quatrefages). *Mar Biol* 160, 2089–2101.
- Lewit-Bentley, A. and Réty, S. (2000) EF-hand calcium-binding proteins. *Curr Opin Struc Biol* 10, 637–643.
- Li, S., Xie, L., Zhang, C., Zhang, Y., Gu, M. and Zhang, R. (2004) Cloning and expression of a pivotal calcium metabolism regulator: calmodulin involved in shell formation from pearl oyster (*Pinctada fucata*). *Comp Biochem Phys B* 138, 235–243.

- Likens, G.E., Wright, R.F., Galloway, J.N. and Butler, T.J. (1979) Acid rain. *Sci Am* 241, 43-48.
- Lindskog, S. (1997) Structure and mechanism of carbonic anhydrase. *Pharmacol Ther* 74, 1-20.
- Livak, K. J. and Schmittgen, T.D. (2001) Analysis of relative gene expression data using real-time quantitative PCR and the $2^{-\Delta\Delta C_T}$ method. *Methods* 25, 402-408.
- Lohbeck, K.T., Riebesell, U. and Reusch, T.B.H. (2012) Adaptive evolution of a key phytoplankton species to ocean acidification. *Nat Geosci* 5, 346-351.
- Lombardi, C., Cocito, S., Gambi, M.C., Cisterna, B., Flach, F., Taylor, P.D., Keltie, K., Freer, A. and Cusack, M. (2011a) Effects of ocean acidification on growth, organic tissue and protein profile of the Mediterranean bryozoan *Myriapora truncata*. *Aquat Biol* 13, 251-262.
- Lombardi, C., Gambi, M.C., Vasapollo, C., Taylor, P. and Cocito, S. (2011b) Skeletal alterations and polymorphism in a Mediterranean bryozoan at natural CO₂ vents. *Zoomorphology* 130, 135-145.
- Lombardi, C., Rodolfo-Metalpa, R., Cocito, S., Gambi, M.C. and Taylor, P.D. (2011c) Structural and geochemical alterations in the Mg calcite bryozoan *Myriapora truncata* under elevated seawater pCO₂ simulating ocean acidification. *Mar Ecol* 32, 211-221.
- Lopez, J.V., Ledger, A., Santiago-Vázquez, L.Z., Pop, M., Sommer, D.D., Ranzer, L.K., Feldman, R.A., Kerr, R.G. (2011) Suppression subtractive hybridization PCR isolation of cDNAs from a Caribbean soft coral. *Electron J Biotechn* 14, 8-9.
- Lucey, N.M., Lombardi, C., DeMarchi, L., Schulze, A., Gambi, M.C. and Calosi, P. (2015, in press) To brood or not to brood: Are marine invertebrates that protect their offspring more resilient to ocean acidification? *Nature* 5: doi: 10.1038/srep12009.
- Lunt, D.H., Zhang, D.-X., Szymura, J.M. and Hewitt, O.M. (1996) The insect cytochrome oxidase I gene: evolutionary patterns and conserved primers for phylogenetic studies. *Insect Mol Biol* 5, 153-165.
- Lüthi, D., Le Floch, M., Bereiter, B., Blunier, T., Barnola, J.-M., Siegenthaler, U., Raynaud, D., Jouzel, J., Fischer, H., Kawamura, K. and Stocker, T.F. (2008) High-resolution carbon dioxide concentration record 650,000–800,000 years before present. *Nature* 453, 379-382.

- Mackenzie, J.M. and Epstein, H.F. (1980) Paramyosin is necessary for determination of nematode thick filament length in vivo. *Cell* 22, 747-755.
- MacNicol, M., Jefferson, A.B. and Schulman, H. (1990) Ca²⁺/calmodulin kinase is activated by the phosphatidylinositol signaling pathway and becomes Ca²⁺-independent in PC12 cells. *J Biol Chem* 265, 18055-18058.
- Mangun, W.R. and Henning, D.H. (1999) Managing the environmental crisis. Incorporating competing values in natural resource administration. 2nd Edition. Durham: Duke University Press.
- Martin, S. and Gattuso, J.-P. (2009) Response of Mediterranean coralline algae to ocean acidification and elevated temperature. *Glob Change Biol* 15, 2089-2100.
- Martin, S., Richier, S., Pedrotti, M.-L., Dupont, S., Castejon, C., Gerakis, Y., Kerros, M.-E., Oberhänsli, F., Teyssié, J.-L., Jeffree, R. and Gattuso, J.-P. (2011) Early development and molecular plasticity in the Mediterranean sea urchin *Paracentrotus lividus* exposed to CO₂-driven acidification. *J Exp Biol* 214, 1357-1368.
- Means, A.R. and Dedman, J.R. (1980) Calmodulin-an intracellular calcium receptor. *Nature* 285, 73-77.
- Means, A.R., VanBerkum, M.F.A., Bagchi, I., Lu, K.P. and Rasmussen, C.D. (1991) Regulatory functions of calmodulin. *Pharmacol Therapeut* 50, 225-270.
- Melzner, F., Thomsen, J., Koeve, W., Oschlies, A., Gutowska, M.A., Bange, H.W., Hansen, H.P. and Körtzinger, A. (2013) Future ocean acidification will be amplified by hypoxia in coastal habitats. *Mar Biol* 160, 1875-1888.
- Meron, D., Rodolfo-Metalpa, R., Cunning, R., Baker, A.C., Fine, M. and Banin, E. (2012) Changes in coral microbial communities in response to a natural pH gradient. *ISME J* 6, 1775-1785.
- Miao, J., Pan, L., Zhang, W., Liu, D., Cai, Y. and Li, Z. (2014) Identification of differentially expressed genes in the digestive gland of manila clam *Ruditapes philippinarum* exposed to BDE-47. *Comp Biochem Phys C* 161, 15-20.
- Michaelidis, B., Ouzounis, C., Paleras, A. and Pörtner, H.O. (2005) Effects of long-term moderate hypercapnia on acid-base balance and growth rate in marine mussels *Mytilus galloprovincialis*. *Mar Ecol Prog Ser* 293, 109-118.

- Miles, H., Widdicombe, S., Spicer, J.I. and Hall-Spencer, J. (2007) Effects of anthropogenic seawater acidification on acid-base balance in the sea urchin *Psammechinus miliaris*. *Mar Pollut Bull* 54, 89-96.
- Miller, M.A., Pfeiffer, W. and Schwartz, T. (2010) Creating the CIPRES Science Gateway for inference of large phylogenetic trees. In: *Gateway Computing Environments Workshop (GCE)* pp 1-7.
- Millero, F.J., Feistel, R., Wright, D.G. and McDougall, T.J. (2008) The composition of standard seawater and the definition of the reference-composition salinity scale. *Deep-Sea Res Pt I* 55, 50-72.
- Millero, F.J., Woosley, R., Ditrolio, B. and Waters, J. (2009) Effect of ocean acidification on the speciation of metals in seawater. *Oceanography* 22, 72-85.
- Moore, C.J. (2008) Synthetic polymers in the marine environment: a rapidly increasing, long-term threat. *Environ Res* 108, 131-139.
- Mortimer, C.E. and Müller, U. (2014) *Chemie. Das Basiswissen der Chemie*, 11. Auflage. Stuttgart: Thieme.
- Moy, A.D., Howard, W.R., Bray, S.G. and Trull, T.W. (2009) Reduced calcification in modern Southern Ocean planktonic foraminifera. *Nat Geosci* 2, 276-280.
- Moya, A., Tambutté, S., Bertucci, A., Tambutté, E., Lotto, S., Vullo, D., Supuran, C.T., Allemand, D. and Zoccola, D. (2008) Carbonic anhydrase in the scleractinian coral *Stylophora pistillata*. Characterization, localization, and role in biomineralization. *J Biol Chem* 283, 25475-25484.
- Moya, A., Huisman, L., Ball, E.E., Hayward, D.C., Grasso, L.C., Chua, C.M., Woo, H.N., Gattuso, J.-P., Forêt, S. and Miller, D.J. (2012) Whole transcriptome analysis of the coral *Acropora millepora* reveals complex responses to CO₂-driven acidification during the initiation of calcification. *Mol Ecol* 21, 2440-2454.
- Nilsson, G.E., Dixon, D.L., Domenici, P., McCormick, M.I., Sørensen, C., Watson, S.-A. and Munday, P.L. (2012) Near-future carbon dioxide levels alter fish behaviour by interfering with neurotransmitter function. *Nature Climate Change* 2, 201-204.
- Nosengo, N. (2003) Fertilized to death. *Nature* 425, 894-895.
- NRC (1987) Committee on biological markers of the National Research Council. Biological markers in environmental health research. *Environ Health Persp* 74, 3-9.

- O'Donnell, M.J., Todgham, A.E., Sewell, M.A., Hammond, L.M., Ruggiero, K., Fangue, N.A., Zippay, M.L. and Hofmann, G.E. (2010) Ocean acidification alters skeletogenesis and gene expression in larval sea urchins. *Mar Ecol Prog Ser* 398, 157-171.
- Ochei, J. and Kolhatkar, A. (2000) Medical Laboratory Science: Theory and Practice. New Dehli: Tata-McGraw-Hill.
- Oglesby, L.C. (1968) Responses of an estuarine population of the polychaete *Nereis limnicola* to osmotic stress. *Biol Bull* 134, 118-138.
- Orchard, C.H. and Kentish, J.C. (1990) Effects of changes of pH on the contractile function of cardiac muscle. *Am J Physiol-Cell Ph* 258, 967-981.
- Ouellette, A.J. and Bevins, C.L. (2001) Paneth cell defensins and innate immunity of the small bowel. *Inflamm Bowel Dis* 7, 43-50.
- Packer, R.K. and Dunson, W.A. (1972) Anoxia and sodium loss associated with the death of brook trout at low pH. *Comp Biochem Physiol* 41, 17-26.
- Padan, E. and Schuldiner, S. (1993) Na⁺/H⁺ antiporters, molecular devices that couple the Na⁺ and H⁺ circulation in cells. *J Bioenerg Biomembr* 25, 647-669.
- Padan, E., Venturi, M., Gerchman, Y. and Dover, N. (2001) Na⁺/H⁺ antiporters. *Biochim Biophys Acta* 1505, 144-157.
- Padan, E., Tzuberly, T., Herz, K., Kozachkov, L., Rimon, A. and Galili, L. (2004) NhaA of *Escherichia coli*, as a model of a pH-regulated Na⁺/H⁺ antiporter. *Biochim Biophys Acta* 1658, 2-13.
- Padan, E., Kozachkov, L., Herz, K. and Rimon, A. (2009) NhaA crystal structure: functional-structural insights. *J Exp Biol* 212, 1593-1603.
- Pan, T.-C.F., Applebaum, S.L. and Manahan, D.T. (2015) Experimental ocean acidification alters the allocation of metabolic energy. *P Natl Acad Sci USA* 112, 4696-4701.
- Parker, L.M., Ross, P.M. and O'Connor, W.A. (2009) The effect of ocean acidification and temperature on the fertilization and embryonic development of the Sydney rock oyster *Saccostrea glomerata* (Gould 1850). *Glob Change Biol* 15, 2123-2136.
- Parker, L.M., Ross, P.M., Raftos, D., Thompson, E. and O'Connor, W.A. (2011) The proteomic response of larvae of the Sydney rock oyster, *Saccostrea glomerata* to elevated pCO₂. *Australian Zoologist* 35, 1011-1023.

- Peakall, D.B. (1994) The role of biomarkers in environmental assessment (1). Introduction. *Ecotoxicology* 3, 157-160.
- Perry, S.F., Shahsavarani, A., Georgalis, T., Bayaa, M., Furimsky, M. and Thomas, S.L.Y. (2003) Channels, pumps, and exchangers in the gill and kidney of freshwater fishes: Their role in ionic and acid-base regulation. *J Exp Zool Part A* 300, 53-62.
- Pespeni, M.H., Sanford, E., Gaylord, B., Hill, T.M., Hosfelt, J.D., Jaris, H.K., LaVigne, M., Lenz, E.A., Russell, A.D., Young, M.K. and Palumbi, S.R. (2013) Evolutionary change during experimental ocean acidification. *P Natl Acad Sci USA* 110, 6937-6942.
- Petsko, G.A. and Ringe, D. (2004) Protein Structure and Function. London: New Science Press Ltd.
- Pettibone, M.H. (1963) Marine Polychaete worms of the New England region. *Bulletin of the United States National Museum* 227, 1-356.
- Pfaffl, M.W. (2001) A new mathematical model for relative quantification in real-time RT-PCR. *Nucleic Acids Res* 29: doi: 10.1093/nar/29.9.e45.
- Piantadosi, C.A. (2003) The Biology of Human Survival: Life and Death in Extreme Environments. New York: Oxford University Press.
- Pocklington, P. and Wells, P.G. (1992) Polychaetes key taxa for marine environmental quality monitoring. *Mar Pollut Bull* 24, 593-598.
- Pörtner, H.O., Bock, C. and Reipschläger, A. (2000) Modulation of the cost of pHi regulation during metabolic depression: a ³¹P-NMR study in invertebrate (*Sipunculus nudus*) isolated muscle. *J Exp Biol* 203, 2417-2428.
- Pörtner, H.O., Langenbuch, M. and Reipschläger, A. (2004) Biological impact of elevated ocean CO₂ concentrations: lessons from animal physiology and earth history. *J Oceanogr* 60, 705-718.
- Porzio, L., Buia, M.C. and Hall-Spencer, J.M. (2011) Effects of ocean acidification on macroalgal communities. *J Exp Mar Biol Ecol* 400, 278-287.
- Porzio, L., Garrard, S.L. and Buia, M.C. (2013) The effect of ocean acidification on early algal colonization stages at natural CO₂ vents. *Mar Biol* 160, 2247-2259.
- PrimerDesign (2008) Products for Real-Time PCR, Technical bulletin 02, 40-67.

- Ramanathan, N., Simakov, O., Merten, C.A. and Arendt, D. (2013) Ocean on a chip: microfluidics as a gateway to functional marine ecology. In *17th International Conference on Miniaturized Systems for Chemistry and Life Sciences*. Freiburg pp 1102-1104.
- Rasmussen, C.D. and Means, A.R. (1989) Calmodulin is required for cell-cycle progression during G1 and mitosis. *EMBO J* 8, 73-82.
- Recordati, G. and Bellini, T.G. (2004) A definition of internal constancy and homeostasis in the context of non-equilibrium thermodynamics. *Exp Physiol* 89, 27-38.
- Redfield, A.C. and Walford, L.A. (1951) A study of the disposal of chemical waste at sea. Report of the committee for investigation of waste disposal. Washington: National Academy of Science-National Research Council.
- Reipschläger, A. and Pörtner, H.O. (1996) Metabolic depression during environmental stress: the role of extracellular versus intracellular pH in *Sipunculus nudus*. *J Exp Biol* 199, 1801-1807.
- Reish, D.J., Anderson, F.E., Horn, K.M. and Hardege, J. (2014) Molecular phylogenetics of the *Neanthes acuminata* (Annelida: Nereididae) species complex. *Memoirs of Museum Victoria* 71, 271-278.
- Ricevuto, E., Lorenti, M., Patti, F.P., Scipione, M.B. and Gambi, M.C. (2012) Temporal trends of benthic invertebrate settlement along a gradient of ocean acidification at natural CO₂ vents (Tyrrhenian Sea). *Biol Mar Mediterr* 19, 49-52.
- Ricevuto, E., Kroeker, K.J., Ferrigno, F., Micheli, F. and Gambi, M.C. (2014) Spatio-temporal variability of polychaete colonization at volcanic CO₂ vents indicates high tolerance to ocean acidification. *Mar Biol* 161, 2909-2919.
- Ricevuto, E., Vizzini, S. and Gambi, M.C. (2015) Ocean acidification effects on stable isotope signatures and trophic interactions of polychaete consumers and organic matter sources at a CO₂ shallow vent system. *J Exp Mar Biol Ecol* 468, 105-117.
- Riddle, D.L., Blumenthal, T., Meyer, B.J. and Priess, J.R. (1997) *C. elegans* II, 2nd Edition, Section II, The Organization, Structure, and Function of Muscle. New York: Cold Spring Harbor Laboratory Press.
- Riebesell, U., Zondervan, I., Rost, B., Tortell, P.D., Zeebe, R.E. and Morel, F.M. (2000) Reduced calcification of marine plankton in response to increased atmospheric CO₂. *Nature* 407, 364-367.

- Ries, J.B., Cohen, A.L. and McCorkle, D.C. (2009) Marine calcifiers exhibit mixed responses to CO₂-induced ocean acidification. *Geology* 37, 1131-1134.
- Rodolfo-Metalpa, R., Houlbrèque, F., Tambutté, É., Boisson, F., Baggini, C., Patti, F.P., Jeffree, R., Fine, M., Foggo, A., Gattuso, J.-P. and Hall-Spencer, J.M. (2011) Coral and mollusc resistance to ocean acidification adversely affected by warming. *Nature Climate Change* 1, 308-312.
- Röhl, I., Schneidder, B., Schmidt, B. and Zeeck, E. (1999) L-Ovothiol A: The egg release pheromone of the marine polychaete *Platynereis dumerilii*: Annelida: Polychaeta. *Z Naturforsch* 54, 1145-1147.
- Ronquist, F., Teslenko, M., Van der Mark, P., Ayres, D.L., Darling, A., Höhna, S., Larget, B., Liu, L., Suchard, M.A. and Huelsenbeck, J.P. (2012) MrBayes 3.2: Efficient Bayesian phylogenetic inference and model choice across a large model space. *Syst Biol* 61, 539-542.
- Rosa, R. and Seibel, B.A. (2008) Synergistic effects of climate-related variables suggest future physiological impairment in a top oceanic predator. *P Natl Acad Sci USA* 105, 20776-20780.
- Rosa, R.D., Santini, A., Fievet, J., Bulet, P., Destoumieux-Garzón, D. and Bachère, E. (2011) Big defensins, a diverse family of antimicrobial peptides that follows different patterns of expression in hemocytes of the oyster *Crassostrea gigas*. *PLoS One* 6: doi:10.1371/journal.pone.0025594.
- Rossoll, D., Bermudez, R., Hauss, H., Schulz, K.G., Riebesell, U., Sommer, U. and Winder, M. (2012) Ocean acidification-induced food quality deterioration constrains trophic transfer. *PLoS one* 7: doi:10.1371/journal.pone.0034737.
- Rouse, G.W. and Fauchald, K. (1997) Cladistics and polychaetes. *Zool Scr* 26, 139-204.
- Rouse, G.W. and Pleijel, F. (2001) Polychaetes, New York: Oxford University Press.
- Royal Society (2005) Ocean acidification due to increasing atmospheric carbon dioxide. London: The Royal Society.
- Ryu, S., Liu, B. and Qin, F. (2003) Low pH potentiates both capsaicin binding and channel gating of VR1 receptors. *J Gen Physiol* 122, 45-61.
- Sabine, C.L., Feely, R.A., Gruber, N., Key, R.M., Lee, K., Bullister, J.L., Wanninkhof, R., Wong, C.S., Wallace, D.W.R., Tilbrook, B., Millero, F.J., Peng, T.-H., Kozyr,

- A., Ono T. and Rios, A.F. (2004) The oceanic sink for anthropogenic CO₂. *Science* 305, 367-371.
- Salisbury, J., Green, M., Hunt, C. and Campbell, J. (2008) Coastal acidification by rivers: a threat to shellfish? *Eos, Transactions, American Geophysical Union* 89, 513.
- Scaps, P. (2002) A review of the biology, ecology and potential use of the common ragworm *Hediste diversicolor* (O.F. Müller) (Annelida: Polychaeta). *Hydrobiologia*, 470, 203-218.
- Schalkhausser, B., Bock, C., Stemmer, K., Brey, T., Pörtner, H.O. and Lannig, G. (2013) Impact of ocean acidification on escape performance of the king scallop, *Pecten maximus*, from Norway. *Mar Biol* 160, 1995-2006.
- Schneider, S., Fischer, A. and Dorresteijn, A.W. (1992) A morphometric comparison of dissimilar early development in sibling species of *Platynereis* (Annelida, Polychaeta). *Roux's Arch Dev Biol* 201, 243-256.
- Selye, H. (1975) Homeostasis and heterostasis. In: Day, S.B. (eds.) *Trauma, Clinical and Biological Aspects*. New York: Springer US pp 25-29.
- Sewell, M.A., Millar, R.B., Yu, P.C., Kapsenberg, L. and Hofmann, G.E. (2014) Ocean acidification and fertilization in the Antarctic sea urchin *Sterechinus neumayeri*: the importance of polyspermy. *Environ Sci Technol* 48, 713-722.
- Sherwood, L., Klandorf, H. and Yancey, P.H. (2005) *Animal Physiology, From Genes to Organisms*. Belmont: Brooks/Cole, Cengage Learning.
- Shimogawara, K., Fujiwara, S., Grossman, A. and Usuda, H. (1998) High-efficiency transformation of *Chlamydomonas reinhardtii* by electroporation. *Genetics* 148, 1821-1828.
- Shine, J. and Dalgarno, L. (1974) The 3'-terminal sequence of *Escherichia coli* 16S ribosomal RNA: Complementarity to nonsense triplets and ribosome binding sites. *P Natl Acad Sci USA* 71, 1342-1346.
- Shirayama, Y. and Thornton, H. (2005) Effect of increased atmospheric CO₂ on shallow water marine benthos. *J Geophys Res* 110: doi:10.1029/2004JC002618.
- Shugart, L.R., McCarthy, J.F. and Halbrook, R.S. (1992) Biological markers of environmental and ecological contamination: an overview. *Risk Analysis* 12, 353-360.

- Siggaard-Andersen, O. (2005) Acid-Base Balance. In: *Encyclopedia of Respiratory Medicine*. New York: Academic pp 1-6.
- Simakov, O. (2013) Linking micro- and macro-evolution at the cell type level. Insights into long-term evolution of cell types from comparative genomics, population sampling and development of *Platynereis dumerilii*. Doktorarbeit, Universität Konstanz.
- Sinning, A. and Hübner, C.A. (2013) Minireview: pH and synaptic transmission. *FEBS Lett* 587, 1923-1928.
- Slepkov, E.R., Rainey, J.K., Sykes, B.D. and Fliegel, L. (2007) Structural and functional analysis of the Na⁺/H⁺ exchanger. *Biochem J* 401, 623-633.
- Smith, R.I. (1955) On the distribution of *Nereis diversicolor* in relation to salinity in the vicinity of Tvärminne, Finland, and the Isefjord, Denmark. *Biol Bull* 108, 326-345.
- Smith, R.I. (1958) On reproductive pattern as a specific characteristic among Nereid polychaetes. *Syst Biol* 7, 60-73.
- Smith, V.J., Desbois, A.P. and Dyrinda, E.A. (2010) Conventional and unconventional antimicrobials from fish, marine invertebrates and micro-algae. *Mar Drugs* 8, 1213-1262.
- Solomon, S., Plattner, G.-K., Knutti, R. and Friedlingstein, P. (2009) Irreversible climate change due to carbon dioxide emissions. *P Natl Acad Sci USA* 106, 1704-1709.
- Solomon, E., Berg, L. and Martin, D. (2011) *Biology*. 9th Edition. Belmont: Brooks/Cole.
- Sommer, A., Klein, B. and Pörtner, H.O. (1997) Temperature induced anaerobiosis in two populations of the polychaete worm *Arenicola marina* (L.). *J Comp Physiol B* 167, 25-35.
- Spanier, K.I., Leese, F., Mayer, C., Colbourne, J.K., Gilbert, D., Pfrender, M.E. and Tollrian, R. (2010) Predator-induced defences in *Daphnia pulex*: Selection and evaluation of internal reference genes for gene expression studies with real-time PCR. *BMC Mol Biol* 11: doi:10.1186/1471-2199-11-50.
- Starcevic, A., Dunlap, W.C., Cullum, J., Shick, J.M., Hranueli, D. and Long, P.F. (2010) Gene expression in the scleractinian *Acropora microphthalma* exposed to high solar irradiance reveals elements of photoprotection and coral bleaching. *PLoS One* 5: doi:10.1371/journal.pone.0013975.

- Stobbart, R.H. (1971) Evidence for Na^+/H^+ and $\text{Cl}^-/\text{HCO}_3^-$ Exchanges during independent sodium and chloride uptake by the larva of the mosquito *Aedes aegypti* (L.). *J Exp Biol* 54, 19-27.
- Stock, D., Gibbons, C., Arechaga, I., Leslie, A.G.W. and Walker, J.E. (2000) The rotary mechanism of ATP synthase. *Curr Opin Struc Biol* 10, 672-679.
- Stumpp, M., Dupont, S., Thorndyke, M.C. and Melzner, F. (2011) CO_2 induced seawater acidification impacts sea urchin larval development II: Gene expression patterns in pluteus larvae. *Comp Biochem Phys A* 160, 320-330.
- Suarez-Ulloa, V., Gonzalez-Romero, R. and Eirin-Lopez, J.M. (2015) Environmental epigenetics: A promising venue for developing next-generation pollution biomonitoring tools in marine invertebrates. *Marine Pollution Bulletin* 98, 5-13.
- Supuran, C.T. (2011) Carbonic anhydrase inhibition with natural products: novel chemotypes and inhibition mechanisms. *Mol Divers* 15, 305-316.
- Szyk, A., Wu, Z., Tucker, K., Yang, D., Lu, W. and Lubkowski, J. (2006) Crystal structures of human α -defensins HNP4, HD5 and HD6. *Protein Sci* 15, 2749-2760.
- Takahashi, K. and Nadal-Ginard, B. (1991) Molecular cloning and sequence analysis of smooth muscle calponin. *J Biol Chem* 266, 13284-13288.
- Takayama, Y., Kamimura, Y., Okawa, M., Muramatsu, S., Sugino, A. and Araki, H. (2003) GINS, a novel multiprotein complex required for chromosomal DNA replication in budding yeast. *Gene Dev* 17, 1153-1165.
- Tamura, K., Stecher, G., Peterson, D., Filipowski, A. and Kumar, S. (2013) MEGA6: Molecular evolutionary genetics analysis version 6.0. *Mol Biol Evol* 30, 2725-2729.
- Tardent, P. (2005) Meeresbiologie, Eine Einführung, 3., unveränderte Auflage. Stuttgart: Georg Thieme Verlag KG.
- Taylor, S., Wakem, M., Dijkman, G., Alsarraj, M. and Nguyen, M. (2010) A practical approach to RT-qPCR-Publishing data that conform to the MIQE guidelines. *Methods* 50: doi:10.1016/j.ymeth.2010.01.005.
- Tedesco, D. (1996) Chemical and isotopic investigations of fumarolic gases from Ischia island (southern Italy): Evidences of magmatic and crustal contribution. *J Volcanol Geoth Res* 74, 233-242.

- Tessmar-Raible, K. and Arendt, D. (2003) Emerging systems: between vertebrates and arthropods, the Lophotrochozoa. *Curr Opin Genet Dev* 13, 331-340.
- Theil, E.C. (1987) Ferritin: structure, gene regulation, and cellular function in animals, plants and microorganisms. *Ann Rev Biochem* 56, 289-315.
- Thomsen, J., Gutowska, M.A., Saphörster, J., Heinemann, A., Trübenbach, K., Fietzke, J., Hiebenthal, C., Eisenhauer, A., Körtzinger, A., Wahl, M. and Melzner, F. (2010) Calcifying invertebrates succeed in a naturally CO₂-enrich coastal habitat but are threatened by high levels of future acidification. *Biogeosciences* 7, 3879-3891.
- Thomsen, J. and Melzner, F. (2010) Moderate seawater acidification does not elicit long-term metabolic depression in the blue mussel *Mytilus edulis*. *Mar Biol* 157, 2667-2676.
- Tierney, A.J. and Atema, T. (1988) Amino acid chemoreception: effects of pH on receptors and stimuli. *J Chem Ecol* 14, 135-141.
- Todgham, A.E. and Hofmann, G.E. (2009) Transcriptomic response of sea urchin larvae *Strongylocentrotus purpuratus* to CO₂-driven seawater acidification. *J Exp Biol* 212, 2579-2594.
- Tomanek, L., Zuzow, M.J., Ivanina, A.V., Beniash, E. and Sokolova, I.M. (2011) Proteomic response to elevated PCO₂ level in eastern oysters, *Crassostrea virginica*: evidence for oxidative stress. *J Exp Biol* 214, 1836-1844.
- Toulmond, A. and Tchernigovtzeff, C. (1984) Ventilation and respiratory gas exchanges of the lugworm *Arenicola marina* (L.) as functions of ambient PO₂ (20–700 torr). *Resp Physiol* 57, 349-363.
- Tripp, B.C., Smith, K. and Ferry, J.G. (2001) Carbonic anhydrase: new insights for an ancient enzyme. *J Biol Chem* 276, 48615-48618.
- Tseng, Y.-C., Hu, M.Y., Stumpp, M., Lin, L.-Y., Melzner, F. and Hwang, P.-P. (2013) CO₂-driven seawater acidification differentially affects development and molecular plasticity along life history of fish (*Oryzias latipes*). *Comp Biochem Phys A* 165, 119-130.
- Tunnicliffe, V., Davies, K.T.A., Butterfield, D.A., Embley, R.W., Rose, J.M. and Chadwick Jr, W.W. (2009) Survival of mussels in extremely acidic waters on a submarine volcano. *Nat Geosci* 2, 344-348

- Turner, L.M., Ricevuto, E., Gallucci, A.M., Gambi, M.C. and Calosi, P. (2015) Energy metabolism and cellular homeostasis trade-offs provide the basis for a new type of sensitivity to ocean acidification in a marine polychaete at a high CO₂ vent: adenylate and phosphagen energy pools vs. carbonic anhydrase. *J Exp Biol* doi: 10.1242/jeb.117705.
- Urho, L., Hildén, M. and Hudd, R. (1990) Fish reproduction and the impact of acidification in the Kyrönjoki River estuary in the Baltic Sea. *Environ Biol Fish* 27, 273-283.
- Van der Oost, R., Beyer, J. and Vermeulen, N.P.E. (2003) Fish bioaccumulation and biomarkers in environmental risk assessment: a review. *Environ Toxicol Phar* 13, 57-149.
- Vidal-Dupiol, J., Zoccola, D., Tambutté, E., Grunau, C., Cosseau, C., Smith, K.M., Freitag, M., Dheilily, N.M., Allemand, D. and Tambutté, S. (2013) Genes related to ion-transport and energy production are upregulated in response to CO₂-driven pH decrease in corals: new insights from transcriptome analysis. *PloS One* 8: doi:10.1371/journal.pone.0058652.
- Visser, M.E. (2008) Keeping up with a warming world; assessing the rate of adaptation to climate change. *P Roy Soc B-Biol Sci* 275, 649-659.
- Vitousek, P.M., Mooney, H.A., Lubchenco, J. and Melillo, J.M. (1997) Human domination of Earth's ecosystems. *Science* 277, 494-499.
- Vizzini, S., Tomasello, A., Di Maida, G., Pirrotta, M., Mazzola, A. and Calvo, S. (2010) Effect of explosive shallow hydrothermal vents on $\delta^{13}\text{C}$ and growth performance in the seagrass *Posidonia oceanica*. *J Ecol* 98, 1284-1291.
- Walker, C.H., Sibly, R.M., Hopkin, S.P. and Peakall, D.B. (2012) Principles of Ecotoxicology, 4th Edition. Boca Raton: CRC Press Taylor & Francis Group.
- Walsh, P.J. and Milligan, C.L. (1989) Coordination of metabolism and intracellular acid-base status: ionic regulation and metabolic consequences. *Can J Zool* 67, 2994-3004.
- Wang, T. and Brown, M.J. (1999) mRNA quantification by real time TaqMan polymerase chain reaction: validation and comparison with RNase protection. *Anal Biochem* 269, 198-201.

- Wang, T., Cheung, V.T.F., Anson, M. and Li, Y.S. (2001) Ozone and related gaseous pollutants in the boundary layer of eastern China: overview of the recent measurements at a rural site. *Geophys Res Lett* 28, 2373-2376.
- Watanabe, Y., Yamaguchi, A., Ishida, H., Harimoto, T., Suzuki, S., Sekido, Y., Ikeda, T., Shirayama, Y., Takahashi, M.M., Ohsumi, T. and Ishizaka, J. (2006) Lethality of increasing CO₂ levels on deep-sea copepods in the western North Pacific. *J Oceanogr* 62, 185-196.
- Weiss, H., Friedrich, T., Hofhaus, G. and Preis, D. (1991) The respiratory-chain NADH dehydrogenase (complex I) of mitochondria. *Eur J Biochem* 197, 563-576.
- Westheide, W. and Hass-Cordes, E. (2001) Molecular taxonomy: description of a cryptic *Petitia* species (Polychaeta: Syllidae) from the island of Mahé (Seychelles, Indian Ocean) using RAPD markers and ITS2 sequences. *J Zool Syst Evol Research* 39, 103-111.
- Wheatly, M.G. and Henry, R.P. (1992) Extracellular and intracellular acid-base regulation in crustaceans. *J Exp Zool* 263, 127-142.
- Widdicombe, S. and Needham, H.R. (2007) Impact of CO₂-induced seawater acidification on the burrowing activity of *Nereis virens* and sediment nutrient flux. *Mar Ecol Prog Ser* 341, 111-122.
- Widdicombe, S. and Spicer, J.I. (2008) Predicting the impact of ocean acidification on benthic biodiversity: what can animal physiology tell us? *J Exp Mar Biol Ecol* 366, 187-197.
- Widdicombe, S., Dupont, S. and Thorndyke, M. (2010) Laboratory experiments and benthic mesocosm studies. In: Riebesell, U., Fabry, V.J., Hansson, L. and Gattuso, J.-P. (eds.) *Guide to best practices for ocean acidification research and data reporting*. Luxembourg: Publications Office of the European Union.
- Wilson, R.W., Millero, F.J., Taylor, J.R., Walsh, P.J., Christensen, V., Jennings, S. and Grosell, M. (2009) Contribution of fish to the marine inorganic carbon cycle. *Science* 323, 359-362.
- Wittmann, A.C. and Pörtner, H.-O. (2013) Sensitivities of extant animal taxa to ocean acidification. *Nature Climate Change* 3, 995-1001.
- Won, E.-J., Kim, R.-O., Rhee, J.-S., Park, G.S., Lee, J., Shin, K.-H., Lee, Y.-M. and Lee, J.-S. (2011) Response of glutathione S-transferase (*GST*) genes to cadmium

- exposure in the marine pollution indicator worm, *Perinereis nuntia*. *Comp Biochem Phys C* 154, 82-92.
- Wong, K.K.W., Lane, A.C., Leung, P.T.Y. and Thiyagarajan, V. (2011) Response of larval barnacle proteome to CO₂-driven seawater acidification. *Comp Biochem Physiol* 6, 310-321.
- Wood, H.L., Spicer, J.I., Lowe, D.M. and Widdicombe, S. (2010) Interaction of ocean acidification and temperature; the high cost of survival in the brittlestar *Ophiura ophiura*. *Mar Biol* 157, 2001-2013.
- Wu, B.L., Sunm R.P. and Yang, D.J. (1984) The Nereidae of the Chinese coast. China Ocean Press, Beijing, Springer Verlag, Heidelberg, New York, Tokyo.
- Xu, B.-E., Stippec, S., Chu, P.-Y., Lazrak, A., Li, X.-J., Lee, B.-H., English, J.M., Ortega, B., Huang, C.-L. and Cobb, M.H. (2005) WNK1 activates SGK1 to regulate the epithelial sodium channel. *P Natl Acad Sci USA* 102, 10315-10320.
- Zeebe, R.E. and Wolf-Gladrow, D. (2001) CO₂ in seawater: Equilibrium, Kinetics, Isotopes. Amsterdam: Elsevier.
- Zeeck, E., Harder, T. and Beckmann, M. (1998) Uric acid: the sperm-release Pheromone of the marine polychaete *Platynereis dumerilii*. *J Chem Ecol* 24, 13-22.
- Zeng, H., Huang, J., Li, W., Huang, H. and Ye, H. (2011) Identification of differentially expressed genes in the thoracic ganglion of the mud crab, *Scylla paramamosain* during ovarian maturation. *Mar Biol Res* 7, 617-622.
- Zhai, Y., Lin, Q., Zhou, X., Zhang, X., Liu, T. and Yu, Y. (2014) Identification and validation of reference genes for quantitative real-time PCR in *Drosophila suzukii* (Diptera: Drosophilidae). *PloS One* 9: doi: 10.1371/journal.pone.0106800.
- Zhang, H., Pan, L., Tao, Y., Tian, S. and Hu, Y. (2013) Identification and expression of differentially expressed genes in clam *Venerupis philippinarum* in response to environmental pollutant hexabromocyclododecane (HBCD). *J Exp Mar Biol Ecol* 445, 166-173.
- Zhao, Q.-P., Moon, S.-U., Na, B.-K., Kim, S.-H., Cho, S.-H., Lee, H.-W., Kong, Y., Sohn, W.-M., Jiang, M.-S. and Kim, T.-S. (2007) *Paragonimus westermani*: Biochemical and immunological characterizations of paramyosin. *Exp Parasitol* 115, 9-18.

- Zheng, S., Qiu, X., Chen, B., Yu, X., Lin, K., Bian, M., Liu, K., Huang, H. and Yu, W. (2011) Toxicity evaluation of benzo[*a*]pyrene on the polychaete *Perinereis nuntia* using subtractive cDNA libraries. *Aquat Toxicol* 105, 279-291.
- Zippay, M.L. and Hofmann, G.E. (2010) Effect of pH on gene expression and thermal tolerance of early life history stages of red abalone (*Haliotis rufescens*). *J Shellfish Res* 29, 429-439.
- Zimmer, R.K. and Butman, C.A. (2000) Chemical signaling processes in the marine environment. *Biol Bull* 198, 168-187.